SUBMERGENCE EFFECTS ON JET BEHAVIOR IN SCOUR BY A PLANE WALL JET

A Thesis
Submitted to the College of Graduate Studies and Research
In Partial Fulfillment of the Requirements
for the
Degree of Master of Science
in the
Department of Civil and Geological Engineering
University of Saskatchewan
Saskatoon, Saskatchewan

by

BISHNU PRASAD GAUTAM

PERMISSION TO USE

The author has agreed that the library, University of Saskatchewan, may make this thesis freely available for inspection. Moreover, the author has agreed that permission for extensive copying of this thesis for scholarly purposes may be granted by the professors who supervised the thesis work recorded herein or, in their absence, by the head of the Department or the Dean of the College in which the thesis work was done. It is understood that due recognition will be given to the author of this thesis and to the University of Saskatchewan in any use of the material in this thesis. Copying or publication or any other use of the thesis for financial gain without approval by the University of Saskatchewan and the author's written permission is prohibited.

Requests for permission to copy or to make any other use of material in this thesis in whole or part should be addressed to:

Head of the Department of Civil and Geological Engineering
University of Saskatchewan
Engineering Building
57 Campus Drive
Saskatoon, Saskatchewan
Canada, S7N 5A9

ABSTRACT

In this study, the effects of submergence on local scour in a uniform cohesionless sediment bed by a plane turbulent wall jet and the resulting flow field were investigated experimentally. Here, submergence is defined as the ratio of the tailwater depth to the thickness of the jet at its origin. The main focus was to determine scour dimensions at an asymptotic state, examine whether there was similarity in the velocity profiles for the flow in the scour hole, and to determine the growth of the length scales and decay of the maximum velocity of the jet. Also examined were the relationships between the scales for the velocity field in the scour hole and the scour hole size.

In the experiments, the range of submergence was varied from 3-17.5, whereas the range of densimetric Froude number and the ratio of the boundary roughness to the gate opening (relative boundary roughness) were varied from 4.4-6.9 and 0.085-0.137 respectively. The velocity field in the scour hole at asymptotic state was measured using a SonTek 16-MHz MicroADV. Time development of the characteristic dimensions of the scour hole was also measured.

The dimensions of the scour hole were found to increase with increasing submergence for all experiments with a "bed-jet" flow regime. In the bed-jet flow regime, the jet remains near the bed throughout the scouring process. Further, the time development of the scour hole dimensions were observed to increase approximately linearly with the logarithm of time up to a certain time before the beginning of asymptotic state for experiments with either the bed-jet or surface-jet flow regimes.

The flow field results showed that the velocity profiles in the region of forward flow and the recirculating region above the jet were similar in shape up to about the location of the maximum scour depth. Relationships describing this velocity profile, including its velocity and length scales, were formulated. The decay rate of the maximum velocity, the growth of the jet half-width, and the boundary layer thickness were also studied. The decay and the growth rate of the jet length scales were found to

be influenced by the submergence ratio, densimetric Froude number, and the relative boundary roughness.

Two distinct stages in the decay of the maximum streamwise velocity, with distance along the direction of flow, were observed for the jet flows having a bed-jet flow regime. The first stage of velocity decay was characterized by a curvilinear decay of velocity, which followed that of a wall jet on a smooth, rigid bed for streamwise distance approximately equal to 2L. For the surface-jet flow regime, the decay of velocity was observed to be similar to that of a free-jump on a smooth, rigid bed for a streamwise distance approximately equal to L. Here, L is defined as the streamwise distance measured from the end of the rigid apron to where the maximum streamwise velocity in the jet is half the velocity of the jet at the end of apron. The streamwise maximum velocity of the jet was then seen to increase in what was called the recovery zone.

A relationship for the streamwise decay of the maximum velocity within the scour hole is proposed. Moreover, other scales representing the flow inside the scour hole such as the streamwise distance from the end of the apron to where the streamwise maximum velocity starts to deviate from curvilinear to linear decay and the streamwise distance to where maximum streamwise velocity starts to increase are suggested. Some new results on the velocity distribution for the reverse flow for a “bed-jet” flow regime are also presented. Finally, some dimensionless empirical equations describing the relationship between the jet scales for the jet flow in a scour hole and the scour hole size are given.

ACKNOWLEDGEMENTS

I wish to express my sincere appreciation and gratitude to my respected supervisor, Dr. Kerry Mazurek, for her invaluable guidance, endless support and encouragement throughout the course of my M.Sc. program. Her continued constructive comments, criticisms, suggestions and input were instrumental in seeing this thesis in its present form.

I would also like to thank to my advisory committee members, Dr. Jim Kells and Dr. Gordon Putz, for their constructive comments, suggestions and feedback. The author would like to acknowledge the time and support of my advisory committee chair, Dr. Jitendra Sharma. I would also like to thank Dr. Jim Bugg for allowing the use of the plotting software.

I wish to extend my sincere thanks to Mr. Dale Pavier and Mr. Brennan Pokoyoway for their prompt support and guidance in building the experimental setup in the Hydrotechnical Laboratory throughout the laboratory program of my work.

Gratitude is also expressed to the Natural Sciences and Engineering Council of Canada (NSERC) for providing funds for the research through my supervisor's NSERC grant.

Last, but not the least, I owe a debt of gratitude to my wife, Bindu, for her patient love, unwavering support and encouragement, and for the care of our children that enabled me to complete my studies in a timely manner.

DEDICATION

This thesis is dedicated to my Grandfather, the Late Rukmagat Gautam.

TABLE OF CONTENTS

LIST OF TABLES

LIST OF FIGURES

LIST OF SYMBOLS

A	function of tailwater depth ratio
B	constant
b	vertical distance from bed to the point where $u = u_m/2$ and $du/dy < 0$ (jet half-width)
b_0	opening of sluice gate (jet thickness at origin)
b_{ma}	jet half-width, b at location of maximum scour depth at asymptotic state
b_r	value of y_s where $u_r = 0.75u_s$
c, c'	coefficients
D_{50}	bed material size for which 50% is finer by weight
D_i	bed material size for which i% is finer by weight
F_0	densimetric Froude number
F_r	flow Froude number
g	acceleration due to gravity
H	flume height
k_s	equivalent sand roughness
l	length of rigid apron downstream of sluice gate
L	length scale equal to the value of x (measured from the end of rigid apron) where $u_m/U_{0A} = 0.5$
L_e	surface eddy length measured from the sluice gate opening
m, m'	coefficients
M	forward flow momentum flux per unit width
M_0	momentum flux per unit width (measured at x = 100 mm)
Q	flow rate
R^2	correlation coefficient
R_a^2	adjusted correlation coefficient
R_e	jet Reynolds Number at origin (sluice gate)
s	submergence ratio, $s = y_t/b_0$
S	submergence factor, $S = (y_t - y_2)/y_2$
S_g	specific gravity of bed material

$S^{\#}$	value of S for a WJL jump with the same length scale L as the wall jet (Wu and Rajaratnam 1995)
S^{*}	critical value of S to distinguish between WJL and FJL jumps (Wu and Rajaratnam 1995)
t	time
u	longitudinal time-averaged velocity component at any point
u'	velocity fluctuation in x direction
u_m	maximum value of u at any x-section
u_{ms}	maximum value of u_s
u_{md}	value of u_m at $x = X_d$
u_r	time-averaged velocity for reverse flow
u_s	time-averaged surface velocity (for reverse flow)
u_{sm}	maximum velocity of u_s in streamwise direction
U_0	velocity of flow under the sluice gate (velocity of jet at its origin)
U_{0A}	maximum u velocity measured at the section at the end of rigid apron
$\sqrt{\overline{u'^2}}$	root-mean-square of velocity fluctuation in x-direction
$\sqrt{\overline{(u'^2)_m}}$	maximum value of root-mean-square of velocity fluctuation at any section
$\sqrt{\overline{(u'^2)_{mA}}}$	maximum value of root-mean-square of velocity fluctuation in the x-direction velocity at the end of rigid apron
v	time-averaged velocity in vertical direction
v'	velocity fluctuation in y-direction
$\sqrt{\overline{v'^2}}$	root-mean-square of velocity fluctuation in y-direction velocity
w	time-averaged velocity component in transverse direction
w'	velocity fluctuation in transverse direction
W	flume width
$\sqrt{\overline{w'^2}}$	root-mean-square velocity of velocity fluctuation in transverse direction
x_s	longitudinal distance from the jet efflux (gate opening)
x_d	distance of maximum mound height from edge of apron
x_{da}	distance of maximum mound height from edge of apron at asymptotic state

x_m	distance of maximum scour depth from edge of apron
x_{ma}	distance of maximum scour depth from edge of apron at asymptotic state
x_0	length of scour hole from the edge of apron
x_{0a}	length of scour hole from the edge of apron at asymptotic state
x_{0A}	distance measured from the edge of the rigid apron in streamwise direction
x_{0d}	distance of downstream toe of the mound measured from the edge of apron
x_{0da}	distance of downstream toe of the mound measured from the edge of apron at asymptotic state
X_0	distance from the sluice gate opening, where the second stage of velocity decay begins
X_d	value of x where decay of u_m starts to deviate from curvilinear to linear decay (measured from the edge of apron)
X_r	value of x_{0A} where u_m starts to increase/recover
y	vertical distance from channel boundary (rigid apron bed level)
y_m	water depth above top of mound
y_{ma}	water depth above top of maximum mound height at asymptotic state
y_0	water surface elevation just downstream of sluice gate (at x = 100 mm)
y_1	supercritical sequent depth
y_2	subcritical sequent depth
y_e	water surface elevation at $x = L_e$
y_s	distance below the free water surface in reverse flow region
y_{sb}	thickness of sand bed
y_t	tailwater depth
y'	vertical distance from the plane of u_m
z	coordinate in the transverse direction
δ	boundary layer thickness
δ_1	vertical distance, y from the boundary to where u = 0 for the jet
δ_2	vertical distance, y_s from the water surface (reverse flow) at which $u_r = 0$
δ_3	length scale for outer mixing layer
δ_A	the vertical distance from the plane of u_m to the plane where $u = u_m/2$
δ_{ma}	boundary layer thickness at maximum scour depth

δ_w	depression water depth measured at x = 100 mm
δ_{wa}	depression water depth measured at x = 100 mm at asymptotic state
Δ_m	maximum mound height
Δ_{ma}	maximum mound height at asymptotic state
$\Delta\rho$	difference between mass density of the particle and eroding fluid
ε_m	maximum scour depth
ε_{ma}	maximum scour depth at asymptotic state
ε_0	scour depth at the end of rigid apron
ε_{0a}	scour depth at the end of rigid apron at asymptotic state
η	non-dimensional ordinate (= y/b)
ν	kinematic viscosity of fluid
μ	dynamic viscosity of the eroding fluid (water)
ρ	density of the fluid
σ_g	geometric standard deviation of the bed material

CHAPTER 1: INTRODUCTION

1.1 Background

Flows over and through hydraulic structures such as spillways, weirs and sluices in canals often issue in the form of turbulent water jets. These jet flows create localized scour around such structures, which can be constructed on materials ranging from loose beds of sand and gravel to stiff clays to rocks. These jets are typically capable of producing sizable scour holes in loose sediment beds and fine-grained materials that may endanger the integrity of the structures and lead to their failure. For proper design of hydraulic structures against excessive scour, engineers must predict the rate of growth and maximum possible size of the scour hole (Breusers and Raudkivi 1991). They also may need to protect against scour. An understanding of the role of the various parameters that affect the scouring process and the jet behavior during scour is very important. In addition to the safety of hydraulic structures, understanding of the jet behavior during scour is also important because of the increasing use of jets in other applications. For example, recently-developed dredging vessels use high-velocity jets to mobilize accumulated sediment (Hogg et al. 1997).

A significant number of studies have been conducted by researchers on erosion by different types of jets. Among these studies, work on local scour due to a plane wall jet has been given much attention (see for example, Tarapore 1956; Rajaratnam 1981; Rajaratnam and MacDougall 1983; Balachandar and Kells 1997; Chatterjee and Ghosh 1980; Ali and Lim 1986; Aderibigbe and Rajaratnam 1998; Kells et al. 2001; Ahsan 2003). A classical plane wall jet is a rectangular jet of large aspect ratio that flows tangentially along a smooth boundary into a stationary or slowly moving fluid under very deep tailwater conditions (Rajaratnam 1965b, 1976). Flow under sluice gates, at outlets with rectangular cross-sections, and hydraulic jumps or submerged hydraulic

jumps in rectangular channels all behave similarly to plane wall jets (Rajaratnam 1965b; Wu and Rajaratnam 1995). The work on scour by these jets has been primarily experimental in nature due to complexities of the turbulent jet flows and their interaction with the sediment beds. These flows are unsteady and highly turbulent and the boundaries are continuously changing with time (Breusers and Raudkivi 1991).

One outstanding issue in the study of plane wall jet behavior on rough, rigid and mobile beds (which are also mostly rough) is the effect of submergence on the jet. It appears that the submergence has a significant effect on jet behavior (Ead and Rajaratnam 2002, 2004). Submergence has typically been defined in two different ways: (1) as a submergence ratio, $s = y_t/b_o$, where y_t is the tailwater depth and b_o is the thickness of the jet at its origin (the nozzle) (Ali and Lim 1986; Ahsan 2003; Ead and Rajaratnam 2004); or (2) as a submergence factor, $S = (y_t - y_2)/y_2$, where y_2 is the subcritical sequent depth for the flow through the nozzle and y_t is the depth of flow in the receiving channel, or tailwater depth (Rajaratnam 1965a; Wu and Rajaratnam 1995). For mobile beds, some have observed that the size of the scour hole produced by a jet under shallow submergence is less than that produced for a deep submergence (Kells et al. 2001; Mazurek and Ahsan 2005).

More information is available on the effect of submergence on the plane wall jet behavior for smooth rigid boundaries. It has been seen that the maximum velocity of the jet decays more quickly in a shallower flow (Johnston 1978; Ead and Rajaratnam 2002). Submergence effects on the velocity profiles, growth of the jet length scales, and the decay of the velocity along the streamwise direction of such jets have been investigated and reported in the literature (Long et al. 1990; Wu and Rajaratnam 1995; Ead and Rajaratnam 2002).

The focus of this study is to investigate the effects of submergence on plane wall jet behavior in a scour hole and to examine if there is a relationship between the scales for the jet flow in the scour hole and the scour hole size.

1.2 Objectives

The objectives of this thesis are as follows:

- To study the effects of submergence on the time development of the scour hole produced by a plane wall jet and its characteristic dimensions at asymptotic state;
- To study the effects of submergence on the jet behavior in the scour hole from the point of view of similarity in velocity profiles, growth of length scales, and the decay of the velocity scale along the streamwise direction;
- To compare the scales for the jet with the size of the scour hole; and
- To compare the length scales of the jet flow developed for rigid, rough boundaries by Ead and Rajaratnam (2004) to that found for the mobile boundary case.

1.3 Practical significance

In many cases, the diffusion of fluid jets into a large body of slower moving fluid, such as mixing of effluents from sewers into rivers, creates localized erosion near structures (Ali and Lim 1986). Diffusion of such jets is significantly influenced by the submergence (Wu and Rajaratnam 1995; Ead and Rajaratnam 2004). One can also observe varied submergence under circumstances such as the passage and receding of flood waters and emptying and refilling of channels (Faruque et al. 2007), and during the regular operation of flow through hydraulic structures (for example, sluice gates and spillways).

Moreover, much effort has been expended to identify the scaling parameters for identifying jet flow characteristics such as mean velocity, turbulence, and shear stresses for jet flows near rigid boundaries (Rajaratnam 1965a; Long et al. 1990; Wu and Rajaratnam 1995, Ead and Rajaratnam 2002 & 2004). Therefore, comparing jet behavior on rigid and mobile boundaries through a comparison of jet scales (a main objective of this study) is beneficial because, if they exhibit similar behavior, the more detailed and easy to run experiments on rigid beds can be used as a guide for analysing jet behavior for mobile bed conditions. In addition, if one can relate the features of the flow to the

scour hole size, only some simple measurements of the shape of the scour hole would provide a reasonable estimation of the flow field in the scour hole. Knowledge of the flow field in the scour hole is also important for the development of computer models for scour.

1.4 Organization of thesis

This thesis consists of five chapters. The second chapter includes a review of previous studies on jet behavior of plane wall jets on rigid boundaries. This is followed by a review of the studies of scour by such jets acting on a cohesionless erodible boundary. Chapter 3 describes the experimental setup, testing program, and tools and software that were used for data measurement and analysis. Chapter 4 gives the results of the experiments and detailed analysis of the experimental data. Finally, Chapter 5 gives the conclusions developed from the study and recommendations for further work.

CHAPTER 2: LITERATURE REVIEW

2.1 Introduction

In this chapter, since the plane turbulent wall jet is the scouring agent to be investigated in the present study, the general behavior and characteristics of these jets on smooth and rough rigid beds are discussed first. The effect of an offset of the jet from the wall is also briefly reviewed. Next, the general features of scour by plane wall jets are discussed, followed by a review of previous research where the jet flow within a scour hole was measured. Finally, some definitions of the asymptotic or equilibrium state of scour are given.

2.2 The plane turbulent wall jet

A "classical" plane wall jet is a rectangular jet of large aspect ratio that flows tangentially along a smooth rigid boundary into a stationary or slowly moving fluid under very deep tailwater conditions (Rajaratnam 1965b, 1976). However, exactly what constitutes "deep tailwater" is still a topic of research. The velocity profile of these jets and the nomenclature used to describe the jet are shown in Figure 2.1. Herein, b_0 is the thickness of the jet at its origin; U_0 is the mean velocity of the jet at its origin; x_s is the distance along the direction of flow from the jet origin; u_m is the maximum streamwise velocity measured at some distance x_s through the depth of flow; y is the normal distance from the boundary; δ is the thickness of the boundary layer growing on the wall; b is the normal distance from the boundary at which the velocity, u, is equal to half the maximum velocity, (i.e. $u_m/2$) and du/dy is negative; and δ_1 is the normal distance from the boundary at which the velocity, u, is equal to zero.

As discussed in Rajaratnam (1976), for the flow shown in Figure 2.1, as the jet leaves the nozzle, there is a pronounced velocity discontinuity between the jet and the surrounding fluid. The velocity discontinuity generates eddies, which result in mixing of the jet with the fluid lying above the jet. On the wall side of the jet, a boundary layer forms. While the jet initially is at a velocity U_0 throughout its thickness, the mixing layer on its side exposed to the surrounding fluid and boundary layer grow to decrease the jet velocity to less than U_0. The region where the jet velocity remains at U_0 is called the potential core and its length is typically $6.5b_0$ (Rajaratnam 1976). Beyond the end of the potential core region, the flow becomes fully developed (i.e. the shape of velocity profiles measured at any x_s distance are similar).

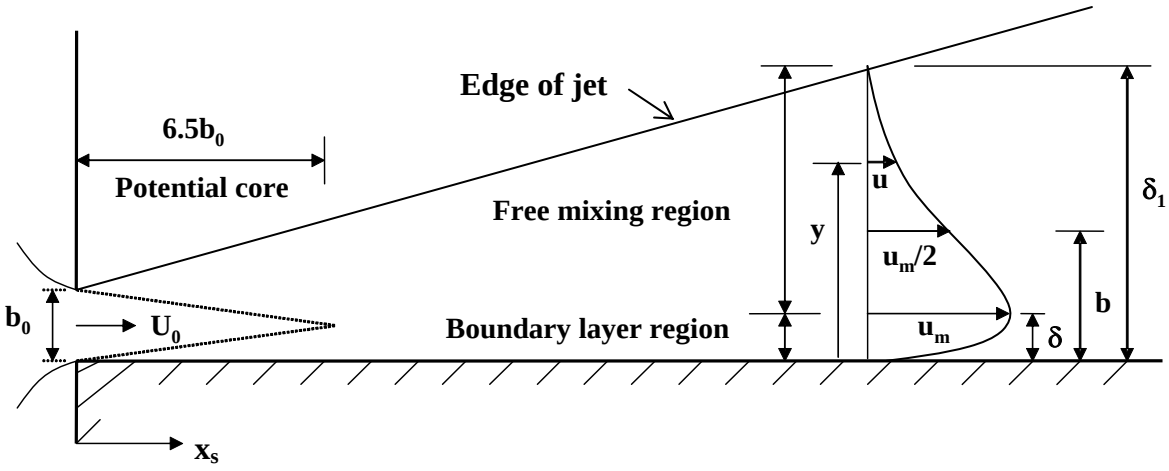

Figure 2.1 Definition sketch of a plane wall jet (adapted from Rajaratnam 1976)

At any typical section in the region of developed flow, the velocity, u, increases from zero at the wall to a maximum value of u_m at a distance where $y = \delta$, called the boundary layer region, and then decreases to zero again at a large distance from the bed ($y = \delta_1$), in the region called the free mixing region. For $x > 20b_0$, the velocity profiles in the jet have been shown to be geometrically similar (Rajaratnam 1976). Verhoff (1963) showed that these velocity profiles can be described by (Rajaratnam 1976):

$$\frac{u}{u_m} = 1.48\eta^{1/7}\left[1 - erf(0.68\eta)\right] \qquad [2.1]$$

where, $\eta = y/b$. Based on experimental data, Rajaratnam (1976) suggested the decay of u_m in the streamwise direction could be described by

$$\frac{u_m}{U_0} = \frac{3.50}{\sqrt{x_s / b_0}} \qquad [2.2]$$

for x_s/b_0 from 20 to approximately 100.

2.3 Plane wall jet behavior under varied submergence (for rigid beds)

In the case of a horizontal wall jet, such as the case of the flow issuing from underneath a rectangular sluice gate of high aspect ratio, the behavior of the flow is greatly affected by the depth in the downstream channel (the tailwater depth). Here, only rigid bed conditions are considered and it is assumed that the jet or flow under the sluice gate is supercritical. Under minimum tailwater conditions, a supercritical stream forms. With increasing tailwater depth, a free hydraulic jump will form until the tailwater depth equals the subcritical sequent depth for the flow under the gate. With further increases in tailwater depth, a submerged hydraulic jump forms. Eventually, when the flow through the opening becomes very deeply submerged, the flow will act like a classical wall jet (Wu and Rajaratnam 1995).

In the 1960's, Rajaratnam (1965b) conducted a number of experiments where he measured the flow in both free and submerged hydraulic jumps, from which he proposed that those flows were similar in behavior to classical wall jets. He found that, for the bottom portion of the flow below the roller in the hydraulic jump, the flow in the jump behaved similar to a classical wall jet, although for the jumps the jet is under an adverse pressure gradient (i.e. the pressure increases along the direction of flow because the depth increases). He observed for both the free and submerged jumps that the velocity distribution was similar and closely followed the curve for the classical wall jet to $\eta = 1$ (where, $\eta = y/b$); beyond for $\eta > 1$,) the velocity in the jumps decayed more quickly than the wall jet. The growth of the length scale, b, as defined above (i.e. jet half-width) was found to be:

$$\frac{b}{b_0} = m\left(\frac{x_s}{b_0}\right) + c \qquad [2.3]$$

where the coefficients m and c were considered a weak function of the supercritical Froude number, $F_r = U_0 \big/ \sqrt{gb_0}$, and thought to be essentially independent of the submergence factor, $S = (y_t - y_2)/y_2$, where, y_t is the tailwater depth downstream of the gate and y_2 is the subcritical sequent depth, as calculated using the Belanger equation

$$\frac{y_2}{y_1} = \frac{1}{2}(\sqrt{1+8F_r^2} - 1) \qquad [2.4]$$

where, y_1 is the supercritical sequent depth. Similarly, the decay of the maximum velocity u_m was found to be described by

$$\frac{u_m}{U_0} = c' - m'\left(\frac{x_s}{b_0}\right) \qquad [2.5]$$

in which the coefficients m' and c' were dependent on the submergence factor, S.

Later, Long et al. (1990) conducted an extensive experimental study of the flow characteristics of submerged hydraulic jumps on a smooth bed. They measured the velocity, turbulence intensity and Reynolds stresses at the centreline of submerged hydraulic jumps with a laser Doppler anemometer. Long et al. (1990) introduced a new length scale for the decay of velocity of these jets, L, which was defined as the distance from the inlet where $u_m/U_0 = 0.5$. This was used instead of the conventional length scale, b_0. It was found that if the length scale L was used to normalize the longitudinal distance, the decay of u_m/U_0 behaved similarly in free jumps, submerged jumps and wall jets for x_s/L up to about 1.5. For a value greater than 1.5, they found the decay of velocity in submerged hydraulic jumps occurred more quickly than for the wall jet. Moreover, they found that the length scale L was capable of bringing together onto one curve for the streamwise variation of the maximum turbulence shear stresses and intensities for submerged jumps under varied experimental conditions. They further proposed a relationship between length scale, L and the inlet Froude number, $F_r = U_0 \big/ \sqrt{gb_0}$ and submergence factor, $S = (y_t - y_2)/y_2$ that was proposed to be equally applicable to free jumps, submerged jumps, and wall jets:

$$\frac{L}{b_0} = \frac{49}{1 + 27 \times 10^{-0.5S} F_r^{-2}} \quad [2.6]$$

Wu and Rajaratnam (1995) continued this study of jets on smooth, rigid boundaries and compared the velocity distributions, decay of maximum velocity, and growth of the length scale of the jet, b, for jets under a full range of submergence (free jumps, submerged jumps and wall jets). They concluded that the submerged wall jet is the transition between the free jump and the wall jet and divided the flow behaviors into three regimes based on submergence: free-jump-like; wall-jet-like; and classical wall jet. Using L as the length scale (as defined by Long et al. 1990), they developed empirical relationships for the decay of maximum velocity, u_m in the longitudinal direction, which applied for submerged hydraulic jumps, and another for free jumps, given respectively as:

$$\frac{u_m}{U_0} = 0.50 / \sqrt{x_s / L} \quad [2.7]$$

$$\frac{u_m}{U_0} = 1.173 - 0.843 \frac{x_s}{L} + \left(\frac{x_s}{L} \right)^2 \quad [2.8]$$

For classical wall jet behavior, they found $L \approx 60 b_0$, which applied for $S > S^{\#}$, where $S^{\#}$ is a function of F_r and is given by the equation

$$S^{\#} = 15.28 F_r^{-0.81} - 1 \quad [2.9]$$

For free-jump-like behavior, they found L can be given by Equation 2.10, which applies for $S < S^*$, where S^* is also a function of F_r and is given by Equation 2.11.

$$L = \left(5.06 + 2.91 F_r\right) b_0 \quad [2.10]$$

$$S^* = 12 F_r^{-1.3} \quad [2.11]$$

For wall-jet-like behavior, S should be between S^* and $S^{\#}$. In this case, L is a function of F_r and S as given by

$$L = 7.26 F_r^{-0.64} (1 + S) b_0 \quad [2.12]$$

Ead and Rajaratnam (2002) performed a laboratory study of plane turbulent wall jets on smooth beds. They investigated the effects of tailwater depth on the jet

characteristics by measuring the time-averaged longitudinal velocity u within the jumps using a Prandtl tube. Experiments were conducted for different values of Froude number, F_r, and submergence ratio, y_t/b_0, ranging from 4-8 and 25-50, respectively. They found the velocity profiles taken at different streamwise locations were similar. They went back to analyzing the velocity decay based on b_0 as length scale. With this, they found the existence of two stages in the streamwise decay of mean maximum velocity. In the first stage, the decay was found to be independent of the submergence ratio and showed the same behavior as plane wall jets with large submergence. In this region, the streamwise decay of normalized velocity scale was given by:

$$\frac{u_m}{U_0} = \frac{4.00}{\sqrt{x_s / b_0}} \qquad [2.13]$$

The second stage of the velocity decay was found to start from a particular distance X_d from the gate and was characterized by a more rapid, linear decay rate that was a function of y_t/b_0 and which could be described by

$$\frac{u_m}{U_0} = A\left(\frac{x_s}{b_0}\right) + B \qquad [2.14]$$

where B = constant with a value equal to 0.82, and A and X_d are functions of the submergence ratio, y_t/b_0, and given by

$$A = 7 \times 10^{-5}\left(\frac{y_t}{b_0} - 100\right) \qquad [2.15]$$

$$\frac{X_d}{b_0} = 2.85\left(\frac{y_t}{b_0} - 2.00\right) \qquad [2.16]$$

Equations 2.15 and 2.16 suggest that, as submergence decreases, the velocity decay in the second stage occurs more quickly. There is also a decrease in the length of the first stage of decay. For the flow in the recirculating area above the jet, the eddy length, L_e, was found to be equal to the length of a free jump plus an extra length equal to four times the submergence factor, S.

Following these works, Liu et al. (2004) studied the turbulence characteristics of free hydraulic jumps of lower Froude numbers than previously studied by taking

detailed velocity measurements using a MicroADV. The streamwise variation of the maximum time-averaged streamwise velocity, u_m, for a range of the F_r = 2.0-2.5, the decay of velocity was observed similar to the plane wall jet curve when plotted using L as the scale for b_0 instead of the free jump curve suggested by Wu and Rajaratnam (1995), which was developed for $F_r > 4$. They developed a relationship between L/y_2 and F_r. They also showed that b/b_0 against x_s/b_0 was a linear relationship (up to x_s/b_0 of 20).

Ead and Rajaratnam (2004) studied the effects of boundary roughness and tailwater depth on the centreline profiles of streamwise velocity in the streamwise direction for plane turbulent wall jets on rough beds. In their experiments, two types of corrugated sheets with the same sinusoidal corrugations of wavelength of 65 mm, but different amplitudes (12.7 and 21.8 mm) were used to create a rough boundary. The roughness, k_s was taken equal to the amplitude of the sinusoidal corrugations (k_s = 12.7 and 21.8 mm). The ranges of F_r and y_t/b_0 for their experiments were 4-8 and 10.3-18.5, respectively. Ead and Rajaratnam (2004) found that the dimensionless velocity profiles at different sections similar as that for a classical wall jet; however, there was some difference in the value of the normalized boundary layer thickness, δ/b. A higher value of δ/b = 0.35 was found for wall jets with rough boundaries as compared to the corresponding value of δ/b = 0.16 for the classical wall jet.

With regard to the decay of the maximum velocity and the growth of the length scales of the jets, Ead and Rajaratnam (2004) observed two distinct stages, named the first and second stages. They further observed that the decay of the normalized maximum velocity u_m/U_0 at any section with the normalized longitudinal distance, x_s/L could be described by a single equation for smooth and rough boundaries (see Figure 2.2) in the first stage of velocity decay. The decay appeared to be independent of submergence ratio and boundary roughness. However, for the second stage, the decay of velocity was found to be more rapid than in the first stage, as shown in Figure 2.2, and it was a function of both submergence and roughness. The distance, X_0 from the jet origin, where the second stage of velocity decay begins was found to be a function of submergence ratio, y_t/b_0, with

$$\frac{X_0}{b_0} = 2.85\left(\frac{y_t}{b_0} - 2.0\right) \qquad [2.17]$$

With regard to the growth of the boundary layer and jet half-width, Ead and Rajaratnam (2004) found that the growth of these features was suddenly increased at the point corresponding to the second stage of velocity decay. Further, they also observed a significant increase in the growth of half-width, b with the increase of relative boundary roughness as compared with that for a smooth boundary. In contrast to these findings, in a similar type of study (velocity measurement for a flow downstream of a sluice gate arrangement by laser Doppler anemometer (LDA)), Tachie et al. (2004) found the spread rate of the jet half-width, b, was nearly independent of bed roughness. However, as in Ead and Rajaratnam (2004), a faster decay of velocity scale, u_m on rough beds than those on smooth beds has also been reported by Dey and Sarkar (2006b). They have also reported that the growth of the jet half-width, b, on smooth and rough beds were faster than in classical wall jet.

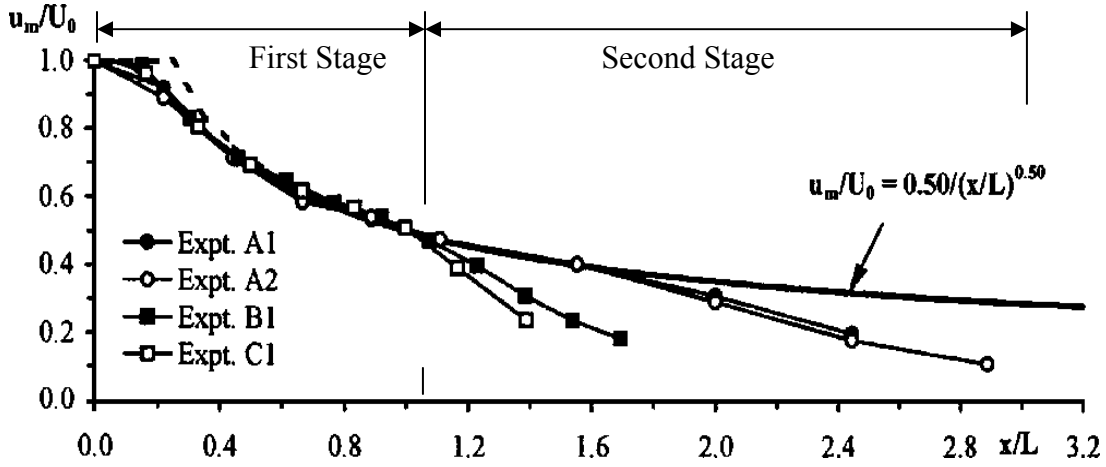

Figure 2.2 Variation of the maximum velocity with distance (adapted from Ead and Rajaratnam 2004)

In a recent experimental study of deeply submerged flow (y_t/b_0 = 20, and F_r = 3-7.2) issuing from a slot on smooth and rough boundaries (k_s/b_0 = 0.000, 0.212, and 0.379), Shabayek (2007a) attempted to identify the type of submerged flow (i.e.

either as submerged jumps or wall jets) by analyzing the velocity data measured by a Prandtl tube. Shabayek (2007a) reported values of the normalized boundary layer thickness, δ/b, of 0.30, and 0.40 for boundaries with k_s/b_0 of 0.212 and 0.379, respectively; these are much higher than the value for classical wall jets ($\delta/b = 0.16$). Other interesting observations include that, for the flow fields in the recirculating region above the jet, the occurrence of the maximum velocity was found close to the surface, and the eddy length, L_e was found to be significantly influenced by the boundary roughness. For the constant value of F_r and y_t/b_0, a decrease in eddy lengths was observed for any increase in the value of normalized boundary roughness. A similar observation of the effects of boundary roughness on eddy length is also reported in a recent study of hydraulic jumps on rough beds by Carollo et al. (2007) and Shabayek (2007b).

2.4 Influence of an offset of the jet from the wall in jet flow behavior

As mentioned previously, this study primarily focuses on the investigation of scour development and jet flow behaviour inside a scour hole produced by a plane turbulent wall jet. The general behavior and the characteristics of such jets flowing over a rigid boundary have been discussed in the previous section. Unlike for the case of rigid bed boundary, for mobile bed boundary case, the planar jet, which is parallel to and flush with the flat bed initially does not stay parallel to and flush with bed due to the formation of scour hole and mound in the course of scouring. In other words, the jet needs to pass through a negative step (the scour hole) and then a positive step (mound of material deposited at the end of the scour hole). Therefore, it is believed that the development of such steps could affect the jet (initially wall jet) behavior; thus, it makes it somewhat different from those observed in the case of rigid bed boundary. Further, as the mound (a positive step) is located relatively far from the jet efflux, its effects in jet diffusion are likely insignificant compared with the negative step, which is located very close to the jet efflux.

There have been a few experimental studies pertaining to the effects of a negative step on the jet flow behavior of a horizontal rectangular jet issuing through a

slot reported in the literature (Matthews and Whitelaw 1973; Coates 1976; Johnston 1978; Johnston 1990). Johnston (1978) reported that the presence of an offset (even a small value) near to the jet efflux significantly influences the diffusion of the jet. He suggested that, due to the presence of the offset, a clockwise eddy (separation bubble) with low pressure is developed between the bottom of the jet efflux and the bed thereby resulting in the jet being deflected towards the solid boundary. He further reported that the length of separation bubble or eddy below the jet is influenced by the offset distance; he found the jet behavior after the reattachment point similar to a re-attached wall jet. Matthews and Whitelaw (1973) found the change in jet-like nature of the flow near the slot region due to the presence of backward-facing step. Coates (1976) and Johnston (1990) investigated the flow fields inside a scour hole produced by a jet under shallow tailwater conditions and observed a significant influence of the offset distance in the flow regimes to be developed inside the scour hole. They have reported three flow regimes, called the bed-jet, surface-jet, and bed-surface flow regimes depending upon the offset distance.

There also exists a large number of experimental studies that consider the effects of negative steps on the behaviour of hydraulic jump. In such a study, Sharp (1974) observed the formation of different regimes of jumps depending upon the tailwater and the height of the negative step. A significant increase in the stability of the hydraulic jump with the presence of a negative step was also reported in some studies on hydraulic jumps in negative step (Moore and Morgan 1957; Hager and Bretz 1986). Armenio et al. (2000) found a large fluctuation in the pressure at the bottom of the jumps due to the presence of the negative step.

2.5 Plane wall jet behavior under varied submergence for erodible beds

2.5.1 General features

A good number of studies on local scour by plane wall jets on mobile beds, mostly in clean coarse sands, under varied submergence have been reported in the literature (for example, Laursen 1952; Tarapore 1956; Chatterjee and Ghosh 1980; Rajaratnam 1981; Rajaratnam and Macdougall 1983; Ali and Lim 1986; Balachandar

and Kells 1997; Aderibigbe and Rajaratnam 1998; Balachandar et al. 2000; Kells et al. 2001; Ahsan 2003; Mazurek and Ahsan 2005). It is known that the scour profiles and flow regimes are strongly affected by the tailwater depth (Coates 1976; Johnston 1978; Ali and Lim 1986; Johnston 1990; Balachandar et al. 2000; Kells et al. 2001; Ahsan 2003; Mazurek and Ahsan 2005). Johnston (1990) suggested that there was three regimes of flow for the jet within a scour hole with varied submergence, the "bed-jet" regime, the "surface-jet" regime, and "bed-surface" regime. A method to predict these regimes was developed.

At higher submergences, the bed-jet regime tends to form, where the jet always attaches itself to the bed (Rajaratnam 1981; Johnston 1990; Ahsan 2003). The scour hole produced by a bed-jet process has a mound that forms downstream of the scour hole. The scour hole grows in a regular manner up to some time, beyond which the scour slows to a rate for which the scour hole, for all practical purposes, can be said to have reached its largest size, called the asymptotic or equilibrium state (Tarapore 1956; Rajaratnam 1981; Mazurek and Ahsan 2005). The main dimensions of a scour hole grow approximately linearly with the logarithm of time for most of the scouring process. It was also seen that the shape of the scour hole profiles are similar throughout the development of the scour hole (Laursen 1952; Tarapore 1956; Rajaratnam 1981; Ali and Lim 1986; Dey and Sarkar 2006a).

At very shallow submergences, the jet is always attached to the free surface, called the "surface-jet" regime (Johnston 1990). Since the jet is attached to the free surface and not to the bed, the scour hole and mound tend to be longer and shallower than for the deep submergence case. A regular growth of the scour hole and asymptotic state have been observed for this regime (Ahsan 2003).

For intermediate submergences, the jet first attaches to either the free surface or to the bed and then begins to 'flick' intermittently from one boundary to the other at some point in the scouring process. This is the "bed-surface" regime. For this regime, an entirely different and complex form of scour hole development occurs, with an

intermittent scouring action by the jet (Johnston 1990; Balachandar and Kells 1997; Balachandar et al. 2000; Kells et al. 2001; Ahsan 2003; Mazurek and Ahsan 2005; Faruque et al. 2007). While the jet is attached to the bed, the scour hole grows in size; however, when the jet is attached to the free surface, a vortex created by this flow near the bed tends to fill in the scour hole. This process results in a very unusual development of the scour hole with many interesting features such as formation of secondary mound and slumping back of mound materials to the scour hole. This jet oscillation between the boundaries, or "jet flicking", has been observed both early on experiments (within a few seconds) and very late in experiments (after more than 40 hours) (Mazurek and Ahsan 2005). In a preliminary experiments for the work describe herein, jet flicking was not observed until 33 hours into the experiment (with $F_0 = 6.5$ and $s = 10$). Balachandar and Kells (1997) found these scour holes did not reach asymptotic state even after 144 hours and asymptotic state in this regime has not been observed. Similarity of the scour hole profiles throughout the development of scour hole has also not been observed.

2.5.2 Parameters influencing scour in cohesionless materials

Many different parameters have been thought to affect scour below a sluice gate (by a plane wall jet) in cohesionless materials. These include: the velocity of flow under the gate (the jet origin), U_0; the gate opening or thickness of the jet at its origin, b_0; the density of eroding fluid, ρ; the difference in density between the bed material and the eroding fluid, $\Delta\rho$; the viscosity of the eroding fluid, μ; the acceleration due to gravity, g; the mean grain diameter of the sediment, D_{50}; the grain size distribution; the tailwater depth, y_t; the time from the beginning of scour, t; the length of the rigid apron, l (Dey and Sarkar 2006a); and the channel width, W (Faruque et al. 2007). These parameters are usually grouped into dimensionless terms using dimensional analysis. Note that herein the discussion is restricted to the cases where jet-flicking was not observed.

From dimensional considerations, Rajaratnam (1981) suggested that the maximum scour depth, ε_m, at asymptotic state (or any characteristic dimension of the scour) developed by a plane wall jet under deep tailwater conditions could be written as

$$\varepsilon_m = f\{U_0, b_0, \rho, g\Delta\rho, \mu, D_{50}\} \quad [2.18]$$

which by dimensional analysis reduces to:

$$\frac{\varepsilon_m}{b_0} = f\left[F_0 = \frac{U_0}{\sqrt{g\frac{\Delta\rho}{\rho}D_{50}}}, R_e = \frac{\rho U_0 b_0}{\mu}, \frac{b_0}{D_{50}}\right] \quad [2.19]$$

The first term, $F_0 = U_0 / \sqrt{g\,\Delta\rho/\rho\, D_{50}}$ is called the densimetric Froude number. It represents the ratio of the shear stresses on the bed to the buoyant weight of the particle (Aderibigbe 1996), or the tractive forces to the resisting forces for erosion of the soil particle (Ahsan 2003). The second term R_e is the jet Reynolds number. The third term, b_0/D_{50} accounts for the effects of relative bed roughness. Rajaratnam (1976) suggested that the effect of Reynolds number on the jet can be neglected if it is greater than a few thousand. Similarly, he suggested that the effect of relative roughness, b_0/D_{50} can also be neglected unless it is very small (Rajaratnam and Berry 1977). This was followed by Aderibigbe and Rajaratnam (1998), whose analysis of their own results and those from previous researchers appeared to show no significant effect of relative roughness on scour. However, this is in contrast with more recent work of Dey and Sarkar (2006a). Johnston (1990) had also considered the roughness important. Most past studies where scour by wall jets was analyzed have followed the approach of Rajaratnam (1981).

Ali and Lim (1986) suggested the need to incorporate the effects of submergence on scour depth development for shallow tailwater with $y_t/b_0 < 16$. They have also considered the roughness effects on scour development. To account for submergence in analyzing scour, Ahsan (2003) included an additional parameter, y_t/b_0, to Equation 2.19, which represented the influence of tailwater depth at asymptotic state. Similarly, Dey and Sarkar (2006a) suggested three additional parameters, l/b_0, y_t/b_0, and D_{50}/b_0 to Equation 2.19, which represent the influence of length of rigid apron, tailwater depth, and the boundary roughness, respectively, on the value of the maximum scour depth at the asymptotic state. According to Faruque et al. (2007), a non-dimensional parameter

for the channel width, W/b_0, also needs to be considered. In an experimental study on scour development in shallow tailwater due to an offset jet, neglecting the effects of surface tension, viscosity, and buoyancy, and assuming that the scouring reached an asymptotic condition, Johnston (1990) suggested four non-dimensional parameters, namely the densimetric Froude number, slot offset, submergence, and relative roughness to represent any flow fields inside the scour hole.

Considering the findings of aforementioned researchers, it can be concluded that the flow fields and the development of scour at asymptotic state due to a plane wall jet (at no offset) is influenced by the following non-dimensional parameters: the densimetric Froude number, F_0; submergence ratio, y_t/b_0; relative roughness, D_{50}/b_0; length of rigid apron, l/b_0; and width of channel, W/b_0.

2.5.3 Assessment of asymptotic scour depth and time to asymptotic state

In considering the time development of local scour due to jets, Rouse (1940) proposed a hypothesis of infinite scour (the scour hole will keep growing indefinitely). However, later Laursen (1952) challenged Rouse's hypotheses stating the existence of a limit to the extent of scour hole and that this limit was approached asymptotically. However, it is pertinent to note here that Laursen (1952) neither described the time required to attain such an asymptotic state nor the criteria to identify the occurrence of such a state.

Later, through an experimental study on scour below a submerged sluice gate, Tarapore (1956) proved Laursen's hypothesis. He also proposed a method to identify the occurrence of the asymptotic state. For that, he plotted the scour hole length against the logarithm of time of scouring and reported the existence of three stages in the scouring process. In the first stage of scouring, Tarapore (1956) observed an approximately linear (with constant positive slope) growth of the scour hole length with the logarithm of time of scouring and named it the "logarithmic law". However, after a certain time of scouring, he noticed the departure of such a plotted line from its constant positive slope and observed a slower growth rate of the scour hole length. He considered this a

transition phase between the first and the third phase that was observed for a relatively short period. After a very long period of scouring, he noticed that the deviated line was following a horizontal asymptote and the growth rate of the scour hole was much slower than in previous two stages. He referred to this stage as a beginning of the asymptotic state and used it as the criteria to determine the limiting size or the asymptotic state of the scouring process. Figure 2.3 shows the schematic illustration of the three distinct stages of the scouring process noticed by Tarapore (1956).

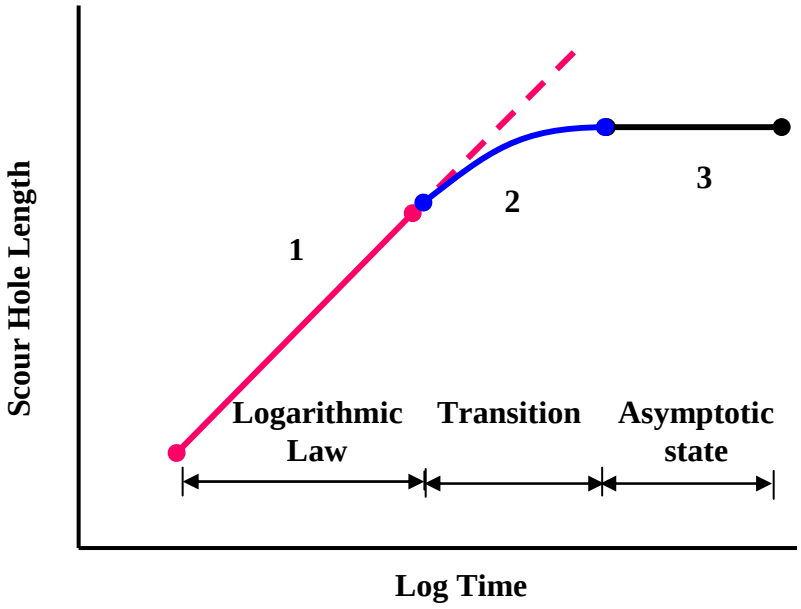

Figure 2.3 Schematic illustration of the three stages of the scouring process noticed in the study of Tarapore (1956)

Tarapore (1956) also reported that time to asymptotic state appeared to depend on the size of sediment and the jet exit velocity. A bigger sediment and higher inlet velocity resulted in a scour hole that reached asymptotic state earlier. In his experiment with finer size sediment (D_{50} = 0.7 mm), occurrence of asymptotic state was not noticed even after seven weeks of scouring. However, an asymptotic state was observed for bigger sediment (D_{50} = 4.4 mm) after six days.

Several researchers have carried out studies on scour by plane wall jets, where the scour hole at asymptotic state was supposedly measured (Chatterjee and Ghosh

1980; Rajaratnam 1981; Rajaratnam and MacDougall 1983; Aderibigbe and Rajaratnam 1998; Ahsan and Mazurek 2005; Sarkar and Dey 2007). Most of those studies have followed the criteria almost the same as that developed by Tarapore (1956), but have inserted some additional parameters/criteria to define the asymptotic state. Table 2.1 summarizes the test conditions, criteria to define the asymptotic state, and the typical time to reach the asymptotic state of these studies. The lower value of time to asymptotic state is observed for lower values of F_0, whereas the effect of y_t/b_0 on the time to asymptotic state is unclear (Mazurek and Ahsan 2005).

Considering the observations of the previous studies, it appears that, except for the experiments where one can expect the unstable jet behavior or jet flicking phenomena, there exists an asymptotic state for the scour hole. However, how long it takes to occur and how it is affected by various experimental parameters is still seemingly a topic of research.

Table 2.1 Summarized key information on the test conditions, criteria used to assess the asymptotic state, and the typical time to reach the asymptotic state

Studies	**Major test conditions**			**Criteria used**	**Time to asymptotic state (hrs.)**
	D_{50} (mm)	**F_0**	**y_t/b_0**		
Chatterjee and Ghosh (1980)	0.76 & 4.30	3.5 – 18.0	6 – 14	No grain movement at location of maximum scour	Not specified
Kurniawan et al. (2004)	2.00	4.7 – 4.9	2.2 – 4.4	No sediment transport throughout the measuring section	91.8 – 117.9
Rajaratnam (1981)	1.20 & 2.38	4.4 – 12.9	15 - 107	Almost constant value of maximum scour depth and maximum mound height	8 - 64
Rajaratnam and MacDougall (1983)	1.00 & 2.38	4.3 – 18.3	1	Scour profile independent with time	6 - 41
Aderibigbe and Rajaratnam (1998)	6.75	1.8 – 10.7	12 - 60	Insignificant sediment transport over mound	5 - 52
Mazurek and Ahsan (2005)	2.08	1.4 – 6.2	1 - 20	Deviation from logarithmic law and insignificant change in maximum scour depth for a period of 6 hours (largest change in the overall scour depth over that period was 0.4 %)	0.9 – 41.2
Dey and Sarkar (2006a)	1.86	5.7 – 8.3	6.6 – 14	Not specified	after 12
Sarkar and Dey (2007)	0.8, 1.86, & 3.0	2.3 – 2.9	17 - 17	Not specified	10 - 12

2.5.4 Jet behavior within the scour hole

In order to understand jet behavior during scour, a number of studies have been conducted to measure the velocity profiles within a scour hole. This has typically been done by either making a fixed model that simulates the shape of the scour hole or by taking measurements after the scour hole has reached the asymptotic state. This has been done for both deep and shallow submergences, but not for the jet-flicking regime (for example, Chatterjee and Ghosh 1980; Nik Hassan and Narayan 1985; Ali and Lim 1986; Kurniawan et al. 2004; Dey and Sarkar 2006b; Sarkar and Dey 2007).

Using a Pitot tube, Chatterjee and Ghosh (1980) measured velocity profiles over a rigid horizontal apron of length equal to 600 mm as well as inside the scour hole of erodible beds of sand and gravel (D_{50} = 0.76 mm and 4.3 mm respectively) for y_t/b_0 = 6 – 14. In their experiments, jets were produced by flow issuing below a sharp-edged sluice gate of opening b_0 equal to 20, 30, 40, and 50 mm into a rectangular channel 600 mm wide. The velocities inside the scour hole were measured in the centreplane of the flume along the x-direction once the scour hole profiles reached asymptotic state. Based on observations of the characteristics of jet diffusion inside the scour hole, they considered the flow situation inside the scour hole to be the case of a plane wall jet. The rate of growth of the boundary layer on the bed, δ, was greater for the gravel bed than for the sand. They concluded that diffusion of the jet was influenced by the size of the bed material. The boundary layer growth also appeared to be influenced by the tailwater depth. However, this does not show up in their equations for boundary layer growth. For the velocity decay, they proposed two separate equations, one for the sand bed (see Equation 2.20) and other for the gravel bed (see Equation 2.21) to predict the streamwise variation of u_m inside the scour hole at equilibrium state, given by

$$\frac{u_m}{U_0} = 0.980\left(\frac{l}{b_0}\right)^{2.28}\left(\frac{x}{b_0}\right)^{-2.47} \qquad \text{(for sand bed)} \qquad [2.20]$$

$$\frac{u_m}{U_0} = 3.548\left(\frac{l}{b_0}\right)^{1.51}\left(\frac{x}{b_0}\right)^{-1.695} \qquad \text{(for gravel bed)} \qquad [2.21]$$

where, l is the length of the rigid apron. Considering the velocity decay in these equations, it is important to note here that even though some of the experiments by

Chatterjee and Ghosh (1980) include relatively shallow submergence (with the minimum y_t/b_0=6), the effects of tailwater depth in the diffusion of jet in streamwise and vertical direction have not been noticed.

In an experimental study almost similar to Chatterjee and Ghosh (1980) but with higher submergence ratio (s=20–50), Nik Hassan and Narayanan (1985) measured mean velocity profiles using a Pitot-static tube for the flow over a rigid flat apron as well as in a rigid model simulating the shape of the scour hole made by "freezing" the erodible sand bed. Experiments were carried out in a rectangular flume 915 mm wide with a sluice gate arrangement with a b_0 equal to 5, 10, or 15 mm. Three sizes of uniform sand of D_{50} equal to 1.65, 0.8, or 0.5 mm were used to make up the sand bed. After analyzing the mean velocity data measured in the streamwise as well as in the vertical direction of flat rigid apron and inside the rigid scour hole, Nik Hassan and Narayanan (1985) suggested that limited tailwater and the development of scour hole could influence the velocity distribution for the flow over a rigid apron as well as in scour hole. Furthermore, using the maximum time-averaged velocity, u_m and the vertical distance of separation, δ_3 from the plane of u_m to the plane where the velocity is $u_m/2$ as velocity and length scales respectively, they reported the existence of similarity in the velocity profiles of the outer mixing layer for the whole range of experiments. They also suggested a single empirical equation to describe such velocity profiles as

$$\frac{u}{u_m} = e^{-0.693\left(\frac{y'}{\delta_3}\right)^{1.5}} \qquad [2.22]$$

where, y' is the vertical distance measured upward from the plane of u_m. However, unlike in the outer mixing layer, the similarity of time-averaged longitudinal velocity profile was not observed in the case of inner (shear) layer for the whole range of test runs. Further, using the maximum mean velocity at the end of the rigid apron, u_{mA}, and the vertical distance of separation from the plane of u_{mA} to the plane where the velocity is $0.5u_{mA}$, δ_A, as velocity and length scales respectively, they also suggested empirical relationships (Equation 2.23 and 2.24) for the longitudinal decay of the maximum mean velocity, u_m in the scour hole.

$$\frac{u_m}{u_{mA}} = e^{-0.138\left(\frac{x_{0A}}{\delta_A}\right)^{1.055}} \qquad \text{for } 0 < \frac{x_{0A}}{\delta_A} < 4.28 \qquad [2.23]$$

$$\frac{u_m}{u_{mA}} = 0.61\left(\frac{x_{0A}}{\delta_A}\right)^{-0.1} \qquad \text{for } \frac{x_{0A}}{\delta_A} \geq 4.28 \qquad [2.24]$$

where, x_{0A} is the horizontal distance measured from the edge of the rigid apron.

Ali and Lim (1986) also performed an extensive investigation on the localized scour caused by two-dimensional wall jets in shallow submergence (s=1-5) by measuring velocity distributions inside the scour hole by making fixed models of scour profiles and using a stream flow miniature meter. Analysing the experimental results, they reported that the behavior of the jets is significantly influenced by the tailwater depth and there exists similarity in the velocity profiles for sections up to that of maximum scour depth, irrespective of the period of scouring. The vertical angle made by a line joining the loci of local maximum horizontal velocity was observed to be significantly influenced by the tailwater depth. A higher value of this vertical angle was observed for lower tailwater depth. This was resulted a deeper scour hole.

In an experimental study to investigate the flow pattern inside a scour hole (at asymptotic state) produced by a submerged planar (initially) jet (created by a sharp-edged sluice gate) passing over an erodible boundary made of a uniformly graded sand of D_{50} = 2 mm, Kurniawan et al. (2004) carried out the measurement of three components of instantaneous velocity inside a scour hole (with the bed made rigid by spraying a special glue on the sand bed after the scour hole reached asymptotic state) using Nortek's ADV with a side-looking probe. An Acoustic Doppler Velocity Profiler (ADVP) was also used to measure the vertical profiles of the three-dimensional instantaneous velocities. Experiments were run for a relatively low value of densimetric Froude number ($F_0 \approx 4.7$) and two submergence ratios (s = 2.4 & 4.4). Two experiments were run without a rigid apron, while in one experiment a rigid apron of 0.10 m length was provided downstream of the sluice gate. From the results of the velocity measurements, they observed the decay of local maximum velocity, u_m, for all the

experiments with a free-jet like velocity distribution and with weak return flows at the top and the bottom. However, interestingly for the experiments run for the same value of F_0 and s, they clearly observed two distinct types of flow fields inside the scour hole depending on whether the jet leaves the sluice gate directly or is followed by a rigid apron. For the flow in the absence of an apron, the issuing jet was inclined and impinged somewhere on the downstream face in the scour hole (a flow field similar to that of "bed-jet" flow regime as observed in Johnston (1990)), while for the flow with an apron the jet mainstream remained outside the scour hole and attached closer to the surface (a flow field similar to that of "surface-jet" flow regime as observed in Johnston (1990)). For the second case, the scour hole was observed shallower as compared the scour hole in the first case. Their study reveals that the flow field inside the scour hole could be influenced by the length of the protective apron.

Hill and Younkin (2006) carried out an experimental study to measure the flow fields within a scour hole produced by a plane turbulent jet in an erodible bed made of glass beads instead of natural sediments under deep tailwater conditions. For that, they developed a number of roughened fixed-bed models simulating the scour hole bed-form geometry (initial flat-bed to the ultimate size) and carried out extensive velocity measurement using Particle Image Velocimetry. After analyzing the velocity data, they reported the presence of a strong clockwise recirculation zone (clockwise eddy) between the bottom of jet and the bed of the scoured boundary in the region of the upstream face of the scour hole. Further, they also found the attachment of the jet on the downstream face of the scour hole; the velocity fields were observed to be similar to the case of a re-attached wall jet.

In an experimental study, Dey and Sarkar (2006b) measured profiles of the time-averaged velocity components, turbulence intensity components and Reynolds stress at different streamwise locations on a rigid apron as well as in the scour hole (produced by a submerged two-dimensional jet) using an acoustic Doppler velocimeter. For the velocity measurements inside the scour hole, they made a number of fixed bed models simulating the geometry of intermediate and equilibrium scour hole profiles. Using the

velocity data, they plotted Reynolds stress profiles (vertical) within the scour hole in order to determine the variation of bed shear stress on scoured beds. With the use of the calculated bed shear stress along the scoured bed, they suggested a relationship between shear stress and the scour hole size and shape. Furthermore, they proposed a method (based on shear stress variation along the scour hole) for the computation of the equilibrium scour profiles and the time-variation of maximum scour depth. The results obtained from their proposed computation method for scour hole geometry and the experimental data were found to be reasonably close.

Recently, in an experimental study on the effects of upward seepage velocity on the characteristics dimensions of the scour hole and the resulting flow fields due to horizontal submerged jets within the scour hole, Sarkar and Dey (2007) carried out extensive velocity measurements inside the scour hole at the asymptotic state (observed after 12 hours) using SonTek's 3-D down-looking MicroADV probe at sampling times of 3 to 10 minutes (decided based upon the expected turbulence intensity). For the velocity measurement in the zone located 5 cm below the free surface, where the measurements using a down-looking ADV probe were not possible, they caged the ADV probe in a water-filled tube with its lower surface made of Mylar film transparent to the acoustic waves but retaining the water. Considering the size of the scour hole and the flow fields for different seepage velocities, they suggested that any increase in seepage velocity results in a decrease of all the characteristics lengths of the scour hole, whereas the decay rate of the submerged jet was observed to increase for any increase in the seepage velocities.

In conclusion, it is pertinent to note here that none of above studies on erodible boundaries have reported the effects of submergence on the velocity profiles, decay of maximum mean velocity, u_m, variation of turbulence intensities and the growth of length scales, b and δ as the jets passes through the scour hole.

CHAPTER 3: EXPERIMENTAL SETUP AND EXPERIMENTS

3.1 Introduction

In order to achieve the research objectives, an extensive experimental study was conducted in the Hydraulics Lab of the University of Saskatchewan. In the study, a scour hole was allowed to form in a sand bed downstream of a sluice gate (to produce scour by a plane turbulent wall jet), under several experimental conditions, until the scour hole reached asymptotic state. During the development of the scour hole, the characteristic dimensions of the scour profiles were measured to assess whether an asymptotic state occurred. Once the scour hole reached asymptotic state, extensive measurements of the velocity profiles in the centreline vertical plane of the channel in the streamwise direction were carried out using a 16-MHz Microacoustic Doppler Velocimeter (16-MHz MicroADV). This chapter gives the details of the experimental setup, testing program, and measurements.

3.2 Experimental setup

The experiments were performed in a rectangular glass-walled flume that was 0.5 m wide, 0.5 m deep, and 4.9 m long. Figure 3.1 shows a schematic of the experimental setup. The jet issued from under a sluice gate, which had a curved guiding vane attached to the back of the gate to produce a jet of thickness equal to the gate opening, b_0. There was a short (50 mm long), smooth, rigid apron below the gate followed by a sediment bed. Water was pumped from a reservoir beneath the flume through a magnetic flow meter (resolution of 0.01 L/s) that was installed in the supply line and then into the flume head tank. The overflow of the flume was returned to the reservoir so that the flow in the experiments was recirculated. One gate opening of 16 mm was used for all of the experiments. The MicroADV was mounted on a computer-controlled motorized traverse that moved in the vertical direction only. The positioning

of the ADV in the transverse direction was controlled using a manually operated traverse, with the position determined through the use of a measuring tape (resolution of 1 mm). Along the direction of flow, the positioning of the traverse system was determined using a measuring tape attached to the top of the flume (resolution of 2 mm).

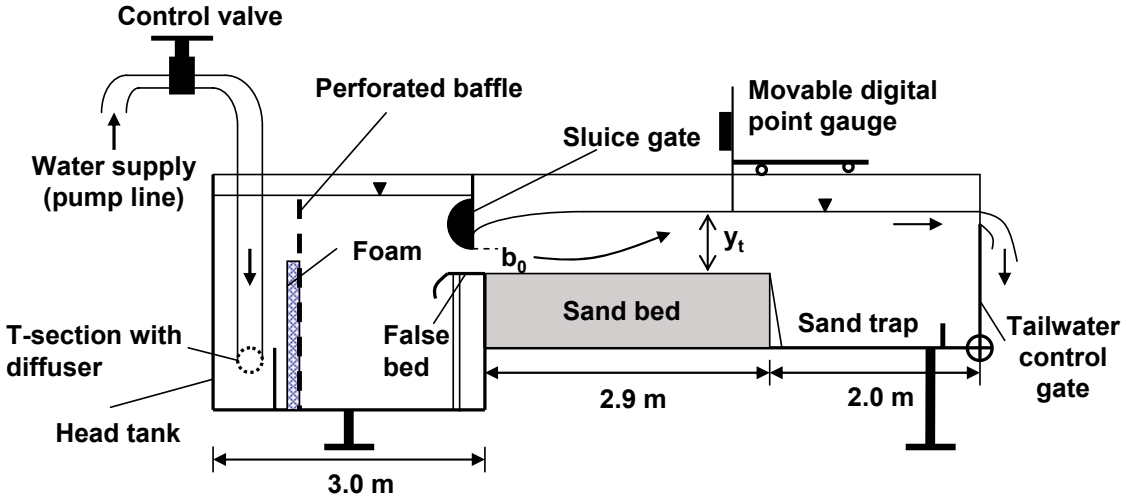

Figure 3.1 Schematic of experimental setup

Within the flume, to create the sand bed, a sediment recess of 2900 mm length and the same width as the flume was constructed downstream of the apron. A height adjustable false bed made of polyvinyl chloride (PVC) plastic was built within the head tank so that the depth of the sediment recess, y_{sb}, could be adjusted to allow for varied sand bed thickness in the experiments. Two depths of sediment bed were used and these were 200 and 260 mm. The required bed depth was estimated using the predicted maximum scour depth from Aderibigbe and Rajaratnam (1998). This was done in order to maximize the available tailwater. For a given sand bed thickness, the tailwater depth was chosen so that the total depth due to the sand bed and the tailwater depth would not exceed the maximum available flume height (500 mm).

Two clean, uniform sands were used in the experiments (a Sil 10/20 and a Sil 9), which were both obtained from Sil Silica Industrial Minerals of Edmonton, Alberta, Canada. The specific gravity, S_g, of the sands was 2.65 and this value was taken from

the manufacturer. A sieve analysis was carried out to determine the grain size distribution of these sands, the results of which are shown in Figure 3.2. It was found that the Sil 9 sand had an average grain size D_{50} = 2.20 mm and a geometric standard deviation, $\sigma_g = \sqrt{D_{84}/D_{16}}$, of 1.33, where D_i is bed material size for which i% is finer by weight. The Sil 10/20 sand had a D_{50} = 1.33 mm with a $\sigma_g = 1.20$. Since the σ_g for each sand was less than 1.35, the sands can be considered uniform (Breussers and Raudkivi 1991).

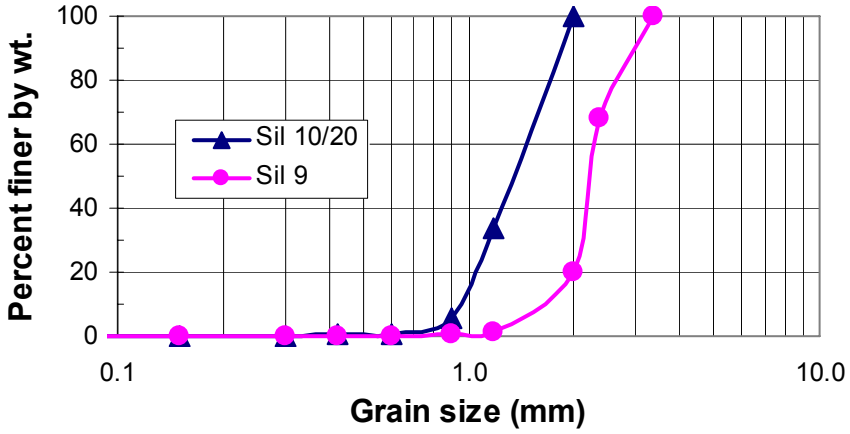

Figure 3.2 Grain size distribution of sands used in experiments

At the start of each test, the sand bed was levelled to be flush with the top of the rigid apron. It was then covered by a 1.5 mm thick aluminium sheet of 1700 mm length and 498 mm width so that any effects due to varied flow rate on the scour hole at the start of the test could be minimized. Next, the digital point gauge used for measuring the vertical dimensions of the scour hole was set to zero with respect to the top level of the sand bed. After this, the desired flow rate was set using the magnetic flow meter and the tailwater depth was set by adjusting the height of the tailgate located at the downstream end of the flume. The tailwater depth was measured at the end of sand bed, which was 2900 mm from the edge of rigid apron. Once the flow rate reached a steady state and the desired tailwater level was established, the experiment was initiated by carefully removing the aluminium sheet.

3.3 Measurements

3.3.1 Scour measurement

This experimental study consisted of two types of measurements: (1) measurements of the scour hole and its development; and (2) measurements that include the water surface profile and velocity profiles. The time development of the characteristic dimensions of the scour hole and mound along the centreline of the flume were measured using a digital point gauge. Several characteristic dimensions of the scour hole were measured at approximately equal logarithmic intervals of time (for example, 5, 10, 20, 40, 60, 120 and 240 minutes) beginning after about 5 minutes from the initiation of the experiment until asymptotic state was considered to be reached. These characteristic dimensions were the maximum scour depth, ε_m; the distance to maximum scour depth from the downstream edge of the apron, x_m; the length of scour hole, x_0; the distance to maximum mound height from the apron, x_d; the maximum mound height, Δ_m; and the distance to the downstream toe of the mound from the apron, x_{od}. Definitions of these measurements are shown in Figure 3.3.

The water surface elevation at locations E, F, G and I were also measured in conjunction with the scour measurements. These locations are shown in Figure 3.3. The measurements of water surface at those points were taken so that the variation of the depression in water depth in the reverse flow region, δ_w, the water depth over mound peak, y_m and the tailwater depth, y_t over time could be determined. This data was collected for the benefit of future researchers who might be interested in modelling the process of scour hole development. The length of surface eddy, L_e, above the scour hole was also measured using a measuring tape with the help of flow visualization using dye at the times of scour measurement. Once the scour hole was considered to have reached an asymptotic state, three longitudinal scour hole profiles were measured: one at the centre of the flume; and two at ±150 mm away from the centreline.

In order to decide the occurrence of the asymptotic state, the dimensions of the scour hole (ε_m and x_m) were plotted against the logarithm of time from initiation of the test. This plot normally follows a straight line (Tarapore 1956). Any marked departure of

the line towards a horizontal asymptote was considered as the beginning of the asymptotic state of the scour. After the beginning of the asymptotic state, experiments were run until the variation in the vertical and horizontal dimensions of the scour hole were found within about ±1 mm and ±2 mm respectively for a measurement interval of 4 hours. The ε_m and x_m were taken as the main controls in deciding the asymptotic state, however changes in other scour hole characteristics dimensions x_0, Δ_m, x_d and x_{od} were also given due consideration by plotting them versus log(t) so that any significant change in the scour profile during velocity measurement would not be expected. In order to confirm that there was no large scale change in scour profile during the velocity measurement, in each experiment a centreline scour profile was taken after the completion of velocity measurements and this was compared with the profile taken before the start of the velocity measurements. Though some small scale movement of sediment in the scour hole was observed during the velocity measurement, the comparison of measured profiles before and after velocity measurement revealed the absence of any large scale variation in scour profile during the velocity measurement. This comparison is discussed further in Section 4.2.

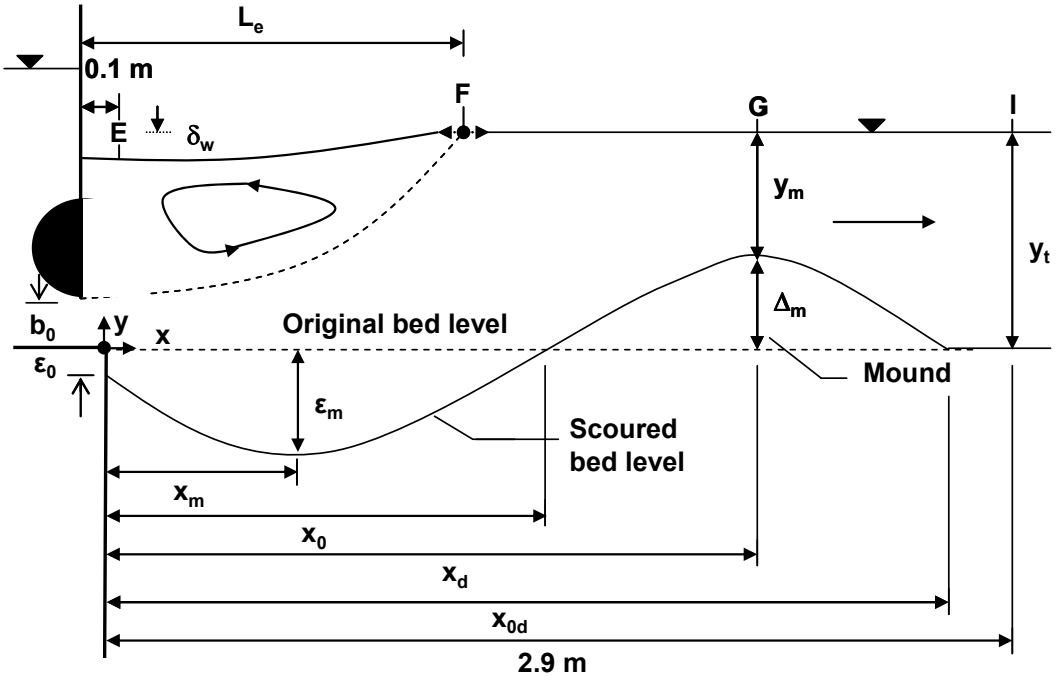

Figure 3.3 Definition sketch for the major measurement parameters (scour and water surface profiles)

3.3.2 Velocity measurements

Extensive measurements were taken of the velocity profiles along the centreline of the flume at different streamwise distances starting from the end of the rigid apron to the maximum mound height. The spacing of the vertical profiles was determined by considering the rate of decay of the maximum velocity, u_m, and the growth rate of the boundary layer, δ, in the streamwise direction for the "bed-jet" flow regime. Smaller spacings were used in the region where the decay of u_m and growth of δ in the streamwise direction were found to be relatively high. A horizontal spacing of 50 mm was maintained up to the end of the surface roller. Beyond that point spacings ranging from 100 mm to 200 mm was used. Similarly, the vertical spacing between two velocity measurements in a profile was determined by considering the velocity gradient in the vertical direction after conducting some preliminary tests. For the inner layer (boundary layer) with a higher velocity gradient, closer spacings when compared with that used in the outer mixing layer and the reverse flow region were used. The vertical spacing was restricted by the height of the sampling volume (5.6 mm) of the MicroADV. In each test, before the velocity measurements were undertaken, a detailed grid arrangement was developed which showed the longitudinal and vertical locations for each measurement. A sketch of a typical grid is shown for experiment 2F6.9Y200 in Figure 3.4.

The velocity measurements were mostly carried out using a 16 MHz MicroADV with 3D down-looking probe with sampling rate of 25 Hz, supported by use of a 2D side-looking probe with sampling rate of 50 Hz for shallow flows and measurements 50 mm below the water surface, where measurements using the 3D probe were not possible. No measurements were possible at locations less than 50 mm ($\approx 3b_0$) from the jet exit due to restrictions posed by the geometry of the ADV probes and the flume support structures. Figure 3.5 shows the ADV with a 3D down-looking probe as a velocity measurement was taken. Details of the operation of the ADV are discussed in the following section.

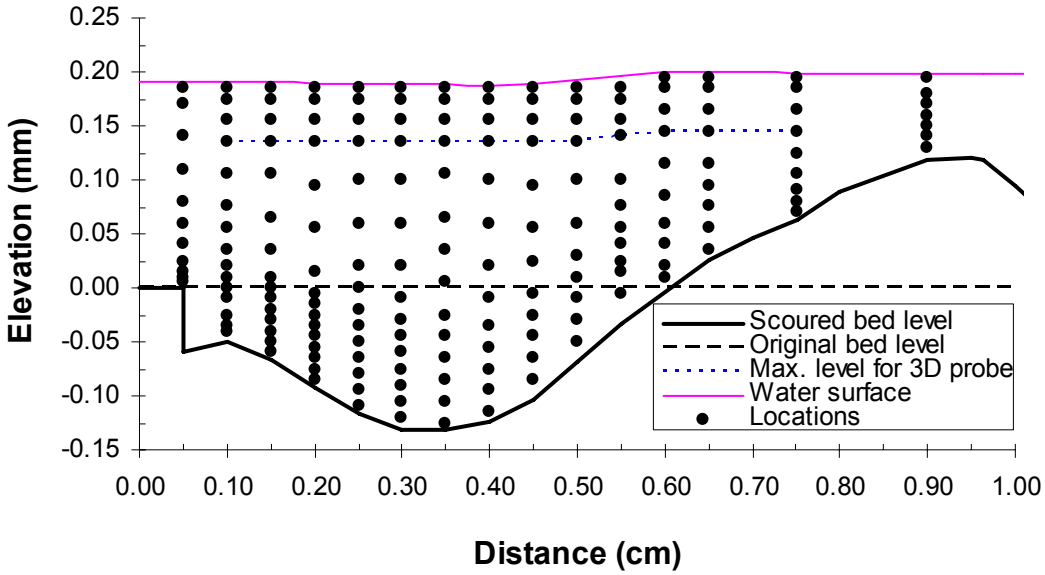

Figure 3.4 Sketch of a typical grid used for the velocity measurements performed in Expt. 2F6.9Y200

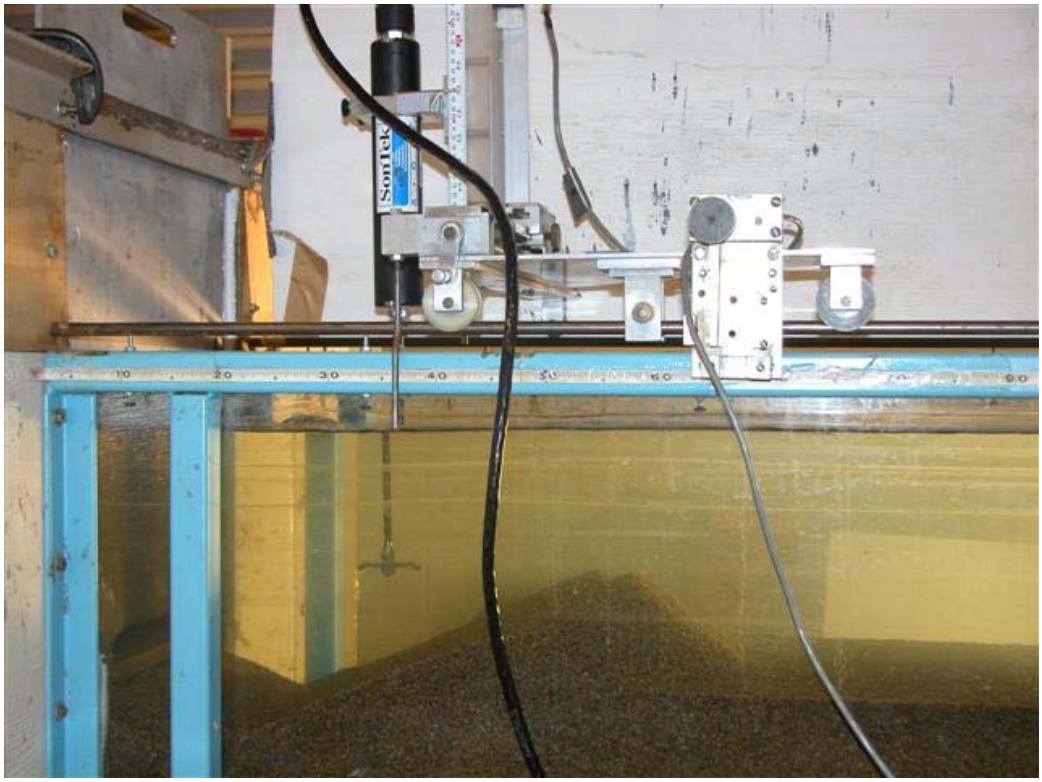

Figure 3.5 ADV with 3D probe

3.3.2.1 Acoustic Doppler Velocimeter (ADV)

The measurements were carried out primarily with a SonTek 16-MHz MicroADV with a 3D down-looking probe of 7 cm diameter head (Figure 3.6(a)). A 2D side-looking probe of 7 cm wide head was also used for shallow flows and the portion of the flow 50 mm below from the water surface (Figure 3.6(b)). The ADV probe consists of an acoustic sensor and two or three acoustic receivers for 2D or 3D probes, respectively, and one acoustic transmitter mounted on a stainless steel stem. Figure 3.7 illustrates the various components of a typical ADV probe. The sampling volume is the volume of water (equal to 0.09 cm^3) in which the ADV makes velocity measurements and is located 5 cm away from the acoustic transmitter. The default height and the diameter of the sampling volume are 5.6 mm and 4.5 mm, respectively. The probe also consists of a signal conditioning module made up of a cylindrical Delrin housing with internal receiver electronics. One end of the conditioning module is connected to the acoustic receiver using the stem, while the other end with a high-frequency cable using an underwater connector (SonTek/YSI 2007).

According to SonTek/YSI (2007), the ADV measures turbulence and the three components of the velocity vector (for the 3D probe) using a Doppler processing technique. In this technique, two pulses of sound of known frequency that are separated by a time lag are sent by the transmitter of the instrument through the sampling volume. As the acoustic waves or energy pass through the sample volume, they are reflected off particulate matter present in the flow. Some of the reflected acoustic waves travel back along the axis of the ADV receiver, where it is sampled and processed by the electronics provided in the instruments for the measurement of change in phase of the waves. The change in the phase divided by the time between the pulses gives the velocity of the particles in the water. The accuracy of the MicroADV is 1% of the measured velocity, or ± 2.5 mm/s (SonTek/YSI 2007).

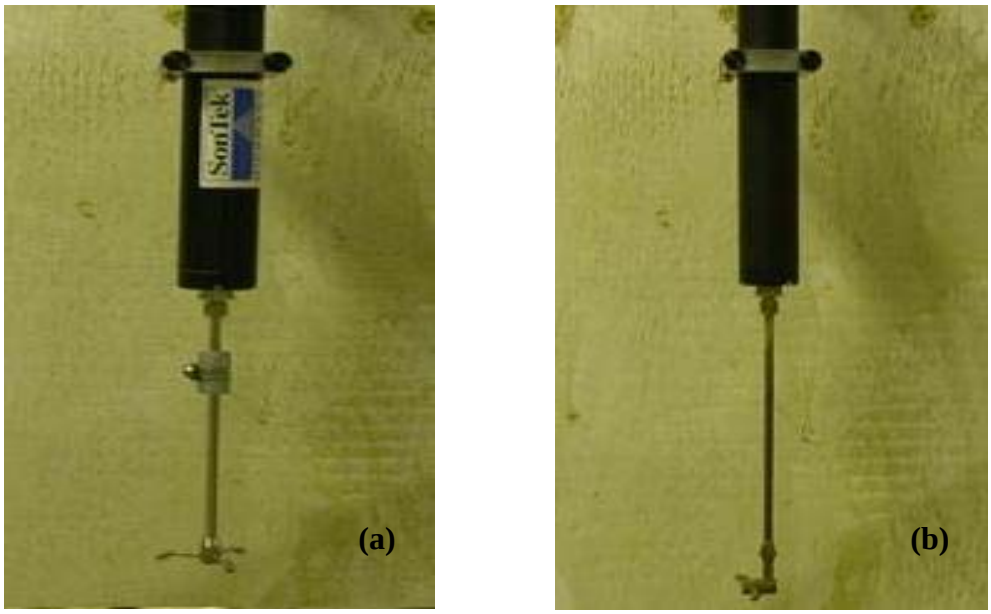

Figure 3.6 ADV Probes (a) 3D Down-looking (b) 2D Side-looking

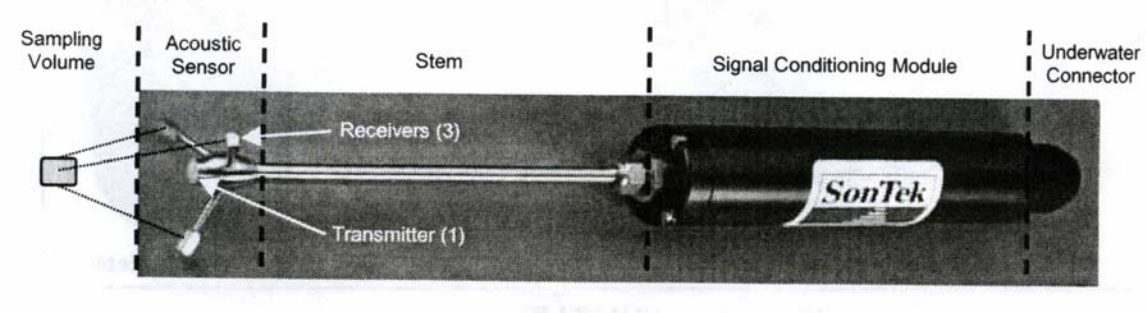

Figure 3.7 Components of a typical ADV probe (adapted from SonTek/YSI 2001b)

3.3.2.2 Acquisition of the ADV data

Velocity data measured by the ADV were collected through the use of a computer using SonTek's Horizon ADV software (Version 1.04.0.6). Using the Horizon software, ADV records nine values of three parameters (i.e. velocity, signal strength, and correlation) for each sample and reports them in XYZ (Cartesian) coordinates relative to the probe orientation. A sampling duration of five minutes was used for each measurement. This was decided by measuring velocity in different locations of scour hole for different sampling durations of 30, 60, 120, 180, 240, 300, 360, 480, and 600 seconds. The typical variation of time-averaged x-direction velocity, u, and $\sqrt{\overline{u'^2}}$ (RMS)

with sampling time is shown in Figure 3.8(a-b) and Figure 3.9(a-b), where x is the horizontal distance from the gate and y is the vertical distance from the scoured bed. For clarity, two separate plots, one for higher velocity and other for lower velocity are presented. From Figure 3.8(a-b) and Figure 3.9(a-b), it is observed that the variation of the velocity after a sampling time of 300 s (5 min) as compared to a velocity given by 600 s (10 min) of sampling time varied by less than the ADV accuracy (i.e. 1% of measured velocity, or ± 2.5 mm/s).

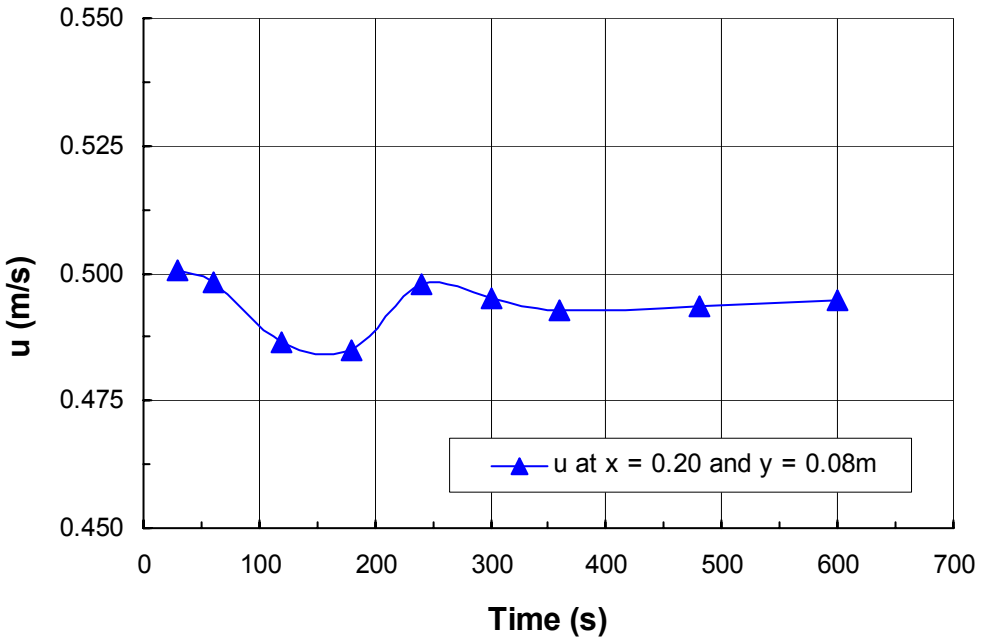

(a)

Figure 3.8 Time-averaged x-direction velocity versus sampling duration for (a) high velocity (b) low velocities

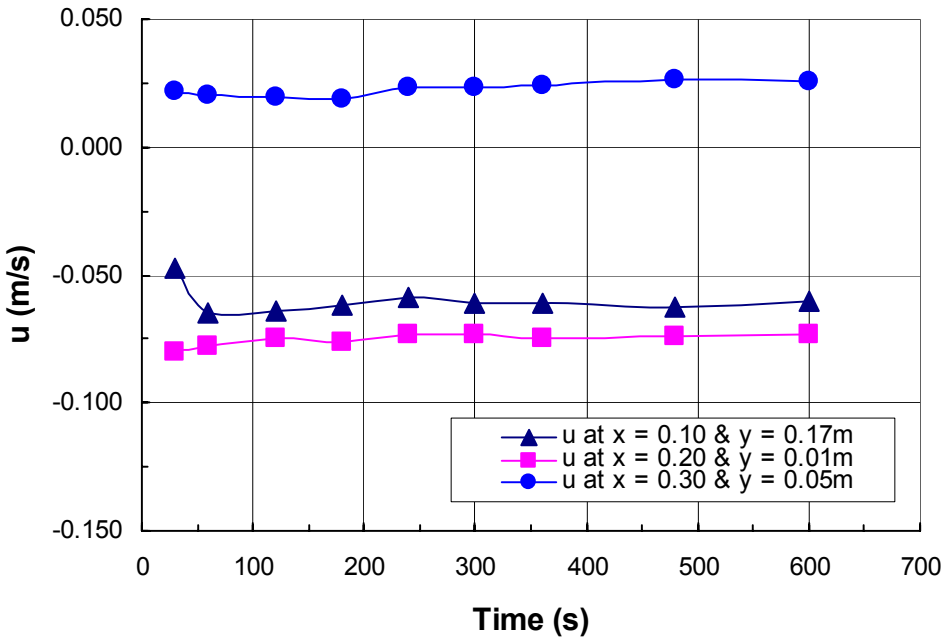

(b)

Figure 3.8 cont'd

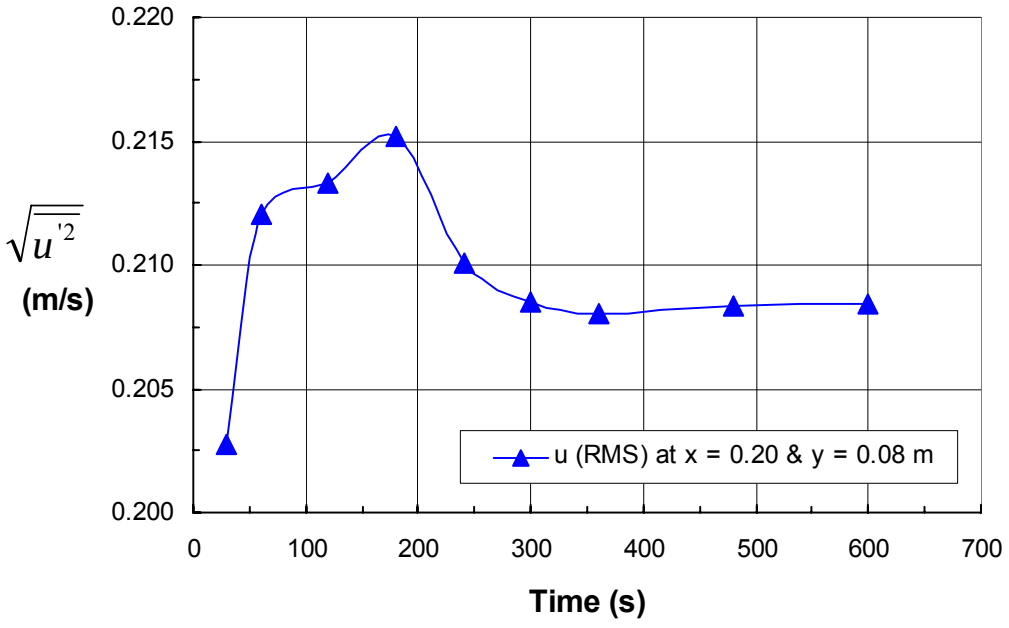

(a)

Figure 3.9 Time-averaged x-direction velocity (RMS) versus sampling duration for (a) high velocity (b) low velocities

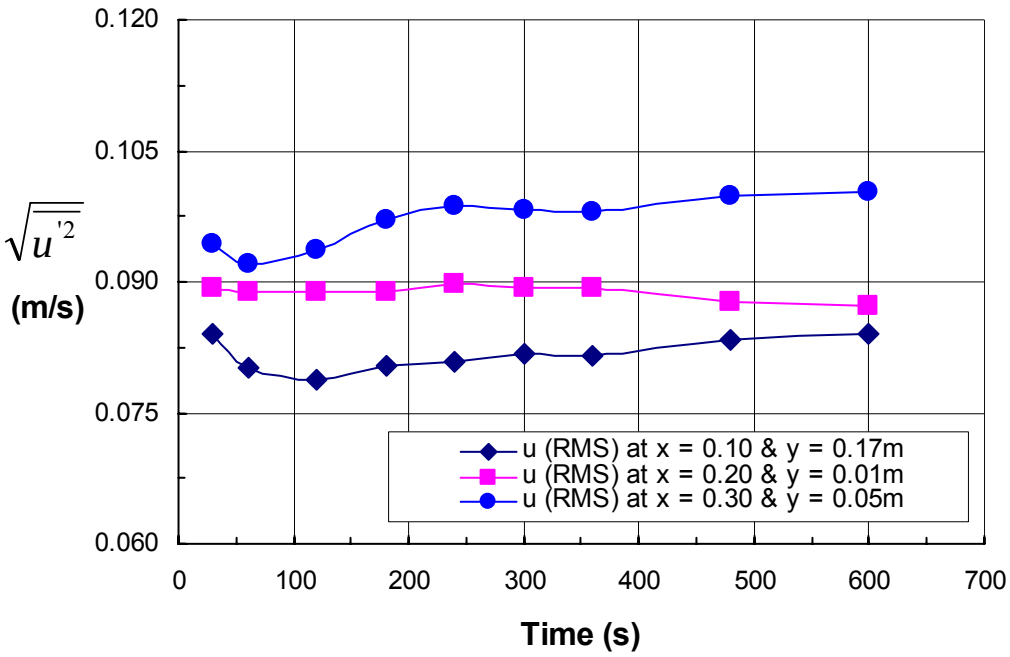

(b)

Figure 3.9 cont'd

3.3.2.3 ADV data quality and processing

The quality and accuracy of the ADV measured velocity data are primarily determined by two parameters: the signal-to-noise ratio (SNR); and the correlation score (COR). The parameter SNR primarily indicates presence of seeding material in the flow, whereas the COR parameter indicates the relative consistency of the behavior of the scattered particulates in the sampling volume during the sampling period (Wahl 2000). COR is expressed as a percentage (%). A higher value of COR indicates that the velocity measurements are reliable and have less noise, while a lower COR value indicates that the output velocity is dominated by noise and the ADV is operating in a difficult measurement condition (SonTek/YSI 2007).

For good quality data in field or laboratory environments, the ADV manufacturer SonTek recommends a SNR value of at least 5 dB while measuring average flow velocities, and 15 dB or higher when measuring instantaneous velocities and turbulence quantities (SonTek/YSI 2001a). The SNR is a measure of the intensity of the reflected

acoustic signal, which is derived from signal amplitude by subtracting the ambient noise level and converting to units of dB (SonTek/YSI 2001a). Therefore, in order to have good quality ADV measurements, it was attempted to keep the SNR greater than 15 dB. To achieve this, silica powder was added to the flow to serve as seeding material in the experiments any time the value of SNR was less than 15 dB. Silica powder was used because it is inexpensive and non-reactive to chemical agents (which would have otherwise disrupted other experiments in the lab).

SonTek/YSI (2001a) recommends 70% as the minimum acceptable COR for good quality ADV data. However, some researchers have reported that it may not always be possible to achieve high correlation values, especially when the ADV is used in highly turbulent or aerated flow. A lower COR does not necessarily mean that the measured data are not good (Wahl 2000; Martin et al. 2002; Liu et al. 2004; SonTek/YSI 2007). Wahl (2000) reported that measurements with correlation values much less than 70% can sometimes still give good data when the SNR value is high and the flow is relatively turbulent. Later, SonTek/YSI (2007) suggested that low correlation values in some cases do not bias the mean velocity measurements. It only affects the short-term variability in velocity data (i.e. increases the noise). Therefore, SonTek recommends that correlation values as low as 30% can be used as a filtering criterion if one is taking mean velocity measurements. Similarly, Martin et al. (2002) suggested that for turbulent flows one can use a COR value as low as 40% to filter measured velocity data when calculating time-averaged velocities if after filtering 70% of the data is retained.

In this study, viewing and post-processing of the collected velocity data were carried out using WinADV (Version 2.024), which was developed by Tony L. Wahl of the Water Resources Research Laboratory of the U.S. Bureau of Reclamation. Filtering of the data was based on the COR and SNR values. Phase-Space Threshold Despiking, as developed by Goring and Nikora (2002) and modified by Tony L. Wahl, was also used for filtering the data. Samples with good correlation score (average COR of more than 70%) were filtered based on a COR of at least 70% and an SNR of 15 dB for both average flow velocities and turbulence quantities as recommended by SonTek/YSI

(2001a). For the samples with an average correlation less than 70%, the data were filtered based on a COR of 40% and an average SNR of 15 dB for the time-averaged velocity measurements as recommended in Martin et al. (2002), in order to avoid a significant loss of velocity data especially near to the bed and in areas with high turbulence. A detailed comparison of several filtering methods for ADV data (minimum/maximum threshold filter, acceleration threshold filter, phase-space threshold filter, and velocity correlation filter) can be found in Cea et al. (2007) for highly turbulent flows. They found that no filtering method could be considered to be clearly superior to the others.

3.3.2.4 Tests of accuracy of ADV

In order to check the accuracy of the ADV readings, a total of twelve experiments were carried out in a separate rectangular flume of 10.3 m length, 0.8 m width, and 0.6 m depth. In the tests, the fully developed open-channel flow vertical velocity profile was measured for mean velocities in the range of 0.18-0.73 m/s and flow depths of 0.11-0.25 m. Both smooth and rough beds were tested. The velocity measurements at the section were taken using an ADV with 3D down-looking probe, an ADV with 2-D side-looking probe, and a Prandtl (or Pitot-Static) tube. The 2D and Prandtl tube measurements matched well. However, flows with a mean velocity greater than 0.6 m/s showed departure of the 3D ADV measurements from the 2D ADV and Prandtl measurements in the upper part of the flow. Some results are shown in Figures 3.10 and 3.11.

Two additional experiments were also conducted in measuring the velocity field in scour holes that reached asymptotic state as initial trials before the main experiments. These were carried out in the same experimental setup for the experiments describe the previous sections. Velocity profiles were taken both with the 2D and 3D ADV probes. For an experiment with a gate opening of 16 mm, a sand size of 2.2 mm, and a flow rate in the channel of 8 L/s, the data for the time-averaged streamwise vertical velocity profiles in the scour hole taken with the 2D and 3D probes matched very well (even near the boundaries). This is shown in Figure 3.12.

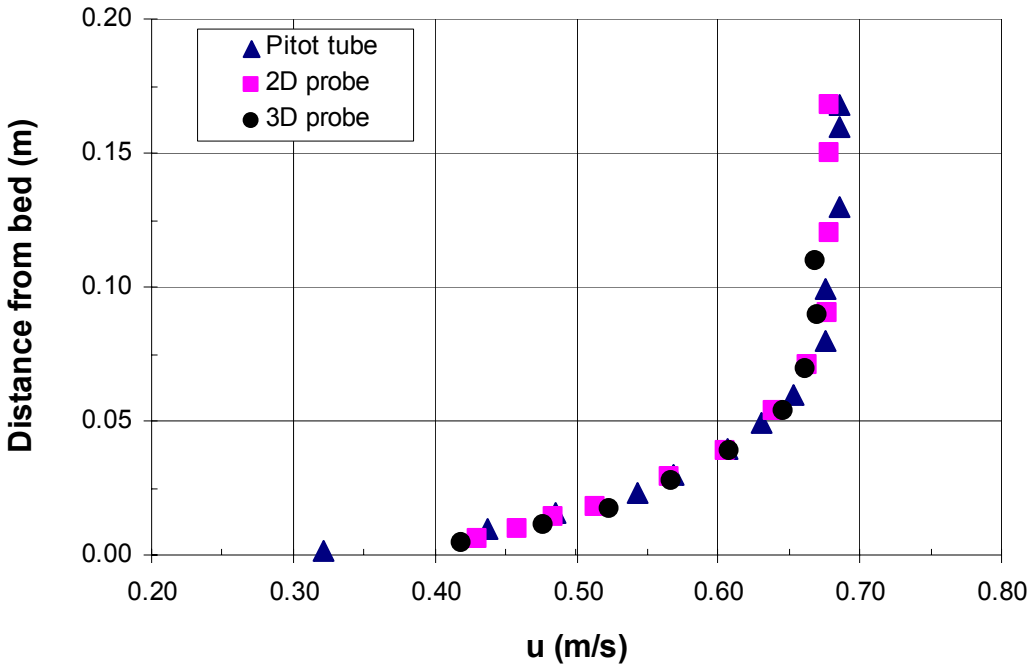

Figure 3.10 Velocity profiles using the data measured by Pitot tube, 3D down-looking, and 2D side-looking ADV probes (mean velocity 0.59 m/s)

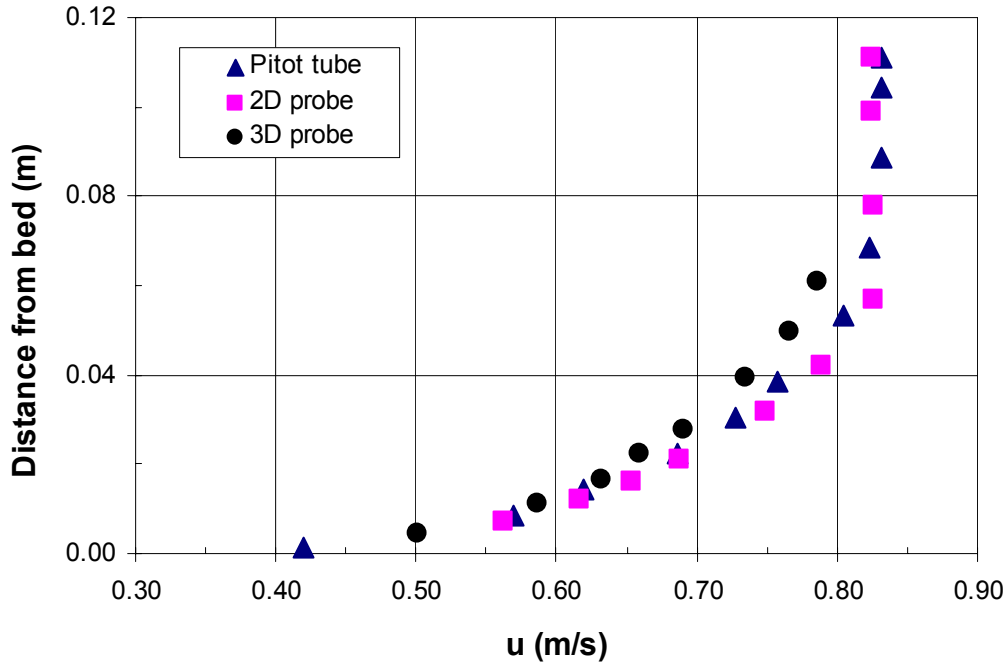

Figure 3.11 Velocity profiles using the data measured by Pitot tube, 3D down-looking, and 2D side-looking ADV probes (mean velocity 0.71 m/s)

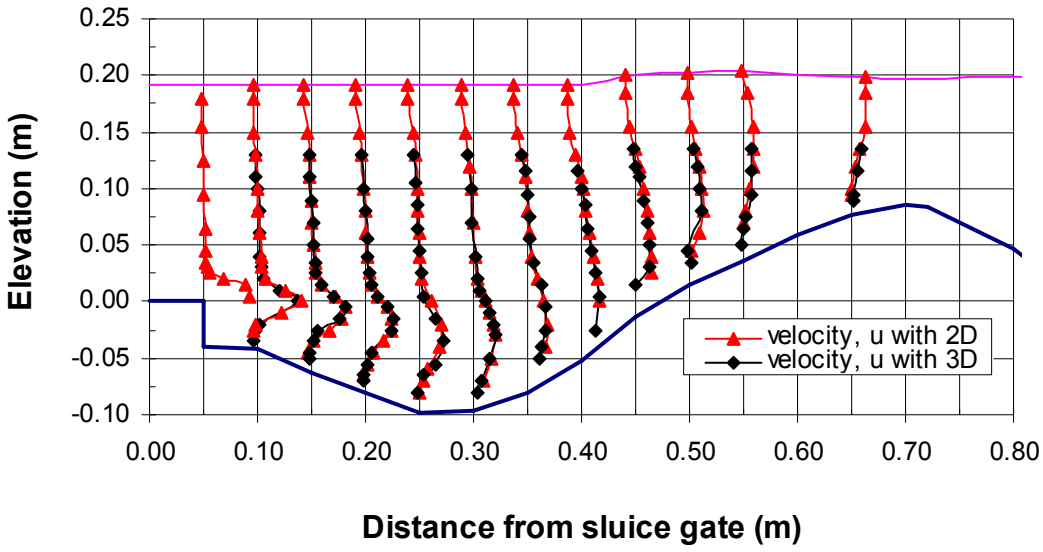

Figure 3.12 Velocity profiles using the data measured by 3D down-looking, and 2D side-looking ADV probes within scour hole

Based on the results of these preliminary experiments, it was decided that no correction was needed for the ADV measurements near the boundary as done by Liu et al. (2004). Since the velocities in the scour holes were all less than 0.6 m/s, no other corrections were made to the filtered ADV data.

3.4 Experiments

For development of the testing program, the main experimental variables that were considered were the velocity of flow under the gate, U_0; the average grain diameter of the sediment, D_{50}; and the tailwater depth, y_t. These three parameters were combined into the dimensionless parameters known to affect scour and the flow (as discussed in Chapter 3): the densimetric Froude number, $F_0 = U_0 / \sqrt{gD_{50}(S_g - 1)}$; the source Froude number, $F_r = U_0 / \sqrt{gb_0}$; submergence ratio, $s = y_t / b_0$; submergence factor, $S = (y_t - y_2)/y_2$; and boundary roughness, D_{50}/b_0. Here S_g is the specific gravity of bed material. The range of F_0, F_r, s, and S were chosen so that only the bed-jet or surface-jet flow regimes would be observed in the scour hole. The prediction of the flow regime for the experimental conditions was made using the criteria outlined in Johnston (1990).

Attempts were made to cover a wide range of submergence in designing the experiments without seeing the unstable bed-surface jet flow regime. Furthermore, the effects of jet Reynolds number, $R_e = U_0 b_0 / \nu$, on the development of scour and flow field are not taken into consideration.

In total, 18 experimental runs (four series) with different submergence ratio (s = 3-17.5), submergence factor (S = 0.0-6.4), densimetric Froude number (F_0 = 4.4-6.9), and source Froude number (F_r = 1.99-3.28) were designed and conducted (see Table 3.1). The gate opening, b_0 = 16 mm, was kept fixed. Two different bed roughness of relative roughness, D_{50}/b_0 = 0.137 and 0.085 were tested. The experiments were named as, for example, 1F5.3Y280, where the 1, F5.3, and Y280 represent the series number, densimetric Froude number and tailwater depth (in mm), respectively. A duplicate of the experiment 1F5.3Y160 with the name as 1F5.3Y160 (R) was also designed. Here, R indicates this was a replicate experiment. The experiments were divided into four different experimental series. The first series was taken as the base condition, where only the submergence ratio, s, was changed. The second series was intended mainly to observe the effect of densimetric Froude number (F_0) (and therefore F_r) for a constant submergence ratio. In the third series, the s, S, and F_r are kept constant and the densimetric Froude number is changed. In the final series, the s and F_0 are kept constant, but the relative roughness is different than the tests in Series 1. This was done because it was inconclusive from previous literature whether relative bed roughness had a significant effect on scour.

Table 3.1 Details of experiments

Test No.	D_{50} (mm)	b_0 (mm)	y_{sb} (mm)	y_t (mm)	$s = y_t/b_0$	S	Q (L/s)	U_0 (m/s)	F_0	F_r	R_e
1F5.3Y280	2.20	16	200	280	17.5	4.6	8.0	1.00	5.3	2.52	12232
1F5.3Y240	2.20	16	200	240	15.0	3.8	8.0	1.00	5.3	2.52	12232
1F5.3Y200	2.20	16	200	200	12.5	3.0	8.0	1.00	5.3	2.52	12232
1F5.3Y160	2.20	16	200	160	10.0	2.2	8.0	1.00	5.3	2.52	12232
1F5.3Y160 (R)	2.20	16	200	160	10.0	2.2	8.0	1.00	5.3	2.52	12232
1F5.3Y144	2.20	16	200	144	9.0	1.9	8.0	1.00	5.3	2.52	12232
1F5.3Y120	2.20	16	200	120	7.5	1.4	8.0	1.00	5.3	2.52	12232
1F5.3Y48	2.20	16	200	48	3.0	0.0	8.0	1.00	5.3	2.52	12232
2F6.9Y200	2.20	16	260	200	12.5	2.0	10.4	1.30	6.9	3.28	15902
2F5.9Y200	2.20	16	260	200	12.5	2.6	8.9	1.11	5.9	2.81	13609
2F4.4Y200	2.20	16	260	200	12.5	3.9	6.7	0.84	4.4	2.11	10245
3F6.7Y240	1.36	16	260	240	15.0	3.8	8.0	1.00	6.7	2.52	12232
3F6.7Y200	1.36	16	260	200	12.5	3.0	8.0	1.00	6.7	2.52	12232
3F6.7Y48	1.36	16	260	48	3.0	0.0	8.0	1.00	6.7	2.52	12232
4F5.3Y280	1.36	16	200	280	17.5	6.4	6.3	0.79	5.3	1.99	9633
4F5.3Y240	1.36	16	200	240	15.0	5.4	6.3	0.79	5.3	1.99	9633
4F5.3Y200	1.36	16	200	200	12.5	4.3	6.3	0.79	5.3	1.99	9633
4F5.3Y160	1.36	16	200	160	10.0	3.2	6.3	0.79	5.3	1.99	9633

CHAPTER 4: RESULTS, ANALYSIS, AND DISCUSSION

4.1 Introduction

The results of the experiments and the analysis of the data are discussed in this chapter. The main focus of the discussion is the submergence effects on the time development of the scour hole and the flow fields inside the scour hole. Analysis of the scour and velocity data is undertaken in order to better understand the flow in the scour hole and to examine the relationship between the scales for the flow in the scour hole and the scour hole size. Finally, a discussion on the experimental uncertainty is presented.

4.2 Observations of scour

4.2.1 Time development of scour

In this study, velocity measurements were not taken within a scour hole until it reached asymptotic conditions. As such, the typical growth of the scour holes and the condition of the scour holes at asymptotic state are discussed first. Figure 4.1(a-e) shows the time development of the main dimensions of the scour hole for experiments with varied y_t/b_0, but constant F_0 and D_{50}/b_0. These dimensions include the maximum scour depth, ε_m; the distance to maximum scour depth, x_m; the length of scour hole, x_0; the maximum mound height, Δ_m; and the distance to maximum height of the mound, x_d. For clarity, the Δ_m, x_0 and x_d data from Experiment 1F5.3Y48 (surface-jet flow regime) are not included in Figure 4.1 as the value of those dimensions were found to be significantly different from the values for the other experiments (which had a bed-jet flow regime). From Figure 4.1, it is evident that at all submergences where the bed-jet regime was observed ($s > 3.1$), the scour hole dimensions grow in a regular manner and approximately linearly with the logarithm of time up to a certain time before they deviate to a horizontal asymptote. This deviation is considered to be the beginning of

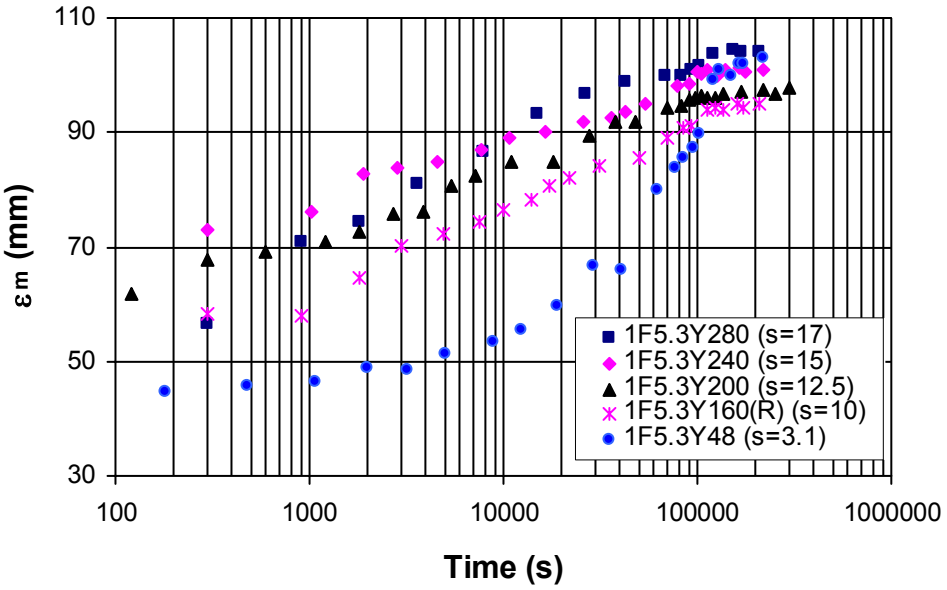

(a)

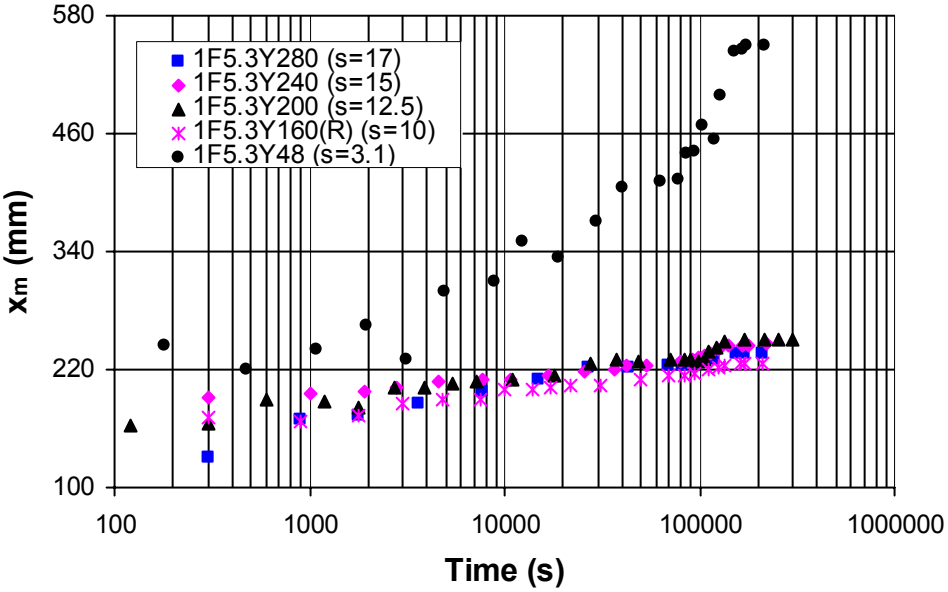

(b)

Figure 4.1 Development of the scour hole with time for F_0=5.8 with varied submergence (a) ε_m (b) x_m (c) x_0 (d) Δ_m (e) x_d (d) Δ_m and (e) x_d

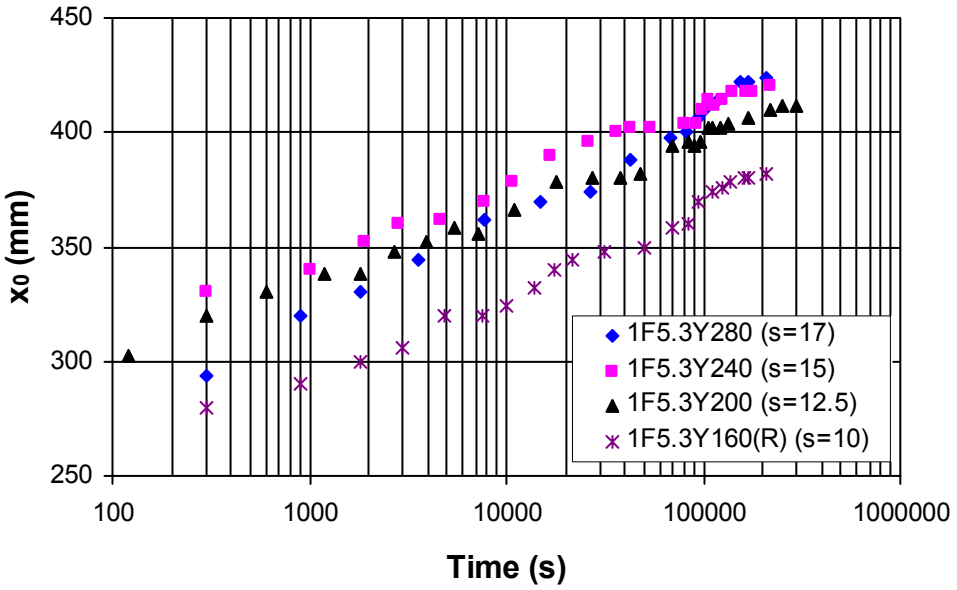

(c)

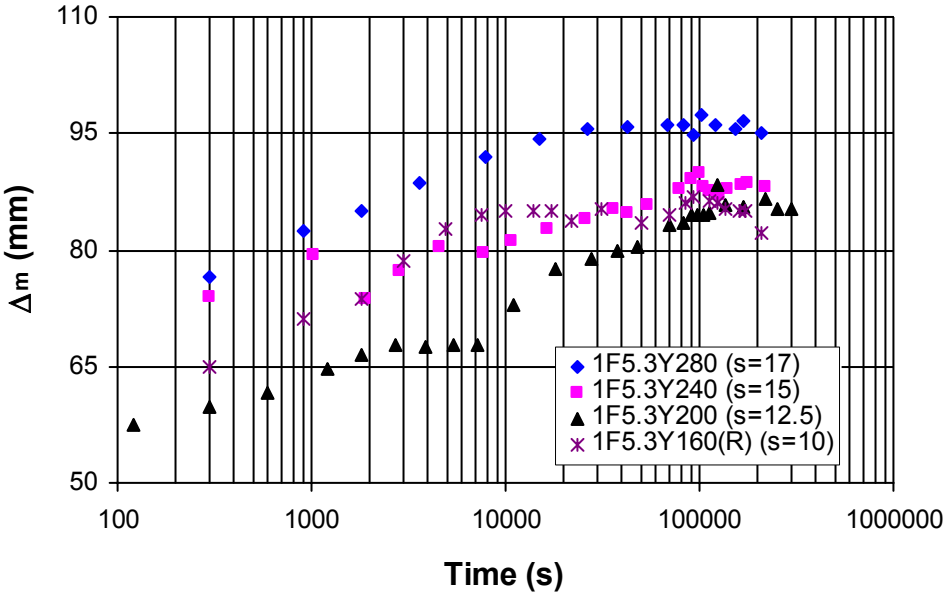

(d)

Figure 4.1 cont'd

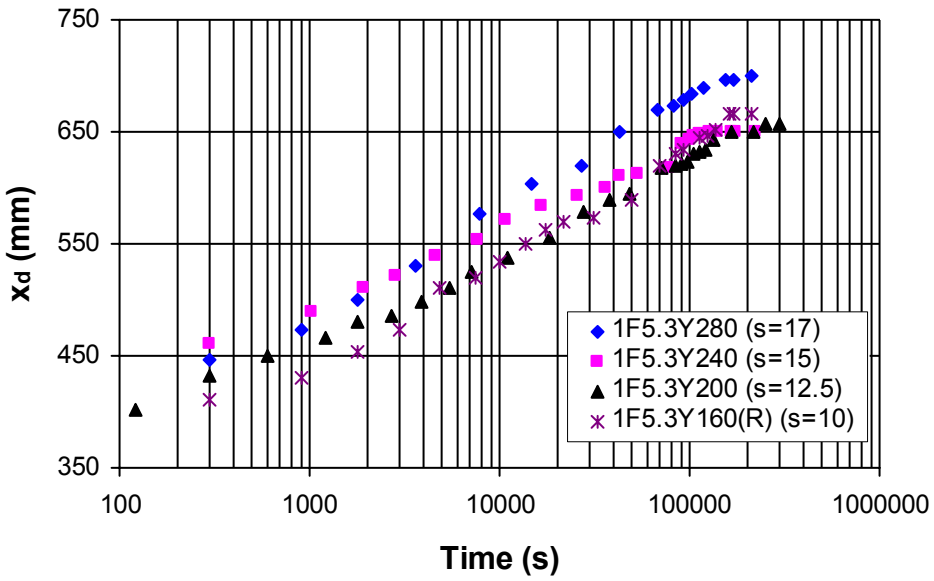

(e)

Figure 4.1 cont'd

asymptotic state (Tarapore 1956; Rajaratnam 1981; Mazurek and Ahsan 2005). The data for the time development of the scour hole dimensions for all the experiments is given in Appendix A.

The scour hole growth in all the experiments plotted in Figure 4.1(a-e) do not show sudden discontinuities, which would be observed for the jet-flicking that characterizes the bed-surface jet regime (Johnston 1990; Kells et al. 2001; Ahsan 2003). In Figure 4.1(b), the scour hole growth data looks somewhat irregular in the early stages of the test (i.e. the plot looks "bumpy"). However, it is believed that this behavior is in fact due to the difficulties in measuring the scour hole instead of the occurrence of the bed-surface jet flow regime behavior. There is much movement of the sediment inside the scour hole at these times. In comparison, the bed-surface jet flow regime was observed for two experiments (1F5.3Y144 and 1F5.3Y120); the growth of scour hole for these experiments is shown in Figure 4.2. Jet-flicking is seen late in the test. As such, no further measurements were taken for these experiments.

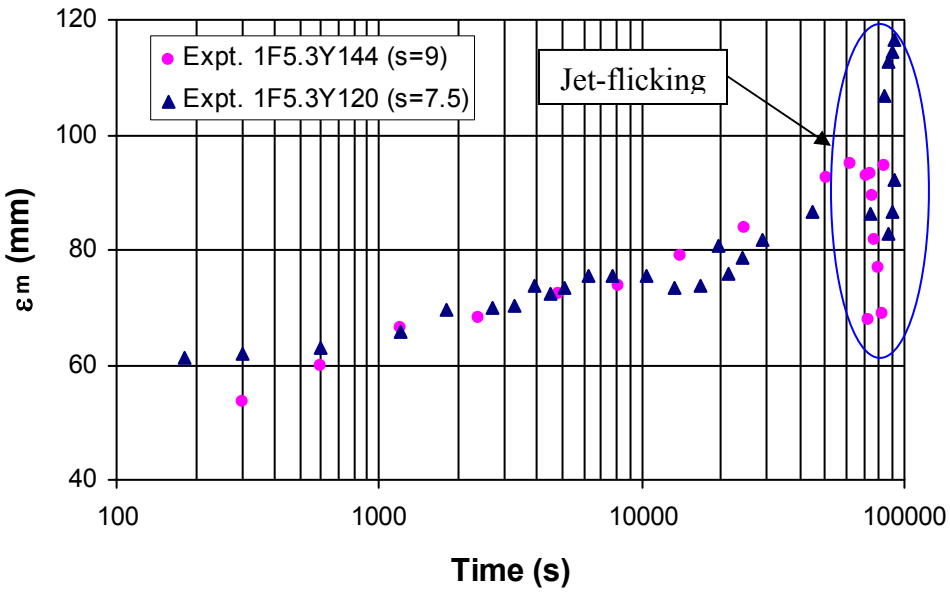

Figure 4.2 Growth of ε_m over time in experiments with a "bed-surface" flow regime

From the results given in Figure 4.1(a), it is apparent that ε_{ma} (the maximum scour depth at asymptotic state) increases with an increase in submergence except for the Experiment 1F5.3Y48 in which s = 3. In Experiment 1F5.3Y48, a "surface-jet" flow regime was observed rather than the "bed-jet" flow regime as observed in the other experiments. It is believed that the general trend of deeper scour holes for deeper submergence is due to slower velocity decay in deeper submergences. Under shallower conditions, the jet tends to entrain more negative momentum from the roller over top of the jet, which "slows down" the jet (Ead and Rajaratnam 2002). However, it is unclear why there is more scour for the very shallow tailwater test. This result is in contrast to the findings of Kells et al. (2001) and Ahsan (2003). The other dimensions x_{0a}, x_{da}, and Δ_{ma} (at asymptotic state) all were found to increase with increasing submergence, but this was not true for x_{ma}, which is the distance to maximum scour depth (Figure 4.1(b)).

In order to assess whether the boundary roughness had an effect on the depth of scour hole development, a few experiments with the same F_0 and s but different relative boundary roughness, D_{50}/b_0 (0.137 and 0.085) were conducted. Figure 4.3(a-b) shows the growth of ε_m with time for those experiments. From the plot, it appears that for a given F_0 and s, the magnitude of ε_{ma} (ε_m at asymptotic state) increases with increasing

relative roughness. The increase in the value of ε_{ma} with an increase in D_{50}/b_0 from 0.085 to 0.137 between Experiments 4F5.3Y200 and 1F5.3Y200 was 17.96% and for experiments 4F5.3Y160 and 1F5.3Y160 was 23.97%. To compare these results to tests run under the same experimental conditions, the difference in ε_{ma} for Experiments 1F5.3Y160(R) and 1F5.3Y160 was only 3.32%.

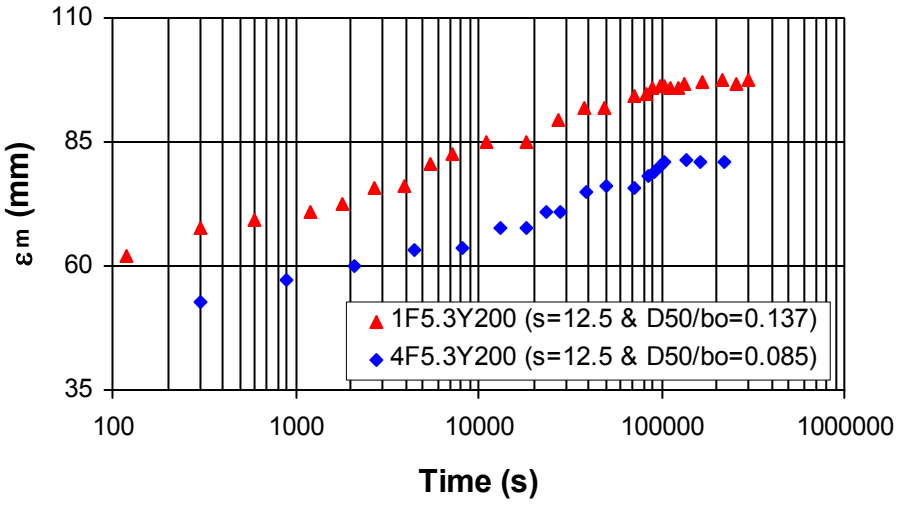

(a)

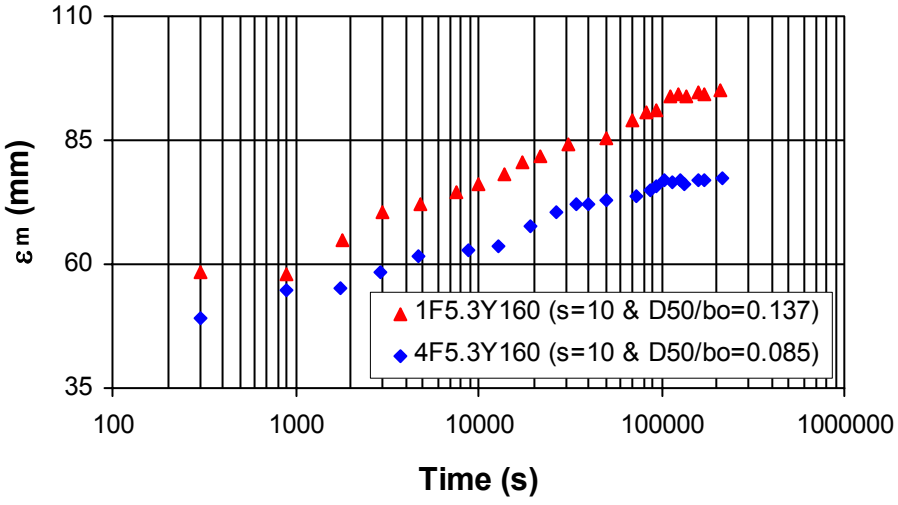

(b)

Figure 4.3 Development of ε_m with time for varied relative roughness of D_{50}/b_0 = 0.137 & 0.085 (a) y_t/b_0 = 10 & F_0 = 5.8 (b) y_t/b_0 = 10 & F_0 = 5.8

Table 4.1 gives a summary of the scour hole dimensions at the asymptotic state for all the experiments. Included in Table 4.1 is the duration of the experiment, T_e and the time to reach the asymptotic state, T_{bas}. As discussed previously, T_{bas} was determined by plotting the main dimensions of the scour hole, mainly, ε_m and x_m against the logarithm of time. A marked change in trend of the data towards a horizontal asymptote was considered to be the beginning of asymptotic state. It is important to note here that these values are only estimates as it is difficult to quantify exactly when the transition to asymptotic state occurs. Figure 4.4(a-b) gives the results of the time taken to reach asymptotic state for experiments with varied F_0 and s. From the plot in Figure 4.4(a), it is evident that an increase in F_0 for fixed value of D_{50}/b_0 (i.e. increasing jet velocity) increases T_{bas}. This result is in contrast to the results of Tarapore (1956), where a decrease in T_{bas} for increased jet velocity is reported. The effect of submergence on T_{bas} (Figure 4.4(b)) is unclear.

Table 4.1 Scour and flow measurements at asymptotic state

Test No.	D_{50} (mm)	s = y_t/b_0	U_0 (m/s)	F_0	δ_{wa} (mm)	ε_{0a} (mm)	L_e (mm)	x_{ma} (mm)	ε_{ma} (mm)	x_{0a} (mm)	x_{da} (mm)	Δ_{md} (mm)	y_{ma} (mm)	x_{0da} (mm)	T_e (hr)	T_{bas} (hr)	Flow Regime*
1F5.3Y280	2.20	17.0	1.11	5.9	7.4	35.3	560	236	104.5	420	696	95.7	178.9	850	58	33.3	BJ
1F5.3Y240	2.20	15.0	1.06	5.6	10.1	41.2	540	244	101.3	418	650	88.3	136.2	788	61	29.4	BJ
1F5.3Y200	2.20	12.5	1.07	5.7	11.6	38.7	530	250	97.1	406	650	85.5	112.7	788	83	29.2	BJ
1F5.3Y160	2.20	10.0	1.05	5.6	9.6	41.4	530	240	98.1	410	688	81.1	77.3	826	78	39.3	BJ
1F5.3Y160 (R)	2.20	10.0	1.10	5.8	10.6	35.8	450	222	94.9	380	666	85.0	75.8	804	59	37.8	BJ
1F5.3Y48	2.20	3.1	1.02	5.4	-	26.8	-	500	102.1	1050	1450	23.4	32.7	2850	60	33.2	SJ
2F4.4Y200	2.20	12.5	0.88	4.7	7.1	35.6	450	196	73.0	332	480	56.3	144.2	572	59	20.3	BJ
2F5.9Y200	2.20	12.5	1.18	6.2	12.7	41.4	540	260	109.6	450	700	98.4	97.3	880	59	28.0	BJ
2F6.9Y200	2.20	12.5	1.35	7.2	12.1	48.7	600	306	132.1	550	896	120.7	76.6	1096	70	41.5	BJ
3F6.7Y240	1.36	15.0	1.09	7.3	7.3	42.4	590	260	121.4	474	786	135.3	102.3	990	54	26.0	BJ
3F6.7Y200	1.36	12.5	1.07	7.2	7.8	39.7	540	250	116.1	468	780	119.0	80.0	960	59	22.6	BJ
3F6.7Y48	1.36	3.1	1.09	7.3	-	19.3	190	550	113.1	1410	2400	11.8	37.2	2850	40	22.8	SJ
4F5.3Y280	1.36	17.5	0.87	5.8	4.0	34.9	550	202	81.8	350	618	84.3	194.7	762	58	30.6	BJ
4F5.3Y240	1.36	15.0	0.85	5.7	4.3	37.5	500	200	86.0	356	604	82.9	156.9	760	61	29.0	BJ
4F5.3Y200	1.36	12.5	0.87	5.9	5.0	36.1	460	200	81.1	340	580	82.9	113.1	722	61	31.4	BJ
4F5.3Y160	1.36	10.0	0.89	6.0	5.1	36.7	410	192	77.1	328	562	73.3	88.3	740	60	37.4	BJ
1F5.3Y144	2.20	9.0	1.00	5.3	9.4	40.7	500	230	94.6	394	660	81.2	61.4	782	-	NA	BSJ
1F5.3Y120	2.20	7.5	1.00	5.3	-	-	-	264	116.5	480	-	-	-	-	-	NA	BSJ

***BJ - Bed-jet, SJ - Surface-jet, BSJ - Bed-surface jet**

Note: The origin for all the longitudinal distances of the scour hole profile is from the edge of rigid apron (length of apron = 50 mm)

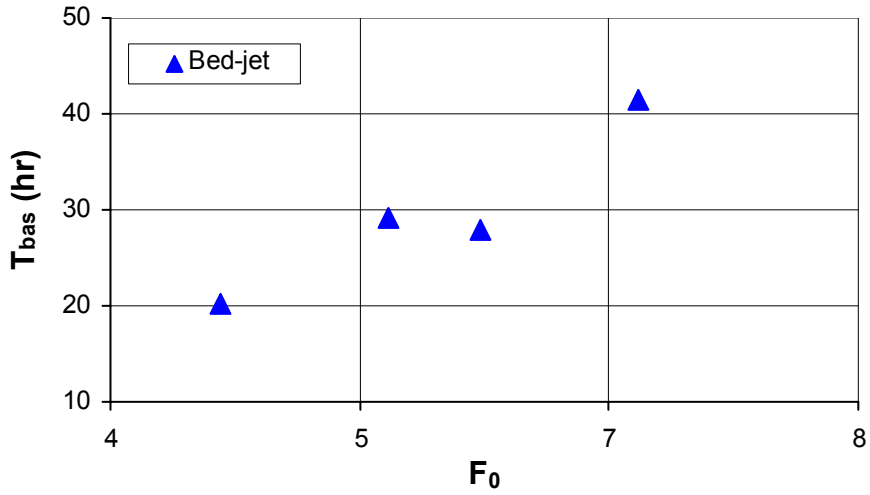

(a)

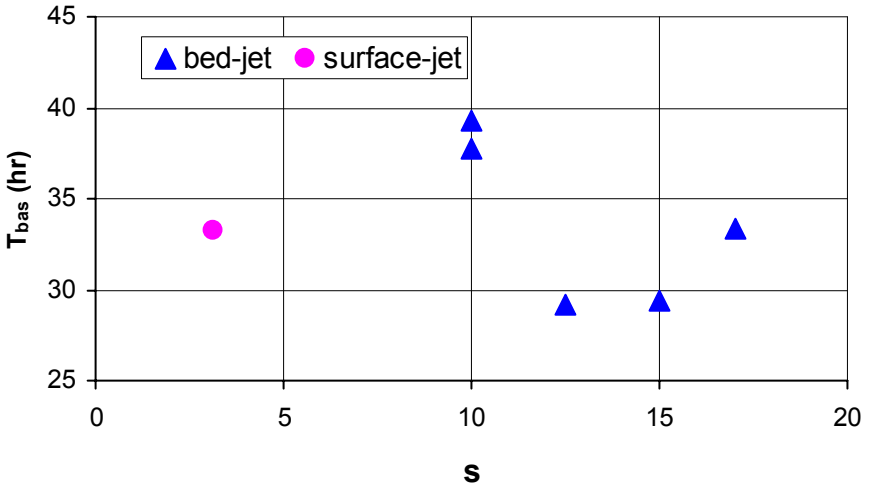

(b)

Figure 4.4 Influence on T_{bas} of (a) F_0 and (b) s

4.2.2 Scour hole profiles at asymptotic state

Figure 4.5(a-c) gives the scour hole profiles taken along the centreline of the flume at asymptotic state with varied F_0, s, and D_{50}/b_0. As expected, F_0 has a strong influence on the overall scour hole size (Figure 4.5(a)). Similarly, an increase in the scour hole size with an increase in submergence ratio was observed (see Figure 4.5(b)) except for the experiment 1F5.3Y48 with s=3.1 with the surface-jet regime. For the experiment with s = 3.1, a relatively low mound located far from the edge of rigid apron was observed. Further, for a given value of F_0 and s, an increase in scour hole size was observed for an increase in the value of D_{50}/b_0 (Figure 4.5(c)).

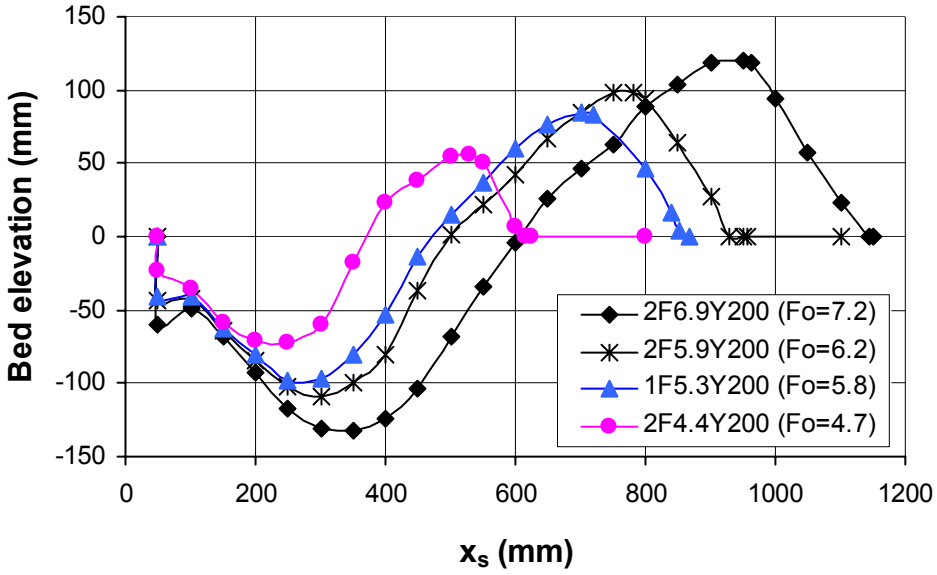

(a)

Figure 4.5 Asymptotic scour profiles along streamline under varied (a) F_0 (b) s (c) D_{50}/b_0

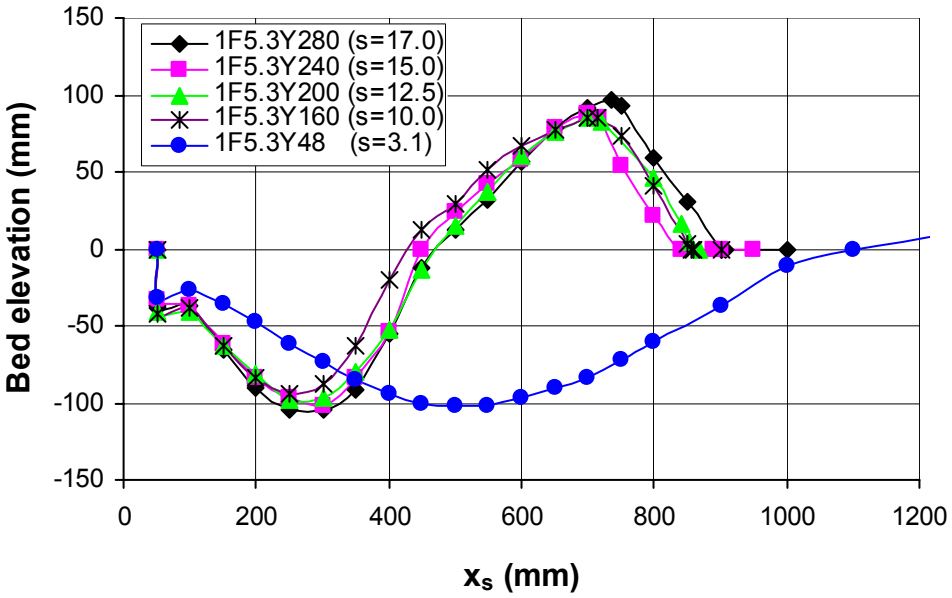

(b)

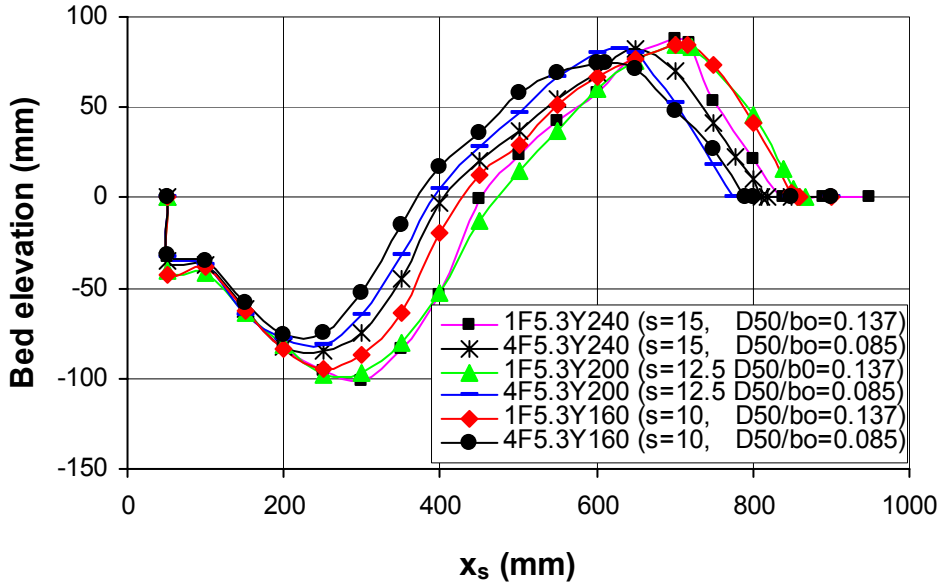

(c)

Figure 4.5 cont'd

Figure 4.6(a-c) shows a typical variation of scour hole profiles across the channel width (at the centreline (CL), 150 mm right of the centreline (ROC) and 150 mm left of the centreline (LOC) under varied submergence ratio. The measurements of the profiles were taken at predefined locations at spacing of 50 mm. Results of the plotted profiles clearly shows submergence effects on the variation of scour hole across the width of the flume. It appears that the lower submergence, s=3.1 (Figure 4.6(c)) results in a more significant variation in scour profile as compared with the higher submergences, s = 17 & 10 (Figure 4.6(a) & (b)). It is noted that the flow regime for s = 3.1 was a "surface-jet", whereas for other submergences, it was a "bed-jet" flow regime. It can also be noted in Figure 4.6(c) that, although there exists significant variation in the scour hole profile across the width of the flume, the variation is reasonably symmetrical. This suggests that the jet velocity across the channel width was symmetrical. Similar results were observed for the experiments conducted with the lower value of D_{50}/b_0. The data for asymptotic state scour profiles for all the experiments are presented in Appendix B.

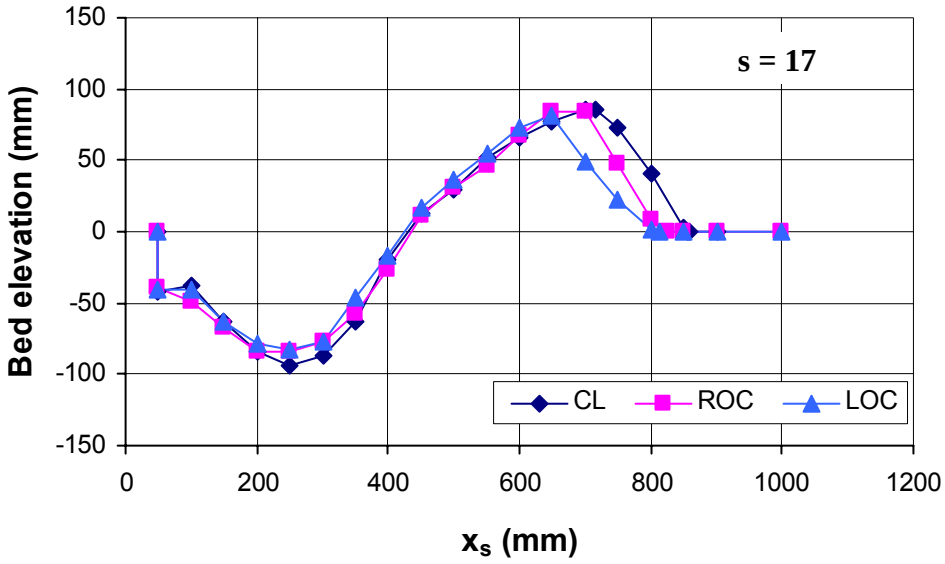

(a)

Figure 4.6 Scour profiles across channel width under varied submergence ratio (a) s = 17 (Expt. 1F5.3Y280) (b) s=10 (Expt. 1F5.3Y160) (c) s=3 (Expt. 1F5.3Y48)

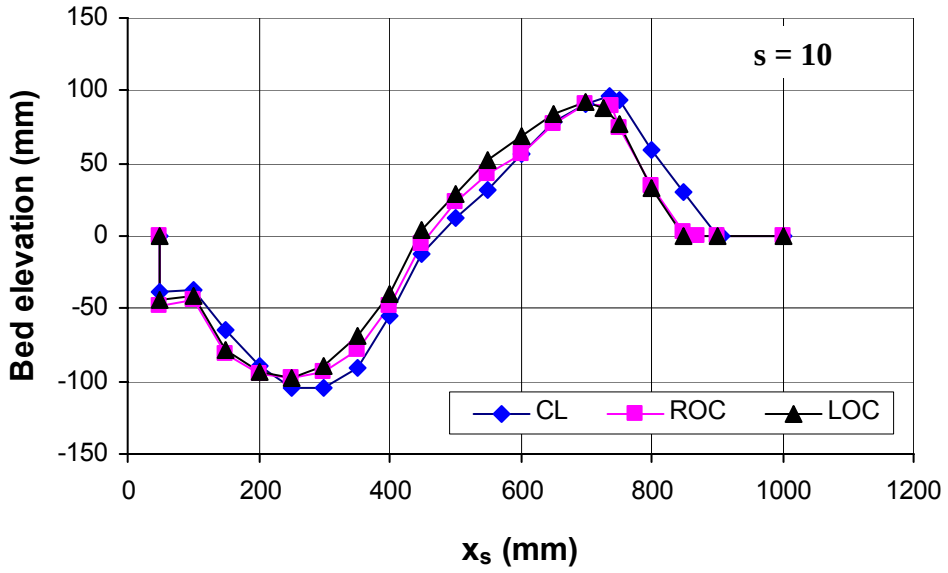

(b)

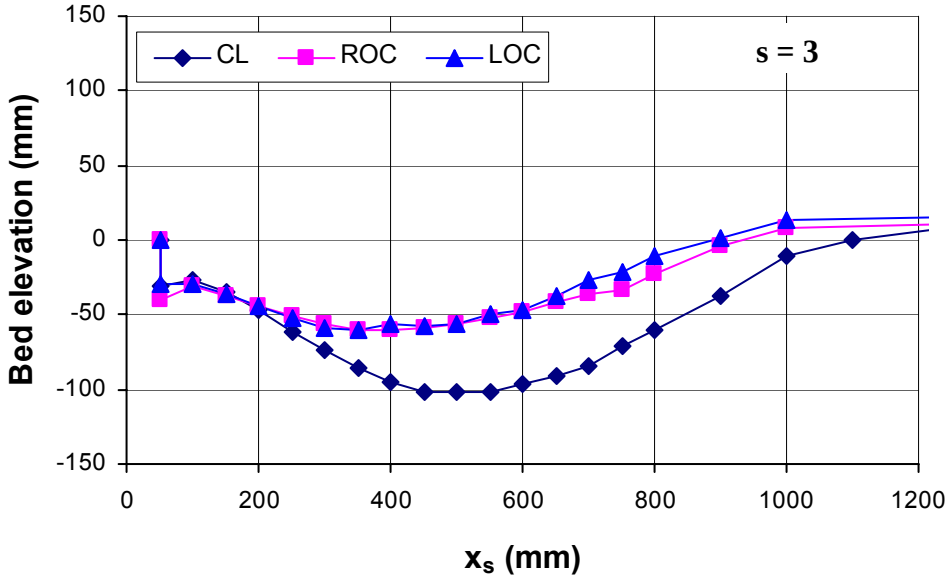

(c)

Figure 4.6 cont'd

In order to confirm that no significant change in scour profile occurred during the velocity measurements, a centreline scour profile was also taken after the completion of velocity measurements and this was compared with the profile taken before the start of the measurements. Though some movement of sediment in the scour hole was observed during the velocity measurements, the comparison of the profiles measured before and after the velocity measurements reveals the absence of any large scale change in scoured profiles during velocity, which took up to 15 hours. As an example, Figure 4.7 shows the comparison of scour profile taken before and after completion of velocity measurements for experiment 1F5.3Y200.

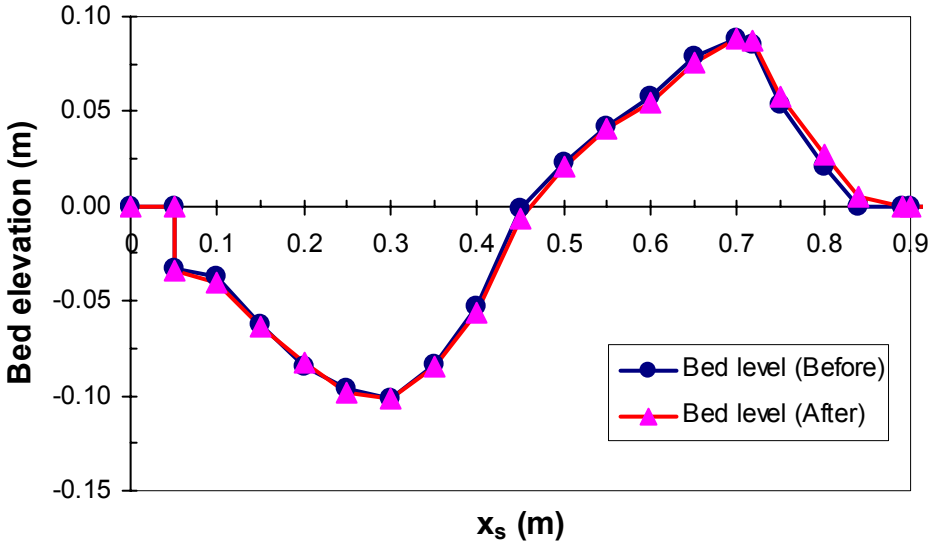

Figure 4.7 Scour profiles before and after velocity measurement of a different of 15 hours (Expt. No. 1F5.3Y240)

4.3 Observations of flow in the scour holes

4.3.1 Flow field in scour hole

For general observations of the flow patterns in the scour hole, Figure 4.8(a-b) and 4.9(a-b) gives typical velocity fields in experiments with the same F_0 and D_{50}/b_0, but different submergence. The time-averaged velocities in the x and y directions are plotted as velocity vectors in Figure 4.8(a-b) and contour plots of the same data are given in Figure 4.9(a-b). The x-direction velocity is u and the y-direction velocity is v. The

magnitude and the direction of the dimensionless vector are $(u^2 + v^2)^{0.5}/U_{0A}$ and arc tan(v/u), respectively, where U_{0A} is the maximum u velocity at the section measured at the end of the apron. The flow field near to the gate and water surface (within about 60 mm) are not shown in Figures 4.8(a-b) and 4.9(a-b) since it was not possible to measure the complete flow fields in those areas due to limitations with the use of the ADV. In Figures 4.8 and 4.9, a line representing the loci of $u = u_m$ is shown.

As in the case of a submerged hydraulic jump on a smooth rigid horizontal bed, it is seen that the jet travels along the bed and an eddy forms above the jet with much slower velocities than the jet itself. However, unlike in the case of the submerged hydraulic jump, two eddies in the clockwise direction at the upstream and downstream ends of the scour hole (near to the scoured bed) are also clearly noticeable (see Figure 4.9(a-b)). Also, the velocity decays in the x-direction, but is also seen to recover after the end of the reverse flow at top of the mound (see Figure 4.8(a-b)). The size of all the eddies increase with increasing submergence. Unlike for the low submergence value of $y_t/b_0 = 10$, a reverse flow over the mound peak can also be clearly observed for the higher value of $y_t/b_0 = 17$ (see Figure 4.8(a-b)).

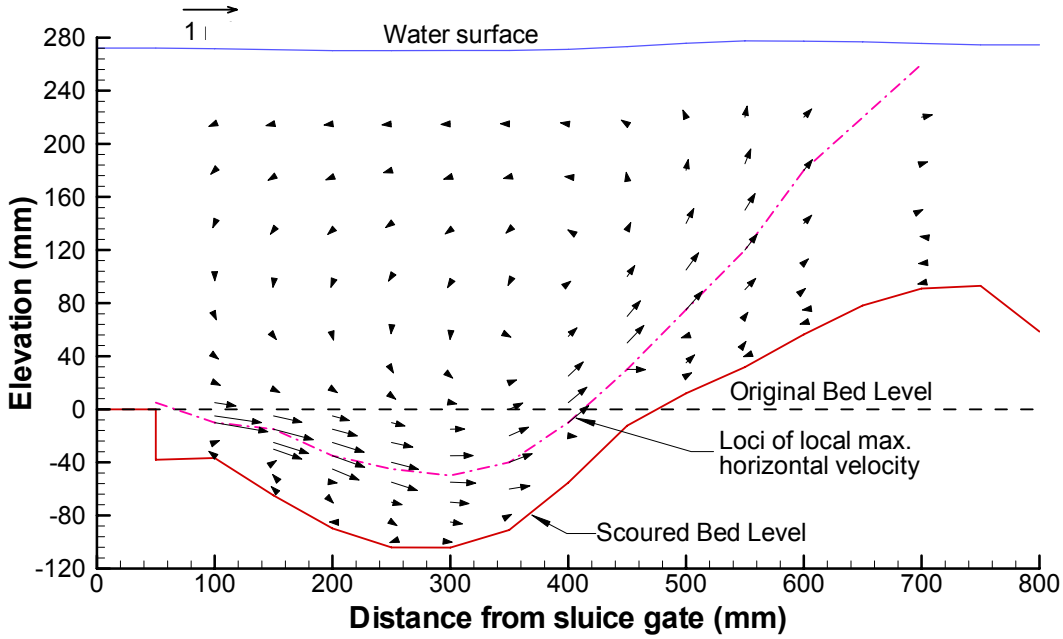

(a)

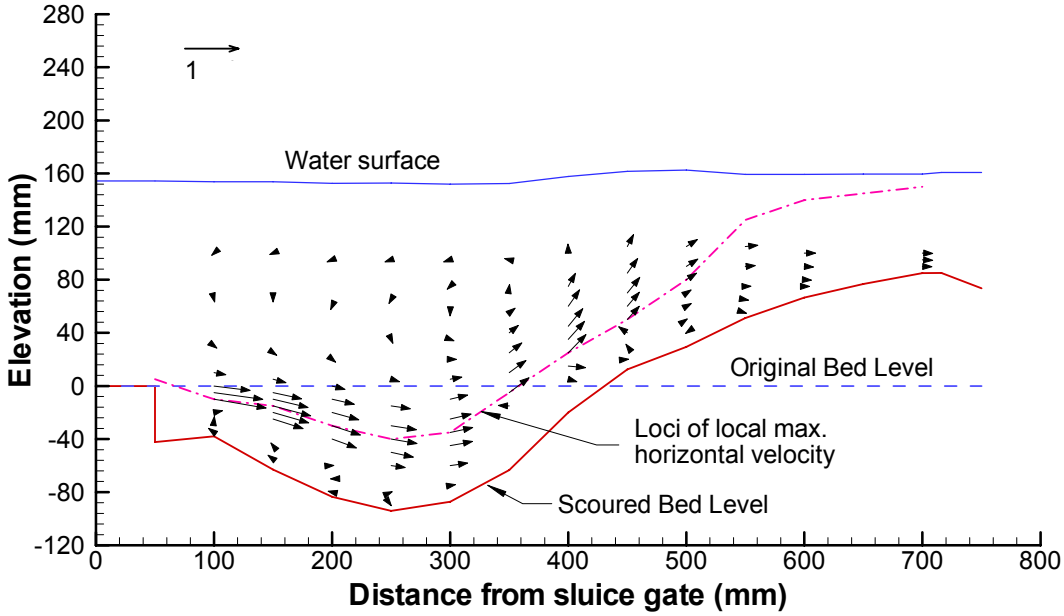

(b)

Figure 4.8 Dimensionless velocity vectors for varied y_t/b_0 for F_0 = 5.8 and D_{50}/b_0 = 0.137 (a) y_t/b_0 = 17 (Expt. 1F5.3Y280) (b) y_t/b_0 = 10 (Expt. 1F5.3Y160

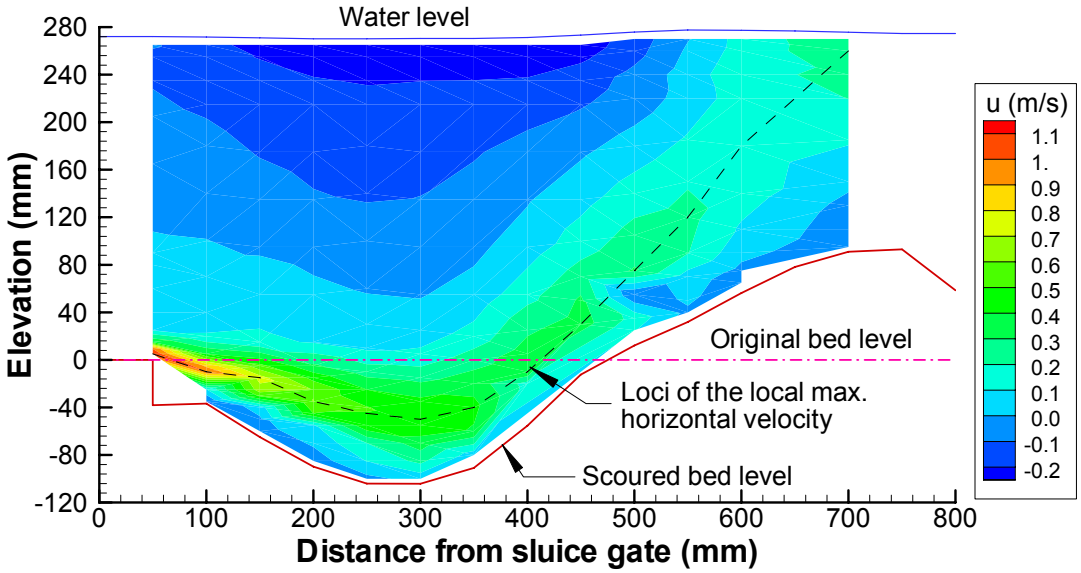

(a)

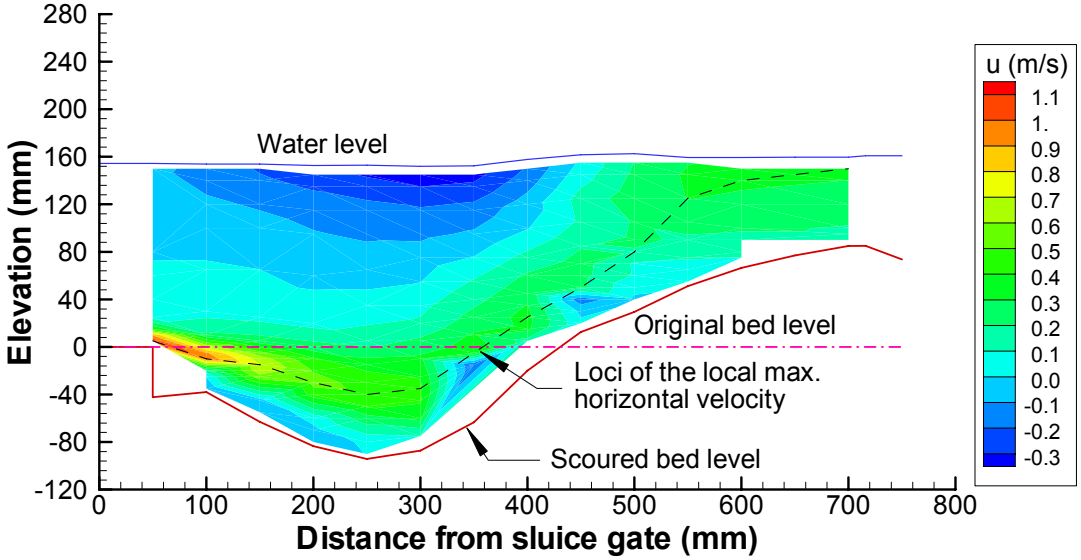

(b)

Figure 4.9 Velocity contours of horizontal velocities, u (m/s) for varied y_t/b_0 at F_0 = 5.8 and D_{50}/b_0 = 0.137 (a) y_t/b_0 = 17 (Expt. 1F5.3Y280) (b) y_t/b_0 = 10 (Expt. 1F5.3Y160 (R))

Figure 4.10(a-b) shows the dimensionless velocity vectors for varied y_t/b_0 for a higher F_0 = 7.2, with also a different sand with a D_{50}/b_0=0.085. Considering the results shown in Figure 4.10(a-b), a similar type of flow field as that observed for the coarser sand in Figure 4.8(a-b) was observed. However, for this case, there is an absence of reverse flow over the mound even for the higher submergence (y_t/b_0=15), as observed for the coarse sand.

Figure 4.11 shows typical velocity profiles for the time-averaged x-direction velocity inside the scour hole. Similar plots were developed for all experiments for which velocity measurements were taken. These velocity profiles were mainly intended to analyze the jet behaviour inside the scour hole under varied experimental conditions (particularly under varied submergence) from the point of view of similarity in the velocity profiles, growth of the length scales of the jet, and the decay of the maximum velocity along the streamwise direction. Appendix C gives the data for the velocity profiles for all the experiments.

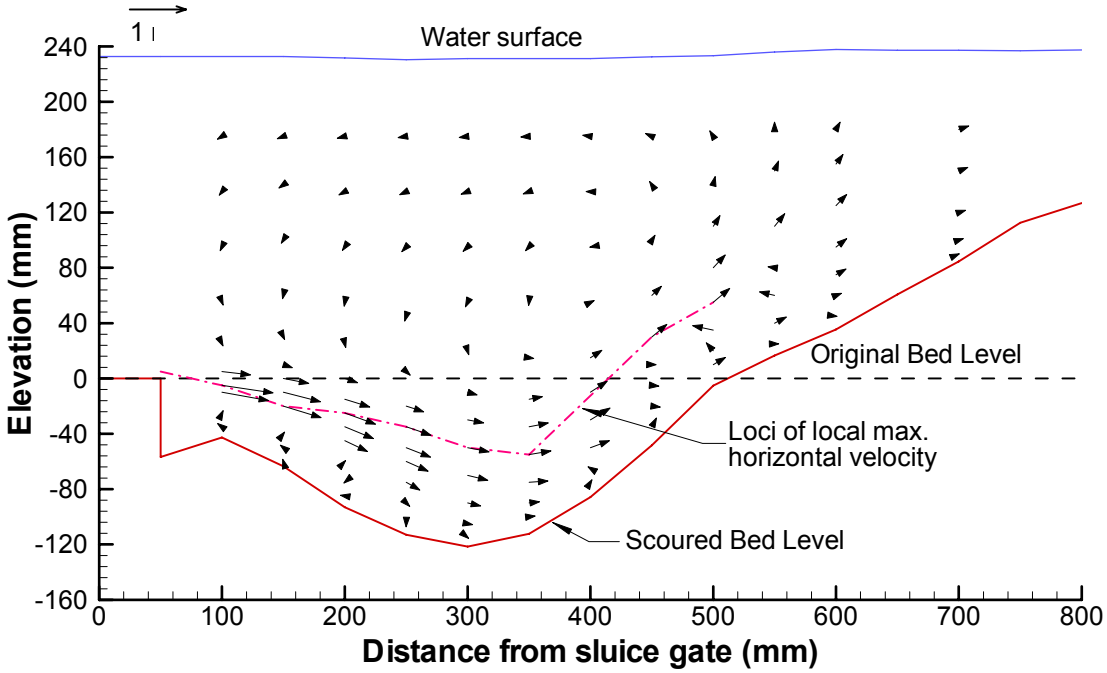

(a)

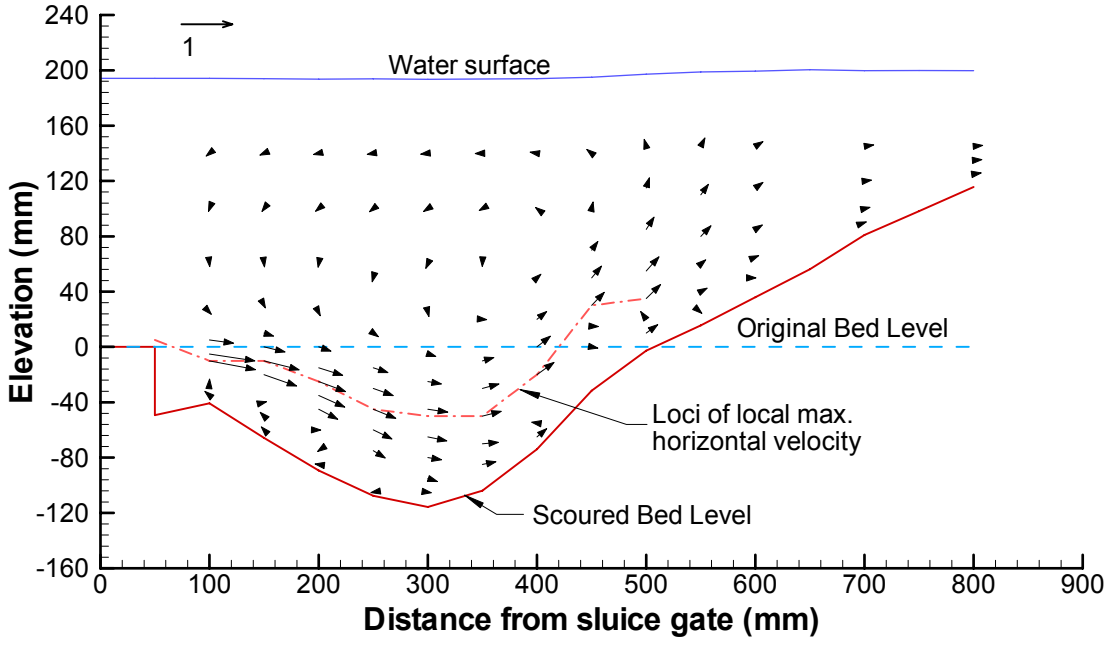

(b)

Figure 4.10 Dimensionless velocity vectors for varied y_t/b_0 for $F_0 = 7.2$ for finer sand of $D_{50}/b_0 = 0.085$ (a) $y_t/b_0 = 15$ (Expt. 3F6.7Y240) (b) $y_t/b_0 = 12.5$ (Expt. 3F6.7Y200)

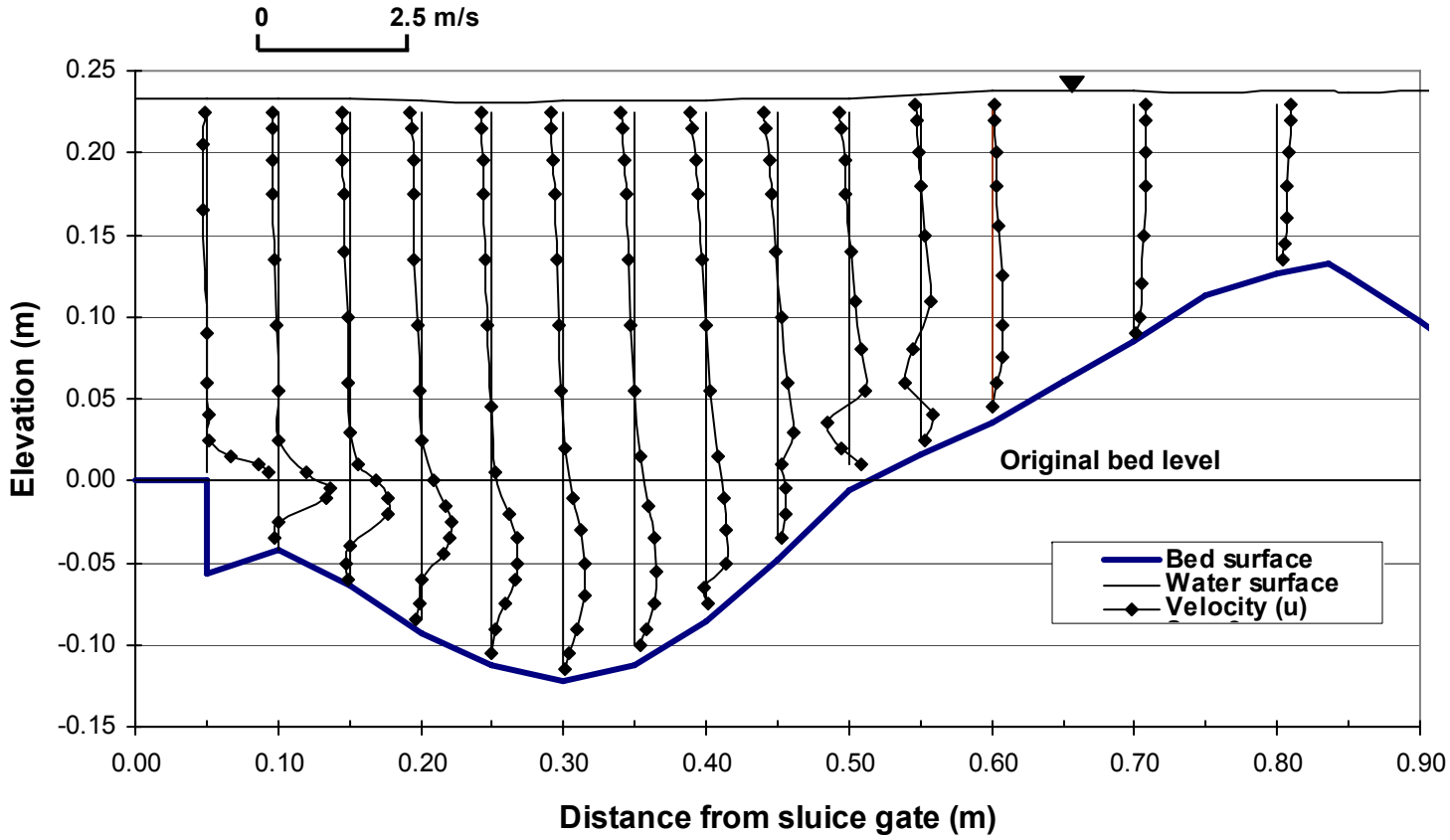

Figure 4.11 Typical velocity profiles (for time-averaged velocity in x-direction) of a bed-jet flow regime (Expt. 3F6.7Y240)

4.3.2 Velocity decay in the scour hole

Figure 4.12(a-b) gives the variation of the time-averaged streamwise maximum velocity in the streamwise or x-direction along the jet centreline for varied submergence. The velocities were normalized using a velocity scale U_{0A} because there were slight variations in U_{0A} between experiments. It is seen that the jet diffusion inside the scour hole (for the bed-jet regime) can be divided into two distinct stages (see Figure 4.12(b)), which is similar for that observed by Ead and Rajaratnam (2002 and 2004) for smooth and rough rigid beds. The first zone is characterized by a curvilinear velocity decay up to a certain distance after that it deviates to a linear decay (second stage) until the jet starts to recover its velocity due to flow acceleration caused by the limited tailwater above the mound. However, unlike for the bed-jet regime, the second stage decay was not observed for the surface-jet regime (see Expt. 1F5.3Y48, Figure 4.12(a)). In this case the first stage decay was followed by the beginning of the recovery of the jet velocity. The decay of normalized velocity for the experiments with two different values of relative roughness (D_{50}/b_0=0.137 and 0.085), but same F_0 and y_t/b_0 are given in Figure 4.13. The result indicates a higher decay of maximum velocity with decreasing value of D_{50}/b_0. It is pertinent to mention that there was a bigger scour hole size for the coarse sand as compared to the finer sand, which might also affect velocity decay.

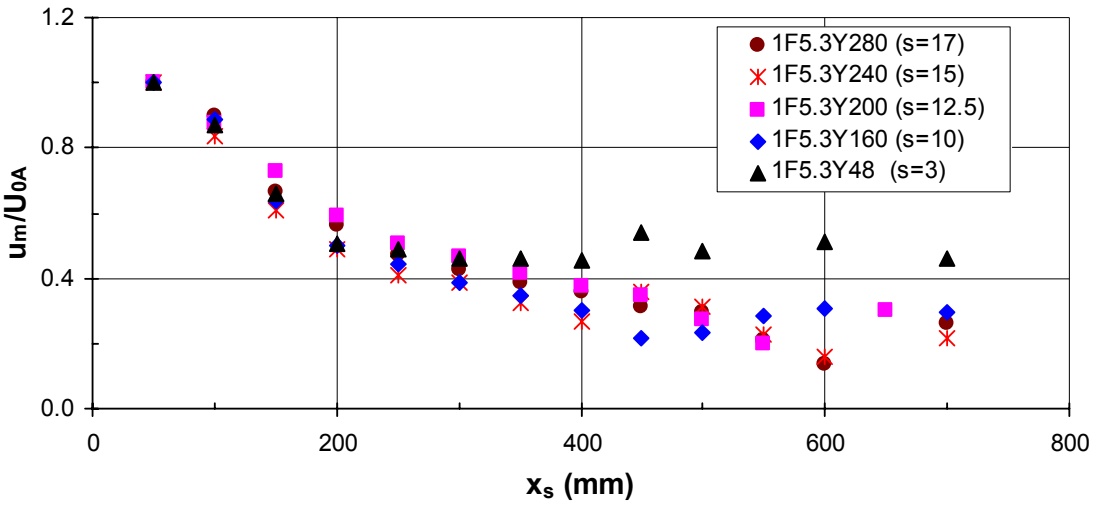

(a)

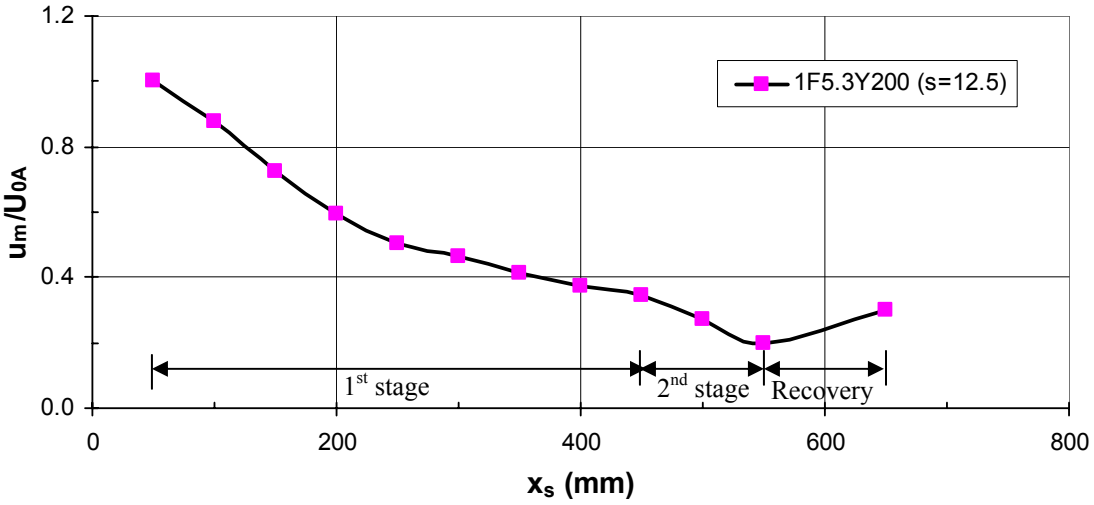

(b)

Figure 4.12 Variation in u_m with distance x_s along the scour hole for (a) varied y_t/b_0 (F_0 = 5.8 & D_{50}/b_0 = 0.137) (b) Experiment 1F5.3Y200 (s=12.5) showing stages in velocity variation

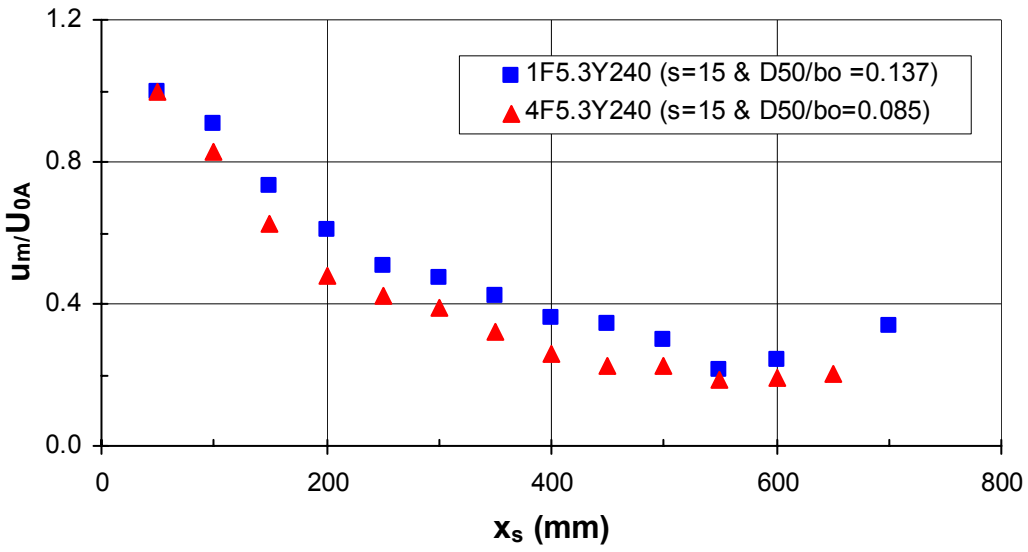

Figure 4.13 Variation in u_m with distance x_s along the scour hole for varied relative roughness (F_0 = 5.8 & y_t/b_0 = 15)

4.3.3 Streamwise variation of boundary layer thickness and jet half-width

As discussed in Chapter 2, the boundary layer thickness, δ, of a jet at any section is defined as a the vertical distance from the scoured bed to the point where $u = u_m$ and $du/dy = 0$. However, it should be noted that for the region near the apron, where a clockwise eddy is observed near the bed, the datum for the boundary layer was taken as the location where $u = 0$. The effect of submergence ratio and the relative boundary roughness on the variation of δ in the streamwise direction is shown in Figure 4.14(a-b). In Figure 4.14, it is seen that the boundary layer initially grows linearly to a certain point, beyond which the growth rate slows and becomes curvilinear. The distance where the curvilinear growth begins to occur is downstream of the location of the maximum scour depth, x_m. Further, it appears that the growth of δ in the non-linear region is more influenced by the change in y_t/b_0 and D_{50}/b_0 than in the region with linear growth. However, whether it increases or decreases with the increased value of those parameters is not clear.

As also discussed in Chapter 2, jet half-width, b, is the distance from the bed to the location where $u = 0.5u_m$ and $du/dy < 0$. Figure 4.15(a-b) gives the growth of b along

the x-direction for experiments with different y_t/b_0 and D_{50}/b_0. Two stages in the growth of b (a linear growth followed by a curvilinear) as those observed for boundary layer growth are also seen.

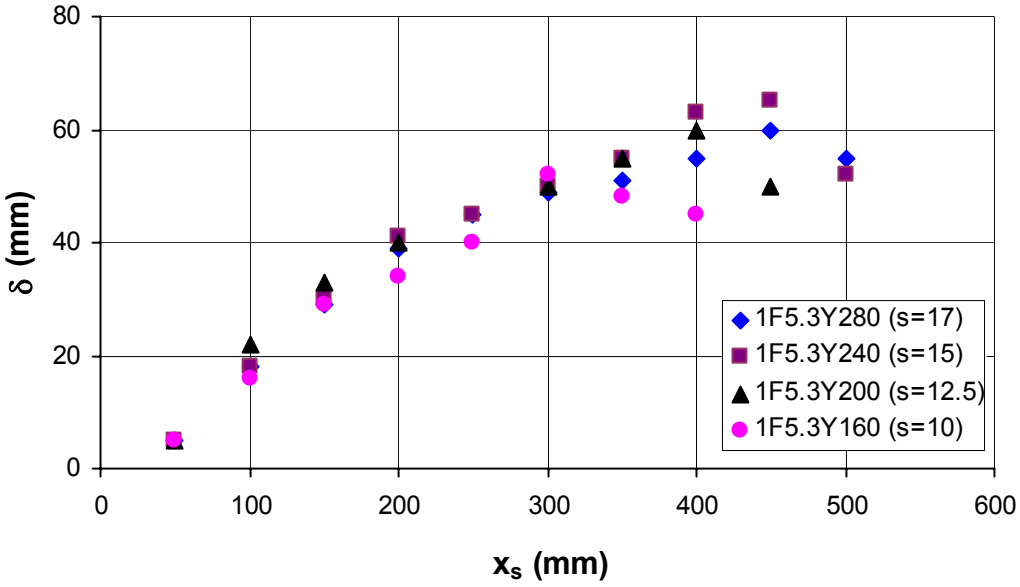

(a)

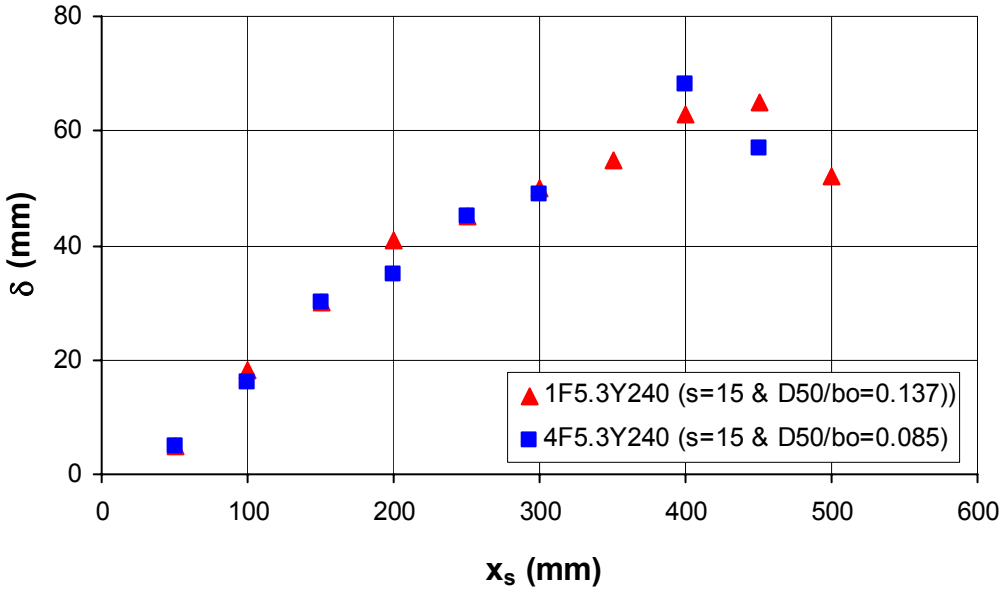

(b)

Figure 4.14 Growth of boundary layer thickness in x-direction for (a) varied y_t/b_0 (F_0 = 5.38 & D_{50}/b_0 = 0.137) (b) varied D_{50}/b_0 (F_0 = 5.8 & y_t/b_0 = 15)

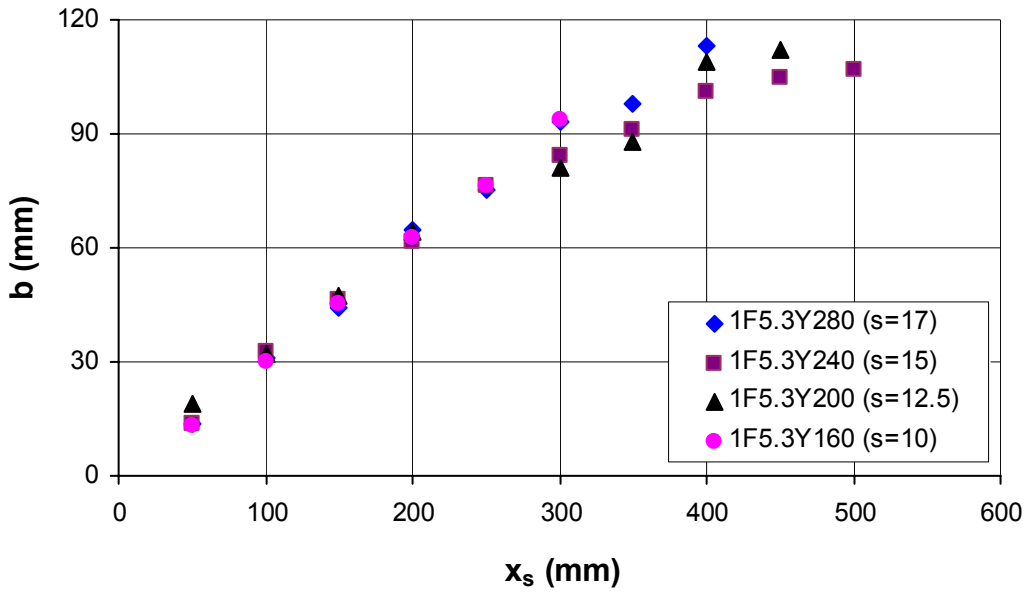

(a)

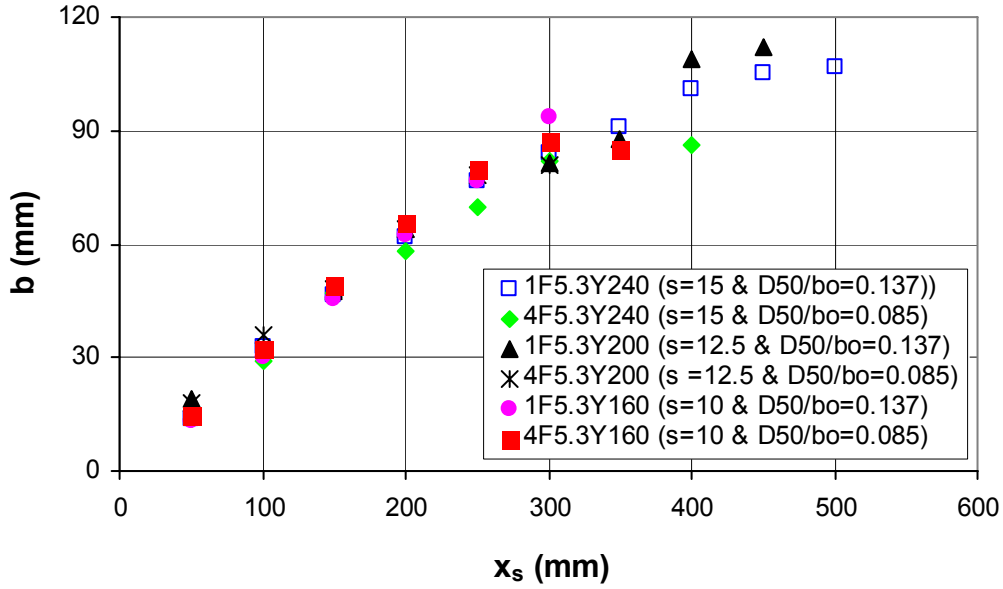

(b)

Figure 4.15 Growth of jet half-width in x-direction for (a) varied y_t/b_0 (F_0 = 5.8 & D_{50}/b_0 = 0.137) (b) varied D_{50}/b_0 (F_0 = 5.8 & y_t/b_0 = 15, 12.5 & 10)

4.4 Analysis of velocity measurements in the scour hole

4.4.1 Overview

In the following sections, an analysis of the velocity data is carried out in order to develop the relationships between the length and velocity scales that describe the characteristics of the jet. Further, attempts are also made to assess whether there exists similarity of velocity profiles under varied experimental conditions in the areas within forward jet flow and recirculating zone above the jet. For clarity, the analyses of the mean velocity in the forward flow near to the bed and reverse flow due to the roller are discussed separately.

Figure 4.16 shows a sketch of a typical velocity profile of the streamwise velocity, where u is the velocity of the forward flow in the streamwise direction and u_r is the velocity in the reverse flow. This applies to the bed-jet flow regime as there is no roller or recirculating zone for the surface-jet flow regime. This figure also serves to define the different velocity and length scales that are used in the following discussion. In Figure 4.16, the subscript m refers to a maximum in a vertical distribution, r refers to parameters pertaining to the reverse flow and y_s is the distance measured vertically downwards from the water surface. The length scale b has been defined as the distance from the bottom of the jet to where the time-averaged velocity $u = 0.5u_m$, and $du/dy < 0$. The length scale b_r applies to the time-averaged velocity in the reverse flow, u_r and is defined as the distance from the water surface to where the time-averaged velocity $u_r = 0.75u_s$ following Wu and Rajaratnam (1995). The symbol δ_1 is the value of y for which $u = 0$ and δ_2 is the height of the backward flow region (measured from the water surface).

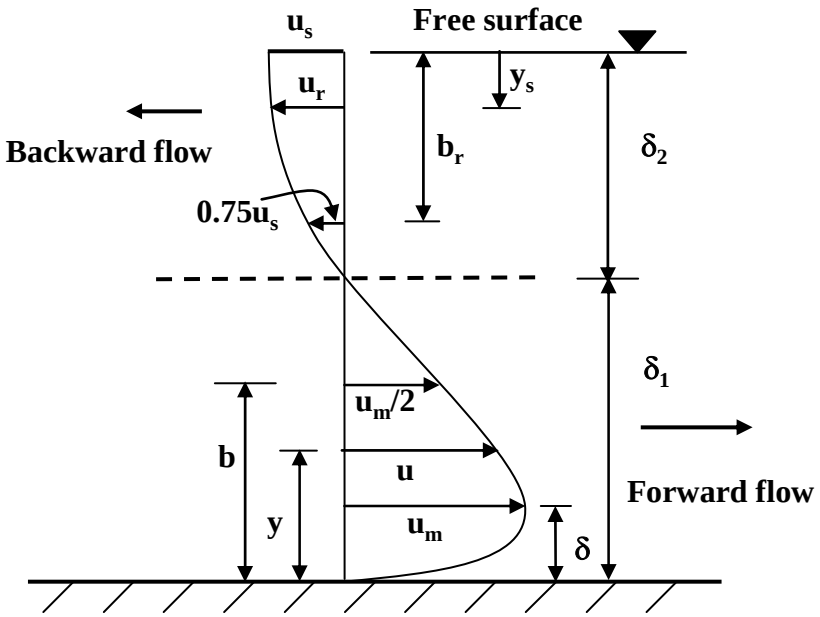

Figure 4.16 A typical velocity profile of time-averaged horizontal velocities, u and u_r in the forward and backward flow region of a "bed-jet" flow regime

4.4.2 Analysis of time-averaged streamwise velocity (in forward flow)

Let us consider the velocity field in the forward flow measured for the 13 experiments where a bed-jet flow regime was observed. The vertical velocity profiles for each experiment were plotted and a typical plot is shown in Figure 4.11. Velocity profiles are plotted in a non-dimensional form in Figure 4.17 for each experiment using u_m as the velocity scale and b as a length scale following Rajaratnam (1976). The data represents profiles from all experiments at different streamwise locations approximately between 100 mm < x < x_m. The velocity profile for the classical wall jet on a smooth rigid boundary as determined by Verhoff (1963) (cited in Rajaratnam (1976)) has also been superimposed on Figure 4.17 for comparison. From the plot, it appears that the velocity profiles in forward flow are similar but are significantly different from the profile for the classical wall jet (Equation 2.1). The thickness δ of the boundary layer is about 0.6b, whereas for the classical wall jet the corresponding value is about 0.16b. The value of 0.6b is even greater than the value of δ equal to 0.35b reported in a study of plane wall jet on rough, rigid boundaries by Ead and Rajaratnam (2004).

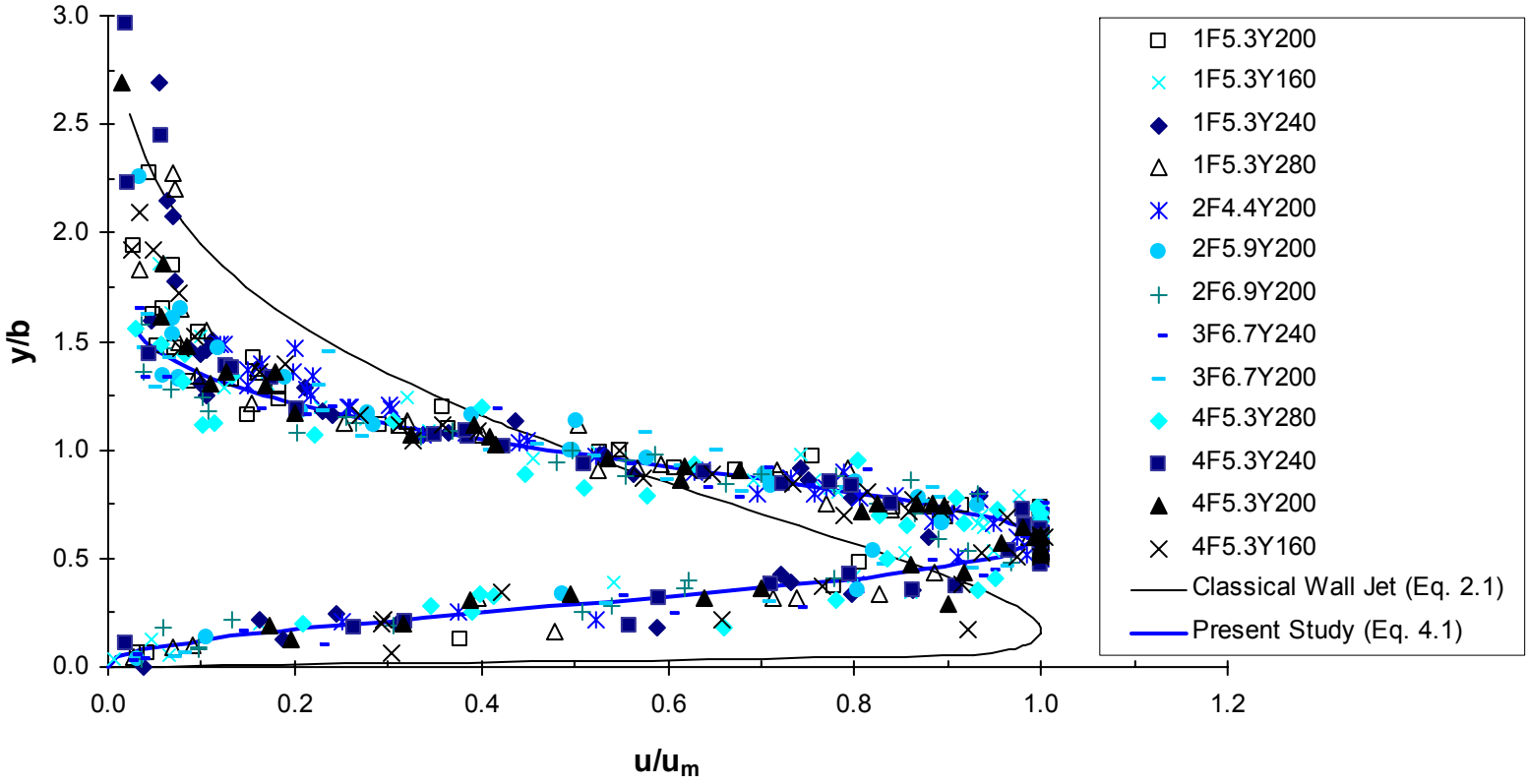

Figure 4.17 Dimensionless vertical velocity profiles for the forward flow (for the bed-jet flow regime) at various longitudinal positions downstream from the gate

Using the data from the present study and following the work of Rajaratnam (1976), a relationship between u/u_m and y/b was developed, which can be expressed as

$$\frac{u}{u_m} = 17.91\left(\frac{y}{b}\right)^{2.34}\left[1 - erf\left\{1.57\left(\frac{y}{b}\right)\right\}\right] \qquad (R^2 = 0.96) \qquad [4.1]$$

where erf is the error function. Figure 4.18 shows dimensionless velocity profiles for Experiment 4F5.3Y280 covering the whole range of scour hole length up to the mound top along with Equation 4.1. From Figure 4.18, it is apparent that the velocity profiles taken after x_s = 300 mm ($x_s > x_m$) and at x_s = 50 mm do not fall on the line representing Equation 4.1. Similar observations were observed for all other experiments. Therefore, while developing the Equation 4.1, only the velocity profiles in the range of 100 mm < x_s < x_m were considered.

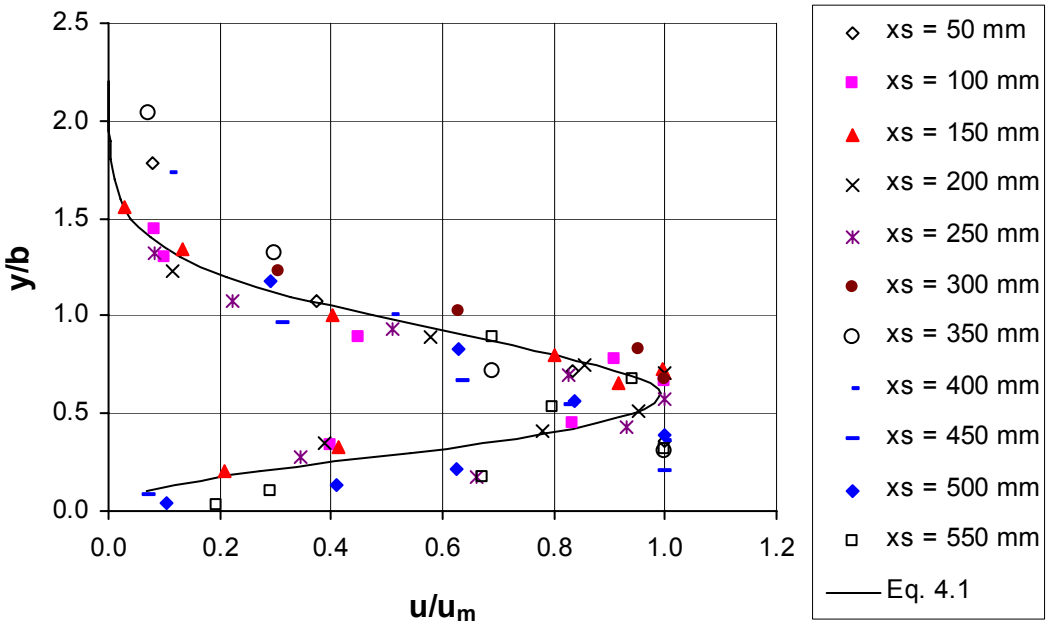

Figure 4.18 Dimensionless longitudinal velocity profiles covering profiles taken over the entire length of the scour hole for Experiment 4F5.3Y280

For the similar velocity profiles in the forward flow, it was necessary to investigate the variation of the maximum velocity u_m and the length scales b and δ with the streamwise distance x. Let us clarify here that x_s is the streamwise distance measured from the sluice gate and x is the streamwise distance measured from the end of the apron. Figures 4.19 and 4.20 show the variation of u_m with x_s in dimensionless form, where u_m is given in terms of the velocity of the jet at the end of the rigid apron, U_{0A}, and x is normalized with L. Here, L is defined as the distance from the edge of the apron to the location where u_m is equal to $0.5U_{0A}$. The values of L were calculated using the data of u_m versus x_s for each experiment using linear interpolation between data points where required. These L values are given in Table 4.2. The decay of maximum velocity for a plane wall jet on a smooth rigid boundary for submerged and free jumps from Wu and Rajaratnam (1995) is also given in Figure 4.19 for comparison.

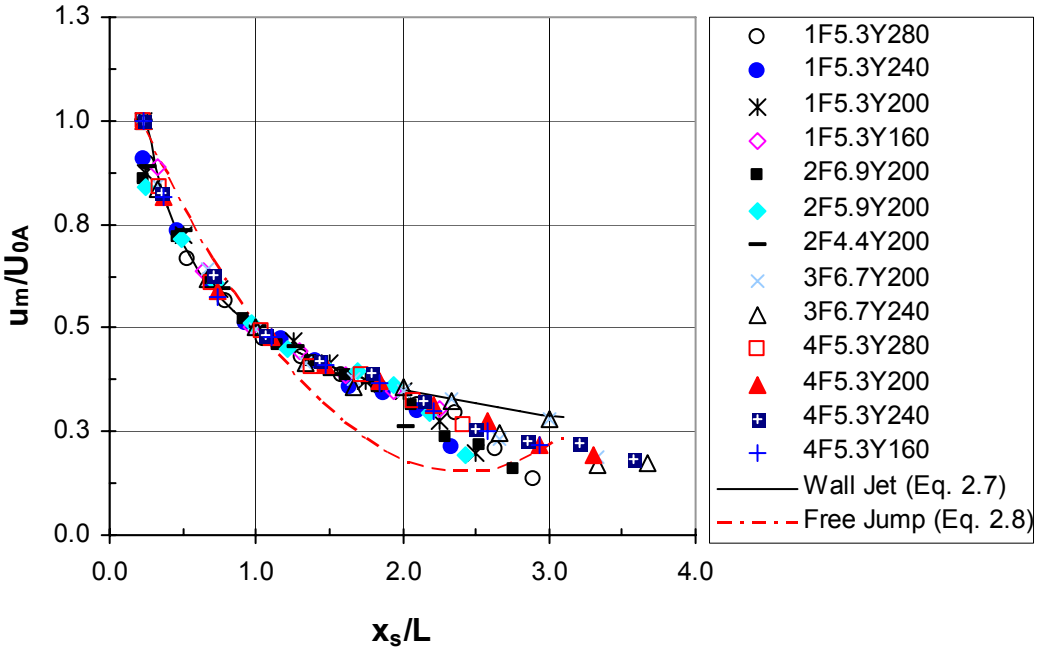

Figure 4.19 Decay of normalized maximum jet velocity, u_m/U_{0A} with normalized distance, x_s/L for bed-jet flow regime

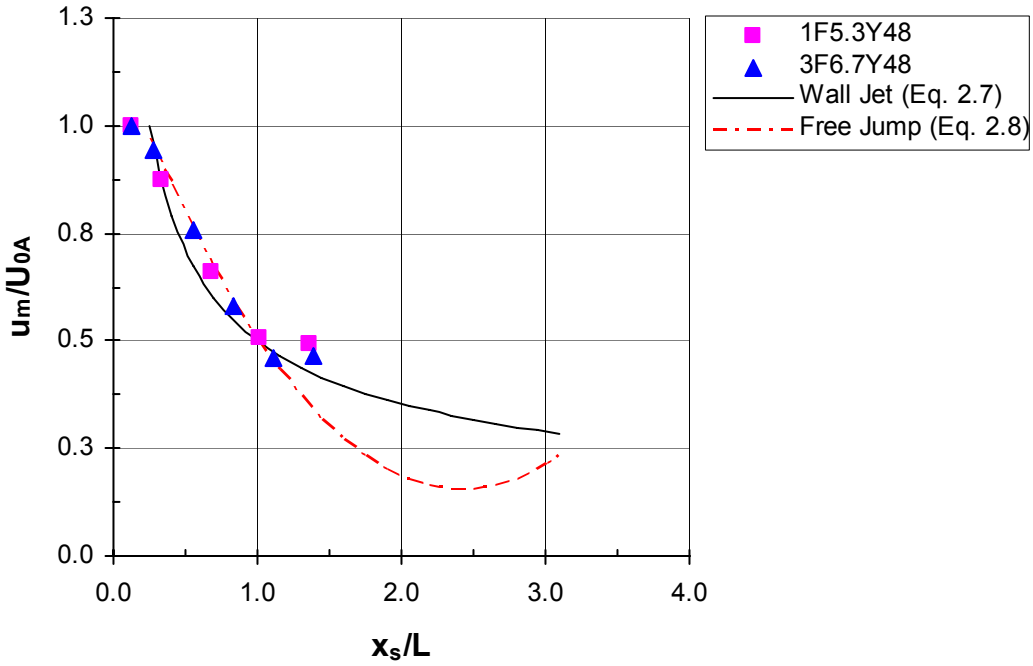

Figure 4.20 Decay of normalized maximum jet velocity, u_m/U_{0A} with normalized distance, x_s/L for "surface-jet" flow regime

Table 4.2 Summary of length scales for velocity profiles

Expt. No.	b_0 (mm)	y_t (mm)	U_{0A} (m/s)	y_2 (mm)	L (mm)	X_d (mm)	X_r (mm)	δ_{ma} (mm)	b_{ma} (mm)
1F5.3Y280	16	272	1.11	55.8	190	450	549	50	97
1F5.3Y240	16	240	1.06	53.1	214	449	501	54	90
1F5.3Y200	16	200	1.07	53.7	200	400	500	55	88
1F5.3Y160	16	160	1.10	55.0	175	250	400	52	94
1F5.3Y48	16	48	1.02	50.8	148	148	148	145	-
2F4.4Y200	16	200	0.88	42.9	198	346	401	45	82
2F5.9Y200	16	200	1.18	59.6	206	400	501	56	107
2F6.9Y200	16	200	1.35	69.7	218	449	600	76	130
3F6.7Y240	16	240	1.09	54.8	150	353	551	70	113
3F6.7Y200	16	200	1.07	53.6	150	353	551	71	120
3F6.7Y48	16	48	1.09	54.6	180	225	225	145	-
4F5.3Y280	16	280	0.87	42.0	145	300	550	49	80
4F5.3Y240	16	240	0.85	41.3	140	322	500	49	82
4F5.3Y200	16	200	0.87	42.5	136	299	450	45	81
4F5.3Y160	16	160	0.86	42.0	136	250	400	51	86

Note: The origin for all the longitudinal distances is taken from the edge of rigid apron (length of apron = 50 mm)

In Figure 4.19, the first stage of velocity decay (for the experiments with the bed-jet flow regime) follows that of a wall jet on smooth and rough rigid beds to x equal to 2L. In Figure 4.20, for the "surface-jet" flow regime, the decay of velocity was observed to be similar to that of a free-jump up to x/L of about 1. It is important to note that the values of length scale, L which were obtained for the flow in the scour hole for both the bed-jet and surface-jet flow regimes, were found to be smaller than that found for submerged jumps (Equation 2.12) and free jump (Equation 2.8) on smooth rigid beds (Wu and Rajaratnam 1995), and plane wall jets on smooth rigid boundaries (Long et al. 1990). Using equivalent sand roughness, k_s, equal to $2D_{50}$ (Chiew 2004), a value of length scale L equal to 480 mm for the Experiment 1F5.3Y280 (k_s/b_0 = 0.275) was observed from the plot of L/b_0 with k_s/b_0 developed for the jet flow in rough, rigid boundary (Ead and Rajaratnam 2004), whereas the observed value of L for that experiment from this study is 190 mm. This result reveals that the decay of velocity for the jet flow inside the scour hole (a rough boundary) is much quicker than that for the jets in rough rigid beds. For the bed-jet regime experiments, the decay in maximum velocity followed the equation developed by Wu and Rajaratnam (1995):

$$\frac{u_m}{U_{0A}} = 0.50\left(\frac{x_s}{L}\right)^{-0.50} \qquad (R^2 = 0.99) \qquad [4.2]$$

Equation 4.2 was found applicable for the range of $0.25L < x_s < X_d$, where X_d is the distance from the edge of the rigid apron to the point where the second stage velocity decay starts. Unlike in the first stage, the decay of maximum velocity in the second stage was more rapid and followed an almost linear decay up to the distance, X_r (defined as a distance from the edge of the rigid apron to where the velocity starts to recover). Similarly, the decay of velocity in the second stage ($X_d < x_s < X_r$) for the "bed-jet" flow regime was found to be described by the equation

$$\frac{u_m}{u_{md}} = 1.00 - 0.91\left(\frac{x_s - X_d}{L}\right) + 0.50\left(\frac{x_s - X_d}{L}\right)^2 \qquad (R^2 = 0.77) \qquad [4.3]$$

where the velocity scale u_{md} is the velocity u_m at $x_s = X_d$ that can be calculated using Equation 4.2 by setting $x_s = X_d$. The values of X_d and X_r obtained (by plotting u_m versus x and through linear interpolation) for all experiments of this study are given in

Table 4.2. No equations for velocity were developed for surface-jet regime due to lack of data.

To analyze the experimental results of X_d and X_r, it was noticed that L appeared to be a function of F_0, y_t/b_0, and D_{50}/b_0.

$$\frac{X_d}{L} = 0.14 + 0.20F_0 + 0.04\left(\frac{y_t}{b_0}\right) + 1.4\left(\frac{D_{50}}{b_0}\right) \qquad (R_a^2 = 0.93) \qquad [4.4]$$

$$\frac{X_r}{L} = 0.12 + 0.31F_0 + 0.16\left(\frac{y_t}{b_0}\right) - 8.71\left(\frac{D_{50}}{b_0}\right) \qquad (R_a^2 = 0.89) \qquad [4.5]$$

Different potential length scales (for example, b_0, y_2, y_t, and L) were tested for the proper selection of length scale for non-dimensionalizing X_d and X_r in Equations 4.4 and 4.5. From the tested scales, L was chosen as it was found more capable of bringing all data points together. Furthermore, the value of densimetric Froude number, F_0 in the above equations was calculated using the measured velocity at the end of the rigid apron, U_{0A}.

Let us consider the development of an equation for length scale L that would be suitable for the jet flow in the scour hole with the bed-jet flow regime. Again, using multiple linear regression analysis and some trial and error, it was found that L could be best described by

$$\frac{L}{y_2} = 3.76 - 0.36F_0 + 0.16\left(\frac{y_t}{b_0}\right) + 12.22\left(\frac{D_{50}}{b_0}\right) \qquad (R_a^2 = 0.87) \qquad [4.6]$$

As in the case of X_d and X_r, different potential length scales were tested for non-dimensionalizing L in Equation 4.6. From that, y_2 was selected as this scale was found more capable of bringing all data points together.

It should be noted that other potential scales for scaling u_m in the variation of u_m with x were tested in addition to L. These include those of Tachie et al. (2004) for plane wall jet flows on rough rigid boundaries in deep tailwater conditions (the momentum-

viscosity scaling); Nik Hassan and Narayanan (1985) for plane wall jet flows on erodible boundaries in deep tailwater (δ_A); and the conventional scale b_0. However, these scales were not capable of grouping the variation of u_m along the scour hole together onto one curve.

Using the velocity profiles developed for the forward flow in the region with similar velocity profiles, the momentum flux per unit width for the experiments with varied y_t/b_0, but fixed F_0 and D_{50}/b_0, was calculated. Figure 4.21 shows the variation of the normalized momentum flux, M/M_{0A} in the x-direction of the scour hole for those experiments, where M_{0A} is the momentum flux at section x_s = 50 mm from the gate. Figure 4.21 also shows that the percentage losses in the initial momentum flux between x_s/b_0 = 3.13 – 12.5 are 32.3, 30.0, and 49.5 for the submergence ratio 17, 15, and 10, respectively. It appears that an increase in y_t/b_0 for a fixed value of F_0 and D_{50}/b_0 decreases the decay of the momentum flux, M.

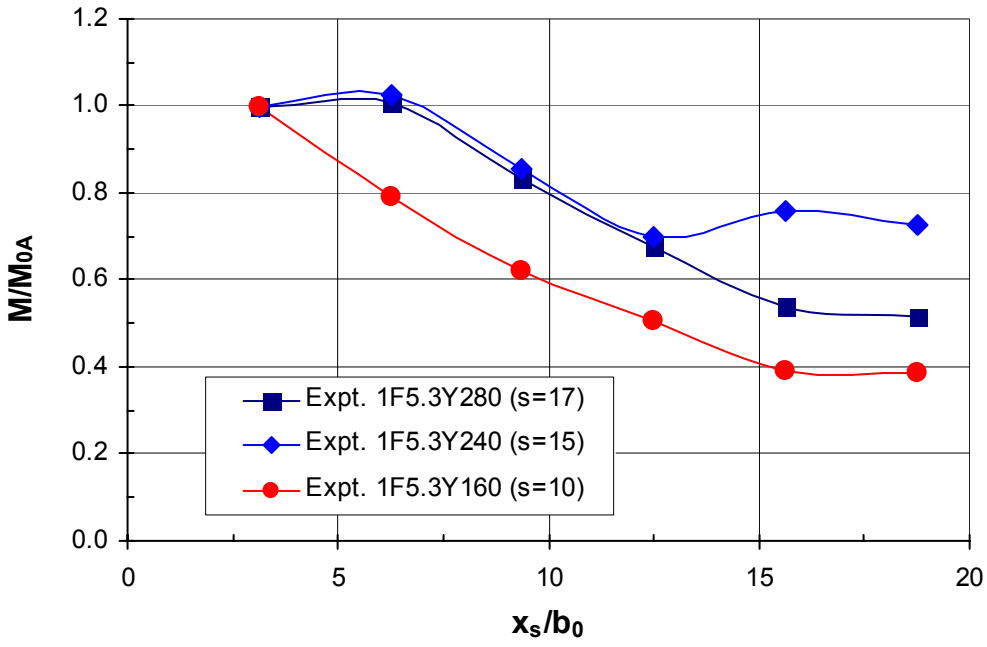

Figure 4.21 Variation of normalized bed-jet momentum flux, M/M_0 with normalized distance, x_s/b_0 for varied y_t/b_0

The growth of the normalized boundary layer thickness, δ/L with the normalized horizontal distance, x_s/L (in the region of similar velocity profiles) for the "bed-jet" flow regime is shown in Figure 4.22. Here, L is chosen for scaling δ and x_s because, as discussed in the previous section, it was observed that the growth of δ was influenced by F_0, y_t/b_0 and D_{50}/b_0 and the length scale L was found to be able to incorporate the effects of those three parameters on the flow fields in the streamwise direction in the scour hole. In addition, other potential scales (for example, b_0, y_2, and y_t) were also tested and were not found suitable. Using the experimental data set, an empirical relationship to describe the streamwise development of δ, which is good for the range of approximately $0.25 < x_s/L < 1.30$, was developed and is given by

$$\frac{\delta}{L} = 0.150\left(\frac{x_s}{L}\right) + 0.073 \qquad (R^2 = 0.94) \qquad [4.7]$$

Figure 4.22 shows the fit of this equation to the experimental data. For comparison of the results of this study with those of Ead and Rajaratnam (2004), a relationship between δ/b_0 versus x_s/b_0 was also developed. From that, a value of 0.14 for the slope of the plot δ/b_0 versus x_s/b_0 was observed, which is much larger than the value of 0.044 found by Ead and Rajaratnam (2004) for plane wall jets on rough boundaries with shallow tailwater.

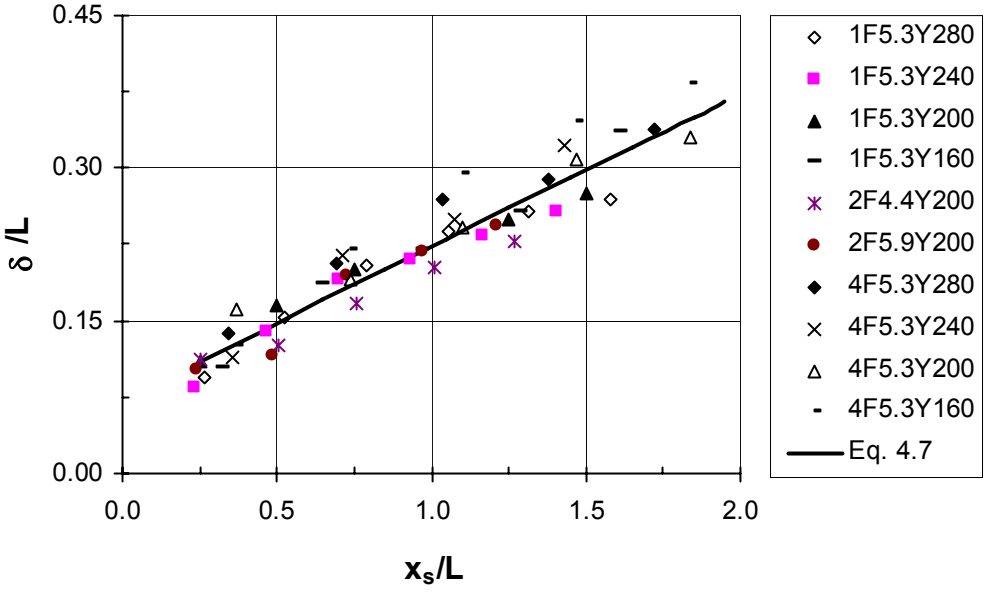

Figure 4.22 Development of dimensionless boundary layer δ

Figure 4.23 shows the growth of the normalized jet-half width b/L with the normalized longitudinal distance x_s/L for all the experiments with the bed-jet flow regime. As in the case of δ, here also L was chosen as a scale for normalizing b and x_s because it worked well compared with other potential scales. As in the case of δ/L, the growth of the b/L was also found to be linear, but with a different growth rate of 0.287 (see Equation 4.8). For the comparison of the results of this study with that of Ead and Rajaratnam (2004), a relationship between b/b_0 versus x_s/b_0 was also developed. From that, a value of 0.287 (the same as that observed using L as length scale) for the slope of the plot b/b_0 versus x_s/b_0 was observed, which is much larger than the value of 0.125 observed by Ead and Rajaratnam (2004) for plane wall jets on rough boundaries. It was also found that the data for b ($0.25 < x_s/L < 1.50$) could be best fit by:

$$\frac{b}{L} = 0.287\left(\frac{x_s}{L}\right) + 0.016 \qquad (R^2 = 0.97) \qquad [4.8]$$

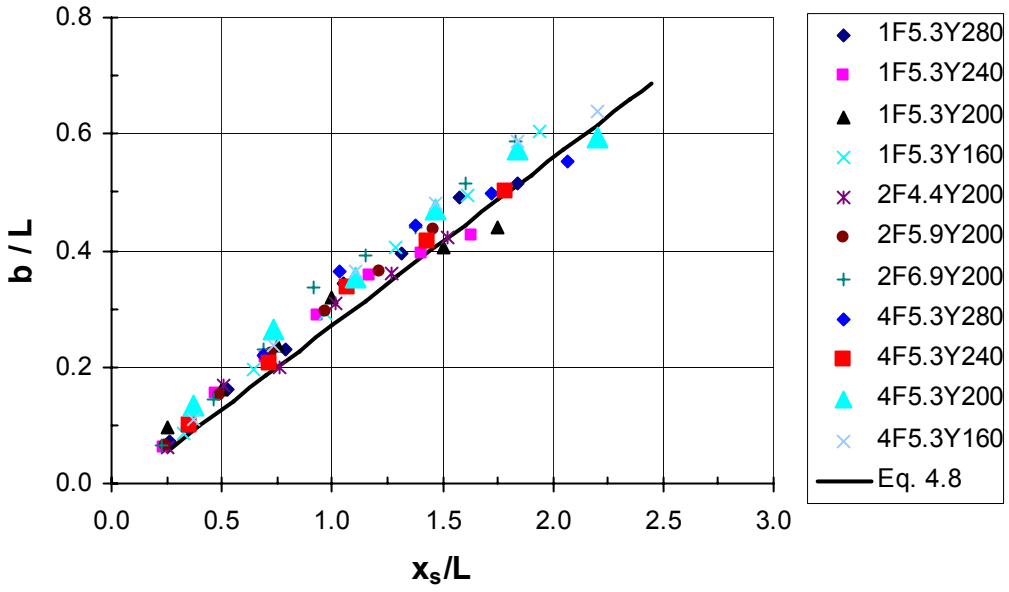

Figure 4.23 Development of dimensionless half-width b

A plot of δ/b with distance along the scour hole, x_s/b_0 is shown in Figure 4.24. Here, for the comparison of the results of this study with that of Ead and Rajaratnam (2004), b_0 is chosen as the length scale for normalizing x_s instead of L. From Figure

4.24, although δ/b seems to get slightly smaller with increasing $x_s/b_{0,}$ δ/b is approximately equal to 0.60 for the present experiments. This value of 0.60 is much larger than the value of 0.35 suggested by Ead and Rajaratnam (2004) for plane turbulent wall jets on rough boundaries. This higher value suggests that the diffusion rate (in vertical direction) of a jet passing through a scour hole is much faster than a jet along a rigid rough boundary.

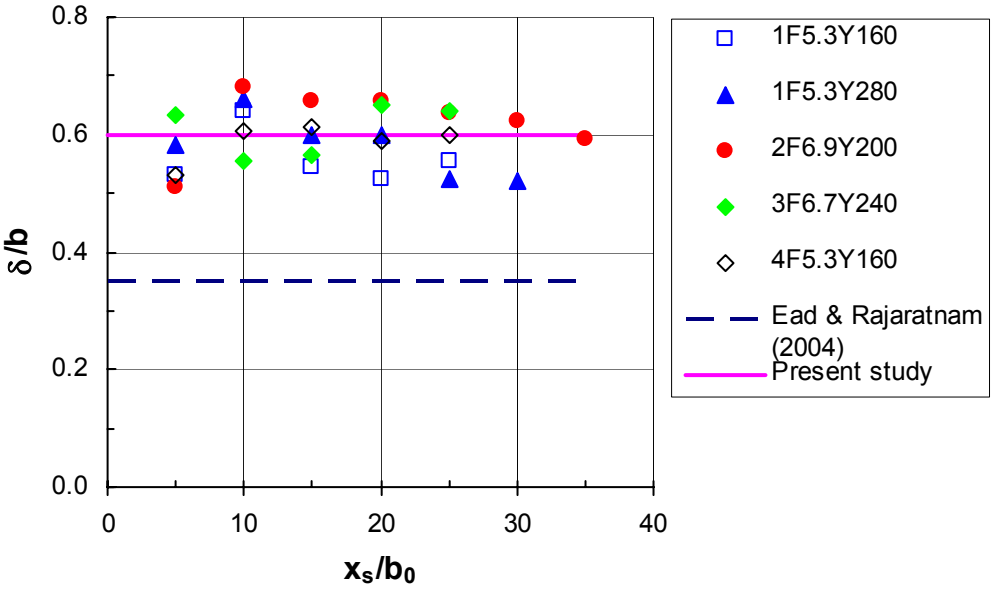

Figure 4.24 Ratio of δ/b for "bed-jet" flow regimes

4.4.3 Analysis of mean flow velocity (in backward flow)

Further analysis of the velocity data obtained from the present study is carried out by plotting the velocity profiles of the backward flow produced by the bed jets, which occurs in the upper portion of the scour hole (near to the gate). It should be noted that the surface velocity, u_s, here actually represents the velocity measured approximately 10 mm from the surface as it was not possible to measure the velocity very close to the water surface due to the limitations of the ADV. Following the approach of Wu and Rajaratnam (1995), Figure 4.25 shows the velocity profiles in a dimensionless form, with u/u_s against y_s/b_r, where, u_s, y_s, and b_r are as described earlier in Figure 4.17. Here, the velocity and length scale u_s and b_r are chosen following Wu and Rajaratnam (1995). From Figure 4.25, it can be seen that the velocity profiles

approximately exhibit geometrical similarity with only some exceptions near to the boundary separating the backward and forward flow and can be described by:

$$\frac{u}{u_s} = 0.025\left(\frac{y_s}{b_r}\right)^2 - 0.300\left(\frac{y_s}{b_r}\right) + 1.038 \qquad (R^2 = 0.96) \qquad [4.9]$$

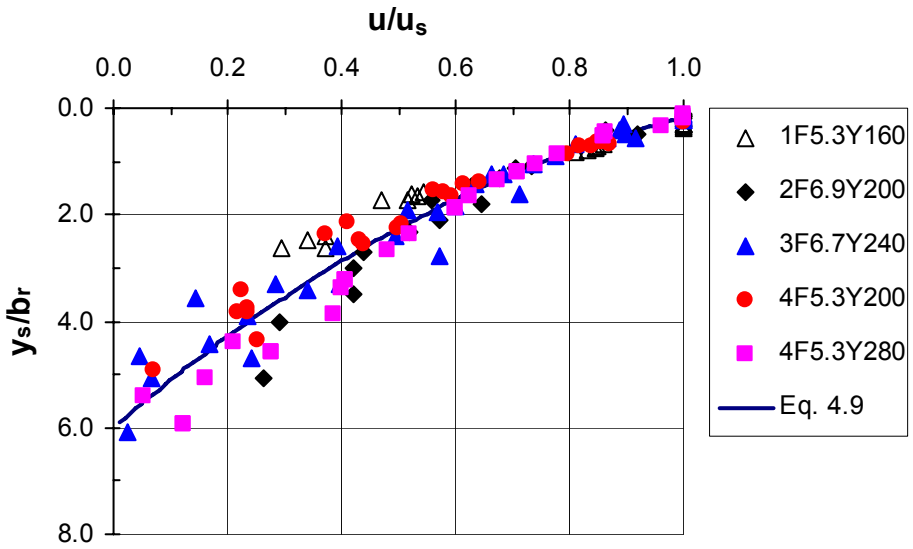

Figure 4.25 Dimensionless reverse flow velocity profiles in a scour hole developed by a bed-jet flow regime

Following Wu and Rajaratnam (1995) for analysis of submerged jumps on smooth beds, analysis of the velocity measurements shows that the normalized length scale, b_r/y_t is equal to 0.11. This value of 0.11 is much lower than the value of 0.20 suggested by Wu and Rajaratnam (1995). Similarly, choosing u_{sm} and L_e as the velocity and length scales again following Wu and Rajaratnam (1995), an empirical relation was developed for u_s in terms of maximum surface velocity, u_{sm}, given by

$$\frac{u_s}{u_{sm}} = -5.466\left(\frac{x_s}{L_e}\right)^3 + 3.268\left(\frac{x_s}{L_e}\right)^2 + 1.285\left(\frac{x_s}{L_e}\right) + 0.189 \qquad (R^2 = 0.96) \qquad [4.10]$$

where L_e is the length of the surface eddy. Figure 4.25 shows the variation of u_s/u_{sm} against x_s/L_e. From Figure 4.26, it appears that u_s is maximum at a distance x_s approximately equal to $0.54L_e$. Further, following the approach almost similar to that

suggested in Wu and Rajaratnam (1995), the other velocity scale, u_{sm} normalized with jet velocity, U_0 was found to be described by

$$\frac{u_{sm}}{U_0} = 1.187 F_0^{-0.654} S^{-0.164} \qquad (R^2 = 0.86) \qquad [4.11]$$

Here, F_0 was used in place of F_r used by Wu and Rajaratnam (1995).

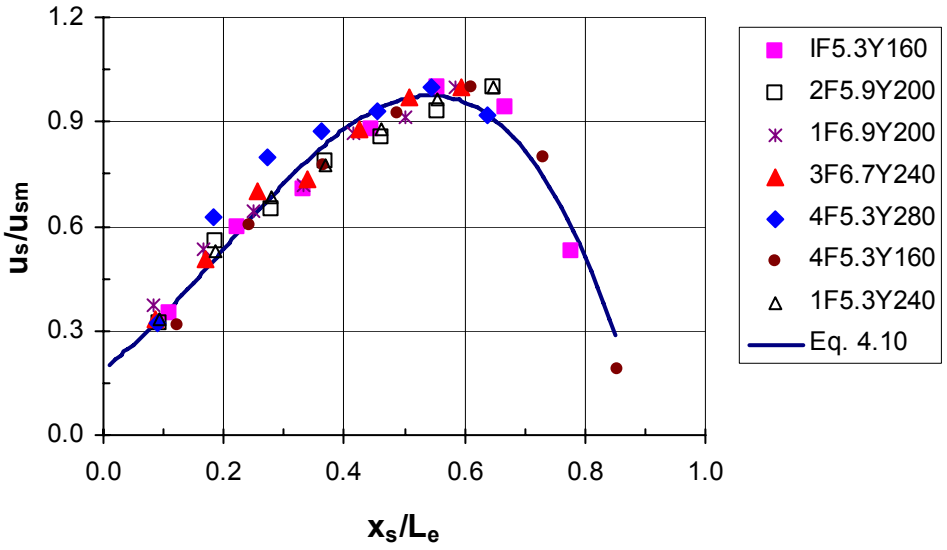

Figure 4.26 Variation of velocity scale u_s along reverse flow

Considering the distance from the sluice gate to the distance where $u_s = 0$ as an eddy length L_e, an equation for L_e for flow in scour holes produced in the "bed-jet" flow regime was formulated as

$$\frac{L_e}{y_2} = 6.34 + 1.20S \qquad (R^2 = 0.96) \qquad [4.12]$$

Comparing the eddy length computed from Equation 4.12 to that of a submerged jump in a rigid smooth boundary as suggested by Wu and Rajaratnam (1995) for an experiment of this study (Expt. 1F5.3Y280), L_e for a bed-jet in an erodible boundary with a scour hole was found to be lower by 33.5% than the L_e for a submerged jump in rigid boundary. However, the present observation of a lower value of L_e agrees with the

observation of Shabayek (2007a) and Carollo et al. (2007), where the length of roller of a submerged jump on rough beds was found appreciably lower than that on smooth bed.

4.4.4 Analysis of turbulence

Following the approach of Long et al. (1990), Figure 4.27 gives the variation of maximum root-mean-square of the fluctuating velocity component in the x-direction of the forward flow normalized with the maximum root-mean-square velocity of the longitudinal velocity component at the end of the rigid apron, $\sqrt{(u'^2)_{mA}}$, $\sqrt{(u'^2)_m}$ with the normalized distance, x_s/L. It is noted that there exists significant variation of $\sqrt{(u'^2)_m}$ along the scour hole. An increase in the RMS value on the downstream face of the scour hole is observed, which is different than that generally observed in submerged jets on a rigid boundary, where a decrease in the value of the RMS value occurs after its maximum value near to the gate opening. The use of length scale for normalizing the horizontal distance, x_s shows that to some extent, the length scale L is capable of grouping the $\sqrt{(u'^2)_m}$ together for different "bed-jet" flow regimes of varying F_0, y_t/b_0, and D_{50}/b_0.

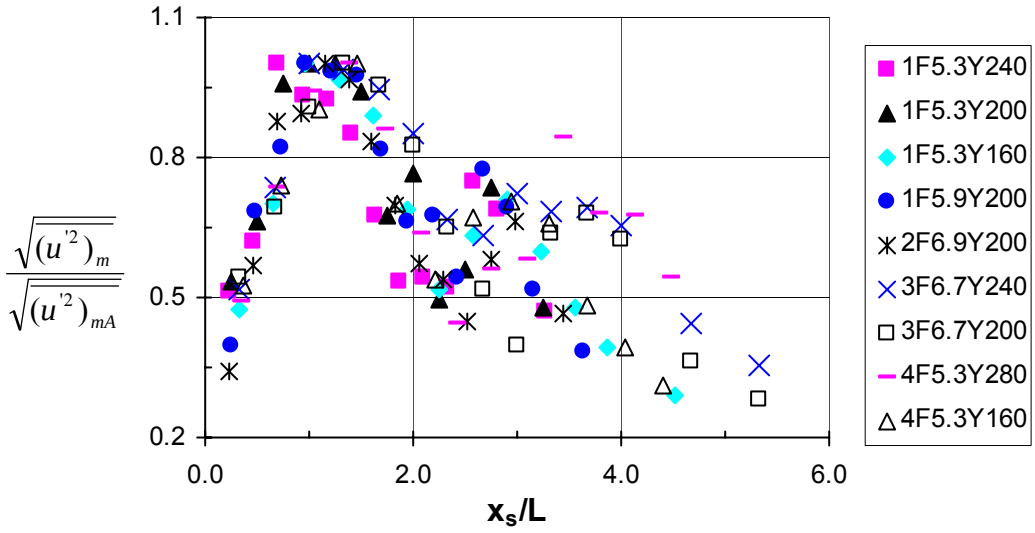

Figure 4.27 Variation of normalized maximum root-mean-square of the fluctuating velocity component against normalized longitudinal distance

4.5 Comparison of the jet scales for scour with the size of the scour hole

In this study, some length scales that can be used to describe the flow or jet behavior in the vertical as well as streamwise directions inside a scour hole produced by a plane wall jet have been identified. They include, L, X_d, X_r, δ, and b for the forward flow and L_e and b_r for the reverse flow. Here, a comparison between the scales for the jet and the scour hole dimensions is given. To describe the scour hole, the dimensions at the asymptotic state are used.

Figure 4.28(a-b) shows the ratio of the variation of the location of the maximum scour depth, x_{ma} and the length of the scour hole, x_{0a} measured for the experiments with a bed-jet flow regime to the jet characteristic length L. The ratio is plotted against the submergence ratio to examine whether there are any submergence effects. It is seen in Figure 4.28(a-b) that the variation of x_{ma}/L and x_{0a}/L with y_t/b_0 (for a bed-jet flow regime) is almost constant and approximately equal to 1.6 and 2.5, respectively. However, for the two experiments with the surface-jet flow regime, relatively higher values of x_{ma}/L and x_{0a}/L approximately equal to 4.2 and 9.4 respectively, were observed.

Similarly, the ratios of x_{ma} and x_{0a} for bed-jet and surface-jet flow regime to the distances X_d and X_r were also investigated. The variation of x_{ma}/X_d, x_{0a}/X_d, x_{ma}/X_r, and x_{0a}/X_r with y_t/b_0 for a bed-jet flow regime were observed approximately constant with the values approximately equal to 0.8, 1.3, 0.6 and 0.9, respectively. The corresponding values for the surface-jet flow regime were 3.2, 7.0, 3.2 and 7.0, respectively.

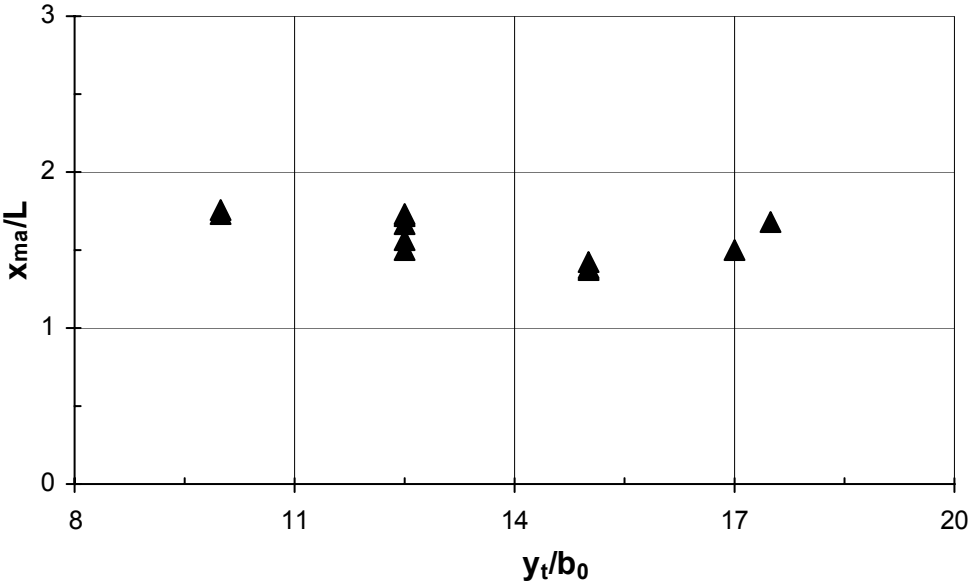

(a)

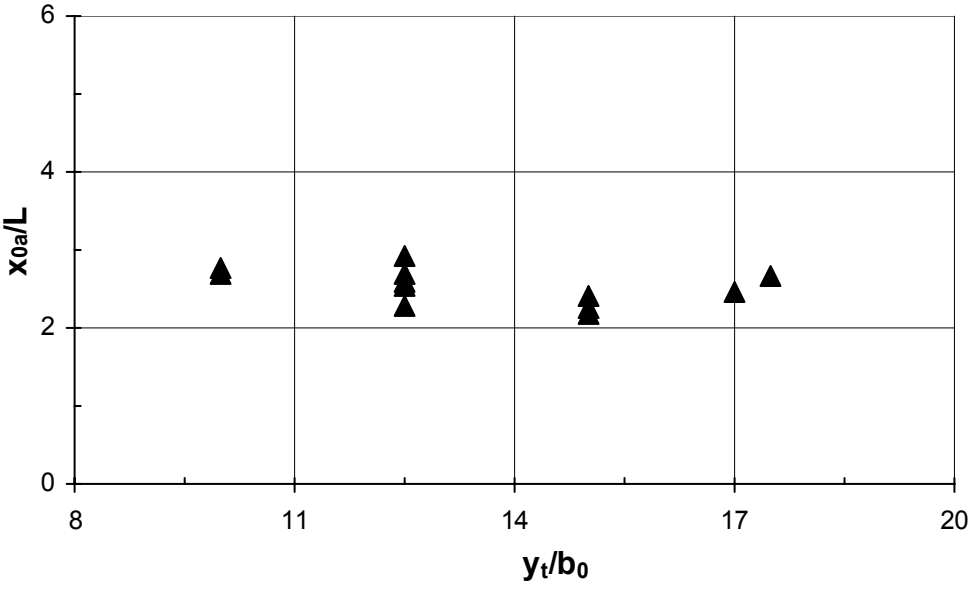

(b)

Figure 4.28 Ratio of x_{ma} and x_{0a} to jet length scale L with submergence ratio (a) x_{ma}/L (b) x_{0a}/L

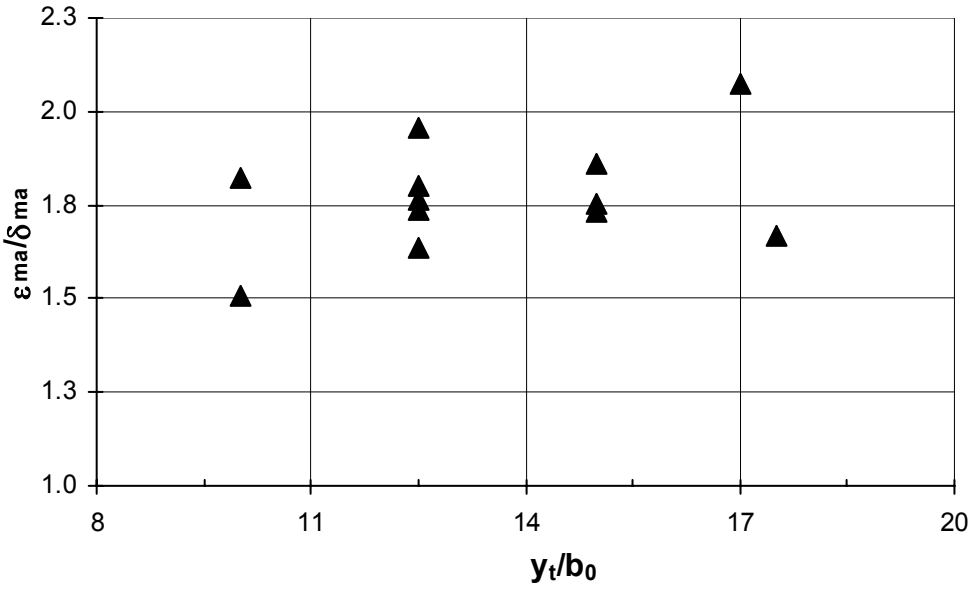

(a)

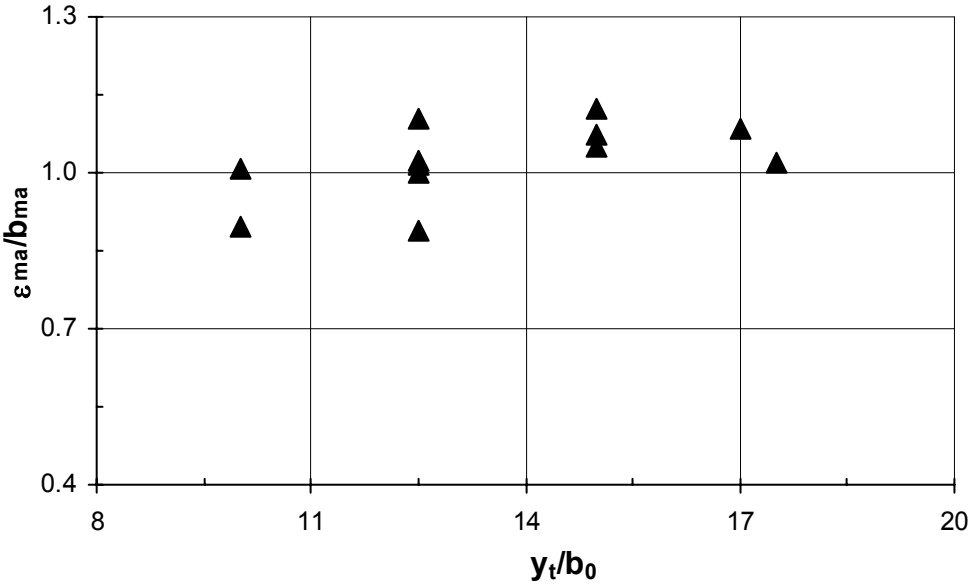

(b)

Figure 4.29 Variation of maximum scour depth made dimensionless with jet length scales δ_{ma} and b_{ma} with submergence ratio (a) $\varepsilon_{ma}/\delta_{ma}$ (b) ε_{ma}/b_{ma}

The ratio of maximum scour depth (for bed-jet flow regime) made dimensionless with two jet scales, δ_{ma} and b_{ma}, with y_t/b_0 is shown in Figure 4.29(a-b). From Figure 4.29(a-b), it appears that the growth of $\varepsilon_{ma}/\delta_{ma}$ and ε_{ma}/b_{ma} are also approximately constant values of 1.8 and 1.0, respectively. A smaller value of $\varepsilon_{ma}/\delta_{ma} \approx 0.7$ was found for surface-jet flow regime.

4.6 Analysis of errors

The analysis of the errors in the measured and derived quantities in the experiments is presented below. The calculations used to estimate the errors are based on the methodology outlined in Topping (1957). The errors calculated are the maximum errors and represent the worst case.

The measurement of the sluice gate opening (b_0) was made using a digital caliper of precision of 0.01 mm, which results an estimated error in the measurement of b_0 equal to 0.06%. However, an average variation of the opening across the flume of about 0.5 mm was observed, which results in an estimated error in the measurement of b_0 equal to 3.12%. The channel width (W) was measured using a measuring tape with the precision of 1 mm, which yields an error in the measurement of W of 0.20%. A magnetic flow meter of precision of 0.01 L/s was used to measure the flow rate, Q, of the tests. Due to fluctuations in the reading showed by the flow meter, flow rate could be read approximately only to the nearest ± 0.20 L/s. This gives the maximum error in the measurement of Q of 3.17%. Using the estimated errors calculated for b_0, W, and Q, the maximum error in the derived jet velocity at gate opening (U_0) can be estimated as 6.49%. Using the errors in U_0 and b_0, the error in the derived source Froude number (F_r) can be estimated as 8.05%. A 3% precision in sieve analysis for aggregates with nominal maximum size of 19 mm is suggested by ASTM C670 (2003). Considering the suggested precision of 3% for D_{50}, the error in the derived source densimetric Froude number (F_0) can be estimated as 7.99%.

All the vertical dimensions of water surface and scour profiles were measured using digital point gauge with precision of 0.01 mm. However, due to free surface

turbulence, tailwater depth (y_t) could be read only to the nearest of about ±1 mm. Similarly, due to the movement of sediments and their gradation/varied size, all the vertical depths and heights of the scour hole and mound could be read only to nearest of approximately $\pm D_{50}$ mm. Considering these accuracy, the maximum estimated error in reading tailwater depth (y_t), maximum scour depth (ε_m), and maximum mound height (Δ_m) can be of 2.08%, 2.89% and 3.92%, respectively. Estimated errors of 4.78% and 2.85% in the derived water depth above mound peak (y_m) and the depression in water surface depth (δ_w) were estimated, respectively. The horizontal characteristic dimensions of scour and water surface profiles: the distance to maximum scour depth (x_m); scour hole length (x_0); distance to maximum mound height (x_d); distance to downstream toe of the mound (x_{0d}); and the eddy length (L_e) were measured using a measuring tape fixed to flume wall with the reading precision of 2 mm. This yields estimated maximum errors for distance of x_m, x_0, x_d, x_{0d}, and L_e of 0.83%, 0.53%, 0.38%, 0.32%, and 0.49%, respectively. Considering the errors estimated for the characteristic dimensions of the scour hole, the estimated errors for ε_m/b_0, Δ_m/b_0, y_m/b_0, x_m/b_0, x_0/b_0, x_d/b_0, and x_{0d}/b_0 become 6.01%, 7.04%, 7.9%, 3.95%, 3.65%, 3.5% and 3.50%, respectively.

According to Lohrmann et al. (1995), the ADV mean flow velocities (u, v, w) are accurate to within 1% of the measured velocity, even though its measurements are controlled by number of parameters. Similarly, the presence of very small errors in the measured instantaneous velocity by the ADV is reported by McLelland and Nicholas (2000). Therefore, following the accuracy range of 1% for measured mean velocities, the estimated error of normalized maximum mean velocities, u_m/U_0 and u_m/U_{0A} can be estimated as 7.49% and 2%, respectively. The errors estimated above are summarized in Table 4.3.

Table 4.3 Maximum errors in measured and derived quantities

Quantity	Maximum errors (%)	Notes
b_0	3.12	
W	0.20	
Q	3.17	
U_0	6.49	
F_r	8.05	
D_{50}	3.00	As suggested by ASTM C670 (2003)
F_0	7.49	
y_t	2.08	
ε_m	2.89	
Δ_m	3.92	Profile for surface-jet regime not considered
y_m	4.78	
δ_m	2.85	
x_m	0.83	
x_0	0.53	
x_d	0.38	
x_{0d}	0.32	
L_e	0.49	
ε_m/b_0	6.01	
Δ_m/b_0	7.04	
y_m/b_0	7.90	
x_m/b_0	3.95	
x_0/b_0	3.65	
x_d/b_0	3.50	
x_{0d}/b_0	3.50	
u, v, w	1.00	As suggested by Lohrmann et al. (1995)
u_m/U_0	7.49	
u_m/U_{0A}	2.00	

CHAPTER 5: SUMMARY, CONCLUSIONS, AND RECOMMENDATIONS

5.1 Summary

Based on the experimental observations and analysis made on the development of a scour hole and the associated flow fields inside the scour hole downstream of a sluice opening due to a plane wall jet, the key findings of the study are summarized as follows:

1. As observed in previous studies, the scour hole dimensions for all submergences in experiments with a bed-jet or a surface-jet flow regime grew in an approximately linear manner with the logarithmic of time up to certain time before they deviate to a horizontal asymptote, called the beginning of the asymptotic state.
2. The magnitude of the maximum scour depth, ε_{ma}, for a given densimetric Froude number and relative boundary roughness was found to increase with increasing submergence ratio for all experiments where the bed-jet flow regime was observed. A similar trend of larger scour hole dimensions for deeper submergence was also found for the other asymptotic state scour hole dimensions x_{0a}, x_{da}, and Δ_{ma}. Later, after the analysis of the velocity data, it was found that the general trend of such deeper scour holes for deeper submergence was due to the faster velocity decay of the jet at shallower submergences.
3. For a given F_0 and s, maximum scour depth, ε_{ma} was found to increase with increasing relative boundary roughness, D_{50}/b_0.
4. The effect of submergence on the variation of scour hole across the width of flume was observed to be significant. A larger variation in scour profiles for lower submergence as compared with the higher submergences was observed.

5. The flow pattern inside the scour hole was observed to be almost similar to that of a submerged hydraulic jump on a smooth rigid horizontal bed, except for the occurrence of two eddies in the clockwise direction at the upstream and downstream ends of the scour hole (near to the scoured bed). The size of those eddies were found to increase with increasing submergence.
6. For the experiments with the bed-jet regime, two distinct stages in the variation of maximum time-averaged streamwise velocity with streamwise distance, normalized using L, as was observed for smooth and rough rigid boundaries (Ead and Rajaratnam 2002 & 2004) were observed for the jet flows inside the scour hole. The first stage of velocity decay was characterized by a curvilinear variation of velocity following the decay curve that of a wall jet on smooth and rough rigid beds to $x_s = X_d$ (or approximately 2L). For the "surface-jet" flow regime, the variation of maximum x-direction velocity was observed similar to that of a free-jump for x_s approximately equal to L. The jet length scale L for scour was defined as the distance from the edge of the apron, where the maximum velocity, u_m is equal to $0.5U_{0A}$ and its value obtained for the flow in the scour hole were found to be smaller than that found for submerged jumps and free jump on smooth and rough rigid beds (Wu and Rajaratnam 1995, Long et al. 1990; Ead and Rajaratnam 2004) indicating a quicker decay of velocity inside the scour hole than for the jets in smooth and rough rigid beds.
7. Unlike in the first stage, the variation of maximum velocity with streamwise distance in the second stage was more rapid and was almost linear up to the point, X_r (defined as a distance from the edge of rigid apron to where the velocity starts to recover). The second stage decay was not observed for the surface-jet regime.
8. A faster decay of maximum velocity, u_m with decreasing value of the submergence ratio, densimetric Froude number and the relative boundary roughness was observed.
9. For a given value of F_0 and D_{50}/b_0, a faster decay of momentum flux per unit channel width in the x-direction with a decrease in the value of y_t/b_0 was found.

10. The jet length scales, L, X_d, and X_r, which describe the jet characteristics in the x-direction, were found to be functions of F_0, y_t/b_0, and D_{50}/b_0. Using those parameters, empirical relationships for L, X_d, and X_r were formulated.
11. As in the case of u_m variation, two stages were also observed in the growth of boundary layer thickness, δ and the jet-half width, b. However, unlike in the decay of u_m, the growth of δ and b in the first stage was linear up to a certain point (approximately equal to x_m), beyond which the growth rates become curvilinear with decreased growth rate. Further, the growth of δ and b in the non-linear region was more influenced by the change in y_t/b_0, and D_{50}/b_0 than in the region with linear growth.
12. The growth of b as compared with the growth of δ was found similar with a constant ratio of $\delta/b = 0.6$ for the first stage, which is much larger than the value of 0.35 reported for rigid rough boundaries (Ead and Rajaratnam 2004).
13. The non-dimensional longitudinal velocity profiles plotted using u_m as the velocity scale and b as a length scale for all the experiments with bed-jet flow regime in the forward flow were found geometrically similar approximately up to x_m, but they were found significantly different from the profiles for the classical wall jet and the plane wall jet on rough, rigid boundaries with much higher value of δ/b equal to 0.6.
14. Using u_s and b_r as velocity and length scales, the velocity distribution in the backward flow was found to be similar. A much lower value of normalized length scale, b_r/y_t equal to 0.11 as compared with the value of 0.20 suggested for submerged jump in smooth rigid boundary (Wu and Rajaratnam 1995) was found for the bed-jet flow regime inside the scour hole indicating higher decay rate of surface velocity in the vertical direction for flows inside the scour hole than for flow in rigid beds.
15. A much lower value of surface eddy length, L_e for a "bed-jet" flow regime in an erodible boundary as compared with that for a submerged jump in rigid boundary was observed.
16. A strong relationship between the scales for the jet flow in a scour hole and the scour hole size was observed from the comparison made between the jet scales

so far identified in this study and the scour hole dimensions at asymptotic state. From this finding, it was also concluded that estimate the features of the flow inside the scour hole from the scour hole size and vice versa.

5.2 Conclusions

The effects of submergence on local scour of uniform cohesionless beds downstream of sluice gate due to plane turbulent wall jets and the resulting flow fields for the range of submergence ratio from 3 - 17.5, the densimetric Froude number from 4.4 – 6.9, and for two values of relative boundary roughness of 0.137 and 0.085 was studied experimentally. In short, it was found that the submergence has a significant influence on the size of the scour hole produced by the jet and the resulting flow fields. The magnitude of the asymptotic state characteristic dimensions of the scour hole such as maximum scour depth, horizontal distance to maximum scour depth, and length of scour hole was found to increase with increasing submergence ratio for a given densimetric Froude number and relative boundary roughness. It appears that the general trend of such bigger scour holes for higher submergence was due to the faster velocity decay of the jet at shallower submergences. As well, it was found that there was less variation of the asymptotic state eroded bed profiles across the channel width for higher submergences. Moreover, time development of scour hole dimensions for all submergences in experiments with a "bed-jet" or a "surface-jet" flow regime were found to grow in an approximately linear manner with the logarithmic of time up to the beginning of the asymptotic state.

The flow field and turbulence structure in the jet flows inside the scoured beds downstream of a sluice gate was measured using a SonTek 16-MHz MicroADV. The velocity distribution, growth of length scales, the variation of the maximum time-averaged velocity in the streamwise direction, and turbulence under varied submergence were analysed. The experimental results showed that the velocity profiles for all the bed-jet flow regimes were found to be similar for all submergence ratios in both the forward and backward flow regions up to maximum scour depth. However, a large departure of the velocity in the scour holes from the corresponding curves of submerged jets on

smooth beds was also observed. Two stages were seen to exist in the variation of the maximum longitudinal velocity in the streamwise direction. The first stage of velocity variation was found to follow that of a wall jet on a smooth and rough rigid bed up to a certain horizontal distance, called X_d upon the use of length scale L in normalizing the streamwise distance. However, the decay of the jet was faster on the scoured bed than in smooth and rough rigid beds in both stages as the value of the jet length scale L obtained for the flow in the scour hole were found to be smaller than that found for submerged jumps and free jump on smooth and rough rigid beds. A similar trend of faster growth of boundary layer thickness and the jet-half width was observed for jets flows in the scour hole as compared with jets on smooth as well as rough rigid beds. The magnitude of the decay of the maximum velocity, growth of boundary layer, and jet-half width all were found to be correlated with submergence ratio, densimetric Froude number, and the relative boundary roughness. Finally, it was found that a strong relationship exists between the scales for the jet flow in a scour hole and the scour hole size.

5.3 Recommendations for future studies

In order to further enhance the understanding of scour and the flow behavior in scour holes, the following is recommended for further studies.

1. The results presented herein are based on the experiments carried out under relatively narrow range of submergence ratio, densimetric Froude number, and the relative roughness. Therefore, this study should be carried on covering a wider range of submergence ratio, densimetric Froude number, and the relative roughness using the same basic set-up in order to ascertain the validity of the proposed velocity and length scales for the jet flow in the scour hole.
2. As only two experiments with “surface-jet” flow regime were studied in the present work, no methods were proposed regarding the velocity and the length scales for this flow regime. Therefore, more studies need to be carried out that cover the large number of experiments covering such flow regime.
3. From the observations of this study, boundary roughness appears to affect both scour hole size and the jet behavior. Therefore, more experiments covering a

wider range of boundary roughness should be carried out so that the effect of boundary roughness on scour and jet data can be analyzed.

4. The effect of the rigid apron length in the development of the scour hole and the associated flow fields was not taken into account while formulating the proposed velocity and length scales for the jet flow in the scour hole. Therefore, its effect as cited in Kurniawan et al. (2004) needs to be studied to ascertain the validity of the relationship between the scour and jet flow data proposed in this study.

REFERENCES

Aderibigbe, O. 1996. Contributions to erosion by jets. Ph.D. Thesis, University of Alberta, Edmonton, Alberta, Canada.

Aderibigbe, O., and Rajaratnam, N. 1998. Effect of sediment gradation on erosion by plane turbulent wall jets. Journal of Hydraulic Engineering, ASCE, **124**(10): 1034-1042.

Ahsan, M.R. 2003. Submergence effects on local scour. M.A.Sc. Thesis, University of Windsor, Windsor, Ontario, Canada.

Ali, K.M.H., and Lim, S.Y. 1986. Local scour caused by submerged wall jets. Proceeding of the Institution of Civil Engineers, Part 2, **81**: 607-645.

Armenio, V., Toscano, P., and Fiorotto, V. 2000. On the effects of negative step in pressure fluctuations at the bottom of a hydraulic jump. Journal of Hydraulic Research, **38**(5): 359-368.

ASTM Standard C670 2003. Standard practice for preparing precision and bias statements for test methods for construction materials. ASTM International, West Conshohocken, PA, USA.

Balachandar, R., and Kells, J.A. 1997. Local channel scour in uniformly graded sediments: the time-scale problem. Canadian Journal of Civil Engineering, NRC Press, **24**(5)**:** 779-807.

Balachandar, R., Kells, J.A., and Thiessen, R.J. 2000. The effect of tailwater depth on the dynamics of local scour. Canadian Journal of Civil Engineering, **27**(1): 138–150.

Breusers, H.N.C., and Raudkivi, A.J. 1991. Scouring. International Association for Hydraulic Research, Hydraulic Structures Design Manual 2. A.A. Balkema, Rotterdam, The Netherlands.

Carollo, F.G., Ferro, V., and Pampalone, V. 2007. Hydraulic jumps on rough beds. Journal of Hydraulic Engineering, **133**(9): 989-999.

Cea, L., Puertas, J., and Pena, L. 2007. Velocity measurements on highly turbulent free surface flow using ADV. Experiments in Fluids, **42**: 333-348.

Chatterjee, S.S., and Ghosh, S.N. 1980. Submerged horizontal jet over erodible bed. Journal of the Hydraulics Division, **106**(11): 1765-1782.

Chiew, Y.M. 2004. Local scour and riprap stability at bridge piers in a degrading channel. Journal of the Hydraulic Engineering, **130**(3): 218-226.

Coates, A.D. 1976. The numerical and experimental studies on the dynamics of fluids. Ph.D. Thesis, Heriot-Watt University, Edinburgh, UK.

Dey, S., and Sarkar, A. 2006a. Scour downstream of an apron due to submerged horizontal jets. Journal of Hydraulic Engineering, **132**(3): 246-331.

Dey, S., and Sarkar, A. 2006b. Response of velocity and turbulence in submerged wall jets to abrupt changes from smooth to rough beds and its application to scour downstream of an apron. Journal of Fluid Mechanics, **556**: 387-419.

Ead, S.A., and Rajaratnam, N. 2002. Plane turbulent wall jets in shallow tailwater. Journal of Engineering Mechanics, **128**(2): 143-155.

Ead, S.A., and Rajaratnam, N. 2004. Plane turbulent wall jets in rough boundaries with limited tailwater. Journal of Engineering Mechanics, **130**(10): 1245-1250.

Faruque, M.A.A., Bey, A., and Balachandar, R. 2007. Role of channel width and varying tailwater depth on the scour caused by a plane wall jet. *In* Proceedings of the 18th Canadian Hydrotechnical Conference, Winnipeg, Manitoba, Canada, 22–24 August. Canadian Society for Civil Engineering, Montreal, Quebec, Canada, on CD.

Goring, D.G., and Nikora, V.I. 2002. Despiking acoustic Doppler velocimeter data. Journal of Hydraulic Engineering, **128**(1): 117-126.

Hager, W.H., and Bretz, N.V. 1986. Hydraulic jumps at positive and negative steps. Journal of Hydraulic Research, **24**(4): 237-253.

Hill, D.F., and Younkin, B.D. 2006. PIV measurements of flow in and around scour holes. Experiments in Fluids, **41**: 295-307

Hogg, A.J., Huppert, H.E., and Dade, W.B. 1997. Erosion by planar turbulent jets. Journal of Fluid Mechanics, **338**: 317-340.

Johnston, A.J. 1978. An experimental study of shallow submerged turbulent jets. Ph.D. Thesis, Heriot-Watt University, Edinburgh, UK.

Johnston, A.J. 1990. Scour hole developments in shallow tailwater. Journal of Hydraulic Research, **28**(3): 341-354.

Kells, J.A., Balachandar, R., and Hagel, K.P. 2001. Effect of grain size on local channel scour below a sluice gate. Canadian Journal of Civil Engineering, **28**: 440-451.

Kurniawan, A., Altinakar, M.S., and Graf, W.H. 2004. Scour depth and flow pattern of eroding plane jets. International Journal of Sediment Research, **19**(1): 15-27.

Laursen, E.M. 1952. Observations on the nature of scour. *In* Proceedings of the Fifth Hydraulic Conference, Bulletin 34, University of Iowa, Iowa City, Iowa, pp. 179-197.

Liu, M., Rajaratnam, N., and Zhu, D.Z. 2004. Turbulence structure of hydraulic jumps of low Froude numbers. Journal of Hydraulic Engineering, **130**(6): 511-520.

Lohrmann, A., Cabrera, R., and Kraus, N.C. 1995. Acoustic Doppler Velocimeter (ADV) for laboratory use. *In* Proceedings of Conference on Fundamentals and Advancements in Hydraulic Measurements and Experimentation, Buffalo, New York, August 1995. American Society of Civil Engineers, New York, USA, pp. 351-365.

Long, D., Steffler, P.M., and Rajaratnam, N. 1990. LDA study of flow structure in submerged hydraulic jump. Journal of Hydraulic Research, **28**(4): 347-460.

Martin, V., Fisher, T.S.R., Millar, R.G., and Quick, M.C. 2002. ADV data analysis for turbulent flows: low correlation problem. Hydraulic Measurement and Experiment Methods, *In* Proceedings of the Specialty Conference on Hydraulic Measurement and Experiment Methods, Estes Park, USA, 28 July – 1 August 2002. American Society of Civil Engineers, New York, USA.

Matthews, L., and Whitelaw, J.H. 1973. Plane-jet flow over a backward-facing step. Heat and Fluid Flow, **3**(2): 133-140.

Mazurek, K.A., and Ahsan, M.R. 2005. Effects of tailwater depth on time evolution of scour by plane wall jets in cohesionless material. In Proceedings of 17th Canadian Hydrotechnical Conference on Hydrotechnical Engineering: Cornerstone of a Sustainable Environment, Edmonton, Alberta, 17-19 August 2005, pp. 1-10 (on CD).

McLelland, S.J., and Nicholas, A.P. 2000. A new method for evaluating errors in high-frequency ADV measurements. Hydrological Processes, **14**: 351-366.

Moore, W.L., and Morgan, C.W. 1957. The hydraulic jump at an abrupt drop. Journal of the Hydraulics Division, **83**(HY6): 1449 (1-21)

Nik Hassan, N.M.K., and Narayanan, R. 1985. Local scour downstream of an apron. Journal of Hydraulics Division, **111**(11): 1371-1385.

Rajaratnam, N. 1965a. Submerged hydraulic jump. Journal of the Hydraulics Division, **91**(HY4): 71-95.

Rajaratnam, N. 1965b. The hydraulic jump as a wall jet. Journal of the Hydraulics Division, **91**(HY5): 107-132.

Rajaratnam, N. 1976. Turbulent jets. Elsevier Scientific Publishing Company, New York.

Rajaratnam, N. 1981. Erosion by plane turbulent jets. Journal of Hydraulic Research, **19**(4): 339-358.

Rajaratnam, N., and Berry, B. 1977. Erosion by circular turbulent jets. Journal of Hydraulic Research, **15**(3): 277-289.

Rajaratnam, N., and MacDougall, R.K. 1983. Erosion by plane wall jets with minimum tailwater. Journal of Hydraulic Engineering, **109**(7): 1061-1064.

Rouse, H. 1940. Criteria for similarity in the transportation of sediment. *In* Proceedings of the Hydraulic Conference. University of Iowa Studies in Engineering. Bulletin 20.

Sarkar, A., and Dey, S. 2007. Effect of seepage on scour due to submerged jets and resulting flow field. Journal of Hydraulic Research, **45**(3): 357-364.

Shabayek, S.A. 2007a. Submerged jumps and wall jets. *In* Proceedings of 18th Canadian Hydrotechnical Conference on Challenges for Water Resources Engineering in a Changing World, Winnipeg, Manitoba, Canada, 22-24 August 2007.

Shabayek, S.A. 2007b. Hydraulic jumps on rough beds. *In* Proceedings of 18th Canadian Hydrotechnical Conference on Challenges for Water Resources Engineering in a Changing World, Winnipeg, Manitoba, Canada, 22-24 August 2007.

Sharp, J.J. 1974. Observation on hydraulic jumps at rounded step. Journal of the Hydraulics Division, **100**(HY6): 787-795.

SonTek/YSI 2001a. Acoustic Doppler velocimeter principles of operation. Technical Documentation, SonTek/YSI, Inc. San Diego, CA, USA.

SonTek/YSI 2001b. ADV field/hydra operation manual. Technical Documentation, SonTek/YSI, Inc. San Diego, CA, USA.

SonTek/YSI 2007. Acoustic Doppler Velocimeter (ADV) details, applications, specifications, and principles of operation. Available from: http://www.sontek.com/product/advm.htm [cited 22 August, 2007}.

Tachie, M.F., Balachandar, R., and Bergstrom, D.J. 2004. Roughness effects on turbulent plane wall jets. Experiments in Fluids, **37**: 281-292.

Tarapore, Z.S. 1956. Scour below a submerged sluice gate. M.Sc. Thesis, University of Minnesota, Minneapolis, Minnesota, USA.

Topping, J. 1957. Errors of observation and their treatment. The Institute of Physics, London, UK.

Verhoff, A. 1963. The two-dimensional turbulent wall jet with and without an external stream, Report 626, Princeton University, Princeton, NJ, USA.

Wahl, T.L. 2000. Analyzing ADV data using WinADV. *In* Proceedings of the Joint Conference on Water Resources Engineering and Water Resources Planning & Management, Minneapolis, Minnesota, USA, 30 July – 2 August 2000.

Wu, S., and Rajaratnam, N. 1995. Free jumps, submerged jumps and wall jets. Journal of Hydraulic Research, **33**(2): 197-212.

APPENDICES

Appendix A: Data for Time Development of Scour Hole Dimensions

Expt. No.	=	1F5.3Y280		Q	=	8.00	l/s		U_0	=	1.00	m/s
F_0	=	5.30		F_r	=	2.52			y_t/b_0	=	17.0	

Date & Time	Time (s)	ε_0 (mm)	y_0 (mm)	L_e (mm)	y_e (mm)	x_m (mm)	ε_m (mm)	x_0 (mm)	x_d (mm)	Δ_m (mm)	y_m (mm)	x_{0d} (mm)	Remarks
6/30/07 11:00	0		270.8	1400	277.3								T = 24.5 ^{0}C
6/30/07 11:05	300	26.7	271.7	530	283.4	130	56.5	294	446	207.1	207.1	530	
6/30/07 11:15	900	26.0	271.0	530	282.8	170	71.0	320	474	201.1	201.1	570	
6/30/07 11:30	1800	27.8	271.2	520	280.2	174	74.5	330	500	195.1	195.1	604	
6/30/07 12:00	3600	26.5	271.5	520	280.5	186	80.8	344	530	192.3	192.3	650	
6/30/07 13:10	7800	32.6	271.5	530	280.0	198	86.5	362	576	188.7	188.7	694	
6/30/07 15:07	14820	36.8	271.8	530	280.7	210	93.2	370	604	186.1	186.1	728	
6/30/07 18:26	26760	36.3	271.2	530	280.3	222	96.7	374	620	182.8	182.8	756	
6/30/07 22:56	42960	35.6	271.5	540	279.3	222	98.8	388	650	181.6	181.6	780	
7/1/07 6:03	68580	34.9	271.9	550	278.0	224	99.8	398	670	180.0	180.0	820	T = 25.0 ^{0}C
7/1/07 9:54	82440	34.6	271.6	550	277.6	224	100.0	400	674	178.5	178.5	826	
7/1/07 13:07	94020	35.6	271.5	550	277.9	226	100.9	406	678	179.5	179.5	828	
7/1/07 15:09	101340	34.8	271.3	550	277.4	228	101.6	410	684	177.3	177.3	830	T = 25.0 ^{0}C
7/1/07 20:15	119700	33.6	271.6	550	277.5	230	103.6	414	690	178.4	178.4	842	
7/2/07 5:55	154500	35.3	270.2	560	277.6	236	104.5	422	696	178.9	178.9	850	T = 25.5 ^{0}C
7/2/07 10:22	170520	36.8	270.9	560	278.0	236	104.1	422	696	177.8	177.8	852	
7/2/07 21:12	209520	37.3	270.6	560	277.5	236	104.1	424	700	179.5	179.5	858	T = 25.5 ^{0}C

Expt. No.	=	1F5.3Y240		Q	=	8.00	l/s		U_0	=	1.00	m/s
F_0	=	5.30		F_r	=	2.52			y_t/b_0	=	15.0	

Date & Time	Time (s)	ε_0 (mm)	y_0 (mm)	L_e (mm)	y_e (mm)	x_m (mm)	ε_m (mm)	x_0 (mm)	x_d (mm)	Δ_m (mm)	y_m (mm)	x_{0d} (mm)	Remarks
6/17/07 8:03	0	0.0	220.1	100	225.9								
6/17/07 8:08	300	29.3	222.5	520	230.8	192	73.1	330	460	161.1	161.1	540	
6/17/07 8:20	1020	33.3	222.9	520	231.2	196	76.2	340	490	154.0	154.0	574	
6/17/07 8:35	1920	35.5	219.6	530	231.9	198	82.8	352	510	155.9	155.9	600	
6/17/07 8:50	2820	35.4	219.7	530	232.0	202	83.9	360	522	151.2	151.2	620	T = 24.5 ^{0}C
6/17/07 9:20	4620	35.8	220.6	530	231.1	208	84.9	362	540	147.5	147.5	628	
6/17/07 10:12	7740	36.3	219.6	530	230.5	210	87.1	370	554	147.1	147.1	654	
6/17/07 11:02	10740	35.6	219.0	546	230.9	210	89.0	378	572	143.2	143.2	693	
6/17/07 12:40	16620	34.2	218.1	560	231.5	214	90.1	390	584	141.3	141.3	700	
6/17/07 15:15	25920	36.1	219.3	570	230.9	218	91.7	396	592	140.3	140.3	706	
6/17/07 18:09	36360	36.3	218.8	580	230.6	220	92.7	400	600	140.7	140.7	710	
6/17/07 19:53	42600	37.9	219.4	580	231.2	224	93.5	402	610	140.5	140.5	726	
6/17/07 22:57	53640	37.0	218.6	590	230.4	224	95.0	402	612	139.3	139.3	732	
6/18/07 6:05	79320	39.0	219.5	600	228.1	228	98.0	404	618	137.7	137.7	760	T = 25.5 ^{0}C
6/18/07 9:26	91380	39.4	220.5	600	227.5	230	98.4	404	640	135.8	135.8	766	
6/18/07 11:34	99060	39.5	220.2	600	227.8	232	100.6	410	642	135.5	135.5	768	
6/18/07 13:29	105960	40.2	220.0	600	228.1	234	100.2	414	646	137.0	137.0	778	
6/18/07 15:22	112740	42.1	220.5	600	228.2	236	100.8	412	648	137.7	137.7	778	
6/18/07 19:05	126120	41.1	220.2	600	228.5	240	99.8	414	650	137.8	137.8	786	
6/18/07 22:55	139920	40.8	220.4	600	228.0	244	100.9	418	650	136.6	136.6	786	
6/19/07 6:12	166140	41.2	218.6	540	228.7	244	101.3	418	650	136.2	136.2	788	T = 25 ^{0}C
6/19/07 9:01	176280	41.5	220.4	540	228.1	244	100.5	418	650	135.6	135.6	788	
6/19/07 21:15	220320	42.7	220.6	540	227.6	246	101.0	420	650	136.8	136.8	790	

Expt. No.	=	1F5.3Y200		Q	=	8.00	l/s		U_0	=	1.00	m/s
F_0	=	5.30		F_r	=	2.52			y_t/b_0	=	12.5	

Date & Time	Time (s)	ε_0 (mm)	y_0 (mm)	L_e (mm)	y_e (mm)	x_m (mm)	ε_m (mm)	x_0 (mm)	x_d (mm)	Δ_m (mm)	y_m (mm)	x_{0d} (mm)	Remarks
5/31/07 10:00	0	0.0	190.8	800	197.3								T = 22.5 ^{0}C
5/31/07 10:02	120	25.0	192.7			164	61.9	302	402	143.4	143.4	478	
5/31/07 10:05	300	27.2	193.9			166	67.8	320	432	142.2	142.2	508	
5/31/07 10:10	600	30.4	190.5	530	203.1	190	69.1	330	450	142.8	142.8	528	
5/31/07 10:20	1200	31.7	191.3			188	70.8	338	466	140.0	140.0	552	
5/31/07 10:30	1800	30.7	191.1			182	72.6	338	480	136.4	136.4	566	
5/31/07 10:45	2700	32.9	191.4			202	75.7	348	486	134.6	134.6	578	
5/31/07 11:05	3900	32.3	191.8			202	76.1	352	498	133.6	133.6	602	
5/31/07 11:30	5400	35.8	192.2			206	80.6	358	510	134.9	134.9	614	
5/31/07 12:00	7201	31.3	189.5			208	82.5	356	525	132.1	132.1	622	
5/31/07 13:04	11040	33.2	190.7			210	84.8	366	538	127.1	127.1	634	
5/31/07 15:02	18120	33.3	191.7	530	202.4	214	85.0	378	556	122.5	122.5	664	
5/31/07 17:40	27600	34.8	189.5	530	202.9	226	89.3	380	578	118.3	118.3	696	
5/31/07 20:32	37920	37.0	191.8	530	201.9	230	91.7	380	590	118.0	118.0	702	
5/31/07 23:27	48420	37.1	191.7	540	201.9	228	92.0	382	594	117.3	117.3	706	
6/1/07 5:33	70380	38.0	190.9	560	202.7	230	94.2	394	618	114.4	114.4	742	
6/1/07 9:14	83640	38.2	190.8	560	203.2	230	94.5	396	620	114.2	114.2	744	T = 22.5 ^{0}C
6/1/07 11:05	90300	39.8	196.2	560	202.9	230	95.8	394	622	112.7	112.7	746	
6/1/07 13:08	97680	39.1	192.6	560	202.8	228	96.1	396	624	112.6	112.6	756	

Expt. No.	=	1F5.3Y200 **(Cont'd)**	Q	=	8.00	l/s	U0	=	1.00	m/s
F_0	=	5.30	F_r	=	2.52		y_t/b_0	=	12.5	

Date & Time	Time (s)	ε_0 (mm)	y_0 (mm)	L_e (mm)	y_e (mm)	x_m (mm)	ε_m (mm)	x_0 (mm)	x_d (mm)	Δ_m (mm)	y_m (mm)	x_{0d} (mm)	Remarks
6/1/07 15:12	105120	40.0	192.6	560	202.5	230	96.4	402	630	113.1	113.1	756	
6/1/07 17:01	111660	38.2	192.4	550	202.1	238	96.0	402	632	112.7	112.7	762	
6/1/07 20:02	122520	38.9	192.0	550	202.5	242	96.0	402	634	109.8	109.8	768	
6/1/07 23:24	134640	38.8	191.7	550	202.1	248	96.8	404	642	112.4	112.4	784	
6/2/07 8:45	168300	38.7	191.6	530	203.2	250	97.1	406	650	112.7	112.7	788	Vel. Measurement
6/2/07 22:15	216900	38.3	191.5	530	202.0	250	97.6	410	650	110.4	110.4	802	End of experiment
6/3/07 8:30	253800	37.3	191.2	530	202.1	250	96.8	412	658	111.5	111.5	818	T = 24.5 ^{0}C
6/3/07 21:15	299700	38.4	192.0	530	202.5	250	97.6	412	662	112.3	112.3	822	

Expt. No.	=	1F5.3Y160		Q	=	8.00	l/s		U_0	=	1.00	m/s
F_0	=	5.30		F_r	=	2.52			y_t/b_0	=	10.0	

Date & Time	Time (s)	ε_0 (mm)	y_0 (mm)	L_e (mm)	y_e (mm)	x_m (mm)	ε_m (mm)	x_0 (mm)	x_d (mm)	Δ_m (mm)	y_m (mm)	x_{0d} (mm)	Remarks
6/7/07 13:45	0		148.8	620	157.3								T = 23.5 ^{0}C
6/7/07 13:46	60	26.9	150.3	460	164.7	138	57.1	302	396	107.7	107.7	474	
6/7/07 13:50	300	27.7	149.0	500	162.2	158	61.1	312	424	105.6	105.6	502	
6/7/07 14:00	900	27.9	150.3	520	160.6	162	65.1	342	448	102.8	102.8	536	
6/7/07 14:15	1800	30.7	148.8	540	160.3	182	69.5	342	476	96.8	96.8	562	
6/7/07 14:35	3000	33.2	147.9	530	159.8	186	69.8	360	502	88.2	88.2	588	
6/7/07 15:06	4860	38.7	148.6	520	160.8	190	71.9	362	516	87.9	87.9	612	
6/7/07 15:40	6900	32.6	148.1	520	160.7	194	72.8	364	526	85.9	85.9	628	
6/7/07 16:10	8700	33.5	146.0	520	160.8	194	72.0	364	534	85.5	85.5	642	
6/7/07 17:00	11700	32.8	149.8	520	161.0	202	76.6	368	542	80.4	80.4	654	
6/7/07 18:00	15300	38.4	148.6	530	159.1	204	77.4	368	558	84.2	84.2	672	
6/7/07 19:45	21600	37.3	150.3	530	159.9	206	79.3	368	574	79.9	79.9	692	
6/7/07 22:55	33000	38.0	150.5	530	161.0	212	85.3	378	588	78.7	78.7	702	
6/8/07 5:17	55920	39.0	150.5	530	160.3	222	90.6	384	628	78.7	78.7	758	
6/8/07 9:05	69600	39.9	150.2	530	160.2	228	92.4	388	640	78.5	78.5	772	
6/8/07 12:01	80160	38.6	151.1	520	160.8	230	93.9	392	662	76.2	76.2	776	
6/8/07 15:15	91800	41.1	151.2	530	159.9	232	93.8	394	666	76.9	76.9	778	
6/8/07 17:31	99960	41.7	149.9	530	160.3	232	94.3	394	672	77.0	77.0	792	
6/8/07 22:46	118860	41.6	150.1	530	160.4	234	96.1	398	678	76.0	76.0	802	
6/9/07 5:02	141420	41.3	149.9	530	160.0	236	97.6	398	686	75.7	75.7	810	
6/9/07 11:45	165600	41.1	150.3	530	160.4	240	97.9	400	686	75.3	75.3	812	T = 24.0 ^{0}C
6/9/07 18:21	189360	41.4	151.2	530	160.8	240	98.1	410	688	77.3	77.3	826	
6/9/07 22:45	205200	41.1	150.3	530	160.4	240	97.9	400	686	75.3	75.3	832	T = 24.5 ^{0}C
6/10/07 5:45	230400	40.0	150.4	530	160.0	240	98.0	416	700	76.8	76.8	840	T = 25 ^{0}C
6/10/07 19:25	279600	39.5	150.9	530	160.5	240	98.5	414	704	76.6	76.6	844	

Expt. No.	=	1F5.3Y160 (R)		Q	=	8.00	l/s		U_0	=	1.00	m/s
F_0	=	5.30		F_r	=	2.52			y_t/b_0	=	10.0	

Date & Time	Time (s)	ε_0 (mm)	y_0 (mm)	L_e (mm)	y_e (mm)	x_m (mm)	ε_m (mm)	x_0 (mm)	x_d (mm)	Δ_m (mm)	y_m (mm)	x_{0d} (mm)	Remarks
7/3/07 9:45	0	0.0	151.5	700	158.5								T = 23 ^{0}C
7/3/07 9:46	60	25.4	153.1	420	161.6	152	60.4	260	380	101.6	101.6	470	
7/3/07 9:50	300	27.1	153.6	420	161.3	172	58.2	280	410	97.9	97.9	512	
7/3/07 10:00	900	28.4	153.2	430	162.5	168	58.1	290	430	89.5	89.5	544	
7/3/07 10:15	1800	29.0	152.0	430	164.3	174	64.7	300	454	84.4	84.4	570	
7/3/07 10:35	3000	32.7	153.1	430	162.5	186	70.3	306	474	81.0	81.0	600	
7/3/07 11:06	4860	32.2	153.3	430	162.5	190	72.3	320	510	77.0	77.0	630	
7/3/07 11:50	7500	28.9	153.5	440	162.9	190	74.4	320	520	75.7	75.7	650	
7/3/07 12:32	10020	37.0	152.1	450	161.2	200	76.3	324	534	73.9	73.9	664	
7/3/07 13:36	13860	30.5	152.3	450	162.1	200	78.2	332	550	75.3	75.3	680	
7/3/07 14:35	17400	33.6	151.6	460	162.0	202	80.6	340	562	75.0	75.0	686	
7/3/07 15:46	21660	34.8	152.6	460	162.5	204	81.9	344	570	76.0	76.0	696	
7/3/07 18:26	31260	34.9	152.4	460	162.3	204	84.0	348	574	74.2	74.2	716	T = 24 ^{0}C
7/3/07 23:40	50100	34.3	152.7	460	162.1	210	85.6	350	590	76.2	76.2	730	
7/4/07 5:05	69600	36.9	152.6	460	162.3	214	89.0	358	620	75.5	75.5	756	
7/4/07 9:00	83700	37.2	152.9	460	162.6	214	90.8	360	630	74.2	74.2	760	T = 24 ^{0}C
7/4/07 11:50	93900	35.0	152.6	460	162.7	216	91.1	370	634	73.6	73.6	770	
7/4/07 16:50	111900	32.0	152.6	460	162.9	220	93.8	374	644	74.4	74.4	774	T = 25 ^{0}C
7/4/07 20:30	125100	32.9	152.1	460	162.7	220	94.1	376	646	74.1	74.1	780	T = 25 ^{0}C
7/4/07 23:30	135900	34.7	153.5	450	163.1	224	94.1	378	652	75.7	75.7	798	
7/5/07 6:30	161100	35.8	152.0	450	162.6	226	94.9	380	666	75.8	75.8	804	
7/5/07 9:15	171000	35.2	152.4	450	162.6	226	94.2	380	666	75.6	75.6	806	T = 25.5 ^{0}C
7/5/07 20:15	210600	37.7	151.8	450	162.7	228	95.0	384	666	76.9	76.9	810	T = 25.5 ^{0}C

Expt. No.	=	1F5.3Y48		Q	=	8.00	l/s		U_0	=	1.00	m/s
F_0	=	5.30		F_r	=	2.52			y_t/b_0	=	3.0	

Date & Time	Time (s)	ε_0 (mm)	y_0 (mm)	L_e (mm)	y_e (mm)	x_m (mm)	ε_m (mm)	x_0 (mm)	x_d (mm)	Δ_m (mm)	y_m (mm)	x_{0d} (mm)	Remarks
6/4/07 11:37	0												T = 21.5 ^{0}C
6/4/07 11:40	180	28.2	37.1			194	44.8	420	494	39.7	39.7	570	Surface Jet
6/4/07 11:45	480	26.0	39.1			170	45.7	352	500	39.9	39.9	640	
6/4/07 11:55	1080	28.7	38.5			190	46.5	382	450	40.2	40.2	738	
6/4/07 12:10	1980	29.2	38.6			214	48.7	430	470	41.4	41.4	810	
6/4/07 12:30	3180	26.4	39.8			180	48.6	440	510	38.5	38.5	900	
6/4/07 13:00	4980	26.8	38.9			250	51.3	460	540	38.7	38.7	950	
6/4/07 14:05	8880	23.6	38.0			260	53.3	506	572	38.1	38.1	1070	
6/4/07 15:02	12300	25.6	38.7			300	55.4	530	570	42.3	42.3	1210	
6/4/07 16:56	19140	27.3	38.5			284	59.8	590	760	41.5	41.5	1380	
6/4/07 19:47	29400	26.3	40.1			320	66.6	650	770	43.4	43.4	610	
6/4/07 22:55	40680	26.9	38.0			356	66.0	690	750	46.5	46.5	1750	
6/5/07 5:05	62880	26.9	39.5			362	80.0	852	2122	29.0	29.0	2152	
6/5/07 9:15	77880	26.7	40.0			364	83.8	870	2150	27.0	27.0	2290	T = 23.5 ^{0}C
6/5/07 11:17	85200	30.8	40.8			390	85.7	894	2250	24.5	24.5	2358	
6/5/07 13:50	94380	29.4	40.7			392	87.2	950	2370	25.3	25.3	2440	
6/5/07 16:07	102600	30.0	42.5			418	89.8	1000	2400	25.6	25.6	2600	
6/5/07 20:49	119520	30.0	42.0			404	99.1	1004	2070	28.9	28.9	2800	
6/5/07 23:37	129600	29.2	43.2			448	101.0	1013	2470	29.0	29.0	2824	
6/6/07 5:26	150540	28.8	45.6			494	99.7	1042	1940	27.5	27.5	2850	>sand bed
6/6/07 9:34	165420	28.2	45.1			496	101.8	1060	1910	27.6	27.6	2850	T = 24.5 ^{0}C
6/6/07 12:01	174240	26.8	42.2			500	102.1	1072	1450	32.7	32.7	2850	T = 24.5 ^{0}C
6/6/07 23:58	217260	26.1	45.9			500	103.1	1100	1500	33.6	33.6	2850	

Expt. No.	=	1F5.3Y144		Q	=	8.00	l/s		U_0	=	1.00	m/s
F_0	=	5.30		F_r	=	2.52			y_t/b_0	=	9.0	

Date & Time	Time (s)	ε_0 (mm)	y_0 (mm)	L_e (mm)	y_e (mm)	x_m (mm)	ε_m (mm)	x_0 (mm)	x_d (mm)	Δ_m (mm)	y_m (mm)	x_{0d} (mm)	Remarks
6/25/07 16:05	0	0.0	135.4	650	144.8								T = 26.5 ^{0}C
6/25/07 16:10	300	24.0	136.7	450	148.7	170	53.5	300	400	94.0	94.0	490	
6/25/07 16:15	600	29.6	136.7	460	148.3	170	59.7	310	420	88.2	88.2	502	
6/25/07 16:25	1200	29.9	136.5	470	147.5	180	66.5	314	438	84.9	84.9	530	
6/25/07 16:45	2400	32.5	134.6	480	146.9	190	68.1	320	472	81.6	81.6	580	
6/25/07 17:25	4800	35.5	135.2	500	145.4	200	72.4	346	508	74.2	74.2	618	
6/25/07 18:20	8100	35.5	133.9	500	145.1	210	73.8	350	530	65.6	65.6	650	
6/25/07 20:00	14100	36.0	133.1	500	145.7	210	78.9	380	560	61.7	61.7	690	
6/25/07 22:54	24540	37.2	134.1	500	145.9	212	83.9	382	586	61.0	61.0	718	
6/26/07 6:01	50160	40.8	135.8	500	146.1	214	92.6	384	632	61.2	61.2	742	T = 28 ^{0}C
6/26/07 9:32	62820	42.9	135.5	500	146.7	214	94.8	384	646	62.9	62.9	758	
6/26/07 11:52	71220	42.2	136.8	500	145.8	214	93.0	390	648	63.3	63.3	772	
6/26/07 12:25	73200	42.3	137.8	500	145.3	214	67.8	390	650	63.6	63.6	772	1st flicking
6/26/07 12:40	74100	41.4	135.7	500	146.0	226	93.2	382	646	64.0	64.0	772	BJ
6/26/07 13:10	75900	43.1	135.9	500	145.8	220	89.3	410	654	60.4	60.4	774	BJ
6/26/07 13:16	76260					210	81.8	380	-50	0.0	0.0	-50	BJ after flicking
6/26/07 14:09	79440	42.9	136.5	500	145.2	220	76.9	412	656	60.5	60.5	778	BJ weak
6/26/07 15:11	83160	43.6	136.2	500	146.1	220	68.8	430	656	63.6	63.6	780	SJ
6/26/07 15:30	84300	40.7	136.1	500	145.5	230	94.6	394	660	61.4	61.4	782	BJ

Expt. No.	=	1F5.3Y120		Q	=	8.00	l/s		U_0	=	1.00	m/s
F_0	=	5.30		F_r	=	2.52			y_t/b_0	=	7.5	

Date & Time	Time (s)	ε_0 (mm)	y_0 (mm)	L_e (mm)	y_e (mm)	x_m (mm)	ε_m (mm)	x_0 (mm)	x_d (mm)	Δ_m (mm)	y_m (mm)	x_{0d} (mm)	Remarks
5/24/07 9:35	0	0.0											T = 19.5 ^{0}C
5/24/07 9:36	60	26.6				148	52.8	290	370	68.4	68.4	432	
5/24/07 9:38	180	29.6				174	61.1	302	402	65.6	65.6	464	
5/24/07 9:40	300	31.8				182	61.8	312	422	63.4	63.4	492	
5/24/07 9:45	600	31.5				184	63.1	332	442	59.5	59.5	534	
5/24/07 9:55	1200	32.8				210	65.9	364	482	52.2	52.2	588	
5/24/07 10:05	1800	32.1				210	69.6	380	514	47.3	47.3	626	
5/24/07 10:20	2700	34.2				210	69.8	394	550	42.9	42.9	656	
5/24/07 10:30	3300	33.0				202	70.2	406	574	41.5	41.5	684	
5/24/07 10:40	3900	33.7				208	73.6	406	596	41.1	41.1	704	
5/24/07 10:50	4500	34.1				232	72.4	416	638	39.5	39.5	724	
5/24/07 11:00	5100	35.9				250	73.4	436	612	37.6	37.6	744	
5/24/07 11:20	6300	34.2				250	75.4	440	634	35.5	35.5	764	
5/24/07 11:45	7800	35.7				252	75.3	452	662	33.6	33.6	790	
5/24/07 12:30	10500	35.4				252	75.6	458	700	32.5	32.5	820	
5/24/07 13:15	13200	36.3				252	73.4	482	714	32.2	32.2	846	SJ weak
5/24/07 14:15	16800	38.8				252	73.6	498	742	30.3	30.3	864	SJ weak

Expt. No.	=	1F5.3Y120 **(cont'd)**	Q	=	109.70	l/s	U_0	=	116.28	m/s
F_0	=	5.30	F_r	=	112.92		y_t/b_0	=	116.7	

Date & Time	Time (s)	ε_0 (mm)	y_0 (mm)	L_e (mm)	y_e (mm)	x_m (mm)	ε_m (mm)	x_0 (mm)	x_d (mm)	Δ_m (mm)	y_m (mm)	x_{0d} (mm)	Remarks
5/24/07 15:00	19500	39.0				264	80.5	478	750	30.8	30.8	878	BJ weak
5/24/07 15:30	21300	37.7				256	75.8	514	764	30.7	30.7	894	SJ weak
5/24/07 16:15	24000	39.6				240	78.5	504	770	32.3	32.3	914	SJ strong
5/24/07 17:35	28800	41.6				240	81.7	492	800	32.0	32.0	922	BJ weak
5/24/07 21:55	44400	44.3				248	86.5	518	832	32.9	32.9	958	BJ weak
5/25/07 6:05	73800	52.8				266	86.3	532	892	33.8	33.8	1010	SJ weak
5/25/07 8:50	83700	53.3				280	106.6	560	896	33.8	33.8	1014	BJ weak
5/25/07 9:40	86700					264	112.6						BJ strong
5/25/07 9:45	87000					264	82.7						SJ strong
5/25/07 10:40	90300	53.0				264	114.4	520	904	35.2	35.2	1014	BJ strong
5/25/07 10:45	90600					264	86.7						SJ strong
5/25/07 11:05	91800					264	116.5	480	-50	0.0	0.0	-50	BJ strong
5/25/07 11:10	92100	54.6				264	92.3	538	904	35.6	35.6	1016	SJ strong
5/25/07 15:13	106680	53.4				264	91.2	546	906	35.1	35.1	1038	SJ strong

Expt. No.	=	2F4.4Y200		Q	=	6.70	l/s		U_0	=	0.84	m/s
F_0	=	4.40		F_r	=	2.11			y_t/b_0	=	12.5	

Date & Time	Time (s)	ε_0 (mm)	y_0 (mm)	L_e (mm)	y_e (mm)	x_m (mm)	ε_m (mm)	x_0 (mm)	x_d (mm)	Δ_m (mm)	y_m (mm)	x_{0d} (mm)	Remarks
6/11/07 9:45	0		194.0	770	199.3								T = 24.5 ^{0}C
6/11/07 9:50	300	28.3	195.1	450	203.8	108	47.8	250	360	150.7	150.7	424	
6/11/07 10:00	900	32.4	195.0	440	202.9	142	56.4	264	372	145.6	145.6	448	
6/11/07 10:20	2100	31.8	194.3	470	203.4	150	58.7	280	392	145.7	145.7	466	
6/11/07 11:00	4500	36.3	194.3	470	203.9	162	61.6	288	404	144.2	144.2	472	
6/11/07 12:20	9300	33.5	194.0	480	202.5	170	63.6	294	422	144.3	144.3	490	
6/11/07 15:00	18900	30.9	194.3	480	203.0	184	66.2	302	436	144.7	144.7	510	
6/11/07 21:55	43800	35.4	195.2	480	202.1	190	69.0	316	454	144.3	144.3	532	
6/12/07 6:01	72960	35.2	194.1	500	202.9	192	72.9	324	468	144.2	144.2	558	T = 23.5 ^{0}C
6/12/07 9:24	85140	35.5	194.6	510	203.2	192	72.2	328	476	142.8	142.8	562	
6/12/07 11:19	92040	35.6	194.5	500	202.9	194	72.9	328	478	143.4	143.4	563	
6/12/07 13:16	99060	35.8	193.6	500	200.8	194	72.8	328	478	144.2	144.2	562	
6/12/07 15:09	105840	35.7	193.6	500	200.8	196	73.0	330	480	144.9	144.9	564	
6/12/07 19:32	121620	35.6	193.0	500	200.8	196	73.1	332	480	144.4	144.4	564	
6/12/07 22:37	132720	35.4	194.1	500	201.1	196	73.3	330	480	143.5	143.5	568	
6/13/07 5:48	158580	35.9	193.3	500	200.5	196	73.7	332	480	144.4	144.4	570	
6/13/07 9:04	170340	35.6	193.7	450	200.8	196	73.0	332	480	144.2	144.2	572	T = 24.0 ^{0}C
6/13/07 20:46	212460	37.8	194.2	450	200.5	196	73.8	334	480	144.3	144.3	576	

Expt. No.	=	2F5.9Y200		Q	=	8.90	l/s		U_0	=	1.11	m/s
F_0	=	5.90		F_r	=	2.81			y_t/b_0	=	12.5	

Date & Time	Time (s)	ε_0 (mm)	y_0 (mm)	L_e (mm)	y_e (mm)	x_m (mm)	ε_m (mm)	x_0 (mm)	x_d (mm)	Δ_m (mm)	y_m (mm)	x_{0d} (mm)	Remarks
6/14/07 10:10	0		188.5	600	202.1								T = 24 ^{0}C
6/14/07 10:15	300	29.0	189.9	510	205.9	162	67.4	350	524	142.1	142.1	550	
6/14/07 10:25	900	38.8	189.9	520	205.5	190	72.3	364	500	134.0	134.0	580	
6/14/07 10:45	2100	32.1	189.6	520	205.0	188	80.3	380	524	131.4	131.4	610	
6/14/07 11:15	3900	34.4	189.8	520	205.2	210	84.7	382	554	128.3	128.3	640	
6/14/07 12:15	7500	35.4	188.3	540	204.2	230	92.1	400	580	120.6	120.6	670	
6/14/07 13:47	13020	36.8	188.7	550	201.8	230	93.9	404	610	109.5	109.5	730	
6/14/07 15:12	18120	36.3	188.3	550	202.3	240	96.0	404	630	104.8	104.8	750	
6/14/07 17:32	26520	39.7	187.8	570	201.1	240	101.6	420	646	102.7	102.7	798	
6/14/07 21:57	42420	42.1	187.1	600	199.6	242	107.1	430	672	98.9	98.9	830	
6/15/07 6:09	71940	40.3	188.2	600	199.2	244	108.9	440	700	96.8	96.8	868	
6/15/07 9:10	82800	38.9	188.4	600	198.6	248	109.1	444	700	96.9	96.9	872	T = 24 ^{0}C
6/15/07 10:55	89100	39.5	188.4	600	198.2	250	109.3	448	700	96.9	96.9	874	
6/15/07 14:14	101040	39.0	188.5	600	198.3	260	109.3	450	700	96.9	96.9	878	
6/15/07 15:46	106560	41.4	186.3	540	199.0	260	109.6	450	700	97.3	97.3	880	
6/15/07 22:57	132420	41.0	188.6	540	198.2	260	109.0	450	700	99.2	99.2	892	
6/16/07 9:27	170220	43.9	187.9	540	199.3	260	109.9	454	720	99.1	99.1	900	T = 25.5 ^{0}C
6/16/07 21:22	213120	39.8	188.9	540	199.0	260	110.6	458	734	101.5	101.5	904	T = 25 ^{0}C

Expt. No.	=	2F6.9Y200		Q	=	10.40 l/s		U_0	=	1.30 m/s		
F_0	=	6.90		F_r	=	3.28		y_t/b_0	=	12.5		

Date & Time	Time (s)	ε_0 (mm)	y_0 (mm)	L_e (mm)	y_e (mm)	x_m (mm)	ε_m (mm)	x_0 (mm)	x_d (mm)	Δ_m (mm)	y_m (mm)	x_{0d} (mm)	Remarks
6/22/07 15:45	0		189.3	850	197.4								T = 18.5 ^{0}C
6/22/07 15:50	300	27.8	186.3	580	203.3	190	75.5	350	550	134.1	134.1	620	
6/22/07 16:00	900	36.8	187.1	580	203.1	200	81.4	360	564	127.7	127.7	660	
6/22/07 16:20	2100	39.2	187.4	580	203.3	240	86.3	380	610	122.1	122.1	710	
6/22/07 16:50	3900	42.5	188.5	580	203.0	250	90.6	410	630	111.3	111.3	774	
6/22/07 17:54	7740	42.9	188.9	590	202.0	270	100.8	430	700	96.5	96.5	850	
6/22/07 20:30	17100	44.5	188.0	590	203.0	264	114.8	460	766	86.1	86.1	940	
6/22/07 23:51	29160	45.0	188.3	600	202.4	268	120.3	490	802	83.7	83.7	980	
6/23/07 5:55	51000	45.0	189.9	600	203.2	274	125.8	508	826	81.9	81.9	1004	
6/23/07 10:12	66420	44.9	189.3	600	201.8	274	128.8	520	840	78.8	78.8	1020	
6/23/07 15:02	83820	47.3	191.1	620	202.9	282	130.1	528	856	78.4	78.4	1038	
6/23/07 17:19	92040	48.4	190.5	640	203.3	290	131.0	530	860	77.9	77.9	1044	
6/23/07 21:11	105960	47.9	191.2	640	203.0	290	131.1	538	870	79.7	79.7	1060	T = 22.5 ^{0}C
6/23/07 23:47	115320	48.1	190.7	640	203.0	292	131.8	550	882	78.7	78.7	1064	
6/24/07 5:58	137580	48.9	190.9	650	201.1	302	131.2	538	892	77.8	77.8	1072	
6/24/07 9:15	149400	49.2	190.7	650	200.8	304	131.9	550	896	77.1	77.1	1074	T = 24.5 ^{0}C
6/24/07 12:13	160080	50.0	190.6	650	200.6	304	131.4	550	896	76.7	76.7	1084	
6/24/07 15:05	170400	48.7	188.9	600	201.0	306	132.1	550	896	76.6	76.6	1096	
6/24/07 22:45	198000	50.0	190.6	600	200.3	306	131.9	550	900	75.0	75.0	1106	T = 25.5 ^{0}C
6/25/07 8:20	232500	50.5	190.1	600	201.1	306	133.0	558	910	76.0	76.0	1122	
6/25/07 13:45	252000	48.7	190.8	600	200.5	308	132.4	562	914	75.2	75.2	1124	T = 25.5 ^{0}C

Expt. No.	=	3F6.7Y240		Q	=	8.00	l/s		U_0	=	1.00	m/s
F_0	=	6.70		F_r	=	2.52			y_t/b_0	=	15.0	

Date & Time	Time (s)	ε_0 (mm)	y_0 (mm)	L_e (mm)	y_e (mm)	x_m (mm)	ε_m (mm)	x_0 (mm)	x_d (mm)	Δ_m (mm)	y_m (mm)	x_{0d} (mm)	Remarks
7/17/07 17:05	0	0.0	230.8	1150	236.6								T = 28.5 ^{0}C
7/17/07 17:11	360	31.4	233.0	470	241.5	190	71.8	320	500	154.4	154.4	610	
7/17/07 17:20	900	32.0	232.0	470	238.1	200	74.7	350	540	148.0	148.0	664	
7/17/07 17:35	1800	31.9	231.8	480	239.5	220	88.2	354	570	140.8	140.8	710	
7/17/07 17:55	3000	35.3	231.3	500	239.1	220	93.3	370	590	130.8	130.8	744	
7/17/07 18:23	4680	31.2	231.5	500	238.1	224	96.1	375	620	128.1	128.1	770	
7/17/07 19:02	7020	34.3	231.9	500	239.3	224	99.6	384	640	122.4	122.4	800	
7/17/07 20:32	12420	35.3	232.5	520	238.8	232	103.8	398	674	118.8	118.8	842	
7/17/07 23:46	24060	36.7	231.8	550	238.0	240	105.4	402	688	113.7	113.7	860	
7/18/07 5:17	43920	36.7	231.9	590	237.9	248	112.4	446	740	110.1	110.1	922	T = 30.0 ^{0}C
7/18/07 9:27	58920	37.1	232.1	600	237.3	250	114.8	456	746	110.0	110.0	934	
7/18/07 12:05	68400	40.5	232.4	600	237.6	250	118.7	456	754	106.0	106.0	954	
7/18/07 14:01	75360	38.5	232.3	600	237.3	258	118.3	456	760	107.1	107.1	954	
7/18/07 15:52	82020	42.8	232.7	600	237.8	260	119.0	460	760	107.4	107.4	960	T = 28.0 ^{0}C
7/18/07 19:06	93660	41.8	232.1	600	237.0	260	121.0	468	770	105.6	105.6	968	
7/18/07 23:29	109440	42.4	232.4	600	237.4	260	120.1	470	772	104.5	104.5	970	
7/19/07 5:10	129900	42.4	230.5	590	237.8	260	121.4	474	786	102.3	102.3	990	T = 29.5 ^{0}C
7/19/07 8:30	141900	42.7	232.3	590	237.8	260	121.1	474	788	101.5	101.5	994	
7/19/07 23:17	195120	43.3	232.5	590	237.1	260	121.6	480	800	102.7	102.7	1000	

Expt. No.	=	3F6.7Y200		Q	=	8.00	l/s		U_0	=	1.00	m/s
F_0	=	6.70		F_r	=	2.52			y_t/b_0	=	12.5	

Date & Time	Time (s)	ε_0 (mm)	y_0 (mm)	L_e (mm)	y_e (mm)	x_m (mm)	ε_m (mm)	x_0 (mm)	x_d (mm)	Δ_m (mm)	y_m (mm)	x_{0d} (mm)	Remarks
7/20/07 11:06	0		194.0	1050	200.2								T = 28 ^{0}C
7/20/07 11:11	300	31.8	193.5	450	205.5	180	77.8	260	480	120.1	120.1	600	
7/20/07 11:22	960	36.4	193.4	470	200.3	190	80.0	340	530	109.1	109.1	660	
7/20/07 11:33	1620	31.9	194.0	480	200.1	200	87.8	350	560	100.8	100.8	690	
7/20/07 12:01	3300	35.8	193.7	480	200.9	210	90.9	366	588	99.5	99.5	740	
7/20/07 13:09	7380	33.6	193.6	500	201.0	228	96.0	394	626	94.8	94.8	778	
7/20/07 14:20	11640	35.1	193.0	500	200.7	230	100.1	410	650	90.9	90.9	810	
7/20/07 15:44	16680	37.5	193.8	510	200.5	230	102.5	412	664	91.9	91.9	836	T = 28.5 ^{0}C
7/20/07 17:49	24180	34.6	193.6	510	199.8	234	105.3	422	686	85.5	85.5	846	
7/20/07 20:32	33960	35.0	193.7	530	200.4	240	107.7	428	692	85.2	85.2	862	
7/20/07 23:13	43620	36.2	193.2	550	199.9	246	111.4	438	716	83.1	83.1	882	
7/21/07 5:02	64560	37.1	193.7	540	200.2	250	116.0	450	740	81.5	81.5	910	
7/21/07 9:39	81180	37.3	193.7	540	200.7	250	117.4	454	744	81.8	81.8	916	T = 28.5 ^{0}C
7/21/07 12:30	91440	39.4	194.0	540	200.3	250	115.5	456	744	81.5	81.5	924	
7/21/07 14:17	97860	40.7	193.9	540	200.6	250	116.6	460	750	83.0	83.0	930	
7/21/07 19:15	115740	39.0	193.2	540	200.2	250	115.8	460	764	79.6	79.6	940	T = 26.5 ^{0}C
7/21/07 23:01	129300	40.3	194.0	540	200.0	246	117.2	464	770	80.5	80.5	950	
7/22/07 5:32	152760	39.7	193.5	540	201.3	250	116.1	468	780	80.0	80.0	960	
7/22/07 9:18	166320	40.1	194.0	540	200.2	254	117.1	470	780	79.9	79.9	960	T = 28 ^{0}C
7/22/07 22:30	213840	38.4	193.7	540	199.9	254	116.2	474	794	79.4	79.4	964	T = 28 ^{0}C

Expt. No.	=	3F6.7Y48		Q	=	8.00	l/s		U_0	=	1.00	m/s
F_0	=	6.70		F_r	=	2.52			y_t/b_0	=	3.0	

Date & Time	Time (s)	ε_0 (mm)	y_0 (mm)	L_e (mm)	y_e (mm)	x_m (mm)	ε_m (mm)	x_0 (mm)	x_d (mm)	Δ_m (mm)	y_m (mm)	x_{0d} (mm)	Remarks
7/23/07 6:47	0												T = 26 ^{0}C
7/23/07 6:57	600	24.2	42.3	150	50.1	200	39.4	430	850	37.3	37.3	1100	
7/23/07 7:10	1380	22.6	43.4	150	50.3	210	41.5	510	850	40.6	40.6	1350	
7/23/07 7:30	2580	23.7	43.1	160	49.0	260	44.5	620	950	39.6	39.6	1700	
7/23/07 8:10	4980	24.9	39.2	170	49.0	340	47.7	810	1250	35.2	35.2	2250	
7/23/07 9:20	9180	23.0	41.9	180	46.7	340	51.3	870	1300	42.6	42.6	2650	
7/23/07 10:35	13680	17.1	42.2	180	52.3	360	61.3	940	1450	37.5	37.5	2850	
7/23/07 12:30	20580	17.5	42.6	180	53.0	390	70.1	1070	1700	34.9	34.9	2850	
7/23/07 13:59	25920	23.1	42.1	180	50.2	390	73.9	1080	1800	40.1	40.1	2850	
7/23/07 15:51	32640	24.1	42.9	180	52.1	400	76.2	1100	1860	38.1	38.1	2850	
7/23/07 17:55	40080	20.3	42.2	180	50.0	430	81.0	1170	1720	36.7	36.7	2850	T = 27.5 ^{0}C
7/23/07 20:17	48600	23.6	42.2	190	51.6	470	91.7	1300	2300	40.2	40.2	2850	
7/23/07 23:41	60840	20.5	43.2	190	52.9	510	96.2	1350	2310	40.0	40.0	2850	
7/24/07 5:35	82080	19.8	42.6	190	52.0	546	112.6	1390	2340	38.0	38.0	2850	
7/24/07 8:52	93900	18.4	43.2	190	53.0	550	113.2	1400	2350	36.1	36.1	2850	T = 26.5 ^{0}C
7/24/07 11:00	101580	19.3	45.7	190	51.3	550	113.1	1430	2400	37.2	37.2	2850	
7/24/07 22:55	144480	22.8	46.0	150	52.5	552	115.3	1450	2402	36.1	36.1	2850	T = 26.5 ^{0}C

Expt. No.	=	4F5.3Y280		Q	=	6.30	l/s		U_0	=	0.79	m/s
F_0	=	5.30		F_r	=	1.99			y_t/b_0	=	17.5	

Date & Time	Time (s)	ε_0 (mm)	y_0 (mm)	L_e (mm)	y_e (mm)	x_m (mm)	ε_m (mm)	x_0 (mm)	x_d (mm)	Δ_m (mm)	y_m (mm)	x_{0d} (mm)	Remarks
7/7/07 10:22	0	0.0	274.9	1100	278.8								T = 28 ^{0}C
7/7/07 10:30	480	34.2	274.5	450	280.2	140	50.9	230	344	216.1	216.1	430	
7/7/07 10:40	1080	33.9	274.6	460	280.3	144	50.9	244	370	211.4	211.4	454	
7/7/07 11:00	2280	30.7	274.3	460	281.3	154	56.3	266	420	204.2	204.2	510	
7/7/07 11:32	4200	29.8	274.2	460	281.8	170	60.3	270	454	203.8	203.8	550	
7/7/07 12:15	6780	29.1	275.0	460	281.6	170	62.7	284	464	200.3	200.3	566	
7/7/07 13:30	11280	29.8	274.8	480	280.4	170	66.0	286	472	200.1	200.1	570	
7/7/07 14:57	16500	28.8	273.9	490	278.5	178	69.0	290	490	198.8	198.8	600	
7/7/07 16:20	21480	29.7	273.5	490	278.0	176	72.9	300	500	195.0	195.0	610	T = 28.5 ^{0}C
7/7/07 18:00	27480	33.4	274.0	490	278.5	182	75.4	306	522	195.5	195.5	634	
7/7/07 20:09	35220	32.7	273.4	490	279.0	182	76.3	314	540	194.1	194.1	654	
7/7/07 23:20	46680	32.5	274.1	510	279.3	186	77.9	330	550	193.9	193.9	670	
7/8/07 5:07	67500	32.0	274.8	530	279.0	196	80.1	338	584	194.3	194.3	706	
7/8/07 9:56	84840	31.7	275.3	540	279.6	200	81.3	342	590	195.0	195.0	720	T = 29 ^{0}C
7/8/07 11:57	92100	35.3	274.9	530	278.9	204	81.1	344	600	193.1	193.1	726	
7/8/07 13:30	97680	35.0	275.2	530	279.4	200	82.1	346	600	194.9	194.9	728	
7/8/07 16:55	109980	36.3	275.0	530	279.6	198	81.8	346	600	194.9	194.9	734	
7/8/07 20:37	123300	34.8	275.4	530	279.4	200	81.9	350	602	196.1	196.1	750	
7/8/07 23:27	133500	35.2	275.1	550	279.7	200	82.6	348	610	195.4	195.4	754	
7/9/07 5:18	154560	34.9	275.5	550	279.5	202	81.8	350	618	194.7	194.7	762	
7/9/07 8:27	165900	34.6	275.7	550	280.0	200	82.1	348	620	195.6	195.6	764	T = 29.5 ^{0}C
7/9/07 20:17	208500	36.0	275.4	550	279.7	202	82.4	350	630	197.5	197.5	768	T = 30 ^{0}C

Expt. No.	=	4F5.3Y240		Q	=	6.30	l/s		U_0	=	0.79	m/s
F_0	=	5.30		F_r	=	1.99			y_t/b_0	=	15.0	

Date & Time	Time (s)	ε_0 (mm)	y_0 (mm)	L_e (mm)	y_e (mm)	x_m (mm)	ε_m (mm)	x_0 (mm)	x_d (mm)	Δ_m (mm)	y_m (mm)	x_{0d} (mm)	Remarks
8/3/07 9:15	0	0.0	235.1	900	239.4								T = 25 ^{0}C
8/3/07 9:20	300	25.9	234.9	400	240.7	140	53.2	240	354	172.3	172.3	402	
8/3/07 9:30	900	27.3	234.5	420	240.0	142	57.3	254	374	169.5	169.5	424	
8/3/07 9:50	2100	30.9	235.0	420	241.0	154	62.8	264	418	165.5	165.5	478	
8/3/07 10:30	4500	29.8	234.1	430	240.9	162	65.3	290	440	162.8	162.8	520	
8/3/07 11:30	8100	32.3	234.7	440	241.0	166	69.4	304	460	159.2	159.2	554	
8/3/07 12:55	13200	33.2	234.6	440	241.4	166	72.5	308	494	155.2	155.2	586	
8/3/07 14:20	18300	33.7	235.2	450	242.1	168	75.6	320	510	154.2	154.2	630	T = 24 ^{0}C
8/3/07 15:49	23640	34.6	234.8	500	240.2	188	79.2	334	542	151.5	151.5	656	
8/3/07 16:57	27720	36.6	233.8	500	238.8	190	81.6	338	554	151.5	151.5	686	
8/3/07 20:05	39000	35.6	232.3	500	238.3	196	84.2	338	560	154.1	154.1	696	
8/3/07 23:16	50460	36.2	234.0	500	236.7	194	85.0	346	578	154.1	154.1	706	
8/4/07 5:11	71760	36.8	232.2	510	237.0	196	84.8	348	590	154.4	154.4	722	
8/4/07 9:07	85920	36.6	232.8	520	235.8	194	85.2	350	594	154.3	154.3	724	T = 25.5 ^{0}C
8/4/07 11:00	92700	36.0	232.8	520	235.2	194	85.5	350	594	153.7	153.7	726	
8/4/07 12:35	98400	36.6	236.0	520	239.5	196	84.6	354	594	156.9	156.9	730	
8/4/07 14:17	104520	36.7	235.7	520	238.6	196	85.5	354	598	155.6	155.6	736	
8/4/07 23:25	137400	34.5	236.0	520	239.1	200	85.9	356	600	155.4	155.4	744	
8/5/07 6:14	161940	37.5	235.2	500	239.5	200	86.0	356	604	156.9	156.9	760	T = 27.5 ^{0}C
8/5/07 22:16	219660	37.9	236.2	500	238.4	200	86.8	360	610	157.7	157.7	768	T = 28 ^{0}C

Expt. No.	=	4F5.3Y200		Q	=	6.30	l/s		U_0	=	0.79	m/s
F_0	=	5.30		F_r	=	1.99			y_t/b_0	=	12.5	

Date & Time	Time (s)	ε_0 (mm)	y_0 (mm)	L_e (mm)	y_e (mm)	x_m (mm)	ε_m (mm)	x_0 (mm)	x_d (mm)	Δ_m (mm)	y_m (mm)	x_{0d} (mm)	Remarks
7/11/07 8:52	0		192.9	950	198.6								T = 22 ^{0}C
7/11/07 8:58	360	26.9	193.4	420	198.5	130	52.8	240	354	141.9	141.9	440	
7/11/07 9:06	840	26.9	193.3	420	200.4	140	57.2	250	380	139.1	139.1	464	
7/11/07 9:20	1680	31.0	193.6	420	200.0	150	59.9	264	402	133.6	133.6	480	
7/11/07 9:35	2580	33.4	192.9	430	198.5	154	63.4	268	414	129.1	129.1	500	
7/11/07 9:55	3780	32.2	192.4	430	199.1	164	63.5	272	424	128.2	128.2	530	
7/11/07 10:28	5760	35.4	193.4	450	199.9	170	67.6	272	450	122.7	122.7	550	
7/11/07 11:00	7680	33.3	192.6	450	199.8	168	67.8	290	460	123.3	123.3	564	
7/11/07 11:57	11100	35.1	191.9	460	199.8	174	70.7	290	476	118.9	118.9	586	T = 27.5 ^{0}C
7/11/07 13:09	15420	35.6	191.7	460	199.6	174	70.9	294	490	116.2	116.2	604	
7/11/07 15:17	23100	33.7	192.8	460	199.2	178	74.9	310	504	115.2	115.2	624	T = 27.5 ^{0}C
7/11/07 17:20	30480	34.5	191.6	460	199.0	190	76.0	316	514	112.5	112.5	644	
7/11/07 18:45	35580	35.2	192.4	460	197.6	190	75.9	318	524	112.5	112.5	656	
7/11/07 20:38	42360	37.4	192.5	460	198.6	190	78.1	320	534	112.6	112.6	660	T = 27 ^{0}C
7/11/07 23:07	51300	37.0	192.0	470	198.0	190	78.9	324	538	112.1	112.1	670	
7/12/07 5:02	72600	35.9	192.4	480	198.0	192	80.3	332	554	111.6	111.6	696	
7/12/07 9:09	87420	35.4	191.9	480	197.7	192	80.8	334	558	111.8	111.8	700	T = 28.5 ^{0}C
7/12/07 11:19	95220	38.9	191.8	480	197.4	200	81.4	336	562	111.1	111.1	702	
7/12/07 13:21	102540	38.4	192.1	480	197.8	200	80.9	336	564	111.8	111.8	702	
7/12/07 16:15	112980	34.8	191.4	480	196.1	200	81.0	340	564	112.4	112.4	704	
7/12/07 22:45	136380	36.6	192.3	480	196.5	200	80.0	340	564	112.6	112.6	714	
7/13/07 5:05	159180	36.1	191.1	460	196.1	200	81.1	340	580	113.1	113.1	722	T = 29.5 ^{0}C
7/13/07 8:30	171480	35.6	191.6	480	196.8	200	81.6	342	580	112.2	112.2	724	
7/13/07 21:25	217980	38.0	190.9	480	197.8	200	81.0	346	580	115.6	115.6	734	T = 30 ^{0}C

Expt. No.	=	4F5.3Y160		Q	=	6.30	l/s		U_0	=	0.79	m/s
F_0	=	5.30		F_r	=	1.99			y_t/b_0	=	10.0	

Date & Time	Time (s)	ε_0 (mm)	y_0 (mm)	L_e (mm)	y_e (mm)	x_m (mm)	ε_m (mm)	x_0 (mm)	x_d (mm)	Δ_m (mm)	y_m (mm)	x_{0d} (mm)	Remarks
7/14/07 9:41	0		155.7	700	160.8								T = 28.5 ^{0}C
7/14/07 9:46	300	30.9	156.8	360	163.0	134	49.2	230	340	105.9	105.9	430	
7/14/07 9:56	900	29.5	157.1	370	161.6	140	54.9	240	370	94.5	94.5	460	
7/14/07 10:10	1740	29.7	157.0	380	161.2	144	55.2	250	386	93.8	93.8	486	
7/14/07 10:30	2940	29.2	156.8	420	161.8	150	58.3	252	410	91.4	91.4	510	
7/14/07 11:00	4740	33.2	157.2	420	162.7	150	61.6	270	430	87.3	87.3	534	
7/14/07 12:07	8760	31.2	157.3	420	163.4	160	62.9	274	454	83.3	83.3	570	
7/14/07 13:16	12900	33.8	156.4	430	163.0	160	63.6	280	462	82.2	82.2	588	
7/14/07 15:01	19200	32.2	157.0	440	163.1	164	67.8	290	478	82.3	82.3	608	
7/14/07 17:09	26880	30.8	157.6	440	163.5	170	70.4	294	496	83.0	83.0	630	T = 29.5 ^{0}C
7/14/07 19:10	34140	31.8	156.6	450	163.7	172	72.0	300	508	81.3	81.3	654	
7/14/07 20:54	40380	34.8	156.6	450	163.4	174	72.2	304	520	84.7	84.7	664	
7/14/07 23:44	50580	33.2	157.6	440	161.9	178	73.0	308	524	85.5	85.5	670	
7/15/07 6:04	73380	34.8	157.0	440	162.0	184	73.7	314	540	85.4	85.4	698	
7/15/07 10:07	87960	36.0	157.6	440	161.6	186	75.1	320	544	86.1	86.1	704	T = 30 ^{0}C
7/15/07 12:01	94800	33.3	157.1	440	162.5	186	75.9	322	550	82.9	82.9	710	
7/15/07 14:30	103740	35.1	157.1	440	161.5	186	76.9	324	550	85.3	85.3	714	
7/15/07 17:17	113760	35.9	157.3	440	161.9	190	76.5	326	552	85.5	85.5	726	
7/15/07 20:36	125700	36.9	157.7	440	162.0	190	76.8	326	554	86.1	86.1	732	T = 30.5 ^{0}C
7/15/07 23:07	134760	37.2	156.4	440	161.5	190	76.2	326	556	86.3	86.3	732	
7/16/07 5:27	157560	36.7	156.5	410	161.6	192	77.1	328	562	88.3	88.3	740	
7/16/07 9:19	171480	37.3	156.6	440	162.9	192	77.0	326	564	88.1	88.1	742	T = 30.5 ^{0}C
7/16/07 21:45	216240	34.8	156.6	440	162.8	192	77.2	326	566	88.1	88.1	750	T = 30.5 ^{0}C

Appendix B: Data for Asymptotic State Scour Hole Profiles

Expt. No.	=	1F5.3Y280	Q	=	8.00	l/s
F_0	=	5.30	U_0	=	1.00	m/s
F_r	=	2.52	y_t/b_0	=	17.0	

Measured at								Remarks
Centre				150 mm right from centre		150 mm left from centre		
Distance (mm)	Bed level (mm)	Water level (mm)	Bed Level at the end of experiment (mm)	Distance (mm)	Bed level (mm)	Distance (mm)	Bed level (mm)	
0	0.0	272.1	0.0	0	0.0	0	0.0	
50	0.0	272.1	0.0	50	0.0	50	0.0	
50	-38.1	272.1	-42.0	50	-48.7	50	-43.7	
100	-36.8	271.6	-37.3	100	-44.0	100	-41.0	
150	-65.0	270.9	-66.6	150	-81.0	150	-78.2	
200	-89.8	270.2	-90.0	200	-95.0	200	-94.1	
250	-104.1	270.2	-103.5	250	-97.4	250	-98.0	
300	-104.2	270.4	-104.0	300	-92.9	300	-90.0	
350	-90.9	270.4	-90.9	350	-78.4	350	-68.3	
400	-55.3	271.1	-60.9	400	-48.0	400	-40.0	
450	-12.4	273.2	-16.4	450	-4.9	450	3.7	
500	12.0	275.8	15.1	500	23.4	500	28.8	
550	31.8	277.6	30.2	550	42.4	550	52.3	
600	56.3	277.3	53.0	600	57.0	600	68.2	
650	78.2	276.8	67.8	650	77.3	650	83.6	
700	90.9	275.7	82.0	700	90.9	700	91.8	
736	96.7	274.6	92.0	738	89.7	726	88.7	
750	93.0	274.5	94.1	750	73.9	750	77.0	
800	58.5	276.1	73.2	800	34.2	800	33.4	
850	30.7	276.5	46.6	850	2.6	850	0.0	
900	0.0	276.6	5.1	870	0.0	900	0.0	
908	0.0	276.8	0.0	900	0.0	1000	0.0	
1000	0.0	277.0	0.0	1000	0.0			

Expt. No.	=	1F5.3Y240	Q	=	8.00	l/s	
F_0	=	5.30	U_0	=	1.00	m/s	
F_r	=	2.52	y_t/b_0	=	15.0		

Measured at								Remarks
Centre				150 mm right from centre		150 mm left from centre		
Distance (mm)	Bed level (mm)	Water level (mm)	Bed Level at the end of experiment (mm)	Distance (mm)	Bed level (mm)	Distance (mm)	Bed level (mm)	
0	0.0	221.0	0.0	0	0.0	0	0.0	
50	0.0	221.0	0.0	50	0.0	50	0.0	
50	-33.1	221.0	-34.1	50	-55.0	50	-41.0	
100	-37.4	220.5	-40.7	100	-71.6	100	-48.9	
150	-62.2	219.9	-64.0	150	-87.3	150	-69.8	
200	-84.2	219.6	-83.0	200	-86.3	200	-87.0	
250	-96.3	219.6	-98.3	250	-87.2	250	-91.7	
300	-101.4	219.1	-101.0	300	-76.6	300	-86.2	
350	-83.3	218.6	-84.4	350	-68.7	350	-75.6	
400	-53.4	219.3	-55.7	400	-52.1	400	-53.7	
450	-1.1	221.4	-6.6	450	-16.1	450	-15.2	
500	23.4	226.7	20.7	500	17.7	500	29.9	
550	42.1	228.7	40.6	550	43.9	550	44.8	
600	58.3	227.4	54.3	600	58.1	600	62.1	
650	78.8	226.0	76.0	650	78.8	650	79.3	
700	88.3	224.5	88.0	700	94.8	700	91.4	
718	85.2	225.6	87.5	720	94.2	710	89.8	
750	53.3	225.7	57.4	750	71.1	750	65.0	
800	21.2	226.2	27.6	800	35.1	800	27.7	
840	0.0	226.2	5.0	850	5.2	830	0.0	
890	0.0	226.2	0.0	854	0.0	850	0.0	
900	0.0	226.2	0.0	1000	0.0	1000	0.0	
950	0.0	226.6	0.0					

Expt. No.	=	1F5.3Y200	Q	=	8.00	l/s
F_0	=	5.30	U_0	=	1.00	m/s
F_r	=	2.52	y_t/b_0	=	12.5	

Measured at								Remarks
Centre				150 mm right from centre		150 mm left from centre		
Distance (mm)	Bed level (mm)	Water level (mm)	Bed Level at the end of experiment (mm)	Distance (mm)	Bed level (mm)	Distance (mm)	Bed level (mm)	
0	0.0	191.6	0.0	0	0.0	0	0.0	
50	0.0	191.6	0.0	50	0.0	50	0.0	
50	-40.4	191.6	-39.0	50	-50.5	50	-37.0	
100	-41.3	191.6	-38.4	100	-61.0	100	-44.1	
150	-63.3	191.6	-64.4	150	-85.2	150	-65.8	
200	-81.1	191.8	-81.6	200	-86.4	200	-79.6	
250	-97.9	192.0	-96.1	250	-82.0	250	-83.4	
300	-96.8	192.2	-96.9	300	-75.8	300	-83.9	
350	-80.1	191.9	-84.4	350	-64.8	350	-73.2	
400	-52.6	191.6	-60.0	400	-47.2	400	-40.4	
450	-13.3	199.9	-9.3	450	-16.0	450	-7.6	
500	15.2	202.6	17.9	500	21.0	500	26.2	
550	36.6	203.2	36.9	550	41.8	550	45.9	
600	59.9	200.9	58.6	600	60.4	600	58.0	
650	75.9	198.3	77.1	650	78.4	650	74.7	
700	84.9	197.0	84.4	700	93.8	700	80.5	
720	83.0	197.8	83.2	720	92.0	710	81.2	
800	46.1	198.5	49.4	800	40.8	750	57.7	
840	15.9	199.0	22.2	840	0.0	800	18.1	
852	4.7	199.0	13.5			840	0.0	
868	0.0	199.0	1.7					

Expt. No.	=	1F5.3Y160	Q	=	8.00	l/s
F_0	=	5.30	U_0	=	1.00	m/s
F_r	=	2.52	y_t/b_0	=	10.0	

Measured at								Remarks
Centre				150 mm right from centre		150 mm left from centre		
Distance (mm)	Bed level (mm)	Water level (mm)	Bed Level at the end of experiment (mm)	Distance (mm)	Bed level (mm)	Distance (mm)	Bed level (mm)	
0	0.0	150.8	0.0	0	0.0	0	0.0	
50	0.0	150.8	0.0	50	0.0	50	0.0	
50	-48.2	150.8	-46.2	50	-56.6	50	-44.5	
100	-41.1	150.3	-39.5	100	-72.9	100	-47.3	
150	-60.6	150.2	-61.0	150	-82.0	150	-64.9	
200	-81.0	149.0	-80.1	200	-84.3	200	-76.9	
250	-94.8	150.0	-96.7	250	-82.4	250	-84.1	
300	-96.8	149.9	-94.1	300	-80.3	300	-82.8	
350	-78.0	149.7	-80.2	350	-67.3	350	-77.5	
400	-47.4	150.6	-50.3	400	-49.9	400	-41.7	
450	-10.8	155.7	-0.4	450	-9.1	450	0.5	
500	13.3	160.7	11.8	500	24.8	500	24.4	
550	32.8	159.3	33.7	550	42.7	550	39.8	
600	55.1	158.0	52.0	600	59.1	600	55.3	
650	67.9	157.9	64.0	650	77.1	650	70.4	
700	79.3	157.7	75.5	700	89.5	700	80.4	
758	81.8	157.5	80.9	750	87.6	736	84.1	
800	45.5	157.5	60.5	800	53.3	800	42.5	
850	5.9	157.7	22.4	850	11.8	850	5.2	
862	0.0	157.7	6.5	866	0.0	862	0.0	
1000	0.0	157.9	0.0	1000	0.0	1000	0.0	

Expt. No.	=	1F5.3Y160 (R)	Q	=	8.00	l/s
F_0	=	5.30	U_0	=	1.00	m/s
F_r	=	2.52	y_t/b_0	=	10.0	

Measured at								Remarks
Centre				150 mm right from centre		150 mm left from centre		
Distance (mm)	Bed level (mm)	Water level (mm)	Bed Level at the end of experiment (mm)	Distance (mm)	Bed level (mm)	Distance (mm)	Bed level (mm)	
0	0.0	154.4	0.0	0	0.0	0	0.0	
50	0.0	154.4	0.0	50	0.0	50	0.0	
50	-42.3	154.4	-42.1	50	-39.6	50	-40.7	
100	-38.0	153.8	-37.7	100	-49.2	100	-41.2	
150	-63.0	153.8	-60.9	150	-67.8	150	-63.5	
200	-83.5	152.6	-83.2	200	-83.9	200	-78.8	
250	-94.2	152.8	-94.5	250	-84.6	250	-83.2	
300	-87.3	152.0	-87.0	300	-77.3	300	-77.1	
350	-63.4	152.4	-61.1	350	-57.6	350	-46.4	
400	-19.9	157.8	-18.8	400	-26.4	400	-16.8	
450	12.4	161.7	6.7	450	11.3	450	17.3	
500	29.4	162.6	30.9	500	31.0	500	36.1	
550	51.2	159.4	46.1	550	46.8	550	55.2	
600	66.5	159.4	62.5	600	67.9	600	73.3	
650	76.9	159.6	75.4	650	84.6	650	80.7	
700	85.0	159.6	82.1	700	83.5	700	48.6	
716	85.0	160.8	82.1	750	48.2	750	22.5	
750	73.6	160.8	77.7	800	8.8	800	1.2	
800	41.3	160.8	46.6	826	0.0	814	0.0	
850	2.7	160.5	9.1	850	0.0	850	0.0	
856	0.0	159.8	3.4	900	0.0	900	0.0	
860	0.0	159.8	0.0	1000	0.0	1000	0.0	
900	0.0	159.8	0.0					

Expt. No.	=	1F5.3Y48	Q	=	8.00	l/s
F_0	=	5.30	U_0	=	1.00	m/s
F_r	=	2.52	y_t/b_0	=	3.0	

Measured at								Remarks
Centre				150 mm right from centre		150 mm left from centre		
Distance (mm)	Bed level (mm)	Water level (mm)	Bed Level at the end of experiment (mm)	Distance (mm)	Bed level (mm)	Distance (mm)	Bed level (mm)	
0	0.0	46.8	0.0	0	0.0	0	0.0	
50	0.0	46.8	0.0	50	0.0	50	0.0	
50	-31.2	46.8	-29.9	50	-39.7	50	-29.9	
100	-26.8	46.8	-26.1	100	-31.0	100	-29.0	
150	-35.5	51.3	-37.2	150	-37.6	150	-36.0	
200	-47.1	50.3	-46.9	200	-44.6	200	-44.6	
250	-61.2	51.3	-62.2	250	-50.5	250	-52.8	
300	-73.7	50.3	-74.1	300	-56.5	300	-59.4	
350	-85.5	51.6	-86.0	350	-60.4	350	-60.4	
400	-94.8	51.6	-95.2	400	-60.9	400	-56.8	
450	-101.3	51.7	-102.0	450	-58.7	450	-57.9	
500	-102.0	51.8	-102.7	500	-56.4	500	-56.2	
550	-102.1	52.6	-104.1	550	-52.0	550	-49.6	
600	-96.8	55.9	-97.1	600	-48.9	600	-46.3	
650	-90.5	55.7	-89.8	650	-41.5	650	-38.1	
700	-84.0	55.8	-84.6	700	-36.0	700	-26.6	
750	-71.5	55.6	-73.8	750	-33.3	750	-21.2	
800	-60.6	55.3	-62.0	800	-23.1	800	-11.3	
900	-37.7	58.6	-39.2	900	-3.7	900	1.2	
1000	-11.0	57.9	-13.0	1000	7.9	1000	13.0	
1100	0.0	56.1	-3.1	1500	13.6	1500	17.3	
1500	23.4	49.5	22.3	2000	10.9	2000	10.0	
2000	20.1	46.6	19.0	2500	11.3	2500	9.1	
2500	20.1	46.2	18.6	2900	6.8	2900	7.4	
2900	18.5	44.6	16.9					

Expt. No.	=	1F5.3Y144		Q	=	8.00	l/s
F_0	=	5.30		U_0	=	1.00	m/s
F_r	=	2.52		y_t/b_0	=	9.0	

Measured at								Remarks
Centre				150 mm right from centre		150 mm left from centre		
Distance (mm)	Bed level (mm)	Water level (mm)	Bed Level at the end of experiment (mm)	Distance (mm)	Bed level (mm)	Distance (mm)	Bed level (mm)	
0	0.0	136.9						
50	0.0	136.9						
50	-48.2	136.9						
100	-41.1	136.8						
150	-60.6	136.8						
200	-81.0	136.5						
250	-94.8	134.7						
300	-96.8	134.3						
350	-78.0	134.3						
400	-47.4	141.1						
450	0.8	144.7						
500	18.3	145.8						
550	37.8	145.4						
600	55.1	144.0						
650	67.9	143.8						
700	79.3	143.2						
740	81.8	143.2						
750	45.5	144.0						
800	5.9	144.1						
862	0.0	144.7						
1000	0.0	144.4						

Expt. No.	=	1F5.3Y120	Q	=	8.00	l/s
F_0	=	5.30	U_0	=	1.00	m/s
F_r	=	2.52	y_t/b_0	=	7.5	

Measured at								Remarks
Centre				150 mm right from centre		150 mm left from centre		
Distance (mm)	Bed level (mm)	Water level (mm)	Bed Level at the end of experiment (mm)	Distance (mm)	Bed level (mm)	Distance (mm)	Bed level (mm)	
0	0.0	113.3		0	0.0	0	0.0	
50	0.0	113.3		50	0.0	50	0.0	
50	-48.5	113.3		50	-73.8	50	-78.7	
100	-56.2	113.3		100	-80.9	100	-77.2	
150	-65.0	113.3		150	-85.0	150	-89.8	
200	-83.0	113.3		200	-91.3	200	-99.2	
250	-83.2	110.2		250	-97.0	250	-92.9	
300	-83.2	110.2		300	-96.5	300	-89.5	
350	-79.8	112.8		350	-76.7	350	-80.3	
400	-74.3	114.3		400	-55.2	400	-68.7	
450	-67.3	117.9		450	-41.5	450	-44.8	
500	-48.8	119.8		500	-19.9	500	-29.6	
550	-28.4	122.8		550	-4.2	550	-14.2	
600	-5.6	121.7		600	20.9	600	6.2	
650	22.0	121.5		650	30.4	650	32.5	
700	31.6	122.6		700	45.5	700	40.5	
750	48.2	122.4		750	57.3	750	54.5	
800	63.8	121.5		800	65.1	800	68.7	
850	77.5	119.2		850	72.8	850	73.3	
900	78.9	117.3		900	76.7	900	76.8	
950	80.2	117.3		950	79.4	950	79.0	
1000	56.5	117.3		1000	77.8	1000	66.6	
1050	21.3	117.5		1050	58.5	1050	4.9	
1088	0.0	117.7		1088	41.7	1088	7.6	
1180	0.0	117.7		1180	0.0	1180	0.0	

Expt. No.	=	2F4.4Y200	Q	=	6.70	l/s
F_0	=	4.40	U_0	=	0.84	m/s
F_r	=	2.11	y_t/b_0	=	12.5	

Measured at								Remarks
Centre				150 mm right from centre		150 mm left from centre		
Distance (mm)	Bed level (mm)	Water level (mm)	Bed Level at the end of experiment (mm)	Distance (mm)	Bed level (mm)	Distance (mm)	Bed level (mm)	
0	0.0	193.9	0.0	0	0.0	0	0.0	
50	0.0	193.9	0.0	50	0.0	50	0.0	
50	-23.2	193.9	-27.3	50	-37.6	50	-27.8	
100	-35.8	193.6	-34.8	100	-48.5	100	-36.6	
150	-58.2	193.7	-55.3	150	-68.0	150	-56.7	
200	-71.5	193.7	-70.0	200	-69.7	200	-68.5	
250	-72.9	193.9	-71.6	250	-64.2	250	-67.1	
300	-59.8	193.9	-60.0	300	-52.2	300	-55.0	
350	-17.6	194.3	-25.5	350	-36.2	350	-18.4	
400	23.3	196.1	18.1	400	38.5	400	29.7	
450	38.6	199.8	37.0	450	42.4	450	41.5	
500	54.9	200.8	53.9	500	59.0	500	63.7	
528	56.3	199.6	55.6	570	84.7	550	82.2	
550	50.3	198.4	57.2	600	69.6	600	59.4	
600	7.2	196.5	20.0	650	31.1	650	18.4	
614	0.0	196.8	10.6	690	0.0	670	0.0	
626	0.0	196.5	0.0	700	0.0	700	0.0	
800	0.0	197.8	0.0	800	0.0	800	0.0	

Expt. No.	=	2F5.9Y200	Q	=	8.90	l/s
F_0	=	5.90	U_0	=	1.11	m/s
F_r	=	2.81	y_t/b_0	=	12.5	

Measured at								Remarks
Centre				150 mm right from centre		150 mm left from centre		
Distance (mm)	Bed level (mm)	Water level (mm)	Bed Level at the end of experiment (mm)	Distance (mm)	Bed level (mm)	Distance (mm)	Bed level (mm)	
0	0.0	188.1	0.0	0	0.0	0	0.0	
50	0.0	188.1	0.0	50	0.0	50	0.0	
50	-44.0	188.1	-44.3	50	-63.0	50	-46.3	
100	-42.4	187.6	-39.8	100	-79.3	100	-53.8	
150	-64.4	187.5	-64.2	150	-90.2	150	-70.8	
200	-84.8	187.5	-82.8	200	-98.7	200	-84.8	
250	-102.5	187.3	-99.0	250	-94.9	250	-93.9	
300	-109.6	186.3	-110.6	300	-87.7	300	-98.9	
350	-99.2	186.2	-102.0	350	-85.6	350	-92.7	
400	-80.6	187.2	-78.1	400	-74.7	400	-78.7	
450	-36.4	190.2	-41.2	450	-43.7	450	-47.2	
500	2.0	194.9	1.7	500	-4.5	500	-6.5	
550	21.3	198.2	18.9	550	20.6	550	13.0	
600	41.9	199.0	37.9	600	39.7	600	47.4	
650	66.7	196.0	61.5	650	58.0	650	60.1	
700	84.9	194.8	80.2	700	78.8	700	78.8	
750	97.8	194.8	94.8	750	92.2	750	95.1	
780	97.5	194.3	94.3	780	94.7	770	95.0	
800	94.0	193.9	95.5	800	90.5	800	82.7	
850	64.7	196.4	74.4	850	63.0	850	40.5	
900	27.9	196.5	38.4	900	27.9	900	4.9	
928	0.0	196.8	15.6	940	0.0	904	0.0	
950	0.0	196.9	5.4	1000	0.0	1000	0.0	
958	0.0	196.9	0.0	1100	0.0	1100	0.0	
1100	0.0	197.0	0.0					

Expt. No.	=	2F6.9Y200	Q	=	10.40	l/s
F_0	=	6.90	U_0	=	1.30	m/s
F_r	=	3.28	y_t/b_0	=	12.5	

Measured at								Remarks
Centre				150 mm right from centre		150 mm left from centre		
Distance (mm)	Bed level (mm)	Water level (mm)	Bed Level at the end of experiment (mm)	Distance (mm)	Bed level (mm)	Distance (mm)	Bed level (mm)	
0	0.0	191.1	0.0	0	0.0	0	0.0	
50	0.0	191.1	0.0	50	0.0	50	0.0	
50	-60.1	191.1	-62.0	50	-77.3	50	-42.9	
100	-49.2	190.7	-48.7	100	-88.3	100	-67.4	
150	-67.6	190.2	-71.8	150	-107.2	150	-92.8	
200	-93.4	189.2	-96.7	200	-110.0	200	-100.8	
250	-117.1	189.1	-115.8	250	-106.9	250	-114.2	
300	-131.2	188.5	-128.2	300	-104.8	300	-120.5	
350	-131.9	188.0	-132.4	350	-100.5	350	-107.3	
400	-124.7	187.5	-126.2	400	-87.5	400	-110.7	
450	-104.3	188.5	-100.6	450	-84.1	450	-91.9	
500	-68.2	191.8	-65.9	500	-58.2	500	-55.3	
550	-34.1	195.7	-35.0	550	-18.4	550	-17.8	
600	-4.4	199.6	-6.4	600	2.2	600	5.6	
650	26.1	200.8	13.4	650	23.8	650	20.5	
700	45.9	200.2	36.1	700	43.2	700	44.2	
750	62.2	198.6	60.0	750	64.5	750	59.6	
800	89.1	198.6	78.9	800	85.8	800	80.4	
850	104.2	197.8	94.8	850	100.9	850	91.0	
900	118.8	198.3	111.6	900	112.8	900	115.5	
950	120.1	197.8	121.6	950	117.9	950	120.1	
964	118.8	197.8	123.8	970	108.5	970	117.0	
1000	94.4	197.8	112.6	1000	88.9	1000	79.2	
1050	57.9	198.3	83.8	1050	53.4	1050	48.3	
1100	23.8	198.2	46.0	1100	18.9	1100	12.6	
1146	0.0	198.8	15.6	1130	0.0	1130	0.0	
1150	0.0	199.0	11.6	1150	0.0	1150	0.0	
1174	0.0	199.4	0.0					

Expt. No.	=	3F6.7Y240	Q	=	8.00	l/s
F_0	=	6.70	U_0	=	1.00	m/s
F_r	=	2.52	y_t/b_0	=	15.0	

Measured at								Remarks
Centre				150 mm right from centre		150mm left from centre		
Distance (mm)	Bed level (mm)	Water level (mm)	Bed Level at the end of experiment (mm)	Distance (mm)	Bed level (mm)	Dist. (mm)	Bed level (mm)	
0	0.0	232.7	0.0	0	0.0	0	0.0	
50	0.0	232.7	0.0	50	0.0	50	0.0	
50	-56.7	232.7	-57.0	50	-59.1	50	-59.5	
100	-42.7	232.7	-43.3	100	-54.7	100	-59.6	
150	-63.5	232.7	-62.2	150	-83.0	150	-81.2	
200	-93.1	231.7	-92.6	200	-106.7	200	-104.6	
250	-112.9	230.5	-114.4	250	-111.3	250	-114.0	
300	-121.6	231.3	-120.1	300	-111.0	300	-119.4	
350	-112.3	231.3	-113.3	350	-100.6	350	-107.4	
400	-85.8	231.3	-90.5	400	-81.9	400	-78.0	
450	-48.4	232.6	-54.4	450	-44.2	450	-37.5	
500	-5.2	233.3	-16.1	500	-14.8	500	-5.8	
550	16.6	236.0	6.5	550	16.1	550	17.7	
600	35.5	237.8	26.5	600	36.8	600	34.3	
650	60.8	237.3	49.3	650	53.2	650	56.6	
700	84.6	237.3	72.6	700	74.0	700	84.3	
750	112.5	236.9	94.4	750	100.0	750	107.3	
800	126.9	237.5	114.3	800	118.8	800	120.4	
836	132.3	237.5	130.8	850	90.7	850	91.6	
850	124.6	237.0	134.5	900	59.6	900	57.1	
900	97.7	237.6	113.0	950	27.0	950	25.3	
950	66.3	237.8	74.6	990	0.0	1000	0.0	
1000	31.2	238.0	42.7	1000	0.0	1100	0.0	
1040	0.0	238.0	16.7	1100	0.0			
1050	0.0	238.0	0.0					
1100	0.0	238.0	0.0					

Expt. No.	=	3F6.7Y200	Q	=	8.00	l/s
F_0	=	6.70	U_0	=	1.00	m/s
F_r	=	2.52	y_t/b_0	=	12.5	

Measured at								Remarks
Centre				150 mm right from centre		150 mm left from centre		
Distance (mm)	Bed level (mm)	Water level (mm)	Bed Level at the end of experiment (mm)	Distance (mm)	Bed level (mm)	Distance (mm)	Bed level (mm)	
0	0.0	194.3	0.0	0	0.0	0	0.0	
50	0.0	194.3	0.0	50	0.0	50	0.0	
50	-49.3	194.3	-50.7	50	-55.4	50	-49.0	
100	-40.7	194.3	-38.4	100	-58.5	100	-52.3	
150	-65.7	194.0	-61.3	150	-81.1	150	-73.8	
200	-89.3	193.6	-84.2	200	-102.1	200	-101.3	
250	-107.6	193.9	-109.7	250	-112.2	250	-107.6	
300	-115.8	193.5	-116.2	300	-104.5	300	-106.1	
350	-103.9	193.6	-109.4	350	-93.7	350	-98.5	
400	-73.9	194.0	-76.8	400	-80.5	400	-69.1	
450	-31.6	195.0	-34.0	450	-46.5	450	-33.0	
500	-2.7	197.3	-11.1	500	-1.9	500	-1.8	
550	15.7	198.8	9.6	550	18.6	550	20.1	
600	36.0	199.4	31.0	600	32.0	600	40.1	
650	56.2	200.4	53.0	650	59.5	650	62.4	
700	80.9	199.8	74.2	700	81.5	700	84.4	
750	98.2	199.9	93.3	750	104.3	750	102.8	
800	115.7	199.7	109.2	800	109.3	790	108.5	
830	119.0	199.7	117.0	810	111.1	800	107.9	
850	116.0	199.7	119.6	850	78.6	850	70.2	
900	76.7	200.1	92.7	900	45.1	900	41.1	
950	41.9	200.1	52.7	950	11.0	950	8.9	
1000	10.0	200.1	16.6	962	0.0	964	0.0	
1010	0.0	200.1	5.6	1000	0.0	1000	0.0	
1014	0.0	200.1	0.0					
1100	0.0	200.1	0.0					

Expt. No.	=	3F6.7Y48	Q	=	8.00	l/s
F_0	=	6.70	U_0	=	1.00	m/s
F_r	=	2.52	y_t/b_0	=	3.0	

Measured at								Remarks
Centre				150 mm right from centre		150 mm left from centre		
Distance (mm)	Bed level (mm)	Water level (mm)	Bed Level at the end of experiment (mm)	Distance (mm)	Bed level (mm)	Distance (mm)	Bed level (mm)	
0	0.0	40.0	0.0	0	0.0	0	0.0	
50	0.0	40.0	0.0	50	0.0	50	0.0	
50	-16.4	40.0	-18.2	50	-26.7	50	-13.5	
100	-18.3	42.7	-20.4	100	-26.3	100	-22.3	
150	-24.4	52.5	-29.2	150	-34.3	150	-27.3	
200	-38.4	51.3	-42.6	200	-49.9	200	-42.8	
250	-56.0	45.3	-66.2	250	-59.4	250	-58.9	
300	-73.8	44.8	-79.2	300	-64.5	300	-76.5	
350	-88.3	55.2	-95.8	350	-67.2	350	-76.5	
400	-96.8	51.0	-105.9	400	-65.2	400	-81.3	
450	-103.4	45.0	-108.7	450	-64.8	450	-83.5	
500	-109.7	52.4	-112.2	500	-65.5	500	-84.6	
550	-113.0	51.5	-114.1	550	-63.4	550	-78.5	
600	-113.9	46.3	-115.2	600	-58.6	600	-72.3	
650	-113.1	51.8	-115.0	650	-56.8	650	-66.4	
700	-107.7	50.5	-112.2	700	-53.1	700	-58.6	
750	-102.5	49.6	-110.0	750	-48.9	750	-50.6	
800	-96.7	51.6	-105.6	800	-44.5	800	-43.4	
900	-77.9	51.1	-89.5	900	-33.8	900	-26.3	
1000	-65.0	53.3	-72.2	1000	-22.7	1000	-11.1	
1200	-32.3	53.6	-42.0	1200	-3.7	1200	7.0	
1400	-7.0	52.8	-10.1	1400	1.8	1400	6.9	
1600	6.6	51.0	2.1	1600	0.4	1600	5.5	
2000	9.4	50.0	12.8	2000	2.4	2000	6.6	
2500	11.8	48.9	13.3	2500	8.5	2500	5.6	
2900	11.6	48.5	12.2	2900	5.3	2900	4.9	

Expt. No.	=	4F5.3Y280	Q	=	6.30	l/s
F_0	=	5.30	U_0	=	0.79	m/s
F_r	=	1.99	y_t/b_0	=	17.5	

Measured at								Remarks
Centre				150 mm right from centre		150 mm left from centre		
Distance (mm)	Bed level (mm)	Water level (mm)	Bed Level at the end of experiment (mm)	Distance (mm)	Bed level (mm)	Distance (mm)	Bed level (mm)	
0	0.0	275.9	0.0	0	0.0	0	0.0	
50	0.0	275.9	5.0	50	0.0	50	0.0	
50	-32.9	275.9	5.0	50	-33.0	50	-36.9	
100	-34.7	275.5	10.0	100	-38.0	100	-41.2	
150	-62.5	275.6	15.0	150	-61.2	150	-61.9	
200	-80.5	274.1	20.0	200	-81.5	200	-80.7	
250	-82.3	275.2	25.0	250	-76.8	250	-80.8	
300	-69.4	275.1	30.0	300	-58.9	300	-64.4	
350	-41.9	275.1	35.0	350	-46.3	350	-31.9	
400	0.9	276.0	40.0	400	3.3	400	7.4	
450	28.5	276.4	45.0	450	32.2	450	36.7	
500	44.4	277.6	50.0	500	45.4	500	48.8	
550	57.7	279.6	55.0	550	57.1	550	61.1	
600	69.4	279.6	60.0	600	66.0	600	74.3	
650	82.8	278.9	62.0	620	66.2	620	74.4	
670	84.0	279.9	65.0	650	58.4	650	64.3	
700	78.1	279.9	70.0	700	28.7	700	33.2	
750	45.5	279.1	74.0	740	0.0	750	0.7	
800	9.9	279.1	75.0	750	0.0	800	0.0	
812	0.0	279.1	80.0	800	0.0	850	0.0	
818	0.0	279.1	85.0	850	0.0			
850	0.0	279.1	0.0					

Expt. No.	=	4F5.3Y240	Q	=	6.30	l/s
F_0	=	5.30	U_0	=	0.79	m/s
F_r	=	1.99	y_t/b_0	=	15.0	

Measured at								Remarks
Centre				150 mm right from centre		150 mm left from centre		
Distance (mm)	Bed level (mm)	Water level (mm)	Bed Level at the end of experiment (mm)	Distance (mm)	Bed level (mm)	Distance (mm)	Bed level (mm)	
0	0.0	236.0	0.0	0	0.0	0	0.0	
50	0.0	236.0	0.0	50	0.0	50	0.0	
50	-35.2	236.0	-35.5	50	-34.5	50	-38.6	
100	-37.3	236.0	-37.9	100	-39.7	100	-40.4	
150	-61.5	235.2	-59.8	150	-63.6	150	-61.5	
200	-82.3	235.2	-77.4	200	-82.5	200	-80.7	
250	-85.1	235.2	-86.8	250	-82.9	250	-84.8	
300	-74.3	234.8	-72.4	300	-67.5	300	-76.2	
350	-45.1	234.9	-46.5	350	-44.7	350	-41.5	
400	-3.1	235.8	-3.4	400	-12.3	400	-0.1	
450	20.8	236.6	23.9	450	23.7	450	22.3	
500	36.6	238.5	38.1	500	45.1	500	42.1	
550	54.7	239.4	55.0	550	56.8	550	57.8	
600	69.0	239.5	67.3	600	66.4	600	71.7	
650	81.9	238.9	80.5	650	58.1	650	60.8	
700	70.1	238.8	76.2	700	29.1	700	30.4	
750	41.6	239.1	50.0	750	0.0	744	0.0	
778	22.2	239.1	31.7	800	0.0	750	0.0	
800	10.0	239.1	18.4	850	0.0	800	0.0	
810	0.0	239.2	9.7			850	0.0	
818	0.0	239.2	0.0					
850	0.0	239.4	0.0					

Expt. No.	=	4F5.3Y200	Q	=	6.30	l/s
F_0	=	5.30	U_0	=	0.79	m/s
F_r	=	1.99	y_t/b_0	=	12.5	

Measured at								Remarks
Centre				150 mm right from centre		150 mm left from centre		
Distance (mm)	Bed level (mm)	Water level (mm)	Bed Level at the end of experiment (mm)	Distance (mm)	Bed level (mm)	Distance (mm)	Bed level (mm)	
0	0.0	191.4	0.0	0	0.0	0	0.0	
50	0.0	191.4	0.0	50	0.0	50	0.0	
50	-32.9	191.4	-33.8	50	-36.5	50	-35.8	
100	-37.6	191.4	-38.0	100	-41.4	100	-37.2	
150	-65.0	191.2	-61.1	150	-60.8	150	-74.3	
200	-78.4	191.1	-78.8	200	-78.9	200	-75.0	
250	-81.6	191.0	-81.0	250	-74.2	250	-75.9	
300	-64.7	191.6	-70.4	300	-62.3	300	-61.6	
350	-31.7	191.4	-31.5	350	-37.8	350	-26.3	
400	4.6	193.2	8.8	400	7.0	400	9.8	
450	28.0	195.0	23.6	450	27.1	450	27.6	
500	47.4	196.1	45.1	500	41.1	500	42.1	
550	67.3	195.5	63.9	550	54.3	550	57.2	
600	79.8	195.4	78.2	600	65.2	600	64.9	
630	82.0	195.5	79.9	650	41.5	650	38.3	
650	79.7	195.5	78.2	700	19.2	700	13.1	
700	52.4	195.5	54.5	730	0.0	720	0.0	
750	18.0	195.3	19.2	750	0.0	750	0.0	
774	0.0	195.3	7.2	800	0.0	800	0.0	
784	0.0	195.3	0.0	850	0.0	850	0.0	
850	0.0	195.5	0.0	900	0.0	900	0.0	
900	0.0	195.7	0.0					

Expt. No.	=	4F5.3Y160	Q	=	6.30	l/s
F_0	=	5.30	U_0	=	0.79	m/s
F_r	=	1.99	y_t/b_0	=	10.0	

Measured at								Remarks
Centre				150 mm right from centre		150 mm left from centre		
Distance (mm)	Bed level (mm)	Water level (mm)	Bed Level at the end of experiment (mm)	Distance (mm)	Bed level (mm)	Distance (mm)	Bed level (mm)	
0	0.0	157.1	0.0	0	0.0	0	0.0	
50	0.0	157.1	0.0	50	0.0	50	0.0	
50	-32.2	157.1	-31.8	50	-32.4	50	-31.0	
100	-34.7	157.0	-34.8	100	-39.2	100	-35.8	
150	-57.8	156.7	-58.6	150	-59.2	150	-58.2	
200	-76.2	156.4	-76.2	200	-72.3	200	-71.2	
250	-75.2	155.9	-74.2	250	-72.2	250	-70.0	
300	-52.3	155.9	-51.8	300	-55.8	300	-49.1	
350	-15.3	157.8	-15.4	350	-22.5	350	-17.4	
400	16.7	160.2	14.5	400	16.1	400	17.1	
450	35.3	161.5	35.5	450	30.1	450	31.1	
500	58.4	161.0	53.8	500	46.8	500	46.6	
550	69.5	160.6	64.3	550	64.8	550	59.9	
600	74.4	160.9	72.0	600	72.9	600	60.1	
610	74.7	161.1	74.8	650	55.5	650	32.2	
650	70.8	161.7	72.0	700	20.5	700	2.0	
700	47.7	161.7	54.6	730	0.0	710	0.0	
750	26.8	161.8	29.3	750	0.0	750	0.0	
790	0.0	161.8	6.0	800	0.0	800	0.0	
800	0.0	161.9	0.0	850	0.0	850	0.0	
850	0.0	161.9	0.0	900	0.0	900	0.0	
900	0.0	161.9	0.0					

Appendix C: Data for the Velocity Profiles

Note: x is the longitudinal distance measured from the sluice gate for all the velocity data summarised in the following tables (i.e. same as x_s used in the main text of the thesis).

Expt. No.: = 1F5.3Y280 **U_0 = 1.00 m/s** **F_0 = 5.3** **y_t/b_0 = 17.0**

At x = 50 mm							At x = 100 mm							At x = 150 mm						
y (mm)	u (m/s)	v (m/s)	w (m/s)	$\sqrt{\overline{u'^2}}$ (m/s)	$\sqrt{\overline{v'^2}}$ (m/s)	$\sqrt{\overline{w'^2}}$ (m/s)	y (mm)	u (m/s)	v (m/s)	w (m/s)	$\sqrt{\overline{u'^2}}$ (m/s)	$\sqrt{\overline{v'^2}}$ (m/s)	$\sqrt{\overline{w'^2}}$ (m/s)	y (mm)	u (m/s)	v (m/s)	w (m/s)	$\sqrt{\overline{u'^2}}$ (m/s)	$\sqrt{\overline{v'^2}}$ (m/s)	$\sqrt{\overline{w'^2}}$ (m/s)
5	1.11		-0.01	0.03		0.02	-35	-0.11	0.07	0.00	0.11	0.05	0.08	-60	-0.05	0.04	0.006			
10	0.98		0.00	0.07		0.03	-25	0.09	0.03	0.00				-50	-0.02	0.02	0.015	0.15	0.09	0.12
15	0.39		0.00	0.10		0.07	-10	1.00	-0.15	0.02				-40	0.05	0.03	0.010			
25	0.10		0.00	0.05		0.06	-5	0.88	-0.11	0.02	0.12	0.05	0.07	-30	0.53	-0.17	0.004	0.25	0.14	0.13
40	0.07		0.01	0.05		0.06	5	0.40	-0.06	0.01	0.15	0.04	0.09	-25	0.66	-0.18	0.008	0.23	0.13	0.12
60	0.05		0.01	0.06		0.06	20	0.10	-0.04	0.01	0.08	0.03	0.08	-15	0.74	-0.18	0.012	0.17	0.07	0.10
80	0.02		0.01	0.05		0.06	40	0.07	-0.05	0.00	0.08	0.04	0.08	-5	0.53	-0.11	0.015	0.21	0.05	0.09
90	0.02		0.00	0.06		0.06	70	0.03	-0.06	0.00	0.08	0.04	0.08	15	0.12	-0.05	0.007	0.10	0.04	0.09
165	-0.05		0.01	0.07		0.06	100	0.00	-0.07	0.00	0.08	0.04	0.06	55	0.05	-0.06	0.003	0.08	0.05	0.07
205	-0.08		0.01	0.07		0.06	140	-0.04	-0.07	0.01	0.08	0.05	0.06	95	-0.01	-0.07	0.004	0.08	0.05	0.06
235	-0.11		0.01	0.07		0.06	180	-0.07	-0.07	0.00	0.08	0.05	0.06	135	-0.06	-0.07	0.008	0.08	0.05	0.06
255	-0.13		0.00	0.08		0.06	215	-0.11	-0.04	0.00	0.07	0.04	0.06	175	-0.11	-0.06	0.002	0.07	0.05	0.07
265	-0.09		0.00	0.08		0.06	235	-0.13		0.01	0.07		0.06	215	-0.14	-0.03	-0.002	0.08	0.05	0.07
At x = 700 mm							255	-0.17		0.00	0.07		0.06	235	-0.17		0.007	0.07		0.07
95	-0.07	-0.01	-0.012	0.06	0.02	0.05	265	-0.17		0.01	0.09		0.06	255	-0.20		0.006	0.07		0.07
110	-0.06	-0.01	-0.012	0.07	0.04	0.07								265	-0.23		0.005	0.07		0.07
130	-0.03	0.00	-0.004	0.08	0.05	0.07														
150	0.02	0.01	0.001	0.11	0.06	0.08														
185	0.11	0.03	0.001	0.12	0.08	0.09														
220	0.20	0.04	0.001	0.10	0.08	0.08														
240	0.23		0.003	0.09		0.08														
260	0.28		-0.002	0.09		0.09														
270	0.29		0.006	0.10		0.10														

Expt. No.: 1F5.3Y280 Cont'd

At x = 200 mm							At x = 250 mm							At x = 300 mm						
y (mm)	u (m/s)	v (m/s)	w (m/s)	$\sqrt{\overline{u'^2}}$ (m/s)	$\sqrt{\overline{v'^2}}$ (m/s)	$\sqrt{\overline{w'^2}}$ (m/s)	y (mm)	u (m/s)	v (m/s)	w (m/s)	$\sqrt{\overline{u'^2}}$ (m/s)	$\sqrt{\overline{v'^2}}$ (m/s)	$\sqrt{\overline{w'^2}}$ (m/s)	y (mm)	u (m/s)	v (m/s)	w (m/s)	$\sqrt{\overline{u'^2}}$ (m/s)	$\sqrt{\overline{v'^2}}$ (m/s)	$\sqrt{\overline{w'^2}}$ (m/s)
-85	-0.06	0.00	0.002				-100	-0.03	-0.01	0.009	0.10	0.04	0.10	-100	0.04	0.00	0.001	0.08	0.03	0.10
-70	0.02	-0.01	0.010	0.14	0.10	0.13	-85	0.11	-0.06	0.009	0.17	0.10	0.15	-85	0.23	-0.03	0.003	0.19	0.10	0.14
-55	0.09	-0.01	0.007				-70	0.20	-0.04	0.007				-70	0.35	-0.02	0.003			
-45	0.50	-0.18	0.014	0.23	0.14	0.12	-55	0.49	-0.13	0.008	0.20	0.11	0.11	-55	0.48	-0.01	0.005	0.18	0.10	0.11
-35	0.60	-0.19	0.014	0.20	0.11	0.11	-40	0.51	-0.11	0.007	0.19	0.09	0.11	-35	0.43	0.00	0.008	0.18	0.09	0.11
-25	0.59	-0.16	0.013	0.20	0.08	0.10	-25	0.40	-0.08	0.006	0.21	0.07	0.11	-15	0.27	0.00	-0.001	0.19	0.07	0.10
-15	0.46	-0.11	0.009	0.24	0.07	0.10	-10	0.25	-0.06	0.000	0.21	0.06	0.09	5	0.12	-0.02	0.005	0.15	0.06	0.09
-5	0.32	-0.08	-0.002	0.22	0.06	0.09	10	0.08	-0.06	-0.003	0.08	0.05	0.07	25	0.05	-0.03	0.000	0.10	0.06	0.08
15	0.09	-0.05	0.006	0.10	0.04	0.08	30	0.04	-0.06	-0.003	0.09	0.05	0.06	55	-0.01	-0.05	-0.002	0.09	0.06	0.08
55	0.02	-0.07	0.001	0.08	0.05	0.06	60	-0.01	-0.07	0.004	0.07	0.06	0.06	95	-0.05	-0.07	0.001	0.07	0.06	0.08
95	-0.03	-0.07	0.004	0.07	0.05	0.06	100	-0.05	-0.08	0.001	0.08	0.06	0.07	135	-0.10	-0.06	0.002	0.07	0.06	0.10
135	-0.09	-0.07	-0.003	0.07	0.05	0.07	140	-0.11	-0.07	0.004	0.07	0.05	0.08	175	-0.13	-0.04	0.002	0.07	0.06	0.10
175	-0.13	-0.05	0.006	0.07	0.05	0.07	180	-0.15	-0.04	-0.001	0.07	0.05	0.09	215	-0.17	-0.01	-0.002	0.07	0.06	0.09
215	-0.16	-0.02	-0.003	0.08	0.05	0.08	215	-0.18	-0.02	0.005	0.07	0.05	0.09	235	-0.20	0.00	0.011	0.08	0.00	0.09
235	-0.20		0.003	0.07		0.08	235	-0.21		0.003	0.08		0.08	255	-0.26	0.00	-0.001	0.07	0.00	0.08
255	-0.23		0.011	0.07		0.07	255	-0.24		0.009	0.08		0.08	265	-0.30	0.00	-0.001	0.08	0.00	0.09
265	-0.27		0.002	0.07		0.08	265	-0.29		0.003	0.07		0.08							

Expt. No.: 1F5.3Y280 Cont'd

At x = 350 mm							At x = 400 mm							At x = 450 mm						
y (mm)	u (m/s)	v (m/s)	w (m/s)	$\sqrt{\overline{u'^2}}$ (m/s)	$\sqrt{\overline{v'^2}}$ (m/s)	$\sqrt{\overline{w'^2}}$ (m/s)	y (mm)	u (m/s)	v (m/s)	w (m/s)	$\sqrt{\overline{u'^2}}$ (m/s)	$\sqrt{\overline{v'^2}}$ (m/s)	$\sqrt{\overline{w'^2}}$ (m/s)	y (mm)	u (m/s)	v (m/s)	w (m/s)	$\sqrt{\overline{u'^2}}$ (m/s)	$\sqrt{\overline{v'^2}}$ (m/s)	$\sqrt{\overline{w'^2}}$ (m/s)
-80	0.04	0.02	0.002				-20	0.16	-0.01	-0.002				30	0.34	0.00	0.005			
-60	0.39	0.05	0.006				-10	0.38	0.28	0.004	0.13	0.10	0.11	50	0.31	0.29	0.008	0.09	0.10	0.10
-40	0.43	0.15	0.007	0.15	0.10	0.11	5	0.35	0.26	0.009	0.12	0.10	0.10	70	0.25	0.26	0.003	0.09	0.12	0.10
-20	0.36	0.14	0.009	0.14	0.09	0.11	25	0.28	0.23	0.006	0.11	0.11	0.11	100	0.14	0.18	-0.002	0.09	0.12	0.10
0	0.25	0.10	-0.002	0.15	0.09	0.11	55	0.16	0.14	-0.001	0.09	0.11	0.09	135	0.07	0.13	0.000	0.09	0.12	0.10
20	0.14	0.05	0.002	0.13	0.08	0.10	95	0.05	0.03	-0.004	0.08	0.09	0.09	175	-0.02	0.08	0.001	0.08	0.10	0.09
55	0.03	-0.02	-0.001	0.07	0.07	0.08	135	-0.01	0.00	-0.012	0.07	0.08	0.09	215	-0.11	0.07	-0.006	0.08	0.09	0.09
95	-0.02	-0.04	0.000	0.07	0.07	0.08	175	-0.06	0.01	-0.006	0.07	0.08	0.10	235	-0.14		-0.004	0.08		0.09
135	-0.06	-0.05	0.005	0.07	0.06	0.09	215	-0.14	0.02	-0.007	0.08	0.07	0.09	255	-0.22		-0.008	0.08		0.10
175	-0.11	-0.03	0.005	0.07	0.06	0.10	235	-0.19		-0.005	0.08		0.09	265	-0.25		-0.004	0.08		0.11
215	-0.17	0.00	-0.001	0.08	0.06	0.09	255	-0.27		-0.001	0.08		0.09	185	-0.29	0.00	-0.036	0.09	0.00	0.12
235	-0.20		0.002	0.08		0.09	265	-0.31		-0.004	0.08		0.10							
255	-0.27		0.001	0.08		0.09														
265	-0.31		-0.003	0.08		0.09														
At x = 500 mm							At x = 550 mm							At x = 600 mm						
25	0.11	0.06	0.009				40	-0.03	-0.01	-0.002	0.08	0.04	0.11	65	-0.07	-0.02	0.001	0.08	0.04	0.08
35	0.16	0.13	0.007				50	0.02	0.03	-0.006	0.15	0.07	0.12	75	-0.03	0.00	0.004	0.12	0.06	0.09
55	-0.09	-0.03	0.002				70	0.06	0.07	-0.001	0.15	0.08	0.12	90	0.03	0.02	0.003	0.17	0.08	0.11
75	0.31	0.31	0.006	0.11	0.09	0.09	90	0.20	0.19	0.007	0.17	0.10	0.12	110	0.09	0.07	-0.002	0.17	0.09	0.11
105	0.24	0.28	0.008	0.10	0.11	0.10	120	0.23	0.26	0.002	0.13	0.09	0.10	140	0.15	0.14	0.002	0.17	0.10	0.12
140	0.15	0.25	0.001	0.10	0.12	0.10	150	0.19	0.28	0.005	0.11	0.10	0.10	180	0.16	0.18	0.000	0.14	0.10	0.11
180	0.04	0.18	-0.009	0.10	0.12	0.11	185	0.11	0.25	0.003	0.10	0.10	0.10	220	0.15	0.14	0.003	0.11	0.10	0.11
220	-0.06	0.12	-0.008	0.11	0.10	0.11	220	0.04	0.19	-0.001	0.10	0.11	0.09	240	0.17		-0.002	0.10		0.08
240	-0.08		-0.004	0.09		0.09	240	0.05		-0.005	0.10		0.09	260	0.14		0.005	0.11		0.09
260	-0.14		0.000	0.09		0.10	260	0.02		-0.007	0.10		0.09	270	0.14		-0.005	0.11		0.10
270	-0.15		-0.008	0.09		0.12	270	-0.01		0.017	0.10		0.12							

Expt. No.: = 1F5.3Y240 **U_0 = 1.00 m/s** **F_0 = 5.3** **y_t/b_0 = 15.0**

At x = 50 mm							At x = 100 mm							At x = 150 mm						
y (mm)	u (m/s)	v (m/s)	w (m/s)	$\sqrt{\overline{u'^2}}$ (m/s)	$\sqrt{\overline{v'^2}}$ (m/s)	$\sqrt{\overline{w'^2}}$ (m/s)	y (mm)	u (m/s)	v (m/s)	w (m/s)	$\sqrt{\overline{u'^2}}$ (m/s)	$\sqrt{\overline{v'^2}}$ (m/s)	$\sqrt{\overline{w'^2}}$ (m/s)	y (mm)	u (m/s)	v (m/s)	w (m/s)	$\sqrt{\overline{u'^2}}$ (m/s)	$\sqrt{\overline{v'^2}}$ (m/s)	$\sqrt{\overline{w'^2}}$ (m/s)
5	1.06		-0.033	0.02		0.02	-30	-0.06	0.06	0.016	0.10	0.05	0.08	-55	-0.03	0.03	0.005	0.09	0.05	0.07
10	0.88		-0.014	0.09		0.04	-20	0.23	0.01	0.025				-45	0.01	0.01	0.032	0.14	0.08	0.11
15	0.38		0.004	0.11		0.07	-10	0.95	-0.13	0.049				-35	0.13	0.00	0.038			
25	0.07		0.018	0.05		0.05	0	0.69	-0.08	0.044	0.14	0.04	0.07	-25	0.56	-0.13	0.032	0.22	0.12	0.13
40	0.06		0.013	0.04		0.05	10	0.23	-0.04	0.020	0.11	0.04	0.07	-15	0.78	-0.16	0.041	0.15	0.08	0.10
60	0.05		0.013	0.05		0.04	20	0.08	-0.03	0.017	0.07	0.03	0.07	-5	0.58	-0.10	0.037	0.21	0.05	0.11
80	0.02		0.016	0.05		0.05	30	0.07	-0.04	0.015	0.07	0.03	0.06	5	0.28	-0.05	0.027	0.16	0.05	0.10
110	0.00		0.015	0.06		0.05	40	0.07	-0.04	0.021	0.07	0.03	0.06	25	0.09	-0.04	0.018	0.10	0.04	0.09
140	-0.03		0.015	0.06		0.05	60	0.05	-0.05	0.013	0.07	0.04	0.06	55	0.05	-0.05	0.013	0.07	0.04	0.05
170	-0.05		0.016	0.07		0.05	90	0.00	-0.06	0.006	0.08	0.04	0.06	85	0.01	-0.05	0.010	0.07	0.05	0.05
200	-0.06		0.012	0.08		0.06	120	-0.02	-0.06	0.007	0.08	0.04	0.07	125	-0.04	-0.05	0.006	0.08	0.05	0.06
215	-0.03		0.014	0.08		0.05	155	-0.06	-0.05	0.000	0.08	0.04	0.07	165	-0.09	-0.03	0.001	0.08	0.05	0.06
							165	-0.07	-0.04	0.006	0.09	0.04	0.07	185	-0.11		0.012	0.07		0.06
							185	-0.09		0.013	0.07		0.05	205	-0.16		0.007	0.08		0.06
							205	-0.11		0.014	0.08		0.06	215	-0.17		0.010	0.09		0.06
							215	-0.11		0.015	0.09		0.05							

Expt. 1F5.3Y240 - Cont'd

At x = 200 mm							At x = 250 mm							At x = 300 mm						
y (mm)	u (m/s)	v (m/s)	w (m/s)	$\sqrt{\overline{u'^2}}$ (m/s)	$\sqrt{\overline{v'^2}}$ (m/s)	$\sqrt{\overline{w'^2}}$ (m/s)	y (mm)	u (m/s)	v (m/s)	w (m/s)	$\sqrt{\overline{u'^2}}$ (m/s)	$\sqrt{\overline{v'^2}}$ (m/s)	$\sqrt{\overline{w'^2}}$ (m/s)	y (mm)	u (m/s)	v (m/s)	w (m/s)	$\sqrt{\overline{u'^2}}$ (m/s)	$\sqrt{\overline{v'^2}}$ (m/s)	$\sqrt{\overline{w'^2}}$ (m/s)
-75	-0.05	0.01	-0.002				-85	0.02	-0.03	-0.005	0.14	0.08	0.12	-85	0.16	-0.03	0.007	0.17	0.09	0.14
-65	0.02	-0.02	0.020	0.14	0.09	0.12	-70	0.17	-0.06	0.023	0.17	0.10	0.13	-70	0.29	-0.03	0.013			
-55	0.12	-0.04	0.033				-55	0.39	-0.11	0.036	0.20	0.11	0.12	-55	0.43	-0.03	0.029	0.19	0.10	0.12
-45	0.13	-0.01	0.039				-40	0.54	-0.11	0.039	0.17	0.09	0.10	-40	0.50	-0.01	0.029	0.15	0.09	0.10
-35	0.51	-0.14	0.030	0.21	0.12	0.12	-25	0.50	-0.08	0.034	0.19	0.07	0.09	-25	0.45	0.01	0.032	0.17	0.08	0.10
-25	0.64	-0.15	0.036	0.17	0.09	0.10	-10	0.28	-0.05	0.024	0.20	0.06	0.09	-10	0.28	0.01	0.020	0.19	0.08	0.09
-15	0.57	-0.11	0.036	0.20	0.07	0.10	5	0.12	-0.05	0.029	0.12	0.05	0.08	5	0.17	-0.01	0.024	0.16	0.07	0.09
-5	0.34	-0.07	0.026	0.20	0.06	0.10	25	0.05	-0.05	0.020	0.09	0.05	0.07	25	0.05	-0.04	0.001	0.10	0.06	0.08
5	0.17	-0.05	0.026	0.15	0.05	0.09	45	0.01	-0.06	0.007	0.09	0.05	0.07	45	0.00	-0.07	0.002	0.07	0.06	0.07
25	0.07	-0.05	0.030	0.07	0.04	0.06	75	-0.03	-0.07	0.002	0.09	0.05	0.08	75	-0.02	-0.07	0.001	0.07	0.06	0.08
55	0.04	-0.05	0.007	0.08	0.05	0.05	105	-0.07	-0.06	-0.007	0.09	0.05	0.08	105	-0.07	-0.06	-0.009	0.07	0.06	0.09
85	-0.02	-0.06	0.008	0.08	0.05	0.06	135	-0.10	-0.04	-0.006	0.09	0.05	0.09	135	-0.10	-0.04	-0.024	0.07	0.06	0.09
125	-0.07	-0.05	0.002	0.08	0.05	0.07	165	-0.13	-0.02	-0.008	0.09	0.05	0.09	165	-0.14	-0.01	-0.017	0.08	0.06	0.09
165	-0.12	-0.02	-0.005	0.08	0.05	0.07	185	-0.15		0.004	0.08		0.08	185	-0.17		-0.001	0.08		0.08
185	-0.14		0.008	0.08		0.07	205	-0.21		0.006	0.08		0.07	205	-0.22		0.000	0.09		0.08
205	-0.18		0.006	0.08		0.07	215	-0.25		0.006	0.08		0.07	215	-0.28		-0.002	0.08		0.08
215	-0.22		0.010	0.08		0.07								At x = 700 mm						
														95	-0.03	-0.013	-0.01	0.07	0.04	0.06
														110	0.01	-0.013	-0.01	0.09	0.05	0.07
														125	0.07	-0.008	0.00	0.10	0.06	0.08
														145	0.16	0.003	0.01	0.10	0.06	0.08
														165	0.24	0.010	0.02	0.09	0.07	0.08
														185	0.29		0.00	0.08		0.08
														205	0.34		-0.01	0.08		0.07
														215	0.36		-0.01	0.08		0.08

Expt. 1F5.3Y240 - Cont'd

At x = 350 mm							At x = 400 mm							At x = 450 mm						
y (mm)	u (m/s)	v (m/s)	w (m/s)	$\sqrt{\overline{u'^2}}$ (m/s)	$\sqrt{\overline{v'^2}}$ (m/s)	$\sqrt{\overline{w'^2}}$ (m/s)	y (mm)	u (m/s)	v (m/s)	w (m/s)	$\sqrt{\overline{u'^2}}$ (m/s)	$\sqrt{\overline{v'^2}}$ (m/s)	$\sqrt{\overline{w'^2}}$ (m/s)	y (mm)	u (m/s)	v (m/s)	w (m/s)	$\sqrt{\overline{u'^2}}$ (m/s)	$\sqrt{\overline{v'^2}}$ (m/s)	$\sqrt{\overline{w'^2}}$ (m/s)
-75	0.04	0.02	0.004				0	0.02	-0.02	0.017				25	0.36	-0.02	0.008			
-60	0.33	0.06	0.017				10	0.37	0.27	0.030	0.12	0.09	0.10	40	0.34	0.31	0.020	0.12	0.09	0.11
-45	0.39	0.06	0.021				25	0.29	0.23	0.018	0.12	0.11	0.10	55	0.31	0.30	0.024	0.10	0.10	0.09
-25	0.44	0.14	0.032	0.13	0.09	0.10	45	0.20	0.15	0.013	0.11	0.12	0.11	75	0.24	0.26	0.014	0.09	0.12	0.10
-5	0.33	0.13	0.027	0.15	0.09	0.11	75	0.08	0.04	-0.001	0.10	0.10	0.10	95	0.16	0.19	0.007	0.09	0.12	0.11
15	0.19	0.06	0.017	0.14	0.09	0.10	105	0.02	0.01	-0.012	0.09	0.08	0.10	115	0.09	0.14	-0.002	0.09	0.12	0.10
45	0.05	-0.02	0.006	0.07	0.07	0.07	135	-0.04	-0.01	-0.013	0.10	0.08	0.10	135	0.03	0.10	-0.003	0.09	0.11	0.10
75	0.00	-0.06	-0.014	0.07	0.07	0.08	165	-0.12	0.01	-0.013	0.10	0.08	0.10	165	-0.07	0.07	-0.015	0.10	0.10	0.09
105	-0.03	-0.06	-0.027	0.07	0.06	0.08	185	-0.17		-0.002	0.09		0.08	185	-0.13		-0.004	0.09		0.09
135	-0.07	-0.03	-0.020	0.07	0.06	0.09	205	-0.27		-0.010	0.09		0.10	205	-0.22		-0.009	0.08		0.10
165	-0.14	-0.01	-0.019	0.08	0.07	0.09	215	-0.32		-0.018	0.09		0.10	215	-0.27		-0.025	0.09		0.11
185	-0.17		-0.009	0.09		0.09														
205	-0.25		-0.009	0.09		0.08														
215	-0.31		-0.008	0.09		0.09														
At x = 500 mm							At x = 550 mm							At x = 600 mm						
45	0.15	-0.02	0.00				50	-0.03	-0.01	0.00	0.08	0.04	0.08	65	-0.03	-0.01	0.00	0.06	0.03	0.07
60	0.13	-0.07	0.00				60	-0.01	0.02	-0.01	0.12	0.06	0.10	75	-0.03	-0.01	0.01	0.10	0.05	0.08
75	0.31	0.32	0.01	0.11	0.08	0.09	75	0.07	0.07	-0.01	0.15	0.07	0.10	90	0.02	0.01	0.01	0.12	0.06	0.09
90	0.27	0.32	0.01	0.12	0.09	0.10	100	0.19	0.19	0.00	0.16	0.09	0.11	110	0.10	0.07	0.01	0.15	0.08	0.10
110	0.22	0.31	0.01	0.10	0.11	0.10	135	0.22	0.26	0.00	0.13	0.09	0.10	140	0.18	0.13	0.01	0.14	0.09	0.10
140	0.12	0.23	0.01	0.11	0.12	0.11	170	0.15	0.22	0.00	0.10	0.10	0.10	170	0.22	0.13	0.01	0.11	0.09	0.09
170	0.01	0.16	-0.01	0.11	0.12	0.11	190	0.14		-0.01	0.10		0.08	190	0.26		-0.01	0.09		0.08
190	-0.03		-0.01	0.09		0.09	210	0.07		-0.02	0.10		0.09	210	0.24		-0.01	0.09		0.08
210	-0.10		-0.01	0.09		0.10	220	0.05		-0.02	0.09		0.10	220	0.22		-0.01	0.10		0.10
220	-0.15		-0.02	0.09		0.12														

Expt. No.: = 1F5.3Y200 U_0 = 1.00 m/s F_0 = 5.3 y_t/b_0 = 12.5

At x = 50 mm							At x = 100 mm							At x = 150 mm						
y (mm)	u (m/s)	v (m/s)	w (m/s)	$\sqrt{\overline{u'^2}}$ (m/s)	$\sqrt{\overline{v'^2}}$ (m/s)	$\sqrt{\overline{w'^2}}$ (m/s)	y (mm)	u (m/s)	v (m/s)	w (m/s)	$\sqrt{\overline{u'^2}}$ (m/s)	$\sqrt{\overline{v'^2}}$ (m/s)	$\sqrt{\overline{w'^2}}$ (m/s)	y (mm)	u (m/s)	v (m/s)	w (m/s)	$\sqrt{\overline{u'^2}}$ (m/s)	$\sqrt{\overline{v'^2}}$ (m/s)	$\sqrt{\overline{w'^2}}$ (m/s)
5	1.07		-0.048	0.02		0.02	-35	-0.09	0.05	0.028	0.08	0.03	0.06	-50	-0.05	0.02	0.017	0.07	0.03	0.07
15	0.97		-0.041	0.06		0.04	-25	-0.06	0.06	0.036	0.10	0.05	0.08	-45	-0.07	0.04	0.016			
20	0.43		0.006	0.11		0.06	-20	0.03	0.03	0.029				-35	0.03	0.02	0.039	0.10	0.06	0.09
25	0.16		0.005	0.07		0.06	0	0.92	-0.11	-0.057				-25	0.16	0.02	0.025			
30	0.08		0.016	0.05		0.06	10	0.50	-0.05	-0.014	0.14	0.04	0.08	-15	0.63	-0.14	-0.033	0.20	0.11	0.11
35	0.07		0.011	0.05		0.05	20	0.14	-0.03	0.013	0.08	0.03	0.06	-5	0.78	-0.16	-0.044	0.14	0.07	0.08
45	0.06		0.015	0.05		0.05	30	0.08	-0.03	0.008	0.07	0.03	0.06	5	0.52	-0.09	-0.022	0.19	0.05	0.09
65	0.04		0.015	0.05		0.05	40	0.07	-0.04	0.015	0.07	0.03	0.06	15	0.23	-0.05	0.004	0.14	0.04	0.08
95	-0.01		0.011	0.06		0.05	60	0.04	-0.04	0.013	0.07	0.04	0.06	25	0.10	-0.04	0.010	0.09	0.04	0.08
125	-0.02		0.014	0.07		0.05	80	0.03	-0.04	0.009	0.07	0.04	0.06	35	0.08	-0.04	0.011	0.09	0.04	0.07
155	-0.05		0.009	0.07		0.05	100	0.00	-0.05	0.009	0.08	0.04	0.06	50	0.05	-0.04	0.013	0.09	0.04	0.07
180	-0.06		0.011	0.09		0.05	110	-0.03	-0.05	0.009	0.08	0.04	0.07	70	0.03	-0.04	0.005	0.09	0.04	0.08
							130	-0.06	-0.05	0.006	0.08	0.04	0.07	90	0.00	-0.04	0.006	0.10	0.05	0.08
							150	-0.07		0.013	0.07		0.06	110	-0.03	-0.04	0.004	0.10	0.05	0.08
							180	-0.09		0.011	0.09		0.06	130	-0.07	-0.04	0.010	0.10	0.05	0.09
														150	-0.11		0.008	0.08		0.07
														180	-0.18		0.007	0.08		0.06

Expt. 1F5.3Y200 - Cont'd

At x = 200 mm							At x = 300 mm							At x = 350 mm						
y (mm)	u (m/s)	v (m/s)	w (m/s)	$\sqrt{\overline{u'^2}}$ (m/s)	$\sqrt{\overline{v'^2}}$ (m/s)	$\sqrt{\overline{w'^2}}$ (m/s)	y (mm)	u (m/s)	v (m/s)	w (m/s)	$\sqrt{\overline{u'^2}}$ (m/s)	$\sqrt{\overline{v'^2}}$ (m/s)	$\sqrt{\overline{w'^2}}$ (m/s)	y (mm)	u (m/s)	v (m/s)	w (m/s)	$\sqrt{\overline{u'^2}}$ (m/s)	$\sqrt{\overline{v'^2}}$ (m/s)	$\sqrt{\overline{w'^2}}$ (m/s)
-70	-0.05	0.00	0.004				-80	0.09	0.00	-0.021				-50	0.27	0.06	-0.016	0.09	0.05	0.10
-65	-0.05	0.01	0.005				-70	0.19	-0.02	-0.012	0.18	0.09	0.12	-40	0.35	0.07	-0.022			
-55	0.07	-0.04	0.036	0.12	0.07	0.10	-50	0.39	-0.03	-0.018				-25	0.41	0.06	-0.019			
-45	0.13	-0.03	0.028				-30	0.50	-0.01	-0.024	0.15	0.09	0.10	-5	0.44	0.13	-0.019	0.13	0.09	0.10
-25	0.61	-0.17	-0.027	0.17	0.10	0.10	-20	0.46	0.00	-0.017	0.17	0.08	0.10	15	0.33	0.11	-0.008	0.14	0.09	0.09
-15	0.63	-0.15	-0.030	0.17	0.07	0.09	-10	0.36	0.01	-0.013	0.20	0.08	0.10	35	0.16	0.04	-0.003	0.12	0.09	0.09
-5	0.50	-0.10	-0.015	0.21	0.06	0.09	0	0.26	0.00	-0.003	0.18	0.07	0.10	55	0.07	-0.02	0.011	0.09	0.07	0.08
5	0.30	-0.07	-0.005	0.19	0.05	0.09	10	0.16	-0.02	0.001	0.17	0.07	0.10	75	0.03	-0.05	0.000	0.08	0.07	0.08
15	0.15	-0.05	0.011	0.12	0.05	0.07	20	0.09	-0.03	0.004	0.13	0.07	0.10	95	-0.01	-0.05	-0.004	0.08	0.06	0.09
25	0.08	-0.05	0.016	0.09	0.04	0.07	40	0.03	-0.06	0.001	0.10	0.06	0.09	115	-0.06	-0.04	0.000	0.08	0.06	0.09
40	0.06	-0.05	0.019	0.09	0.04	0.07	70	-0.03	-0.08	-0.006	0.10	0.06	0.10	130	-0.14	-0.02	0.003	0.10	0.07	0.10
55	0.03	-0.05	0.008	0.09	0.05	0.07	100	-0.06	-0.07	-0.006	0.10	0.06	0.10	150	-0.23		-0.018	0.10		0.09
80	-0.02	-0.05	0.012	0.10	0.05	0.07	130	-0.13	-0.03	-0.002	0.10	0.06	0.10	180	-0.34		-0.005	0.09		0.10
100	-0.04	-0.05	0.008	0.09	0.05	0.08	150	-0.18		-0.013	0.09		0.09							
130	-0.10	-0.03	0.005	0.09	0.05	0.08	180	-0.30		-0.007	0.09		0.08							
150	-0.14		0.002	0.09		0.07														
180	-0.24		0.006	0.08		0.07														

Expt. 1F5.3Y200 - Cont'd

At x = 400 mm							At x = 450 mm							At x = 500 mm						
y (mm)	u (m/s)	v (m/s)	w (m/s)	$\sqrt{\overline{u'^2}}$ (m/s)	$\sqrt{\overline{v'^2}}$ (m/s)	$\sqrt{\overline{w'^2}}$ (m/s)	y (mm)	u (m/s)	v (m/s)	w (m/s)	$\sqrt{\overline{u'^2}}$ (m/s)	$\sqrt{\overline{v'^2}}$ (m/s)	$\sqrt{\overline{w'^2}}$ (m/s)	y (mm)	u (m/s)	v (m/s)	w (m/s)	$\sqrt{\overline{u'^2}}$ (m/s)	$\sqrt{\overline{v'^2}}$ (m/s)	$\sqrt{\overline{w'^2}}$ (m/s)
-25	0.31	0.19	-0.022	0.16	0.08	0.11	15	-0.01	-0.05	-0.024				35	0.03	0.02	-0.018			
5	0.40	0.27	-0.016	0.13	0.09	0.10	30	0.35	-0.03	-0.027				45	-0.04	0.05	-0.019			
25	0.34	0.26	-0.012	0.11	0.10	0.10	50	0.33	0.30	-0.014	0.10	0.09	0.10	80	0.28	0.30	-0.022	0.12	0.08	0.09
45	0.24	0.18	-0.006	0.11	0.11	0.10	70	0.26	0.28	-0.012	0.09	0.11	0.10	100	0.24	0.31	-0.021	0.10	0.09	0.08
65	0.15	0.11	-0.005	0.10	0.12	0.10	90	0.18	0.24	-0.006	0.09	0.13	0.10	120	0.19	0.28	-0.012	0.09	0.10	0.09
85	0.07	0.05	-0.003	0.10	0.11	0.10	110	0.09	0.17	-0.002	0.10	0.13	0.11	135	0.11	0.23	-0.010	0.10	0.11	0.10
100	-0.02	0.01	-0.006	0.09	0.09	0.10	120	0.00	0.13	-0.006	0.10	0.12	0.11	155	0.06		-0.008	0.09		0.08
115	-0.11	0.01	-0.002	0.11	0.09	0.10	135	-0.06	0.10	-0.007	0.10	0.11	0.11	185	-0.05		0.013	0.08		0.12
130	-0.14		-0.011	0.09		0.09	155	-0.14		-0.006	0.09		0.10	At x = 250 mm						
150	-0.29		-0.014	0.09		0.10	185	-0.23		0.004	0.08		0.12	-80	-0.02	-0.01	-0.008			
180	-0.34		-0.008	0.09		0.11								-65	0.12	-0.05	0.001			
At x = 550 mm							At x = 600 mm							-55	0.39	-0.11	0.000			
50	-0.05	-0.01	-0.007	0.08	0.04	0.07	90	0.03	-0.02	-0.013	0.08	0.05	0.07	-35	0.54	-0.11	-0.021	0.18	0.08	0.09
65	0.01	0.03	-0.014	0.12	0.06	0.09	95	0.06	-0.02	-0.011	0.09	0.05	0.08	-15	0.37	-0.06	-0.007	0.21	0.06	0.09
75	0.06	0.06	-0.010	0.12	0.06	0.09	115	0.14	-0.01	-0.012	0.10	0.06	0.08	5	0.10	-0.05	0.011	0.12	0.05	0.08
95	0.17	0.14	-0.015	0.15	0.09	0.10	135	0.25	0.02	-0.014	0.09	0.07	0.08	25	0.03	-0.06	0.012	0.09	0.05	0.07
115	0.20	0.19	-0.020	0.13	0.09	0.09	155	0.32		-0.017	0.08		0.08	45	0.00	-0.06	0.005	0.09	0.05	0.07
135	0.20	0.17	-0.017	0.10	0.09	0.09	185	0.34		-0.031	0.08		0.09	65	-0.03	-0.06	0.000	0.09	0.06	0.08
155	0.21		-0.016	0.09		0.08								85	-0.06	-0.06	0.001	0.09	0.05	0.08
185	0.11		-0.014	0.08		0.11								105	-0.08	-0.04	0.000	0.09	0.05	0.09
														130	-0.12	-0.02	0.001	0.09	0.05	0.09
														150	-0.16		-0.009	0.08		0.08
														180	-0.27		0.004	0.08		0.08

Expt. No.: = 1F5.3Y160 **U_0 = 1.00 m/s** **F_0 = 5.3** **y_t/b_0 = 10.0**

At x = 50 mm						
y (mm)	u (m/s)	v (m/s)	w (m/s)	$\sqrt{\overline{u'^2}}$ (m/s)	$\sqrt{\overline{v'^2}}$ (m/s)	$\sqrt{\overline{w'^2}}$ (m/s)
5	1.05		-0.063	0.04		0.03
10	0.67		-0.052	0.17		0.06
15	0.24		0.004	0.09		0.06
20	0.06		-0.003	0.06		0.06
30	0.05		0.006	0.06		0.06
40	0.03		0.007	0.05		0.05
50	0.01		0.012	0.05		0.05
65	0.00		0.009	0.06		0.05
80	-0.01		0.012	0.06		0.06
95	-0.03		0.009	0.07		0.05
115	-0.05		0.012	0.08		0.06
140	-0.03		0.005	0.08		0.05

At x = 700 mm						
90	0.18		-0.020	0.07		0.06
100	0.21		-0.019	0.07		0.06
110	0.25		-0.021	0.07		0.07
120	0.28		-0.019	0.07		0.06
130	0.30		-0.024	0.07		0.06
140	0.33		-0.027	0.07		0.06
150	0.34		-0.032	0.07		0.06

At x = 100 mm						
y (mm)	u (m/s)	v (m/s)	w (m/s)	$\sqrt{\overline{u'^2}}$ (m/s)	$\sqrt{\overline{v'^2}}$ (m/s)	$\sqrt{\overline{w'^2}}$ (m/s)
-35	-0.06	0.05	0.109	0.09	0.05	0.08
-25	0.00	0.06	0.111	0.09	0.05	0.08
-15	0.13	0.03	0.092			
-10	0.86	-0.12	-0.016	0.11	0.07	0.09
-5	0.83	-0.09	0.004	0.12	0.04	0.08
0	0.32	-0.04	0.014	0.14	0.04	0.09
10	0.06	-0.03	0.004	0.07	0.03	0.07
20	0.04	-0.04	0.008	0.07	0.03	0.06
30	0.02	-0.04	0.009	0.07	0.04	0.06
45	0.00	-0.05	0.005	0.08	0.04	0.06
60	-0.01	-0.05	0.005	0.08	0.04	0.06
75	-0.04	-0.05	0.001	0.08	0.05	0.07
90	-0.06	-0.05	0.004	0.08	0.04	0.07
115	-0.06		0.005	0.08		0.06
145	-0.08		0.009	0.10		0.06

At x = 150 mm						
y (mm)	u (m/s)	v (m/s)	w (m/s)	$\sqrt{\overline{u'^2}}$ (m/s)	$\sqrt{\overline{v'^2}}$ (m/s)	$\sqrt{\overline{w'^2}}$ (m/s)
-55	-0.10	0.04	0.082	0.09	0.05	0.09
-45	0.02	0.01	0.105	0.13	0.09	0.12
-35	0.20	-0.02	0.084			
-25	0.70	-0.16	0.024	0.18	0.11	0.11
-20	0.83	-0.17	0.004	0.13	0.09	0.08
-15	0.82	-0.15	0.008	0.14	0.06	0.08
-10	0.71	-0.11	0.014	0.17	0.05	0.08
0	0.34	-0.06	0.015	0.17	0.05	0.08
10	0.11	-0.04	0.008	0.11	0.04	0.08
30	0.03	-0.04	0.000	0.08	0.04	0.07
50	-0.01	-0.05	0.001	0.09	0.05	0.08
70	-0.04	-0.05	0.004	0.09	0.05	0.07
90	-0.07	-0.05	0.000	0.10	0.05	0.08
115	-0.09		0.003	0.09		0.07
145	-0.16		0.004	0.10		0.06

Expt. 1F5.3Y160 - Cont'd

At x = 200 mm							At x = 250 mm							At x = 300 mm						
y (mm)	u (m/s)	v (m/s)	w (m/s)	$\sqrt{\overline{u'^2}}$ (m/s)	$\sqrt{\overline{v'^2}}$ (m/s)	$\sqrt{\overline{w'^2}}$ (m/s)	y (mm)	u (m/s)	v (m/s)	w (m/s)	$\sqrt{\overline{u'^2}}$ (m/s)	$\sqrt{\overline{v'^2}}$ (m/s)	$\sqrt{\overline{w'^2}}$ (m/s)	y (mm)	u (m/s)	v (m/s)	w (m/s)	$\sqrt{\overline{u'^2}}$ (m/s)	$\sqrt{\overline{v'^2}}$ (m/s)	$\sqrt{\overline{w'^2}}$ (m/s)
-75	-0.07	0.04	0.025	0.10	0.06	0.11	-85	-0.01	0.01	0.004	0.13	0.07	0.14	-85	0.01	0.02	-0.005			
-65	-0.02	0.03	0.032	0.13	0.09	0.12	-75	0.09	-0.02	0.004	0.17	0.11	0.14	-75	0.15	0.03	-0.008	0.18	0.09	0.13
-55	0.08	0.02	0.041				-65	0.14	-0.01	0.015	0.18	0.11	0.13	-65	0.17	0.03	-0.002			
-45	0.40	-0.11	0.030	0.23	0.15	0.13	-60	0.32	-0.08	0.012	0.23	0.14	0.14	-55	0.41	-0.01	0.005	0.20	0.11	0.12
-35	0.64	-0.16	0.022	0.19	0.12	0.11	-55	0.38	-0.09	0.010	0.23	0.14	0.13	-45	0.46	0.00	0.006	0.18	0.11	0.11
-30	0.69	-0.16	0.016	0.17	0.10	0.10	-50	0.49	-0.11	0.011	0.21	0.13	0.12	-35	0.48	0.01	-0.001	0.17	0.10	0.10
-25	0.69	-0.15	0.013	0.17	0.08	0.09	-40	0.56	-0.10	0.007	0.19	0.11	0.11	-25	0.44	0.01	-0.007	0.18	0.10	0.11
-20	0.61	-0.13	0.010	0.20	0.07	0.09	-30	0.56	-0.09	0.004	0.20	0.09	0.10	-15	0.33	0.01	-0.018	0.19	0.09	0.10
-10	0.42	-0.08	0.005	0.23	0.06	0.10	-20	0.44	-0.07	-0.008	0.22	0.08	0.11	-5	0.23	0.00	-0.028	0.17	0.09	0.10
0	0.20	-0.05	-0.003	0.18	0.06	0.09	-10	0.30	-0.05	-0.004	0.22	0.08	0.11	10	0.09	-0.04	-0.007	0.12	0.08	0.09
10	0.08	-0.05	-0.008	0.12	0.05	0.09	10	0.08	-0.06	-0.008	0.12	0.07	0.09	30	0.02	-0.07	0.015	0.10	0.07	0.09
30	0.01	-0.05	0.000	0.09	0.05	0.08	30	0.00	-0.08	0.009	0.10	0.06	0.09	50	-0.03	-0.08	0.032	0.10	0.07	0.09
50	-0.02	-0.06	0.009	0.09	0.06	0.08	50	-0.04	-0.08	0.015	0.10	0.06	0.09	70	-0.08	-0.07	0.040	0.10	0.07	0.09
70	-0.06	-0.06	0.009	0.10	0.06	0.09	70	-0.08	-0.07	0.030	0.10	0.06	0.10	90	-0.13	-0.05	0.039	0.10	0.06	0.10
90	-0.09	-0.05	0.009	0.10	0.06	0.09	90	-0.12	-0.05	0.017	0.11	0.06	0.10	115	-0.17		-0.016	0.11		0.09
115	-0.12		0.002	0.10		0.08	115	-0.15		-0.009	0.10		0.08	145	-0.32		-0.014	0.09		0.10
145	-0.23		0.002	0.10		0.08	145	-0.29		-0.002	0.09		0.08							

Expt. 1F5.3Y160 - Cont'd

At x = 350 mm							At x = 400 mm							At x = 450 mm						
y (mm)	u (m/s)	v (m/s)	w (m/s)	$\sqrt{\overline{u'^2}}$ (m/s)	$\sqrt{\overline{v'^2}}$ (m/s)	$\sqrt{\overline{w'^2}}$ (m/s)	y (mm)	u (m/s)	v (m/s)	w (m/s)	$\sqrt{\overline{u'^2}}$ (m/s)	$\sqrt{\overline{v'^2}}$ (m/s)	$\sqrt{\overline{w'^2}}$ (m/s)	y (mm)	u (m/s)	v (m/s)	w (m/s)	$\sqrt{\overline{u'^2}}$ (m/s)	$\sqrt{\overline{v'^2}}$ (m/s)	$\sqrt{\overline{w'^2}}$ (m/s)
-65	0.09	0.05	-0.010				-30	0.02	0.01	-0.008				5	0.19	0.17	0.004			
-55	0.31	0.11	-0.009	0.17	0.10	0.12	-10	0.10	-0.02	-0.008				15	-0.36	0.15	-0.003			
-45	0.35	0.10	-0.006				0	-0.04	-0.02	-0.002				25	0.27	-0.02	-0.014			
-35	0.21	0.06	-0.003				10	0.34	0.25	-0.007	0.13	0.10	0.10	35	0.18	-0.08	-0.012			
-25	0.42	0.15	-0.006	0.15	0.10	0.10	20	0.31	0.25	-0.013	0.12	0.10	0.10	45	0.29	0.29	-0.013	0.11	0.09	0.10
-15	0.40	0.15	-0.006	0.14	0.10	0.10	30	0.25	0.22	-0.014	0.11	0.11	0.10	55	0.25	0.27	-0.006	0.11	0.10	0.09
-5	0.34	0.13	-0.011	0.14	0.11	0.10	50	0.15	0.15	-0.001	0.10	0.12	0.10	65	0.20	0.25	-0.006	0.10	0.11	0.10
5	0.26	0.10	-0.021	0.14	0.11	0.10	70	0.04	0.08	0.025	0.10	0.11	0.11	75	0.16	0.24	-0.010	0.10	0.11	0.10
15	0.18	0.07	-0.021	0.12	0.10	0.09	90	-0.05	0.06	0.033	0.10	0.11	0.10	95	0.08	0.20	-0.005	0.10	0.11	0.10
30	0.09	0.02	0.010	0.11	0.10	0.10	115	-0.12		-0.003	0.10		0.10	120	-0.01		-0.008	0.10		0.09
50	0.00	-0.03	0.034	0.10	0.08	0.10	145	-0.30		-0.020	0.08		0.12	150	-0.12		-0.006	0.08		0.12
70	-0.06	-0.03	0.052	0.10	0.08	0.10														
90	-0.12	-0.02	0.062	0.10	0.08	0.10														
115	-0.19		-0.011	0.11		0.09														
145	-0.36		-0.020	0.10		0.11														
At x = 500 mm							At x = 550 mm							At x = 600 mm						
25	0.06	0.02	0.006				45	-0.04	-0.02	0.003	0.08	0.04	0.07	70	0.06		-0.02	0.09		0.08
35	-0.05	0.05	-0.007				55	-0.02	-0.01	-0.003	0.09	0.05	0.07	80	0.13		-0.01	0.10		0.08
45	0.13	0.13	-0.015	0.16	0.08	0.10	65	0.07	0.03	-0.008	0.13	0.06	0.08	90	0.19		-0.01	0.11		0.08
55	0.23	0.21	-0.018	0.19	0.10	0.10	75	0.14	0.05	-0.009	0.15	0.08	0.10	100	0.24		-0.02	0.10		0.08
85	0.23	0.23	-0.016	0.11	0.09	0.09	85	0.19	0.07	-0.010	0.14	0.08	0.10	110	0.28		-0.02	0.09		0.08
100	0.19	0.20	-0.014	0.10	0.09	0.09	105	0.24	0.10	-0.014	0.11	0.09	0.09	120	0.32		-0.02	0.08		0.07
125	0.19		-0.019	0.10		0.08	125	0.30		-0.016	0.09		0.08	135	0.33		-0.02	0.08		0.07
155	0.07		-0.023	0.09		0.10	155	0.24		-0.031	0.08		0.10	145	0.33		-0.03	0.09		0.08

Expt. No.: = 1F5.3Y160 (R) **U_0 = 1.00 m/s** **F_0 = 5.3** **y_t/b_0 = 10.0**

At x = 50 mm						
y (mm)	u (m/s)	v (m/s)	w (m/s)	$\sqrt{\overline{u'^2}}$ (m/s)	$\sqrt{\overline{v'^2}}$ (m/s)	$\sqrt{\overline{w'^2}}$ (m/s)
5	1.10		-0.01	0.03		0.02
10	0.88		0.00	0.11		0.05
15	0.39		0.00	0.12		0.07
25	0.06		0.01	0.06		0.06
40	0.04		0.01	0.06		0.06
60	0.02		0.01	0.06		0.06
80	-0.01		0.00	0.07		0.06
150	-0.08		0.00	0.10		0.06

At x = 100 mm						
y (mm)	u (m/s)	v (m/s)	w (m/s)	$\sqrt{\overline{u'^2}}$ (m/s)	$\sqrt{\overline{v'^2}}$ (m/s)	$\sqrt{\overline{w'^2}}$ (m/s)
-35	-0.10	0.07	0.00	0.10	0.05	0.07
-25	0.01	0.04	0.00	0.16	0.08	0.11
-20	0.16	0.03	0.00			
-10	0.97	-0.15	0.05			
-5	0.91	-0.11	0.05			
0	0.67	-0.08	0.03	0.18	0.05	0.08
10	0.22	-0.04	0.02	0.13	0.04	0.08
30	0.05	-0.04	0.01	0.08	0.04	0.07
65	0.01	-0.04	0.01	0.08	0.05	0.06
100	-0.04	-0.03	0.00	0.09	0.05	0.07
120	-0.08		0.00	0.09		0.07
140	-0.13		0.00	0.10		0.07
150	-0.12		0.00	0.10		0.07

At x = 150 mm						
y (mm)	u (m/s)	v (m/s)	w (m/s)	$\sqrt{\overline{u'^2}}$ (m/s)	$\sqrt{\overline{v'^2}}$ (m/s)	$\sqrt{\overline{w'^2}}$ (m/s)
-55	-0.10	0.06	-0.01			
-45	-0.04	0.05	0.01	0.14	0.09	0.11
-25	0.56	-0.16	0.02	0.25	0.14	0.13
-20	0.66	-0.17	0.03	0.22	0.12	0.12
-15	0.70	-0.17	0.03	0.19	0.09	0.11
-10	0.65	-0.14	0.04	0.21	0.07	0.09
-5	0.53	-0.10	0.03	0.23	0.06	0.09
5	0.24	-0.06	0.02	0.18	0.05	0.09
25	0.07	-0.04	0.01	0.08	0.05	0.07
65	0.00	-0.04	0.01	0.09	0.05	0.07
100	-0.06	-0.02	0.00	0.10	0.06	0.08
120	-0.11		0.00	0.10		0.08
140	-0.18		0.00	0.10		0.07
150	-0.21		0.01	0.10		0.07

At x = 700 mm						
90	0.18	0.00	0.00	0.07	0.03	0.06
95	0.19	-0.01	0.01	0.07	0.04	0.06
100	0.19	0.00	0.00	0.07	0.04	0.06
120	0.24		0.00	0.07		0.06
140	0.30		0.00	0.07		0.06
150	0.32		0.00	0.07		0.06

Expt. No.: 1F5.3Y160 (R) Cont'd

At x = 200 mm							At x = 250 mm							At x = 300 mm						
y (mm)	u (m/s)	v (m/s)	w (m/s)	$\sqrt{\overline{u'^2}}$ (m/s)	$\sqrt{\overline{v'^2}}$ (m/s)	$\sqrt{\overline{w'^2}}$ (m/s)	y (mm)	u (m/s)	v (m/s)	w (m/s)	$\sqrt{\overline{u'^2}}$ (m/s)	$\sqrt{\overline{v'^2}}$ (m/s)	$\sqrt{\overline{w'^2}}$ (m/s)	y (mm)	u (m/s)	v (m/s)	w (m/s)	$\sqrt{\overline{u'^2}}$ (m/s)	$\sqrt{\overline{v'^2}}$ (m/s)	$\sqrt{\overline{w'^2}}$ (m/s)
-80	-0.07	0.01	0.00				-90	0.00	0.00	0.00	0.09	0.03	0.09	-75	0.10	0.01	0.01			
-70	-0.03	0.00	0.00				-80	0.02	0.01	0.02				-60	0.33	0.04	0.01			
-60	0.03	0.00	0.01				-60	0.26	-0.03	0.01				-45	0.42	0.07	0.02	0.17	0.11	0.11
-40	0.45	-0.15	0.02	0.24	0.13	0.13	-50	0.41	-0.08	0.02	0.23	0.11	0.12	-35	0.42	0.08	0.02	0.17	0.10	0.11
-30	0.53	-0.15	0.03	0.21	0.10	0.11	-40	0.48	-0.08	0.02	0.20	0.11	0.11	-25	0.39	0.09	0.02	0.17	0.10	0.11
-20	0.50	-0.12	0.03	0.23	0.08	0.11	-30	0.47	-0.07	0.03	0.20	0.09	0.10	-10	0.33	0.07	0.02	0.17	0.09	0.11
-10	0.41	-0.08	0.03	0.25	0.07	0.10	-15	0.36	-0.05	0.02	0.23	0.08	0.10	5	0.22	0.04	0.01	0.16	0.08	0.10
0	0.24	-0.06	0.02	0.21	0.06	0.10	5	0.16	-0.04	0.01	0.15	0.07	0.09	20	0.12	0.00	0.01	0.12	0.07	0.10
20	0.07	-0.05	0.02	0.11	0.06	0.09	35	0.03	-0.06	0.02	0.10	0.07	0.09	35	0.07	-0.02	0.01	0.11	0.07	0.09
60	-0.03	-0.06	0.00	0.11	0.06	0.09	65	-0.04	-0.06	0.00	0.11	0.07	0.09	55	0.00	-0.05	0.00	0.11	0.08	0.10
95	-0.09	-0.03	0.00	0.11	0.06	0.09	95	-0.12	-0.04	-0.02	0.12	0.07	0.10	75	-0.05	-0.05	0.00	0.10	0.08	0.09
115	-0.14		0.00	0.11		0.08	115	-0.16		-0.01	0.11		0.09	95	-0.12	-0.03	-0.02	0.11	0.08	0.09
135	-0.21		-0.01	0.10		0.08	135	-0.25		-0.01	0.10		0.09	115	-0.19		-0.01	0.11		0.09
145	-0.25		0.00	0.10		0.08	145	-0.31		-0.01	0.09		0.09	135	-0.30		-0.02	0.10		0.10

Expt. No.: 1F5.3Y160 (R) Cont'd

At x = 350 mm							At x = 400 mm							At x = 450 mm						
y (mm)	u (m/s)	v (m/s)	w (m/s)	$\sqrt{\overline{u'^2}}$ (m/s)	$\sqrt{\overline{v'^2}}$ (m/s)	$\sqrt{\overline{w'^2}}$ (m/s)	y (mm)	u (m/s)	v (m/s)	w (m/s)	$\sqrt{\overline{u'^2}}$ (m/s)	$\sqrt{\overline{v'^2}}$ (m/s)	$\sqrt{\overline{w'^2}}$ (m/s)	y (mm)	u (m/s)	v (m/s)	w (m/s)	$\sqrt{\overline{u'^2}}$ (m/s)	$\sqrt{\overline{v'^2}}$ (m/s)	$\sqrt{\overline{w'^2}}$ (m/s)
-15	-0.20	0.01	0.01				5	0.16	-0.04	0.01				20	0.02	0.00	-0.01			
-5	0.37	0.25	0.01	0.13	0.10	0.11	15	0.32	-0.03	0.01				30	-0.03	0.03	0.00			
10	0.31	0.20	0.01	0.13	0.10	0.11	25	0.33	0.30	0.02	0.16	0.10	0.15	40	-0.16	0.10	0.00			
25	0.23	0.16	0.00	0.12	0.11	0.11	35	0.30	0.30	0.01	0.12	0.10	0.11	50	0.22	0.22	0.01	0.18	0.10	0.13
40	0.17	0.12	0.00	0.12	0.11	0.10	45	0.27	0.29	0.01	0.12	0.10	0.10	60	0.23	0.23	0.01	0.15	0.10	0.10
55	0.11	0.08	0.01	0.12	0.10	0.10	60	0.21	0.27	0.00	0.11	0.11	0.11	70	0.23	0.26	0.01	0.13	0.09	0.10
75	0.00	0.03	0.00	0.12	0.10	0.11	75	0.13	0.22	0.00	0.11	0.12	0.11	85	0.19	0.24	0.00	0.12	0.10	0.10
95	-0.09	0.02	-0.02	0.10	0.11	0.10	100	-0.01	0.15	-0.01	0.12	0.12	0.11	105	0.12	0.20	0.00	0.11	0.11	0.10
115	-0.16		-0.01	0.10		0.10	120	-0.05		-0.01	0.10		0.09	125	0.14		-0.01	0.10		0.08
135	-0.28		-0.01	0.09		0.10	140	-0.15		-0.01	0.09		0.10	145	0.05		0.00	0.10		0.09
145	-0.34		-0.01	0.09		0.12	150	-0.19		0.00	0.08		0.12	155	0.02		0.00	0.09		0.11
At x = 500 mm							At x = 550 mm							At x = 600 mm						
40	-0.01	-0.01	-0.01	0.08	0.04	0.07	55	0.02	-0.01	0.00	0.06	0.03	0.06	75	0.10	0.00	0.01	0.09	0.05	0.08
50	0.02	0.01	-0.01	0.12	0.05	0.08	65	0.06	-0.01	0.00	0.11	0.06	0.08	80	0.13	-0.01	0.01	0.09	0.05	0.08
60	0.09	0.05	0.00	0.15	0.07	0.09	75	0.11	0.00	0.01	0.11	0.06	0.08	90	0.17	-0.01	0.01	0.09	0.06	0.08
70	0.09	0.05	-0.01	0.13	0.07	0.09	90	0.19	0.02	0.00	0.12	0.07	0.10	100	0.21	0.00	0.01	0.10	0.06	0.09
80	0.19	0.11	0.00	0.15	0.09	0.10	105	0.23	0.02	0.01	0.10	0.08	0.09	120	0.27		0.00	0.09		0.07
90	0.22	0.12	0.01	0.13	0.09	0.09	125	0.30		0.00	0.09		0.08	140	0.32		0.00	0.08		0.06
105	0.21	0.12	0.00	0.11	0.09	0.09	145	0.31		0.00	0.10		0.08	150	0.34		0.01	0.09		0.07
125	0.26		-0.01	0.10		0.08	155	0.29		0.00	0.09		0.10							
145	0.22		0.01	0.10		0.08														
155	0.20		0.00	0.09		0.11														

Expt. No.: = 1F5.3Y48 **U_0 = 1.00 m/s** **F_0 = 5.3** **y_t/b_0 = 3.0**

At x = 50 mm							At x = 100 mm							At x = 150 mm						
y (mm)	u (m/s)	v (m/s)	w (m/s)	$\sqrt{\overline{u'^2}}$ (m/s)	$\sqrt{\overline{v'^2}}$ (m/s)	$\sqrt{\overline{w'^2}}$ (m/s)	y (mm)	u (m/s)	v (m/s)	w (m/s)	$\sqrt{\overline{u'^2}}$ (m/s)	$\sqrt{\overline{v'^2}}$ (m/s)	$\sqrt{\overline{w'^2}}$ (m/s)	y (mm)	u (m/s)	v (m/s)	w (m/s)	$\sqrt{\overline{u'^2}}$ (m/s)	$\sqrt{\overline{v'^2}}$ (m/s)	$\sqrt{\overline{w'^2}}$ (m/s)
5	1.02		-0.040	0.02		0.02	-20	-0.02		0.018	0.09		0.06	-30	-0.03		-0.012	0.06		0.03
10	1.01		-0.050	0.03		0.03	-10	-0.02		0.047	0.08		0.06	-20	0.01		-0.036	0.08		0.06
15	0.92		-0.104	0.07		0.05	-5	0.06		0.056	0.11		0.07	-10	0.07		-0.022	0.09		0.07
20	0.42		-0.084	0.21		0.09	0	0.31		0.047	0.17		0.09	0	0.22		0.008	0.15		0.10
30	-0.13		0.021	0.09		0.06	5	0.61		0.016				10	0.49		0.008	0.21		0.11
40	-0.18		0.054	0.07		0.08	15	0.89		-0.078				20	0.67		-0.041	0.18		0.09
							25	0.40		-0.023				30	0.53		-0.037	0.23		0.10
							35	-0.07		0.001	0.13		0.09	40	0.28		-0.013	0.21		0.11
							40	-0.21		0.002	0.09		0.09	45	0.08		0.038	0.12		0.11
At x = 200 mm							At x = 250 mm							At x = 300 mm						
-35	0.012		-0.01	0.09		0.06	-45	0.01		0.003	0.08		0.06	-55	0.04		0.005	0.09		0.07
-15	0.190		-0.02	0.12		0.09	-25	0.12		-0.004	0.10		0.08	-35	0.15		0.002	0.10		0.08
-5	0.300		-0.01	0.13		0.10	-15	0.23		-0.014	0.11		0.09	-15	0.33		-0.005	0.11		0.09
5	0.436		-0.01	0.14		0.10	0	0.40		-0.014	0.11		0.10	-5	0.39		-0.012	0.10		0.08
15	0.538		-0.02	0.15		0.10	10	0.47		-0.022	0.11		0.09	5	0.45		-0.012	0.10		0.08
25	0.507		-0.04	0.17		0.10	20	0.50		-0.032	0.12		0.08	15	0.48		-0.025	0.09		0.07
35	0.409		-0.02	0.16		0.10	30	0.49		-0.033	0.12		0.08	25	0.51		-0.029	0.09		0.07
45	0.349		0.01	0.14		0.11	40	0.47		-0.026	0.11		0.08	35	0.52		-0.027	0.09		0.07
							45	0.46		-0.015	0.11		0.09	45	0.54		-0.013	0.09		0.08

Expt. 1F5.3Y48 - Cont'd

At x = 350 mm							At x = 400 mm							At x = 450 mm						
y (mm)	u (m/s)	v (m/s)	w (m/s)	$\sqrt{\overline{u'^2}}$ (m/s)	$\sqrt{\overline{v'^2}}$ (m/s)	$\sqrt{\overline{w'^2}}$ (m/s)	y (mm)	u (m/s)	v (m/s)	w (m/s)	$\sqrt{\overline{u'^2}}$ (m/s)	$\sqrt{\overline{v'^2}}$ (m/s)	$\sqrt{\overline{w'^2}}$ (m/s)	y (mm)	u (m/s)	v (m/s)	w (m/s)	$\sqrt{\overline{u'^2}}$ (m/s)	$\sqrt{\overline{v'^2}}$ (m/s)	$\sqrt{\overline{w'^2}}$ (m/s)
-70	0.03		-0.004	0.08		0.07	-75	0.05		-0.008	0.08		0.07	-75	0.09		-0.009	0.09		0.07
-50	0.13		-0.004	0.10		0.08	-55	0.15		-0.007	0.10		0.08	-55	0.19		-0.013	0.09		0.08
-30	0.23		0.001	0.11		0.09	-35	0.24		-0.003	0.10		0.09	-35	0.27		-0.009	0.10		0.08
-10	0.36		-0.007	0.10		0.08	-15	0.34		-0.013	0.09		0.08	-15	0.34		-0.015	0.09		0.08
0	0.40		-0.009	0.09		0.08	5	0.41		-0.021	0.08		0.07	5	0.42		-0.019	0.08		0.07
10	0.44		-0.015	0.09		0.07	15	0.43		-0.025	0.08		0.06	20	0.47		-0.024	0.07		0.06
20	0.46		-0.017	0.08		0.07	25	0.45		-0.025	0.07		0.06	30	0.49		-0.027	0.07		0.06
30	0.47		-0.019	0.08		0.06	35	0.46		-0.023	0.07		0.06	40	0.52		-0.026	0.07		0.06
40	0.47		-0.016	0.08		0.06	45	0.47		-0.017	0.07		0.06	45	0.55		-0.021	0.08		0.07
45	0.47		-0.006	0.08		0.07														
At x = 500 mm							At x = 600 mm							At x = 700 mm						
-75	0.12		-0.021	0.09		0.07	-70	0.16		-0.022	0.09		0.07	-65	0.21		-0.020	0.09		0.07
-55	0.21		-0.014	0.10		0.08	-50	0.25		-0.023	0.09		0.07	-45	0.28		-0.022	0.09		0.07
-35	0.28		-0.015	0.09		0.08	-30	0.31		-0.023	0.09		0.08	-25	0.33		-0.026	0.09		0.07
-15	0.35		-0.021	0.09		0.07	-10	0.37		-0.026	0.09		0.07	-5	0.39		-0.034	0.08		0.07
5	0.41		-0.024	0.08		0.07	10	0.42		-0.025	0.08		0.07	15	0.43		-0.031	0.08		0.07
25	0.45		-0.025	0.07		0.06	30	0.47		-0.031	0.07		0.06	35	0.46		-0.032	0.07		0.07
35	0.47		-0.027	0.07		0.06	45	0.51		-0.028	0.07		0.07	50	0.47		-0.023	0.07		0.07
45	0.49		-0.023	0.08		0.07	50	0.52		-0.015	0.09		0.08	At x = 1000 mm						
														5	0.33		-0.016	0.07		0.06
														15	0.35		-0.022	0.07		0.06
														25	0.37		-0.024	0.07		0.06
														35	0.38		-0.024	0.07		0.06
														45	0.39		-0.025	0.08		0.06
														50	0.38		-0.021	0.09		0.07

Expt. No.: = 2F6.9Y200 **U_0 = 1.30 m/s** **F_0 = 6.9** **y_t/b_0 = 12.5**

At x = 50 mm							At x = 100 mm							At x = 150 mm						
y (mm)	u (m/s)	v (m/s)	w (m/s)	$\sqrt{\overline{u'^2}}$ (m/s)	$\sqrt{\overline{v'^2}}$ (m/s)	$\sqrt{\overline{w'^2}}$ (m/s)	y (mm)	u (m/s)	v (m/s)	w (m/s)	$\sqrt{\overline{u'^2}}$ (m/s)	$\sqrt{\overline{v'^2}}$ (m/s)	$\sqrt{\overline{w'^2}}$ (m/s)	y (mm)	u (m/s)	v (m/s)	w (m/s)	$\sqrt{\overline{u'^2}}$ (m/s)	$\sqrt{\overline{v'^2}}$ (m/s)	$\sqrt{\overline{w'^2}}$ (m/s)
5	1.35		-0.012	0.05		0.05	-40	-0.10	0.07	0.048	0.09	0.04	0.08	-60	-0.09	0.06	0.035	0.10	0.06	0.10
10	1.20		-0.004	0.06		0.05	-35	-0.09	0.07	0.070	0.10	0.05	0.09	-50	-0.05	0.06	0.056	0.11	0.07	0.10
15	0.57		0.014	0.00		0.00	-25	0.04	0.06	0.055				-40	0.09	0.03	0.063			
25	0.08		0.020	0.06		0.06	-10	1.16	-0.15	-0.052	0.10	0.07	0.08	-30	0.52	-0.13	0.014	0.24	0.15	0.16
40	0.05		0.027	0.06		0.06	0	0.90	-0.09	-0.029	0.16	0.05	0.09	-20	0.94	-0.21	-0.032	0.19	0.12	0.11
60	0.02		0.028	0.06		0.06	10	0.30	-0.04	0.004	0.15	0.04	0.10	-10	0.97	-0.17	-0.030	0.18	0.07	0.09
80	0.00		0.020	0.06		0.06	20	0.07	-0.04	0.009	0.09	0.03	0.09	0	0.54	-0.09	-0.006	0.23	0.06	0.10
110	-0.02		0.016	0.06		0.06	35	0.06	-0.04	0.014	0.08	0.04	0.06	10	0.20	-0.05	0.012	0.14	0.05	0.09
140	-0.06		0.017	0.06		0.06	55	0.03	-0.05	0.011	0.09	0.05	0.06	35	0.03	-0.04	0.014	0.10	0.05	0.07
170	-0.10		0.017	0.06		0.06	75	0.00	-0.06	0.011	0.09	0.05	0.07	65	0.00	-0.05	0.006	0.10	0.06	0.07
185	-0.08		0.016	0.06		0.06	105	-0.03	-0.05	0.010	0.09	0.05	0.07	105	-0.05	-0.04	0.009	0.10	0.06	0.07
							135	-0.08	-0.05	0.012	0.09	0.05	0.07	135	-0.11	-0.03	0.011	0.10	0.05	0.08
							155	-0.10		0.011	0.08		0.07	155	-0.14		0.011	0.10		0.07
							175	-0.14		0.008	0.09		0.07	175	-0.18		0.003	0.09		0.07
							185	-0.15		0.013	0.10		0.06	185	-0.21		0.013	0.09		0.07

Expt. 2F6.9Y200 - Cont'd

At x = 200 mm							At x = 250 mm							At x = 300 mm						
y (mm)	u (m/s)	v (m/s)	w (m/s)	$\sqrt{\overline{u'^2}}$ (m/s)	$\sqrt{\overline{v'^2}}$ (m/s)	$\sqrt{\overline{w'^2}}$ (m/s)	y (mm)	u (m/s)	v (m/s)	w (m/s)	$\sqrt{\overline{u'^2}}$ (m/s)	$\sqrt{\overline{v'^2}}$ (m/s)	$\sqrt{\overline{w'^2}}$ (m/s)	y (mm)	u (m/s)	v (m/s)	w (m/s)	$\sqrt{\overline{u'^2}}$ (m/s)	$\sqrt{\overline{v'^2}}$ (m/s)	$\sqrt{\overline{w'^2}}$ (m/s)
-85	-0.06	0.01	0.001	0.13	0.10	0.13	-110	-0.08	0.00	-0.022				-120	-0.03	0.00	-0.019			
-75	0.01	-0.01	0.024	0.14	0.11	0.14	-95	0.01	-0.02	-0.006	0.15	0.11	0.14	-105	0.06	-0.02	0.001			
-65	0.05	0.01	0.039				-80	0.22	-0.12	0.006	0.22	0.16	0.16	-90	0.31	-0.13	0.001	0.25	0.15	0.16
-55	0.11	0.01	0.048				-65	0.44	-0.17	0.016	0.23	0.16	0.15	-75	0.47	-0.16	0.000	0.24	0.15	0.14
-45	0.52	-0.18	0.022	0.25	0.16	0.15	-50	0.65	-0.22	-0.001	0.21	0.13	0.13	-60	0.60	-0.17	0.000	0.20	0.13	0.13
-35	0.74	-0.22	-0.006	0.21	0.14	0.13	-35	0.71	-0.19	-0.011	0.22	0.10	0.12	-45	0.60	-0.14	-0.013	0.23	0.10	0.12
-25	0.83	-0.21	-0.026	0.20	0.10	0.11	-20	0.50	-0.12	-0.010	0.28	0.08	0.13	-30	0.47	-0.10	-0.011	0.27	0.09	0.12
-15	0.72	-0.16	-0.023	0.24	0.08	0.11	0	0.19	-0.07	0.006	0.22	0.08	0.11	-10	0.22	-0.07	0.004	0.24	0.09	0.12
-5	0.42	-0.10	-0.010	0.24	0.07	0.11	20	0.03	-0.07	0.012	0.11	0.06	0.09	20	-0.01	-0.09	0.008	0.12	0.07	0.10
15	0.06	-0.05	-0.001	0.13	0.06	0.09	60	-0.05	-0.07	0.016	0.10	0.07	0.08	60	-0.09	-0.09	0.006	0.10	0.07	0.10
55	-0.01	-0.06	0.017	0.11	0.06	0.08	100	-0.12	-0.06	0.004	0.11	0.07	0.09	100	-0.14	-0.06	-0.005	0.10	0.07	0.11
95	-0.07	-0.05	0.007	0.11	0.06	0.08	135	-0.18	-0.02	-0.002	0.10	0.06	0.09	135	-0.19	-0.02	0.005	0.10	0.07	0.10
135	-0.13	-0.03	0.008	0.10	0.06	0.08	155	-0.20		0.006	0.10		0.09	155	-0.23		0.000	0.10		0.10
155	-0.16		0.007	0.10		0.08	175	-0.26		0.009	0.09		0.08	175	-0.29		-0.005	0.10		0.09
175	-0.22		0.001	0.09		0.08	185	-0.28		0.000	0.09		0.09	185	-0.34		0.005	0.09		0.09
185	-0.25		0.004	0.09		0.08														

Expt. 2F6.9Y200 - Cont'd

At x = 350 mm							At x = 400 mm							At x = 450 mm						
y (mm)	u (m/s)	v (m/s)	w (m/s)	$\sqrt{\overline{u'^2}}$ (m/s)	$\sqrt{\overline{v'^2}}$ (m/s)	$\sqrt{\overline{w'^2}}$ (m/s)	y (mm)	u (m/s)	v (m/s)	w (m/s)	$\sqrt{\overline{u'^2}}$ (m/s)	$\sqrt{\overline{v'^2}}$ (m/s)	$\sqrt{\overline{w'^2}}$ (m/s)	y (mm)	u (m/s)	v (m/s)	w (m/s)	$\sqrt{\overline{u'^2}}$ (m/s)	$\sqrt{\overline{v'^2}}$ (m/s)	$\sqrt{\overline{w'^2}}$ (m/s)
-125	0.04	-0.01	-0.014				-115	0.16	0.01	-0.037				-85	0.26	0.10	-0.027			
-105	0.18	-0.03	-0.020				-95	0.32	0.02	-0.013				-65	-0.02	0.06	-0.012			
-85	0.43	-0.08	-0.012	0.23	0.14	0.15	-75	0.48	0.04	-0.011	0.19	0.12	0.13	-45	0.46	0.21	0.002	0.16	0.12	0.12
-65	0.56	-0.06	-0.012	0.19	0.12	0.13	-55	0.52	0.07	0.000	0.17	0.12	0.12	-25	0.43	0.22	-0.001	0.15	0.12	0.12
-45	0.52	-0.04	-0.011	0.22	0.11	0.13	-35	0.43	0.08	-0.008	0.19	0.12	0.12	-5	0.34	0.19	-0.010	0.15	0.13	0.12
-25	0.33	-0.04	-0.013	0.23	0.10	0.13	-10	0.25	0.03	-0.001	0.19	0.12	0.12	25	0.16	0.10	-0.006	0.13	0.14	0.13
5	0.06	-0.07	-0.014	0.14	0.09	0.12	20	0.06	-0.04	0.001	0.13	0.10	0.12	55	0.03	0.02	-0.009	0.11	0.12	0.12
35	-0.04	-0.10	-0.005	0.11	0.08	0.12	60	-0.06	-0.07	-0.006	0.11	0.09	0.12	95	-0.08	0.01	-0.004	0.11	0.11	0.12
65	-0.09	-0.10	-0.007	0.09	0.07	0.11	100	-0.14	-0.04	-0.005	0.11	0.08	0.12	135	-0.18	0.03	-0.005	0.11	0.10	0.12
105	-0.16	-0.05	0.000	0.10	0.08	0.11	135	-0.20	0.00	-0.014	0.12	0.08	0.12	155	-0.24		-0.018	0.10		0.11
135	-0.20	-0.02	-0.007	0.10	0.07	0.10	155	-0.25		-0.011	0.11		0.11	175	-0.33		-0.013	0.10		0.11
155	-0.26	0.00	-0.001	0.11	0.00	0.10	175	-0.33		-0.014	0.10		0.10	185	-0.37		-0.016	0.10		0.12
175	-0.31	0.00	-0.006	0.10	0.00	0.10	185	-0.39		-0.014	0.10		0.11							
185	-0.36	0.00	-0.003	0.10	0.00	0.10														
At x = 500 mm							At x = 550 mm							At x = 600 mm						
-10	0.42	0.03	-0.008	0.15	0.10	0.12	25	0.32	-0.05	-0.024				10	0.06	0.00	-0.006			
10	0.37	0.02	-0.005	0.14	0.12	0.12	40	0.17	0.00	-0.017				40	-0.13	0.03	-0.020			
30	0.28	0.02	-0.010	0.13	0.14	0.12	55	0.30	0.32	-0.011	0.12	0.11	0.11	60	0.26	0.27	-0.023	0.16	0.10	0.11
60	0.14	0.01	-0.015	0.12	0.15	0.13	75	0.23	0.32	-0.010	0.11	0.13	0.11	85	0.27	0.30	-0.012	0.13	0.12	0.10
100	-0.01	0.00	-0.023	0.12	0.13	0.13	100	0.13	0.26	-0.011	0.12	0.13	0.13	115	0.16	0.26	-0.014	0.12	0.12	0.11
135	-0.13	-0.01	-0.016	0.12	0.12	0.12	140	-0.02	0.18	-0.016	0.12	0.13	0.12	145	0.06	0.19	-0.019	0.12	0.11	0.12
155	-0.16		-0.013	0.10		0.11	155	-0.04		-0.015	0.11		0.11	165	0.09		-0.010	0.10		0.10
175	-0.25		-0.026	0.10		0.12	175	-0.12		-0.016	0.10		0.11	185	0.01		-0.020	0.11		0.10
185	-0.29		-0.019	0.09		0.12	185	-0.16		-0.018	0.10		0.12	195	-0.01		-0.026	0.11		0.11

Expt. 2F6.9Y200 - Cont'd

At x = 650 mm							At x = 750 mm							At x = 900 mm						
y (mm)	u (m/s)	v (m/s)	w (m/s)	$\sqrt{\overline{u'^2}}$ (m/s)	$\sqrt{\overline{v'^2}}$ (m/s)	$\sqrt{\overline{w'^2}}$ (m/s)	y (mm)	u (m/s)	v (m/s)	w (m/s)	$\sqrt{\overline{u'^2}}$ (m/s)	$\sqrt{\overline{v'^2}}$ (m/s)	$\sqrt{\overline{w'^2}}$ (m/s)	y (mm)	u (m/s)	v (m/s)	w (m/s)	$\sqrt{\overline{u'^2}}$ (m/s)	$\sqrt{\overline{v'^2}}$ (m/s)	$\sqrt{\overline{w'^2}}$ (m/s)
35	0.03	0.00	-0.012	0.16	0.08	0.11	70	0.02	-0.01	-0.012	0.08	0.04	0.09	130	0.20		-0.021	0.07		0.07
55	0.06	0.04	-0.005				80	0.06	-0.01	-0.011	0.11	0.06	0.09	140	0.21		-0.015	0.07		0.07
75	0.20	0.15	-0.023	0.18	0.11	0.12	90	0.11	0.01	-0.018	0.12	0.07	0.10	150	0.25		-0.013	0.07		0.07
95	0.20	0.18	-0.020	0.17	0.11	0.12	105	0.14	0.01	-0.014	0.13	0.08	0.11	160	0.27		-0.020	0.07		0.07
115	0.22	0.20	-0.022	0.14	0.10	0.11	125	0.22	0.02	-0.016	0.12	0.08	0.10	170	0.30		-0.024	0.07		0.07
145	0.17	0.16	-0.024	0.11	0.10	0.10	145	0.25	0.03	-0.016	0.11	0.08	0.10	180	0.32		-0.021	0.07		0.07
165	0.24		-0.016	0.10		0.09	165	0.29		-0.014	0.10		0.08	195	0.36		-0.030	0.08		0.08
185	0.20		-0.019	0.11		0.09	185	0.33		-0.016	0.09		0.09							
195	0.18		-0.031	0.11		0.11	195	0.33		-0.032	0.10		0.10							

Expt. No.: = 2F5.9Y200 U_0 = 1.11 m/s F_0 = 5.9 y_t/b_0 = 12.5

At x = 50 mm							At x = 100 mm							At x = 150 mm						
y (mm)	u (m/s)	v (m/s)	w (m/s)	$\sqrt{\overline{u'^2}}$ (m/s)	$\sqrt{\overline{v'^2}}$ (m/s)	$\sqrt{\overline{w'^2}}$ (m/s)	y (mm)	u (m/s)	v (m/s)	w (m/s)	$\sqrt{\overline{u'^2}}$ (m/s)	$\sqrt{\overline{v'^2}}$ (m/s)	$\sqrt{\overline{w'^2}}$ (m/s)	y (mm)	u (m/s)	v (m/s)	w (m/s)	$\sqrt{\overline{u'^2}}$ (m/s)	$\sqrt{\overline{v'^2}}$ (m/s)	$\sqrt{\overline{w'^2}}$ (m/s)
5	1.17		0.008	0.02		0.02	-40	-0.05	0.02	0.022	0.07	0.02	0.05	-50	-0.04	0.04	0.009	0.09	0.04	0.08
10	1.00		0.015	0.10		0.05	-30	-0.09	0.05	0.033	0.09	0.04	0.07	-40	-0.06	0.05	0.036	0.11	0.07	0.09
15	0.50		0.019				-25	-0.08	0.06	0.034	0.09	0.05	0.08	-30	0.06	0.02	0.057	0.15	0.09	0.13
25	0.07		0.025	0.06		0.06	-20	-0.04	0.05	0.045				-10	0.83	-0.19	-0.002	0.16	0.11	0.09
40	0.05		0.020	0.05		0.05	-15	0.03	0.06	0.043	0.13	0.07	0.11	0	0.77	-0.15	-0.008	0.18	0.06	0.09
60	0.03		0.021	0.06		0.05	-5	0.77	-0.12	-0.007	0.16	0.09	0.11	10	0.48	-0.08	0.005	0.19	0.05	0.10
80	0.02		0.015	0.07		0.05	5	0.96	-0.12	-0.012	0.11	0.05	0.08	20	0.17	-0.05	0.014	0.13	0.04	0.09
100	-0.01		0.018	0.07		0.05	15	0.48	-0.05	0.006	0.15	0.04	0.09	40	0.06	-0.04	0.014	0.10	0.04	0.08
120	-0.02		0.015	0.08		0.06	35	0.07	-0.04	0.011	0.09	0.03	0.08	70	0.03	-0.05	0.008	0.08	0.05	0.06
140	-0.05		0.015	0.07		0.06	55	0.05	-0.04	0.012	0.09	0.04	0.08	100	-0.01	-0.04	0.007	0.09	0.05	0.06
160	-0.06		0.013	0.09		0.06	90	0.01	-0.05	0.008	0.10	0.05	0.08	130	-0.07	-0.04	0.003	0.09	0.05	0.07
180	-0.08		0.010	0.09		0.06	130	-0.05	-0.05	0.000	0.10	0.05	0.08	140	-0.08		0.010	0.09		0.07
							140	-0.07		0.011	0.08		0.06	160	-0.13		0.008	0.08		0.07
							160	-0.10		0.006	0.08		0.06	180	-0.19		0.003	0.08		0.07
							180	-0.11		0.006	0.10		0.06							

Expt. 2F5.9Y200 - Cont'd

At x = 200 mm							At x = 250 mm							At x = 300 mm						
y (mm)	u (m/s)	v (m/s)	w (m/s)	$\sqrt{\overline{u'^2}}$ (m/s)	$\sqrt{\overline{v'^2}}$ (m/s)	$\sqrt{\overline{w'^2}}$ (m/s)	y (mm)	u (m/s)	v (m/s)	w (m/s)	$\sqrt{\overline{u'^2}}$ (m/s)	$\sqrt{\overline{v'^2}}$ (m/s)	$\sqrt{\overline{w'^2}}$ (m/s)	y (mm)	u (m/s)	v (m/s)	w (m/s)	$\sqrt{\overline{u'^2}}$ (m/s)	$\sqrt{\overline{v'^2}}$ (m/s)	$\sqrt{\overline{w'^2}}$ (m/s)
-65	0.00	-0.02	0.003	0.13	0.10	0.13	-85	0.00	-0.04	-0.016	0.15	0.10	0.14	-90	0.05	-0.01	-0.023			
-55	0.05	-0.02	0.028	0.15	0.10	0.13	-75	0.06	-0.04	0.004	0.16	0.11	0.14	-80	0.18	-0.06	-0.007	0.18	0.11	0.14
-45	0.12	-0.02	0.053				-60	0.28	-0.12	0.022	0.21	0.13	0.15	-70	0.27	-0.07	0.000	0.21	0.11	0.13
-35	0.43	-0.15	0.020	0.23	0.14	0.14	-45	0.48	-0.15	0.013	0.21	0.12	0.13	-55	0.45	-0.08	0.004	0.20	0.11	0.13
-25	0.63	-0.18	0.005	0.20	0.12	0.12	-30	0.58	-0.15	-0.002	0.19	0.10	0.11	-40	0.53	-0.07	0.009	0.18	0.10	0.11
-15	0.71	-0.18	-0.003	0.17	0.08	0.10	-15	0.50	-0.11	-0.005	0.23	0.08	0.10	-20	0.46	-0.04	0.006	0.21	0.08	0.11
-5	0.59	-0.13	-0.001	0.21	0.07	0.10	0	0.29	-0.07	0.007	0.22	0.07	0.10	-10	0.37	-0.03	0.004	0.23	0.08	0.11
5	0.37	-0.08	0.005	0.22	0.06	0.10	15	0.11	-0.05	0.013	0.14	0.06	0.09	10	0.15	-0.04	-0.004	0.17	0.07	0.10
20	0.13	-0.05	0.020	0.11	0.05	0.08	30	0.04	-0.06	0.008	0.11	0.06	0.08	30	0.03	-0.06	-0.005	0.11	0.06	0.09
40	0.04	-0.05	0.010	0.10	0.05	0.08	50	0.00	-0.07	0.009	0.10	0.06	0.08	50	-0.02	-0.08	-0.003	0.10	0.06	0.10
60	0.02	-0.05	0.008	0.11	0.05	0.08	70	-0.03	-0.07	0.000	0.11	0.06	0.09	70	-0.05	-0.09	-0.007	0.10	0.06	0.10
80	-0.03	-0.06	0.012	0.10	0.05	0.08	100	-0.08	-0.06	-0.001	0.10	0.06	0.09	100	-0.09	-0.07	-0.011	0.11	0.06	0.11
100	-0.05	-0.05	0.005	0.10	0.06	0.08	130	-0.13	-0.04	0.000	0.10	0.06	0.10	130	-0.14	-0.04	-0.010	0.11	0.06	0.11
130	-0.10	-0.04	0.003	0.09	0.05	0.08	140	-0.14		-0.005	0.10		0.09	140	-0.16		-0.017	0.10		0.09
140	-0.11		0.003	0.09		0.08	160	-0.19		-0.008	0.09		0.08	160	-0.21		-0.014	0.10		0.09
160	-0.15		0.000	0.10		0.08	180	-0.26		-0.006	0.09		0.08	180	-0.29		-0.017	0.09		0.08
180	-0.22		0.000	0.08		0.07														

Expt. 2F5.9Y200 - Cont'd

At x = 350 mm							At x = 400 mm							At x = 450 mm						
y (mm)	u (m/s)	v (m/s)	w (m/s)	$\sqrt{\overline{u'^2}}$ (m/s)	$\sqrt{\overline{v'^2}}$ (m/s)	$\sqrt{\overline{w'^2}}$ (m/s)	y (mm)	u (m/s)	v (m/s)	w (m/s)	$\sqrt{\overline{u'^2}}$ (m/s)	$\sqrt{\overline{v'^2}}$ (m/s)	$\sqrt{\overline{w'^2}}$ (m/s)	y (mm)	u (m/s)	v (m/s)	w (m/s)	$\sqrt{\overline{u'^2}}$ (m/s)	$\sqrt{\overline{v'^2}}$ (m/s)	$\sqrt{\overline{w'^2}}$ (m/s)
-80	0.17	0.01	-0.027				-55	-0.06	0.04	-0.010				-10	0.15	-0.03	-0.016			
-65	0.34	0.02	-0.014	0.19	0.11	0.12	-20	0.45	0.21	0.006	0.15	0.10	0.11	10	0.41	0.32	-0.001	0.16	0.09	0.15
-50	0.45	0.04	0.000	0.18	0.11	0.12	10	0.36	0.21	0.009	0.12	0.11	0.10	30	0.37	0.32	0.003	0.12	0.10	0.11
-30	0.48	0.07	0.004	0.16	0.10	0.11	40	0.17	0.10	-0.001	0.11	0.12	0.10	50	0.29	0.28	0.002	0.11	0.12	0.11
-10	0.39	0.06	0.007	0.18	0.10	0.11	70	0.05	0.00	0.000	0.10	0.10	0.10	70	0.21	0.22	-0.002	0.11	0.13	0.11
10	0.21	0.02	0.005	0.17	0.09	0.10	100	-0.02	-0.02	-0.014	0.10	0.09	0.10	90	0.12	0.15	-0.005	0.12	0.14	0.12
40	0.04	-0.05	-0.002	0.10	0.07	0.09	130	-0.11	-0.01	-0.005	0.10	0.09	0.11	110	0.03	0.10	-0.005	0.12	0.13	0.12
70	-0.03	-0.08	-0.013	0.09	0.07	0.10	140	-0.14		-0.019	0.10		0.10	130	-0.04	0.08	0.002	0.11	0.12	0.12
100	-0.07	-0.06	-0.010	0.10	0.07	0.11	160	-0.23		-0.017	0.11		0.10	140	-0.07		-0.009	0.09		0.11
130	-0.14	-0.03	-0.018	0.10	0.07	0.10	180	-0.33		-0.028	0.10		0.11	160	-0.17		-0.017	0.10		0.10
140	-0.16		-0.022	0.10		0.10								185	-0.29		-0.036	0.09		0.12
160	-0.23		-0.020	0.10		0.09														
180	-0.31		-0.023	0.10		0.10														
At x = 500 mm							At x = 550 mm							At x = 600 mm						
20	0.12	0.11	-0.009				35	0.00	-0.01	-0.013	0.09	0.04	0.08	60	-0.04	-0.02	-0.002	0.09	0.04	0.08
35	0.31	-0.04	-0.026				55	0.06	0.07	-0.021	0.16	0.08	0.11	70	-0.01	0.00	0.001	0.11	0.06	0.09
55	0.34	0.33	-0.006	0.13	0.09	0.11	75	0.21	0.22	-0.019	0.18	0.09	0.12	80	0.02	0.02	-0.001	0.12	0.06	0.09
75	0.29	0.33	0.000	0.12	0.10	0.10	95	0.23	0.26	-0.015	0.16	0.09	0.11	100	0.15	0.10	-0.009	0.16	0.08	0.12
95	0.23	0.31	-0.005	0.11	0.12	0.11	115	0.22	0.28	-0.007	0.13	0.09	0.10	120	0.19	0.13	-0.006	0.15	0.09	0.11
115	0.15	0.26	-0.005	0.11	0.13	0.11	140	0.16	0.25	-0.012	0.12	0.10	0.11	140	0.21	0.14	-0.006	0.13	0.09	0.11
135	0.06	0.21	-0.007	0.12	0.13	0.12	150	0.18		0.000	0.10		0.09	150	0.27		0.000	0.10		0.09
145	0.03		0.000	0.10		0.10	170	0.12		-0.008	0.10		0.09	170	0.25		-0.003	0.10		0.08
165	-0.05		-0.010	0.10		0.10	190	0.05		-0.016	0.10		0.10	190	0.21		-0.026	0.10		0.09
190	-0.15		-0.030	0.09		0.12														

Expt. 2F5.9Y200 - Cont'd

At x = 650 mm							At x = 750 mm						
y (mm)	u (m/s)	v (m/s)	w (m/s)	$\sqrt{\overline{u'^2}}$ (m/s)	$\sqrt{\overline{v'^2}}$ (m/s)	$\sqrt{\overline{w'^2}}$ (m/s)	y (mm)	u (m/s)	v (m/s)	w (m/s)	$\sqrt{\overline{u'^2}}$ (m/s)	$\sqrt{\overline{v'^2}}$ (m/s)	$\sqrt{\overline{w'^2}}$ (m/s)
90	0.03		-0.005	0.09		0.08	110	0.10		-0.006	0.08		0.08
100	0.06		0.001	0.10		0.09	120	0.14		-0.012	0.08		0.08
110	0.11		0.001	0.12		0.09	130	0.16		-0.008	0.09		0.08
120	0.16		0.005	0.12		0.09	140	0.20		-0.001	0.09		0.08
130	0.20		0.006	0.11		0.09	150	0.25		0.000	0.09		0.08
140	0.25		0.005	0.11		0.09	170	0.31		0.001	0.08		0.07
160	0.29		-0.001	0.10		0.08	190	0.36		-0.009	0.08		0.07
190	0.32		-0.011	0.09		0.09							

Expt. No.: = 2F4.4Y200 **U_0 = 0.84 m/s** **F_0 = 4.4** **y_t/b_0 = 12.5**

At x = 50 mm							At x = 100 mm							At x = 150 mm						
y (mm)	u (m/s)	v (m/s)	w (m/s)	$\sqrt{\overline{u'^2}}$ (m/s)	$\sqrt{\overline{v'^2}}$ (m/s)	$\sqrt{\overline{w'^2}}$ (m/s)	y (mm)	u (m/s)	v (m/s)	w (m/s)	$\sqrt{\overline{u'^2}}$ (m/s)	$\sqrt{\overline{v'^2}}$ (m/s)	$\sqrt{\overline{w'^2}}$ (m/s)	y (mm)	u (m/s)	v (m/s)	w (m/s)	$\sqrt{\overline{u'^2}}$ (m/s)	$\sqrt{\overline{v'^2}}$ (m/s)	$\sqrt{\overline{w'^2}}$ (m/s)
5	0.88		-0.013	0.03		0.02	-30	-0.07	0.05	0.012	0.08	0.04	0.06	-50	-0.09	0.05	0.014	0.08	0.04	0.07
10	0.59		-0.011	0.11		0.06	-20	0.20	-0.01	0.010				-40	0.01	0.02	0.020	0.12	0.06	0.09
15	0.24		-0.006	0.08		0.06	-10	0.77	-0.10	-0.032	0.06	0.06	0.05	-30	0.24	-0.05	0.009			
25	0.08		0.000	0.03		0.05	-5	0.78	-0.07	-0.029	0.06	0.04	0.04	-20	0.59	-0.12	-0.020	0.16	0.09	0.10
35	0.08		0.002	0.04		0.04	0	0.60	-0.06	-0.022	0.12	0.04	0.08	-15	0.64	-0.12	-0.025	0.12	0.07	0.08
55	0.06		0.006	0.04		0.04	5	0.41	-0.04	-0.015	0.13	0.04	0.08	-10	0.60	-0.10	-0.021	0.14	0.06	0.08
75	0.04		0.009	0.05		0.04	20	0.12	-0.03	0.005	0.05	0.03	0.05	-5	0.51	-0.08	-0.015	0.16	0.05	0.07
95	0.02		0.007	0.05		0.04	35	0.09	-0.03	0.003	0.05	0.03	0.05	10	0.20	-0.04	0.002	0.10	0.03	0.06
115	0.00		0.006	0.06		0.05	55	0.07	-0.03	0.008	0.05	0.03	0.05	30	0.11	-0.03	0.012	0.05	0.03	0.05
135	-0.02		0.007	0.06		0.05	75	0.06	-0.04	0.011	0.06	0.03	0.05	50	0.08	-0.03	0.010	0.06	0.03	0.05
155	-0.03		0.003	0.07		0.05	95	0.03	-0.04	0.006	0.07	0.03	0.05	75	0.05	-0.03	0.007	0.07	0.03	0.05
185	-0.04		0.004	0.08		0.05	115	0.00	-0.05	0.005	0.07	0.04	0.05	105	0.01	-0.03	0.010	0.07	0.04	0.05
							145	-0.02	-0.05	0.004	0.07	0.04	0.06	145	-0.04	-0.04	0.006	0.07	0.04	0.06
							155	-0.05		0.003	0.07		0.05	155	-0.07		-0.001	0.07		0.06
							185	-0.10		0.000	0.09		0.05	185	-0.16		-0.004	0.08		0.06

Expt. 2F4.4Y200 - Cont'd

At x = 200 mm							At x = 250 mm							At x = 300 mm						
y (mm)	u (m/s)	v (m/s)	w (m/s)	$\sqrt{\overline{u'^2}}$ (m/s)	$\sqrt{\overline{v'^2}}$ (m/s)	$\sqrt{\overline{w'^2}}$ (m/s)	y (mm)	u (m/s)	v (m/s)	w (m/s)	$\sqrt{\overline{u'^2}}$ (m/s)	$\sqrt{\overline{v'^2}}$ (m/s)	$\sqrt{\overline{w'^2}}$ (m/s)	y (mm)	u (m/s)	v (m/s)	w (m/s)	$\sqrt{\overline{u'^2}}$ (m/s)	$\sqrt{\overline{v'^2}}$ (m/s)	$\sqrt{\overline{w'^2}}$ (m/s)
-65	-0.07	0.00	0.014	0.10	0.05	0.09	-65	0.07	-0.02	-0.006	0.13	0.06	0.11	-45	0.23	0.04	-0.002			
-55	0.05	-0.02	0.006	0.14	0.07	0.10	-55	0.18	-0.02	0.005	0.17	0.08	0.10	-35	0.35	0.10	-0.012	0.14	0.08	0.08
-45	0.27	-0.08	0.006	0.19	0.09	0.11	-45	0.31	-0.02	-0.008	0.19	0.08	0.10	-25	0.39	0.12	-0.016	0.14	0.07	0.08
-35	0.42	-0.09	-0.006	0.18	0.09	0.10	-35	0.41	-0.01	-0.015	0.16	0.08	0.10	-15	0.40	0.14	-0.012	0.11	0.07	0.08
-25	0.52	-0.09	-0.015	0.14	0.07	0.08	-25	0.46	0.01	-0.016	0.13	0.06	0.08	-5	0.38	0.15	-0.007	0.11	0.06	0.07
-15	0.47	-0.07	-0.012	0.16	0.06	0.08	-15	0.41	0.02	-0.010	0.14	0.06	0.08	5	0.32	0.13	0.002	0.11	0.07	0.07
-10	0.44	-0.05	-0.012	0.17	0.05	0.08	-5	0.32	0.02	-0.005	0.15	0.05	0.08	15	0.25	0.11	0.001	0.11	0.06	0.07
-5	0.38	-0.04	-0.004	0.17	0.05	0.07	15	0.15	0.00	0.013	0.09	0.04	0.05	30	0.15	0.06	0.011	0.08	0.05	0.06
5	0.23	-0.03	0.011	0.14	0.04	0.06	25	0.12	0.00	0.024	0.06	0.04	0.04	40	0.12	0.04	0.013	0.07	0.04	0.05
15	0.14	-0.03	0.018	0.07	0.03	0.05	45	0.09	-0.01	0.018	0.06	0.04	0.04	55	0.09	0.02	0.018	0.06	0.04	0.05
25	0.10	-0.03	0.017	0.06	0.03	0.04	65	0.05	-0.02	0.014	0.06	0.04	0.05	75	0.06	0.00	0.013	0.06	0.04	0.06
45	0.09	-0.03	0.016	0.06	0.04	0.05	85	0.04	-0.02	0.019	0.06	0.04	0.05	95	0.04	0.00	0.009	0.07	0.05	0.06
75	0.05	-0.03	0.015	0.07	0.04	0.05	105	0.01	-0.02	0.006	0.06	0.05	0.06	115	0.01	-0.01	-0.005	0.07	0.05	0.07
105	0.01	-0.03	0.008	0.07	0.04	0.06	145	-0.04	-0.02	-0.005	0.07	0.05	0.07	145	-0.04	-0.01	-0.008	0.08	0.05	0.08
145	-0.06	-0.03	-0.001	0.07	0.04	0.06	155	-0.05		-0.015	0.08		0.06	155	-0.06		-0.014	0.08		0.06
155	-0.07		-0.005	0.08		0.06	185	-0.22		-0.011	0.08		0.06	185	-0.24		-0.018	0.09		0.07
185	-0.19		-0.013	0.08		0.06														

Expt. 2F4.4Y200 - Cont'd

At x = 350 mm						
y (mm)	u (m/s)	v (m/s)	w (m/s)	$\sqrt{\overline{u'^2}}$ (m/s)	$\sqrt{\overline{v'^2}}$ (m/s)	$\sqrt{\overline{w'^2}}$ (m/s)
15	0.34	0.27	-0.005	0.14	0.07	0.12
25	0.33	0.26	-0.005	0.10	0.07	0.08
35	0.30	0.24	0.001	0.08	0.07	0.08
45	0.26	0.21	0.000	0.08	0.08	0.07
55	0.21	0.17	0.003	0.08	0.08	0.07
70	0.15	0.11	0.010	0.07	0.07	0.07
85	0.10	0.06	0.006	0.06	0.06	0.06
100	0.07	0.04	0.003	0.06	0.05	0.06
115	0.04	0.02	-0.002	0.06	0.05	0.06
145	-0.01	0.01	-0.001	0.07	0.05	0.07
155	-0.04	0.00	-0.009	0.07	0.00	0.06
185	-0.27		-0.020	0.09		0.07
194.3	-0.27		-0.020	0.09		0.07

At x = 400 mm						
y (mm)	u (m/s)	v (m/s)	w (m/s)	$\sqrt{\overline{u'^2}}$ (m/s)	$\sqrt{\overline{v'^2}}$ (m/s)	$\sqrt{\overline{w'^2}}$ (m/s)
30	0.15	-0.08	-0.009			
40	0.32	-0.06	-0.014			
50	0.30	-0.03	-0.015			
60	0.30	0.31	-0.010	0.09	0.07	0.08
70	0.28	0.31	-0.012	0.08	0.07	0.08
85	0.24	0.27	-0.008	0.08	0.08	0.08
105	0.18	0.22	-0.005	0.08	0.09	0.08
125	0.10	0.16	-0.004	0.08	0.09	0.08
150	0.02	0.11	-0.010	0.09	0.09	0.08
160	-0.06		-0.004	0.08		0.07
190	-0.23		-0.020	0.07		0.10

At x = 450 mm						
y (mm)	u (m/s)	v (m/s)	w (m/s)	$\sqrt{\overline{u'^2}}$ (m/s)	$\sqrt{\overline{v'^2}}$ (m/s)	$\sqrt{\overline{w'^2}}$ (m/s)
45	-0.03	0.01	-0.005	0.10	0.05	0.07
55	0.05	0.09	-0.006	0.14	0.07	0.08
65	0.08	0.14	-0.007	0.15	0.07	0.09
75	0.20	0.24	-0.008	0.15	0.07	0.09
85	0.21	0.27	-0.011	0.13	0.07	0.08
95	0.23	0.29	-0.013	0.11	0.07	0.08
105	0.22	0.29	-0.010	0.09	0.07	0.07
125	0.16	0.26	-0.012	0.08	0.08	0.07
150	0.11	0.23	-0.014	0.08	0.08	0.08
160	0.08		-0.006	0.07		0.06
190	-0.03		-0.015	0.08		0.09

At x = 500 mm						
60	-0.11	-0.02	0.000	0.05	0.03	0.04
70	-0.09	-0.01	0.001	0.06	0.04	0.05
80	-0.05	0.00	-0.003	0.11	0.05	0.08
90	0.00	0.04	-0.006	0.13	0.06	0.09
105	0.08	0.09	-0.001	0.15	0.07	0.10
120	0.13	0.13	-0.011	0.15	0.08	0.10
140	0.20	0.17	-0.015	0.11	0.08	0.09
160	0.26		-0.002	0.08		0.06
190	0.18		-0.009	0.08		0.08

Expt. No.: = 3F6.7Y240 **U_0 = 1.00 m/s** **F_0 = 6.7** **y_t/b_0 = 15.0**

At x = 50 mm							At x = 100 mm							At x = 150 mm						
y (mm)	u (m/s)	v (m/s)	w (m/s)	$\sqrt{\overline{u'^2}}$ (m/s)	$\sqrt{\overline{v'^2}}$ (m/s)	$\sqrt{\overline{w'^2}}$ (m/s)	y (mm)	u (m/s)	v (m/s)	w (m/s)	$\sqrt{\overline{u'^2}}$ (m/s)	$\sqrt{\overline{v'^2}}$ (m/s)	$\sqrt{\overline{w'^2}}$ (m/s)	y (mm)	u (m/s)	v (m/s)	w (m/s)	$\sqrt{\overline{u'^2}}$ (m/s)	$\sqrt{\overline{v'^2}}$ (m/s)	$\sqrt{\overline{w'^2}}$ (m/s)
5	1.09		0.003	0.03		0.02	-35	-0.08	0.05	0.005	0.11	0.05	0.09	-60	-0.01	0.04	0.001	0.10	0.04	0.07
10	0.90		0.011	0.11		0.05	-25	0.02	0.04	0.013	0.14	0.07	0.11	-50	-0.06	0.04	0.004	0.13	0.09	0.11
15	0.41		-0.002	0.13		0.07	-10	0.83	-0.13	0.050	0.15	0.09	0.10	-40	0.02	0.03	0.011	0.15	0.09	0.12
25	0.06		0.002	0.06		0.07	-5	0.91	-0.12	0.055	0.10	0.06	0.07	-20	0.67	-0.18	0.042	0.20	0.12	0.11
40	0.03		0.004	0.06		0.06	5	0.50	-0.05	0.029	0.18	0.05	0.09	-10	0.66	-0.15	0.039	0.20	0.07	0.10
60	0.01		0.000	0.06		0.06	25	0.02	-0.03	0.002	0.09	0.03	0.08	0	0.45	-0.08	0.021	0.25	0.06	0.10
90	-0.01		0.003	0.06		0.06	55	0.02	-0.04	0.006	0.07	0.04	0.06	10	0.16	-0.05	0.012	0.17	0.05	0.09
165	-0.06		0.004	0.07		0.05	95	-0.03	-0.06	0.001	0.07	0.05	0.06	30	0.02	-0.04	-0.001	0.10	0.04	0.08
205	-0.06		0.003	0.08		0.05	135	-0.05	-0.06	-0.001	0.08	0.05	0.06	60	-0.01	-0.05	-0.004	0.10	0.05	0.08
225	-0.03		0.001	0.08		0.06	175	-0.08	-0.05	-0.002	0.08	0.04	0.06	100	-0.04	-0.05	0.001	0.08	0.05	0.06
							195	-0.09		0.003	0.07		0.05	140	-0.08	-0.05	-0.004	0.08	0.05	0.06
							215	-0.10		-0.007	0.08		0.06	175	-0.11	-0.04	-0.009	0.07	0.04	0.06
							225	-0.09		0.003	0.09		0.06	195	-0.12		0.002	0.08		0.06
														215	-0.14		0.007	0.08		0.06
														225	-0.14		-0.003	0.08		0.06

3F6.7Y240 - Cont'd

At x = 200 mm							At x = 250 mm							At x = 300 mm						
y (mm)	u (m/s)	v (m/s)	w (m/s)	$\sqrt{\overline{u'^2}}$ (m/s)	$\sqrt{\overline{v'^2}}$ (m/s)	$\sqrt{\overline{w'^2}}$ (m/s)	y (mm)	u (m/s)	v (m/s)	w (m/s)	$\sqrt{\overline{u'^2}}$ (m/s)	$\sqrt{\overline{v'^2}}$ (m/s)	$\sqrt{\overline{w'^2}}$ (m/s)	y (mm)	u (m/s)	v (m/s)	w (m/s)	$\sqrt{\overline{u'^2}}$ (m/s)	$\sqrt{\overline{v'^2}}$ (m/s)	$\sqrt{\overline{w'^2}}$ (m/s)
-85	-0.08	0.01	-0.004				-105	0.00	-0.05	-0.006	0.14	0.10	0.14	-115	0.02	-0.01	-0.007	0.10	0.04	0.10
-75	-0.02	-0.01	0.015	0.14	0.10	0.13	-90	0.06	-0.06	-0.002	0.17	0.11	0.14	-105	0.09	-0.01	-0.002			
-60	0.01	0.01	0.021	0.14	0.09	0.12	-75	0.24	-0.12	0.014	0.22	0.14	0.14	-90	0.23	-0.05	0.003			
-45	0.40	-0.17	0.023	0.24	0.15	0.13	-60	0.39	-0.16	0.026	0.22	0.13	0.12	-70	0.36	-0.08	0.019	0.20	0.11	0.12
-35	0.51	-0.18	0.024	0.22	0.12	0.12	-50	0.43	-0.15	0.021	0.21	0.11	0.12	-50	0.38	-0.07	0.021	0.19	0.10	0.11
-25	0.55	-0.17	0.028	0.20	0.09	0.11	-35	0.44	-0.13	0.018	0.21	0.09	0.11	-30	0.28	-0.05	0.016	0.21	0.08	0.11
-15	0.44	-0.12	0.018	0.24	0.07	0.11	-20	0.31	-0.09	0.013	0.23	0.07	0.11	-10	0.17	-0.04	0.009	0.19	0.07	0.10
0	0.23	-0.07	0.006	0.22	0.06	0.10	5	0.07	-0.06	-0.005	0.14	0.06	0.09	20	0.02	-0.06	-0.003	0.09	0.05	0.09
25	0.02	-0.06	-0.004	0.10	0.05	0.08	45	-0.03	-0.08	-0.003	0.08	0.05	0.07	55	-0.04	-0.07	-0.009	0.09	0.06	0.09
55	-0.01	-0.06	0.000	0.08	0.05	0.06	95	-0.08	-0.07	-0.001	0.08	0.06	0.08	95	-0.08	-0.07	-0.007	0.07	0.06	0.09
95	-0.04	-0.05	-0.003	0.08	0.05	0.06	135	-0.12	-0.05	-0.002	0.07	0.06	0.08	135	-0.12	-0.04	-0.010	0.08	0.06	0.09
135	-0.11	-0.05	-0.003	0.08	0.05	0.07	175	-0.14	-0.02	-0.002	0.08	0.05	0.08	175	-0.15	-0.02	-0.005	0.08	0.06	0.08
175	-0.13	-0.03	-0.001	0.08	0.05	0.07	195	-0.16		0.004	0.08		0.08	195	-0.18		0.008	0.08		0.08
195	-0.14		0.006	0.08		0.07	215	-0.18		0.001	0.07		0.07	215	-0.21		0.007	0.07		0.07
215	-0.17		-0.003	0.07		0.07	225	-0.20		0.003	0.08		0.07	225	-0.23		0.007	0.08		0.07
225	-0.19		0.002	0.08		0.07														

Expt. 3F6.7Y240 - Cont'd

At x = 350 mm							At x = 400 mm							At x = 450 mm						
y (mm)	u (m/s)	v (m/s)	w (m/s)	$\sqrt{\overline{u'^2}}$ (m/s)	$\sqrt{\overline{v'^2}}$ (m/s)	$\sqrt{\overline{w'^2}}$ (m/s)	y (mm)	u (m/s)	v (m/s)	w (m/s)	$\sqrt{\overline{u'^2}}$ (m/s)	$\sqrt{\overline{v'^2}}$ (m/s)	$\sqrt{\overline{w'^2}}$ (m/s)	y (mm)	u (m/s)	v (m/s)	w (m/s)	$\sqrt{\overline{u'^2}}$ (m/s)	$\sqrt{\overline{v'^2}}$ (m/s)	$\sqrt{\overline{w'^2}}$ (m/s)
-100	0.11	0.01	0.008	0.15	0.06	0.13	-75	0.03	0.04	0.009	0.10	0.05	0.09	-35	0.08	0.14	0.006	0.18	0.07	0.12
-90	0.19	0.02	0.013				-65	-0.05	0.02	0.011				-20	0.15	-0.01	0.012			
-75	0.34	0.02	0.018				-50	0.34	0.11	0.019	0.16	0.08	0.11	-5	0.13	-0.01	0.014			
-55	0.39	0.06	0.014	0.15	0.11	0.12	-30	0.35	0.19	0.021	0.12	0.10	0.11	10	0.08	0.00	0.012	0.00	0.00	0.00
-35	0.34	0.06	0.017	0.16	0.10	0.11	-10	0.30	0.18	0.018	0.12	0.10	0.10	30	0.27	0.20	0.014	0.10	0.10	0.10
-15	0.24	0.04	0.006	0.16	0.09	0.11	15	0.20	0.12	0.017	0.12	0.11	0.10	60	0.17	0.14	0.014	0.09	0.11	0.10
15	0.08	-0.01	-0.002	0.12	0.08	0.10	55	0.07	0.03	-0.005	0.08	0.10	0.09	100	0.06	0.08	-0.001	0.08	0.11	0.10
55	-0.01	-0.05	-0.002	0.08	0.07	0.09	95	-0.01	0.00	-0.004	0.08	0.09	0.10	140	-0.04	0.05	-0.005	0.09	0.10	0.10
95	-0.06	-0.06	-0.001	0.07	0.07	0.10	135	-0.08	0.00	-0.002	0.08	0.08	0.10	175	-0.11	0.04	-0.009	0.09	0.09	0.09
135	-0.10	-0.03	-0.003	0.08	0.07	0.09	175	-0.14	0.02	-0.003	0.08	0.08	0.08	195	-0.15		-0.003	0.09		0.08
175	-0.15	-0.01	-0.005	0.08	0.07	0.09	195	-0.18		0.005	0.08		0.08	215	-0.22		0.001	0.08		0.09
195	-0.18		0.003	0.08		0.08	215	-0.24		0.000	0.08		0.08	225	-0.25		-0.011	0.08		0.10
215	-0.22		0.005	0.08		0.08	225	-0.27		0.004	0.07		0.10							
225	-0.26		0.004	0.08		0.09														
At x = 500 mm							At x = 550 mm							At x = 650 mm						
10	0.22	0.11	0.019	0.17	0.09	0.11	25	0.07	0.00	0.008	0.12	0.06	0.11	45	0.02	0.00	0.001	0.09	0.05	0.10
20	-0.12	0.13	0.022				40	0.21	0.10	0.014	0.17	0.09	0.11	60	0.10	0.03	0.003	0.15	0.07	0.11
35	-0.36	0.07	0.017				60	-0.27	0.06	0.008				75	0.18	0.09	0.010	0.16	0.08	0.12
55	0.29	0.22	0.017	0.11	0.10	0.11	80	-0.12	0.02	0.011				95	0.19	0.13	0.008	0.15	0.09	0.11
80	0.21	0.20	0.008	0.11	0.11	0.11	110	0.18	0.20	0.011	0.11	0.10	0.10	125	0.19	0.17	0.008	0.13	0.10	0.10
110	0.12	0.17	-0.003	0.11	0.11	0.11	150	0.07	0.16	0.000	0.11	0.11	0.10	155	0.12	0.15	-0.002	0.12	0.09	0.10
140	0.03	0.13	-0.003	0.11	0.11	0.10	180	0.00	0.12	-0.009	0.12	0.10	0.11	180	0.07	0.12	0.003	0.10	0.09	0.09
175	-0.06	0.09	-0.009	0.11	0.10	0.10	200	-0.01		-0.003	0.10		0.09	200	0.10		0.000	0.10		0.08
195	-0.08		-0.004	0.09		0.09	220	-0.07		-0.007	0.09		0.10	220	0.05		-0.001	0.11		0.08
215	-0.15		-0.010	0.08		0.09	230	-0.09		-0.002	0.10		0.11	230	0.04		-0.001	0.10		0.10
225	-0.17		-0.007	0.08		0.11														

Expt. 3F6.7Y240 - Cont'd

At x = 700 mm							At x = 800 mm						
y (mm)	u (m/s)	v (m/s)	w (m/s)	$\sqrt{\overline{u'^2}}$ (m/s)	$\sqrt{\overline{v'^2}}$ (m/s)	$\sqrt{\overline{w'^2}}$ (m/s)	y (mm)	u (m/s)	v (m/s)	w (m/s)	$\sqrt{\overline{u'^2}}$ (m/s)	$\sqrt{\overline{v'^2}}$ (m/s)	$\sqrt{\overline{w'^2}}$ (m/s)
90	0.01	0.00	0.006	0.07	0.03	0.07	135	0.11	0.02	0.000	0.07	0.04	0.07
100	0.08	0.02	0.001	0.11	0.06	0.09	145	0.12	0.02	0.002	0.08	0.05	0.07
120	0.12	0.03	0.004	0.11	0.07	0.08	160	0.15	0.02	0.002	0.08	0.05	0.07
150	0.16	0.06	0.006	0.10	0.08	0.08	180	0.16	0.02	0.004	0.09	0.05	0.08
180	0.18	0.06	0.009	0.09	0.08	0.08	200	0.19		-0.002	0.07		0.06
200	0.20		0.000	0.09		0.07	220	0.22		0.003	0.07		0.07
220	0.20		0.004	0.09		0.08	230	0.24		0.004	0.08		0.07
230	0.19		0.004	0.09		0.09							

Expt. No.: = 3F6.7Y200 **U_0 = 1.00 m/s** **F_0 = 6.7** **y_t/b_0 = 12.5**

At x = 50 mm							At x = 100 mm							At x = 150 mm						
y (mm)	u (m/s)	v (m/s)	w (m/s)	$\sqrt{\overline{u'^2}}$ (m/s)	$\sqrt{\overline{v'^2}}$ (m/s)	$\sqrt{\overline{w'^2}}$ (m/s)	y (mm)	u (m/s)	v (m/s)	w (m/s)	$\sqrt{\overline{u'^2}}$ (m/s)	$\sqrt{\overline{v'^2}}$ (m/s)	$\sqrt{\overline{w'^2}}$ (m/s)	y (mm)	u (m/s)	v (m/s)	w (m/s)	$\sqrt{\overline{u'^2}}$ (m/s)	$\sqrt{\overline{v'^2}}$ (m/s)	$\sqrt{\overline{w'^2}}$ (m/s)
5	1.07		-0.005	0.02		0.02	-35	-0.09	0.06	0.004	0.11	0.05	0.07	-60	-0.06	0.05	0.010	0.09	0.05	0.09
10	0.95		-0.003	0.07		0.03	-25	0.00	0.04	0.020	0.14	0.08	0.11	-50	-0.08	0.06	0.007	0.11	0.07	0.09
15	0.45		0.001	0.13		0.07	-10	0.90	-0.14	0.038				-40	0.05	0.01	0.014			
25	0.05		0.007	0.06		0.06	-5	0.89	-0.11	0.034	0.09	0.06	0.07	-20	0.64	-0.18	0.027	0.21	0.12	0.11
40	0.03		0.006	0.06		0.05	5	0.47	-0.05	0.024	0.17	0.04	0.08	-10	0.69	-0.14	0.030	0.19	0.08	0.09
60	0.02		0.011	0.05		0.05	25	0.04	-0.03	0.002	0.08	0.03	0.07	0	0.41	-0.08	0.011	0.22	0.05	0.09
90	-0.01		0.013	0.07		0.05	60	0.01	-0.04	0.003	0.07	0.04	0.05	10	0.19	-0.05	0.005	0.16	0.05	0.09
165	-0.04		0.007	0.07		0.05	100	-0.02	-0.04	0.000	0.08	0.04	0.05	30	0.03	-0.04	-0.003	0.09	0.04	0.08
190	-0.03		0.009	0.07		0.05	140	-0.07	-0.04	0.004	0.08	0.04	0.06	60	0.01	-0.04	0.005	0.08	0.05	0.06
							160	-0.08		0.002	0.07		0.05	100	-0.04	-0.04	0.000	0.08	0.05	0.06
							180	-0.10		-0.001	0.08		0.05	140	-0.08	-0.03	-0.002	0.08	0.05	0.06
							190	-0.09		0.003	0.08		0.06	160	-0.11		0.006	0.08		0.06
														180	-0.14		0.001	0.08		0.06
														190	-0.14		0.002	0.08		0.06

Expt. 3F6.7Y200 - Cont'd

At x = 200 mm							At x = 250 mm							At x = 300 mm						
y (mm)	u (m/s)	v (m/s)	w (m/s)	$\sqrt{\overline{u'^2}}$ (m/s)	$\sqrt{\overline{v'^2}}$ (m/s)	$\sqrt{\overline{w'^2}}$ (m/s)	y (mm)	u (m/s)	v (m/s)	w (m/s)	$\sqrt{\overline{u'^2}}$ (m/s)	$\sqrt{\overline{v'^2}}$ (m/s)	$\sqrt{\overline{w'^2}}$ (m/s)	y (mm)	u (m/s)	v (m/s)	w (m/s)	$\sqrt{\overline{u'^2}}$ (m/s)	$\sqrt{\overline{v'^2}}$ (m/s)	$\sqrt{\overline{w'^2}}$ (m/s)
-85	-0.07	0.01	-0.008				-105	-0.05	-0.01	0.002				-105	0.07	-0.01	0.014			
-75	-0.02	-0.01	0.004	0.14	0.10	0.13	-75	0.24	-0.11	0.017	0.22	0.13	0.14	-95	0.19	-0.05	0.004	0.20	0.10	0.13
-60	0.04	0.00	0.011	0.00	0.00	0.00	-60	0.37	-0.14	0.020	0.23	0.13	0.12	-80	0.27	-0.03	0.010			
-45	0.38	-0.16	0.021	0.25	0.15	0.12	-45	0.44	-0.14	0.014	0.20	0.12	0.11	-65	0.37	-0.06	0.015	0.19	0.11	0.12
-35	0.51	-0.18	0.024	0.21	0.12	0.12	-30	0.39	-0.11	0.010	0.22	0.08	0.11	-45	0.39	-0.05	0.020	0.18	0.09	0.11
-25	0.53	-0.16	0.019	0.20	0.10	0.11	-15	0.29	-0.07	0.015	0.23	0.07	0.11	-25	0.26	-0.04	0.011	0.20	0.08	0.11
-15	0.47	-0.12	0.020	0.23	0.07	0.10	10	0.10	-0.06	0.003	0.15	0.06	0.09	-5	0.16	-0.04	0.002	0.17	0.07	0.10
0	0.24	-0.06	0.008	0.22	0.06	0.10	50	-0.02	-0.06	-0.003	0.08	0.06	0.07	25	0.02	-0.07	-0.010	0.10	0.06	0.09
25	0.03	-0.05	-0.001	0.10	0.05	0.08	100	-0.08	-0.05	-0.004	0.08	0.06	0.08	60	-0.04	-0.07	-0.003	0.08	0.06	0.09
60	-0.01	-0.05	0.001	0.09	0.05	0.07	140	-0.12	-0.02	-0.006	0.09	0.06	0.08	100	-0.08	-0.04	-0.007	0.08	0.06	0.09
100	-0.06	-0.04	-0.004	0.09	0.05	0.07	160	-0.15		0.000	0.09		0.07	140	-0.14	-0.01	-0.009	0.09	0.06	0.08
140	-0.10	-0.02	-0.002	0.08	0.05	0.07	180	-0.20		0.000	0.08		0.07	160	-0.17		0.002	0.09		0.08
160	-0.12		0.002	0.08		0.06	190	-0.24		0.000	0.08		0.07	180	-0.22		0.003	0.08		0.08
180	-0.17		0.004	0.08		0.07								190	-0.27		0.001	0.08		0.09
190	-0.19		0.001	0.08		0.06														

Expt. 3F6.7Y200 - Cont'd

At x = 350 mm							At x = 400 mm							At x = 450 mm						
y (mm)	u (m/s)	v (m/s)	w (m/s)	$\sqrt{\overline{u'^2}}$ (m/s)	$\sqrt{\overline{v'^2}}$ (m/s)	$\sqrt{\overline{w'^2}}$ (m/s)	y (mm)	u (m/s)	v (m/s)	w (m/s)	$\sqrt{\overline{u'^2}}$ (m/s)	$\sqrt{\overline{v'^2}}$ (m/s)	$\sqrt{\overline{w'^2}}$ (m/s)	y (mm)	u (m/s)	v (m/s)	w (m/s)	$\sqrt{\overline{u'^2}}$ (m/s)	$\sqrt{\overline{v'^2}}$ (m/s)	$\sqrt{\overline{w'^2}}$ (m/s)
-85	0.27	0.04	0.007				-65	0.19	0.13	0.010				0	0.12	-0.02	0.006			
-70	0.31	0.02	0.016				-55	-0.10	0.01	0.011				15	0.13	-0.01	0.006			
-50	0.37	0.07	0.013	0.15	0.10	0.11	-20	0.33	0.19	0.014	0.13	0.10	0.10	30	0.25	0.21	0.007	0.10	0.10	0.10
-30	0.33	0.07	0.012	0.16	0.09	0.11	0	0.26	0.17	0.009	0.13	0.10	0.11	50	0.20	0.18	0.005	0.10	0.11	0.10
-10	0.23	0.05	0.008	0.16	0.09	0.11	20	0.19	0.12	0.004	0.12	0.11	0.11	70	0.12	0.13	-0.002	0.10	0.12	0.10
20	0.09	0.00	-0.006	0.12	0.08	0.09	50	0.08	0.06	0.001	0.11	0.10	0.11	100	0.03	0.10	0.000	0.09	0.12	0.10
60	0.00	-0.04	-0.005	0.10	0.07	0.11	100	-0.03	0.02	-0.006	0.10	0.09	0.10	140	-0.10	0.06	-0.013	0.09	0.10	0.09
100	-0.06	-0.03	-0.005	0.10	0.07	0.10	140	-0.14	0.02	-0.001	0.09	0.08	0.09	160	-0.14		-0.006	0.09		0.09
140	-0.14	0.00	-0.011	0.11	0.07	0.10	160	-0.18		-0.005	0.09		0.08	180	-0.21		-0.011	0.08		0.09
160	-0.18		-0.002	0.09		0.08	180	-0.26		-0.008	0.08		0.10	190	-0.24		-0.012	0.07		0.12
180	-0.25		-0.002	0.09		0.08	190	-0.28		-0.012	0.08		0.11							
190	-0.29		-0.006	0.08		0.10														
At x = 500 mm							At x = 550 mm							At x = 600 mm						
10	0.23	0.13	0.007				25	0.02	-0.01	-0.004	0.11	0.06	0.10	50	0.01	0.00	-0.002	0.10	0.05	0.08
20	-0.11	0.12	0.012				40	0.13	0.05	-0.002	0.17	0.08	0.10	65	0.07	0.02	0.004	0.13	0.07	0.09
35	0.28	0.22	0.014	0.16	0.09	0.14	60	0.10	0.07	-0.001				85	0.14	0.07	0.004	0.15	0.08	0.11
55	0.25	0.22	0.006	0.11	0.10	0.10	80	0.20	0.16	0.001	0.15	0.09	0.11	115	0.15	0.09	0.000	0.13	0.09	0.10
85	0.16	0.19	0.001	0.11	0.11	0.10	110	0.15	0.16	0.002	0.12	0.10	0.10	145	0.15	0.08	0.005	0.11	0.09	0.09
115	0.06	0.16	-0.001	0.11	0.11	0.11	145	0.08	0.13	-0.007	0.12	0.10	0.10	165	0.17		0.000	0.10		0.08
145	-0.04	0.11	-0.009	0.11	0.11	0.11	165	0.09		-0.003	0.10		0.09	185	0.14		0.005	0.10		0.08
160	-0.07		0.000	0.09		0.09	185	0.03		-0.015	0.10		0.08	195	0.14		-0.003	0.10		0.10
180	-0.11		-0.012	0.09		0.09	195	0.05		-0.008	0.11		0.11							
190	-0.13		-0.015	0.08		0.11														

Expt. 3F6.7Y200 - Cont'd

At x = 700 mm							At x = 800 mm						
y (mm)	u (m/s)	v (m/s)	w (m/s)	$\sqrt{\overline{u'^2}}$ (m/s)	$\sqrt{\overline{v'^2}}$ (m/s)	$\sqrt{\overline{w'^2}}$ (m/s)	y (mm)	u (m/s)	v (m/s)	w (m/s)	$\sqrt{\overline{u'^2}}$ (m/s)	$\sqrt{\overline{v'^2}}$ (m/s)	$\sqrt{\overline{w'^2}}$ (m/s)
90	0.03	0.01	-0.003	0.06	0.03	0.07	125	0.15	0.02	0.003	0.06	0.03	0.06
100	0.11	0.02	0.001	0.09	0.05	0.07	135	0.16	0.01	0.000	0.06	0.04	0.06
120	0.14	0.01	0.004	0.09	0.06	0.07	145	0.18	0.02	0.005	0.07	0.04	0.06
145	0.18	0.02	0.003	0.08	0.06	0.08	165	0.22		0.001	0.06		0.06
165	0.20		0.000	0.08		0.07	185	0.25		-0.004	0.06		0.06
185	0.24		0.005	0.08		0.07	195	0.27		0.001	0.07		0.06
195	0.24		0.008	0.09		0.08							

Expt. No.: = 3F6.7Y48 **U_0 = 1.00 m/s** **F_0 = 6.7** **y_t/b_0 = 3.0**

At x = 50 mm							At x = 100 mm							At x = 150 mm						
y (mm)	u (m/s)	v (m/s)	w (m/s)	$\sqrt{\overline{u'^2}}$ (m/s)	$\sqrt{\overline{v'^2}}$ (m/s)	$\sqrt{\overline{w'^2}}$ (m/s)	y (mm)	u (m/s)	v (m/s)	w (m/s)	$\sqrt{\overline{u'^2}}$ (m/s)	$\sqrt{\overline{v'^2}}$ (m/s)	$\sqrt{\overline{w'^2}}$ (m/s)	y (mm)	u (m/s)	v (m/s)	w (m/s)	$\sqrt{\overline{u'^2}}$ (m/s)	$\sqrt{\overline{v'^2}}$ (m/s)	$\sqrt{\overline{w'^2}}$ (m/s)
5	1.09		0.019	0.03		0.03	-15	0.00		0.000	0.02	0.00	0.01	-15	0.02		-0.008	0.08		0.07
10	1.08		-0.020	0.03		0.03	-5	0.03		0.101	0.09	0.00	0.07	-5	0.11		0.026	0.12		0.10
15	0.92		-0.031	0.13		0.05	0	0.24		0.100	0.18	0.00	0.10	5	0.26		0.054	0.18		0.11
20	0.38		-0.006	0.00		0.00	5	0.64		0.067				15	0.64		0.033	0.25		0.11
30	-0.14		0.081	0.10		0.07	10	0.97		0.016	0.12	0.00	0.07	25	0.83		-0.003	0.17		0.08
35	-0.19		0.111	0.11		0.07	15	1.03		-0.019	0.07	0.00	0.05	30	0.72		0.003	0.21		0.09
							20	0.80		-0.009	0.18	0.00	0.08	35	0.55		0.017	0.25		0.10
							25	0.51		0.005	0.24	0.00	0.11	45	0.24		0.078	0.17		0.12
							30	0.16		0.010	0.19	0.00	0.11							
							35	-0.09		0.029	0.12	0.00	0.07							
At x = 200 mm							At x = 250 mm							At x = 300 mm						
-25	0.07		-0.006	0.09		0.08	-45	0.05		0.001	0.09		0.07	-65	0.03		-0.01	0.08		0.07
-15	0.14		0.015	0.11		0.09	-25	0.18		0.018	0.11		0.10	-45	0.14		0.014	0.10		0.09
-5	0.25		0.020	0.14		0.11	-15	0.29		0.016	0.12		0.10	-25	0.26		0.027	0.12		0.11
5	0.41		0.030	0.15		0.11	0	0.46		0.019	0.13		0.10	-10	0.39		0.027	0.12		0.10
15	0.57		0.022	0.16		0.11	10	0.56		0.012	0.12		0.09	5	0.52		0.017	0.12		0.10
25	0.63		0.009	0.15		0.10	20	0.62		-0.001	0.11		0.08	20	0.63		0.001	0.09		0.07
35	0.57		0.013	0.16		0.10	30	0.63		-0.003	0.11		0.08	30	0.68		-0.001	0.09		0.07
45	0.43		0.060				40	0.59		0.022	0.15		0.10	40	0.66		0.010	0.12		0.08

Expt. 3F6.7Y48 - Cont'd

At x = 350 mm							At x = 400 mm							At x = 550 mm						
y (mm)	u (m/s)	v (m/s)	w (m/s)	$\sqrt{\overline{u'^2}}$ (m/s)	$\sqrt{\overline{v'^2}}$ (m/s)	$\sqrt{\overline{w'^2}}$ (m/s)	y (mm)	u (m/s)	v (m/s)	w (m/s)	$\sqrt{\overline{u'^2}}$ (m/s)	$\sqrt{\overline{v'^2}}$ (m/s)	$\sqrt{\overline{w'^2}}$ (m/s)	y (mm)	u (m/s)	v (m/s)	w (m/s)	$\sqrt{\overline{u'^2}}$ (m/s)	$\sqrt{\overline{v'^2}}$ (m/s)	$\sqrt{\overline{w'^2}}$ (m/s)
-85	0.06		-0.010	0.09		0.07	-90	0.16		-0.023	0.09		0.08	-90	0.20		-0.013	0.09		0.07
-65	0.15		0.002	0.10		0.09	-70	0.23		-0.011	0.10		0.09	-70	0.26		-0.021	0.10		0.08
-45	0.24		0.018	0.11		0.10	-50	0.29		0.001	0.11		0.09	-50	0.31		-0.019	0.11		0.08
-25	0.33		0.027	0.11		0.10	-30	0.37		0.003	0.11		0.09	-30	0.36		-0.017	0.11		0.09
-5	0.42		0.019	0.10		0.09	-10	0.44		0.008	0.10		0.09	-10	0.41		-0.017	0.10		0.09
15	0.51		0.011	0.09		0.08	10	0.49		0.008	0.08		0.07	10	0.46		-0.016	0.10		0.08
35	0.54		0.006	0.08		0.06	30	0.52		0.005	0.07		0.07	30	0.50		-0.013	0.08		0.08
45	0.50		0.021	0.11		0.07	45	0.49		0.008	0.07		0.07	45	0.52		-0.003	0.08		0.08
At x = 750 mm							At x = 1000 mm							At x = 1200 mm						
-60	0.24		-0.003	0.09		0.07	-25	0.28		0.004	0.07		0.06	0	0.33	0.00	0.008	0.06	0.00	0.05
-50	0.26		0.000	0.09		0.07	-15	0.30		0.007	0.07		0.06	10	0.35	0.00	0.005	0.06	0.00	0.05
-35	0.29		-0.007	0.09		0.07	0	0.31		0.001	0.07		0.06	25	0.35	0.00	0.002	0.05	0.00	0.05
-15	0.31		-0.011	0.09		0.08	20	0.32		-0.003	0.08		0.06	40	0.35	0.00	0.003	0.06	0.00	0.05
5	0.33		-0.015	0.10		0.08	40	0.33		-0.004	0.08		0.07	50	0.37	0.00	0.005	0.07	0.00	0.06
25	0.36		-0.013	0.10		0.08	50	0.34		-0.001	0.09		0.07							
50	0.40		-0.010	0.11		0.09														

Expt. No.: = 4F5.3Y280 **U_0 = 0.79 m/s** **F_0 = 5.3** **y_t/b_0 = 17.5**

At x = 50 mm							At x = 100 mm							At x = 150 mm						
y (mm)	u (m/s)	v (m/s)	w (m/s)	$\sqrt{\overline{u'^2}}$ (m/s)	$\sqrt{\overline{v'^2}}$ (m/s)	$\sqrt{\overline{w'^2}}$ (m/s)	y (mm)	u (m/s)	v (m/s)	w (m/s)	$\sqrt{\overline{u'^2}}$ (m/s)	$\sqrt{\overline{v'^2}}$ (m/s)	$\sqrt{\overline{w'^2}}$ (m/s)	y (mm)	u (m/s)	v (m/s)	w (m/s)	$\sqrt{\overline{u'^2}}$ (m/s)	$\sqrt{\overline{v'^2}}$ (m/s)	$\sqrt{\overline{w'^2}}$ (m/s)
5	0.86		-0.011	0.03		0.02	-30	-0.01	0.02	-0.007	0.12	0.07	0.10	-55	-0.05	0.03	-0.008	0.10	0.06	0.09
10	0.72		-0.021	0.08		0.04	-20	0.29	-0.05	0.008				-40	0.11	-0.03	0.003	0.17	0.10	0.11
15	0.32		-0.021	0.10		0.06	-15	0.61	-0.12	0.028				-30	0.22	-0.03	0.004			
25	0.07		-0.022	0.04		0.05	-10	0.73	-0.14	0.040				-25	0.48	-0.14	0.013	0.18	0.10	0.09
40	0.05		-0.013	0.04		0.05	-5	0.66	-0.09	0.027				-20	0.52	-0.14	0.017	0.15	0.08	0.08
60	0.02		-0.010	0.04		0.05	5	0.32	-0.04	0.002	0.14	0.04	0.08	-15	0.52	-0.13	0.011	0.15	0.06	0.08
90	0.01		-0.002	0.05		0.04	20	0.07	-0.03	-0.023	0.07	0.03	0.07	-5	0.42	-0.08	0.001	0.18	0.05	0.07
165	-0.04		0.000	0.05		0.04	40	0.06	-0.04	-0.023	0.05	0.03	0.05	5	0.21	-0.05	-0.007	0.15	0.04	0.07
205	-0.07		0.000	0.06		0.04	70	0.01	-0.05	-0.013	0.05	0.03	0.05	20	0.07	-0.04	-0.015	0.06	0.03	0.06
235	-0.08		0.005	0.06		0.05	100	-0.01	-0.06	-0.012	0.05	0.03	0.05	60	0.01	-0.05	-0.018	0.07	0.03	0.06
255	-0.08		-0.004	0.06		0.04	140	-0.04	-0.07	-0.008	0.06	0.04	0.05	100	-0.03	-0.05	-0.012	0.07	0.04	0.06
270	-0.02		-0.009	0.05		0.04	180	-0.07	-0.06	-0.003	0.06	0.04	0.05	140	-0.07	-0.06	-0.005	0.07	0.04	0.05
At x =6 50 mm							220	-0.10	-0.04	0.003	0.06	0.03	0.05	180	-0.10	-0.05	0.004	0.06	0.04	0.06
90	-0.03	0.01	-0.009	0.06	0.02	0.04	240	-0.11		0.006	0.05		0.05	220	-0.12	-0.03	0.001	0.06	0.04	0.05
100	0.00	0.01	0.004	0.07	0.03	0.06	260	-0.13		0.005	0.06		0.05	240	-0.13		0.015	0.06		0.05
115	-0.02	0.01	-0.007	0.06	0.03	0.05	270	-0.08		0.007	0.07		0.04	260	-0.16		0.016	0.05		0.05
145	0.10	0.05	0.014	0.11	0.05	0.08								270	-0.15		0.009	0.06		0.05
185	0.13	0.05	0.011	0.09	0.07	0.07														
225	0.16	0.06	0.016	0.08	0.07	0.07														
245	0.18		0.006	0.07		0.06														
265	0.18		0.011	0.08		0.07														
275	0.15		0.017	0.08		0.09														

Expt. 4F5.3Y280 - Cont'd

At x = 200 mm							At x = 250 mm							At x = 300 mm						
y (mm)	u (m/s)	v (m/s)	w (m/s)	$\sqrt{\overline{u'^2}}$ (m/s)	$\sqrt{\overline{v'^2}}$ (m/s)	$\sqrt{\overline{w'^2}}$ (m/s)	y (mm)	u (m/s)	v (m/s)	w (m/s)	$\sqrt{\overline{u'^2}}$ (m/s)	$\sqrt{\overline{v'^2}}$ (m/s)	$\sqrt{\overline{w'^2}}$ (m/s)	y (mm)	u (m/s)	v (m/s)	w (m/s)	$\sqrt{\overline{u'^2}}$ (m/s)	$\sqrt{\overline{v'^2}}$ (m/s)	$\sqrt{\overline{w'^2}}$ (m/s)
-75	-0.02	-0.01	-0.013				-75	0.12	-0.01	-0.009				-60	0.00	0.03	0.001			
-60	0.16	-0.07	-0.002				-60	0.23	-0.02	0.002	0.17	0.08	0.10	-50	0.10	0.03	0.009			
-45	0.32	-0.10	0.012	0.20	0.10	0.10	-50	0.33	-0.02	0.010				-40	-0.08	0.01	0.007			
-35	0.39	-0.10	0.009	0.18	0.09	0.09	-35	0.35	-0.01	0.011	0.15	0.08	0.08	-30	0.33	0.10	0.008	0.12	0.07	0.08
-25	0.41	-0.10	0.006	0.16	0.07	0.09	-20	0.29	0.00	0.007	0.15	0.06	0.08	-15	0.32	0.12	0.005	0.10	0.07	0.08
-15	0.35	-0.07	-0.003	0.18	0.06	0.08	-5	0.18	-0.01	-0.007	0.14	0.05	0.07	5	0.21	0.09	-0.001	0.10	0.07	0.07
-5	0.24	-0.05	-0.004	0.19	0.05	0.08	15	0.08	-0.02	-0.016	0.09	0.04	0.06	25	0.10	0.03	-0.009	0.08	0.06	0.06
20	0.05	-0.04	-0.014	0.08	0.03	0.07	35	0.03	-0.03	-0.013	0.07	0.04	0.06	60	0.02	-0.02	-0.006	0.06	0.05	0.06
60	-0.01	-0.05	-0.023	0.07	0.04	0.06	65	0.00	-0.05	-0.003	0.06	0.04	0.05	100	-0.03	-0.04	0.012	0.06	0.05	0.07
100	-0.04	-0.06	-0.006	0.07	0.04	0.07	105	-0.03	-0.05	0.002	0.06	0.05	0.06	140	-0.06	-0.04	0.011	0.06	0.05	0.08
140	-0.08	-0.06	0.003	0.07	0.04	0.07	145	-0.08	-0.05	0.009	0.06	0.04	0.07	180	-0.09	-0.03	0.020	0.06	0.04	0.08
180	-0.10	-0.04	0.006	0.07	0.04	0.07	185	-0.10	-0.03	0.013	0.06	0.04	0.07	220	-0.14	0.00	0.009	0.06	0.05	0.07
220	-0.13	-0.02	0.015	0.07	0.04	0.07	220	-0.13	-0.01	0.014	0.06	0.04	0.07	240	-0.16		0.014	0.06		0.07
240	-0.15		0.012	0.06		0.06	240	-0.16		0.019	0.06		0.07	260	-0.19		0.012	0.06		0.07
260	-0.19		0.013	0.05		0.06	260	-0.18		0.013	0.06		0.06	270	-0.23		0.014	0.06		0.07
270	-0.19		0.011	0.06		0.06	270	-0.21		0.010	0.06		0.07							

Expt. 4F5.3Y280 - Cont'd

At x = 350 mm							At x = 400 mm							At x = 450 mm						
y (mm)	u (m/s)	v (m/s)	w (m/s)	$\sqrt{\overline{u'^2}}$ (m/s)	$\sqrt{\overline{v'^2}}$ (m/s)	$\sqrt{\overline{w'^2}}$ (m/s)	y (mm)	u (m/s)	v (m/s)	w (m/s)	$\sqrt{\overline{u'^2}}$ (m/s)	$\sqrt{\overline{v'^2}}$ (m/s)	$\sqrt{\overline{w'^2}}$ (m/s)	y (mm)	u (m/s)	v (m/s)	w (m/s)	$\sqrt{\overline{u'^2}}$ (m/s)	$\sqrt{\overline{v'^2}}$ (m/s)	$\sqrt{\overline{w'^2}}$ (m/s)
-15	-0.09	-0.01	0.011				10	-0.01	0.05	-0.001	0.11	0.04	0.06	35	0.02	0.04	0.014	0.10	0.04	0.07
-5	-0.08	-0.01	0.009				20	-0.41	0.04	0.010				50	0.31	0.16	0.022	0.11	0.05	0.07
5	-0.01	-0.01	0.004				30	0.05	-0.03	0.011				65	-0.44	0.09	0.015			
20	0.28	0.19	0.010	0.09	0.08	0.08	45	-0.02	-0.02	0.005				85	0.26	0.19	0.007	0.09	0.08	0.09
40	0.19	0.14	0.000	0.08	0.08	0.08	65	0.23	0.17	0.001	0.08	0.09	0.08	105	0.20	0.17	0.003	0.08	0.09	0.08
70	0.08	0.06	0.002	0.07	0.07	0.07	100	0.12	0.10	0.003	0.08	0.09	0.08	140	0.10	0.11	0.007	0.08	0.09	0.08
100	0.02	0.01	0.001	0.07	0.07	0.07	140	0.03	0.04	0.012	0.07	0.08	0.08	180	0.00	0.06	0.007	0.08	0.09	0.08
140	-0.04	-0.02	0.016	0.07	0.06	0.07	180	-0.04	0.01	0.018	0.07	0.07	0.08	220	-0.07	0.05	0.006	0.07	0.07	0.08
180	-0.08	-0.01	0.018	0.07	0.06	0.08	220	-0.10	0.02	0.013	0.07	0.07	0.07	240	-0.09		0.013	0.07		0.07
220	-0.13	0.00	0.017	0.06	0.06	0.07	240	-0.13		0.004	0.06		0.07	260	-0.15		0.011	0.06		0.08
240	-0.15		0.008	0.07		0.07	260	-0.20		0.003	0.06		0.07	270	-0.17		0.010	0.07		0.09
260	-0.20		0.016	0.06		0.07	270	-0.22		0.009	0.06		0.09							
270	-0.24		0.011	0.07		0.08														
At x = 500 mm							At x = 550 mm							At x = 600 mm						
50	0.03	0.01	0.006	0.08	0.03	0.08	65	0.04	0.01	0.022	0.10	0.04	0.09	75	0.01	0.00	0.001	0.09	0.04	0.07
60	0.11	0.05	0.017	0.15	0.06	0.08	75	0.06	0.03	0.021	0.13	0.05	0.08	85	0.04	0.02	0.014	0.11	0.04	0.07
70	0.17	0.09	0.014	0.17	0.07	0.08	85	0.13	0.07	0.016	0.13	0.05	0.08	100	0.06	0.03	0.016	0.11	0.05	0.08
90	0.27	0.17	0.014	0.12	0.06	0.07	105	0.20	0.12	0.017	0.13	0.06	0.08	120	0.11	0.07	0.010	0.13	0.06	0.09
110	0.23	0.19	0.008	0.10	0.07	0.08	125	0.16	0.13	0.011	0.13	0.07	0.09	150	0.14	0.09	0.007	0.12	0.07	0.09
140	0.17	0.18	0.009	0.09	0.09	0.08	155	0.19	0.17	0.008	0.10	0.07	0.07	185	0.14	0.09	0.007	0.10	0.08	0.08
180	0.08	0.14	0.010	0.08	0.09	0.08	185	0.14	0.16	0.005	0.09	0.08	0.08	225	0.12	0.08	0.009	0.09	0.08	0.08
220	-0.01	0.10	0.005	0.08	0.09	0.07	225	0.04	0.11	0.011	0.08	0.08	0.07	245	0.13		0.011	0.08		0.07
240	-0.01		0.004	0.08		0.07	245	0.05		0.006	0.09		0.07	265	0.07		0.016	0.08		0.07
260	-0.08		0.008	0.08		0.08	265	0.02		0.011	0.09		0.07	275	0.07		0.018	0.09		0.09
270	-0.10		0.007	0.09		0.10	275	-0.01		0.023	0.09		0.09							

Expt. No.: = 4F5.3Y240 **U_0 = 0.79 m/s** **F_0 = 5.3** **y_t/b_0 = 15.0**

At x = 50 mm						
y (mm)	u (m/s)	v (m/s)	w (m/s)	$\sqrt{\overline{u'^2}}$ (m/s)	$\sqrt{\overline{v'^2}}$ (m/s)	$\sqrt{\overline{w'^2}}$ (m/s)
5	0.85		0.001	0.03		0.02
10	0.69		-0.002	0.08		0.04
15	0.31		-0.010	0.11		0.06
20	0.10		-0.016	0.06		0.05
60	0.02		-0.008	0.05		0.04
100	-0.02		-0.003	0.05		0.05
140	-0.03		-0.001	0.06		0.04
180	-0.05		0.004	0.06		0.04
210	-0.05		-0.001	0.06		0.04
230	-0.02		-0.003	0.05		0.04

At x = 650 mm						
95	0.06	0.01	0.008	0.09	0.04	0.07
105	0.07	0.02	0.012	0.09	0.04	0.07
125	0.12	0.03	0.014	0.10	0.06	0.07
155	0.15	0.04	0.011	0.10	0.06	0.08
185	0.16	0.04	0.012	0.09	0.06	0.08
205	0.17		0.014	0.07		0.06
225	0.17		0.021	0.08		0.07
235	0.16		0.023	0.08		0.09

At x = 100 mm						
y (mm)	u (m/s)	v (m/s)	w (m/s)	$\sqrt{\overline{u'^2}}$ (m/s)	$\sqrt{\overline{v'^2}}$ (m/s)	$\sqrt{\overline{w'^2}}$ (m/s)
-30	-0.08	0.06	-0.005	0.10	0.05	0.07
-20	0.22	-0.03	0.005			
-15	0.50	-0.09	0.023			
-10	0.70	-0.13	0.033			
-5	0.69	-0.10	0.028			
5	0.45	-0.05	0.010	0.16	0.04	0.07
20	0.07	-0.03	-0.006	0.06	0.03	0.05
40	0.04	-0.03	-0.013	0.05	0.03	0.05
70	0.01	-0.05	-0.005	0.05	0.03	0.05
110	-0.02	-0.05	-0.002	0.06	0.03	0.04
150	-0.07	-0.06	-0.002	0.06	0.04	0.05
180	-0.08	-0.04	-0.002	0.06	0.03	0.05
190	-0.09		0.004	0.06		0.05
220	-0.09		0.006	0.07		0.05
230	-0.06		0.001	0.06		0.04

At x = 150 mm						
y (mm)	u (m/s)	v (m/s)	w (m/s)	$\sqrt{\overline{u'^2}}$ (m/s)	$\sqrt{\overline{v'^2}}$ (m/s)	$\sqrt{\overline{w'^2}}$ (m/s)
-55	-0.10	0.05	-0.004	0.07	0.05	0.08
-40	0.01	0.02	-0.009	0.13	0.07	0.09
-30	0.32	-0.11	0.009	0.24	0.13	0.12
-25	0.43	-0.13	0.008	0.21	0.12	0.11
-20	0.52	-0.14	0.015	0.17	0.09	0.09
-15	0.54	-0.13	0.017	0.15	0.07	0.08
-5	0.41	-0.08	0.009	0.19	0.05	0.09
5	0.21	-0.05	-0.007	0.16	0.04	0.07
20	0.07	-0.04	-0.010	0.09	0.03	0.08
60	0.01	-0.05	-0.004	0.06	0.04	0.05
100	-0.03	-0.05	-0.003	0.06	0.04	0.05
140	-0.07	-0.05	0.002	0.06	0.04	0.05
180	-0.09	-0.03	0.003	0.06	0.04	0.05
200	-0.11		0.012	0.06		0.05
220	-0.13		0.014	0.06		0.05
230	-0.10		0.011	0.07		0.05

Expt. 4F5.3Y240 - Cont'd

At x = 200 mm							At x = 250 mm							At x = 300 mm						
y (mm)	u (m/s)	v (m/s)	w (m/s)	$\sqrt{\overline{u'^2}}$ (m/s)	$\sqrt{\overline{v'^2}}$ (m/s)	$\sqrt{\overline{w'^2}}$ (m/s)	y (mm)	u (m/s)	v (m/s)	w (m/s)	$\sqrt{\overline{u'^2}}$ (m/s)	$\sqrt{\overline{v'^2}}$ (m/s)	$\sqrt{\overline{w'^2}}$ (m/s)	y (mm)	u (m/s)	v (m/s)	w (m/s)	$\sqrt{\overline{u'^2}}$ (m/s)	$\sqrt{\overline{v'^2}}$ (m/s)	$\sqrt{\overline{w'^2}}$ (m/s)
-70	0.00	-0.02	0.001	0.13	0.08	0.11	-80	0.02	0.00	-0.004	0.12	0.05	0.12	-60	0.20	0.05	0.002	0.16	0.07	0.11
-55	0.11	-0.03	-0.007	0.16	0.09	0.10	-65	0.20	-0.03	-0.001	0.18	0.09	0.10	-50	0.29	0.07	0.008	0.15	0.08	0.09
-40	0.35	-0.11	0.003	0.20	0.10	0.11	-50	0.33	-0.05	0.006	0.18	0.09	0.10	-40	0.33	0.07	0.002	0.14	0.08	0.08
-30	0.40	-0.11	0.010	0.17	0.09	0.09	-35	0.36	-0.04	0.002	0.15	0.08	0.09	-25	0.33	0.09	-0.001	0.13	0.08	0.09
-20	0.40	-0.09	0.008	0.18	0.07	0.09	-20	0.30	-0.03	0.000	0.16	0.06	0.08	-5	0.24	0.07	-0.005	0.13	0.07	0.09
-10	0.32	-0.07	0.009	0.19	0.06	0.08	-5	0.18	-0.02	-0.005	0.16	0.05	0.08	15	0.13	0.03	-0.009	0.11	0.07	0.08
0	0.17	-0.05	-0.009	0.16	0.05	0.08	15	0.07	-0.03	-0.009	0.10	0.05	0.07	35	0.06	-0.02	-0.008	0.09	0.06	0.08
20	0.05	-0.05	-0.012	0.08	0.04	0.06	35	0.02	-0.05	-0.011	0.06	0.05	0.06	65	0.00	-0.04	0.003	0.07	0.06	0.07
60	-0.01	-0.06	-0.007	0.08	0.04	0.06	65	-0.02	-0.06	-0.004	0.06	0.05	0.06	105	-0.04	-0.05	0.006	0.08	0.05	0.08
100	-0.05	-0.05	-0.004	0.06	0.04	0.05	105	-0.05	-0.06	0.005	0.06	0.05	0.06	145	-0.08	-0.03	0.012	0.09	0.05	0.09
140	-0.08	-0.04	0.002	0.06	0.04	0.06	145	-0.09	-0.03	0.009	0.06	0.05	0.07	180	-0.11	-0.01	0.007	0.07	0.05	0.07
180	-0.12	-0.02	0.002	0.06	0.04	0.07	180	-0.12	-0.01	0.002	0.06	0.04	0.07	200	-0.14		0.012	0.06		0.06
200	-0.13		0.013	0.06		0.06	200	-0.13		0.016	0.06		0.06	220	-0.18		0.012	0.06		0.07
220	-0.16		0.019	0.06		0.06	220	-0.17		0.013	0.06		0.06	230	-0.22		0.007	0.07		0.07
230	-0.14		0.009	0.06		0.05	230	-0.19		0.010	0.07		0.06							

Expt. 4F5.3Y240 - Cont'd

At x = 350 mm							At x = 400 mm							At x = 450 mm						
y (mm)	u (m/s)	v (m/s)	w (m/s)	$\sqrt{\overline{u'^2}}$ (m/s)	$\sqrt{\overline{v'^2}}$ (m/s)	$\sqrt{\overline{w'^2}}$ (m/s)	y (mm)	u (m/s)	v (m/s)	w (m/s)	$\sqrt{\overline{u'^2}}$ (m/s)	$\sqrt{\overline{v'^2}}$ (m/s)	$\sqrt{\overline{w'^2}}$ (m/s)	y (mm)	u (m/s)	v (m/s)	w (m/s)	$\sqrt{\overline{u'^2}}$ (m/s)	$\sqrt{\overline{v'^2}}$ (m/s)	$\sqrt{\overline{w'^2}}$ (m/s)
-25	0.29	0.18	-0.001	0.12	0.08	0.08	20	-0.21	0.00	0.014				35	0.13	0.08	0.012			
-15	0.30	0.16	0.008	0.12	0.07	0.08	30	-0.08	-0.02	0.011				50	0.29	0.17	0.018	0.11	0.06	0.07
0	-0.34	0.06	0.004	0.00	0.00	0.00	45	0.12	-0.02	0.006				70	0.27	0.18	0.015	0.10	0.08	0.09
20	0.24	0.16	-0.002	0.10	0.09	0.09	65	0.20	0.16	0.004	0.08	0.10	0.08	90	0.20	0.17	0.007	0.09	0.09	0.09
40	0.16	0.10	-0.005	0.09	0.09	0.08	90	0.13	0.11	0.002	0.08	0.10	0.08	120	0.12	0.14	0.007	0.09	0.09	0.09
70	0.06	0.02	-0.004	0.07	0.08	0.07	120	0.04	0.06	0.005	0.07	0.09	0.08	150	0.04	0.10	0.005	0.08	0.10	0.08
110	0.00	0.00	0.004	0.06	0.07	0.08	150	-0.02	0.04	0.005	0.07	0.08	0.07	180	-0.03	0.08	0.000	0.07	0.08	0.08
150	-0.06	0.00	0.009	0.07	0.06	0.08	180	-0.08	0.04	0.003	0.07	0.07	0.08	200	-0.07		0.008	0.08		0.07
180	-0.11	0.01	0.005	0.07	0.06	0.07	200	-0.12		0.010	0.07		0.07	220	-0.12		0.001	0.07		0.08
200	-0.13		0.013	0.07		0.07	220	-0.17		0.010	0.07		0.08	230	-0.16		0.010	0.07		0.10
220	-0.19		0.012	0.07		0.07	230	-0.21		0.006	0.07		0.10							
230	-0.23		0.021	0.07		0.08														
At x = 500 mm							At x = 550 mm							At x = 600 mm						
50	0.07	0.03	0.011	0.12	0.04	0.09	65	0.05	0.02	0.008	0.09	0.04	0.08	80	0.05	0.01	0.009	0.08	0.03	0.08
60	0.13	0.06	0.004	0.14	0.06	0.08	75	0.09	0.03	0.011	0.12	0.05	0.09	90	0.06	0.02	0.014	0.10	0.05	0.07
75	0.17	0.10	0.012	0.14	0.06	0.08	90	0.12	0.06	0.014	0.12	0.06	0.08	105	0.10	0.03	0.016	0.10	0.05	0.08
95	0.19	0.15	0.012	0.12	0.07	0.08	105	0.16	0.10	0.015	0.12	0.06	0.08	125	0.14	0.06	0.015	0.10	0.06	0.08
120	0.19	0.17	0.014	0.08	0.08	0.07	125	0.14	0.10	0.007	0.11	0.07	0.08	155	0.16	0.08	0.016	0.09	0.07	0.07
150	0.11	0.15	0.006	0.09	0.09	0.08	155	0.13	0.12	0.009	0.09	0.08	0.07	185	0.14	0.06	0.017	0.08	0.07	0.07
180	0.04	0.11	0.007	0.08	0.09	0.08	185	0.10	0.10	0.008	0.09	0.08	0.07	205	0.15		0.013	0.08		0.06
200	0.01		0.005	0.08		0.08	205	0.09		0.005	0.08		0.07	225	0.14		0.015	0.08		0.07
220	-0.04		0.011	0.08		0.08	225	0.04		0.018	0.08		0.08	235	0.13		0.035	0.09		0.09
230	-0.05		0.017	0.09		0.09	235	0.03		0.025	0.09		0.10							

Expt. No.: = 4F5.3Y200 U_0 = 0.79 m/s F_0 = 5.3 y_t/b_0 = 12.5

At x = 50 mm							At x = 100 mm							At x = 150 mm						
y (mm)	u (m/s)	v (m/s)	w (m/s)	$\sqrt{\overline{u'^2}}$ (m/s)	$\sqrt{\overline{v'^2}}$ (m/s)	$\sqrt{\overline{w'^2}}$ (m/s)	y (mm)	u (m/s)	v (m/s)	w (m/s)	$\sqrt{\overline{u'^2}}$ (m/s)	$\sqrt{\overline{v'^2}}$ (m/s)	$\sqrt{\overline{w'^2}}$ (m/s)	y (mm)	u (m/s)	v (m/s)	w (m/s)	$\sqrt{\overline{u'^2}}$ (m/s)	$\sqrt{\overline{v'^2}}$ (m/s)	$\sqrt{\overline{w'^2}}$ (m/s)
5	0.87		0.001	0.03		0.02	-35	-0.05	0.04	-0.005	0.09	0.04	0.07	-60	-0.05	0.03	-0.001	0.08	0.05	0.08
10	0.74		-0.002	0.08		0.04	-25	0.12	-0.01	0.003	0.17	0.09	0.11	-50	-0.04	0.03	-0.001	0.11	0.07	0.09
15	0.33		-0.006	0.10		0.06	-20	0.35	-0.07	0.009				-40	0.10	-0.03	0.005	0.18	0.11	0.12
25	0.06		0.006	0.04		0.04	-15	0.61	-0.12	0.025				-25	0.47	-0.14	0.017	0.19	0.10	0.10
40	0.04		0.005	0.04		0.04	-10	0.71	-0.12	0.029				-20	0.51	-0.13	0.025	0.16	0.08	0.08
60	0.02		0.005	0.04		0.04	-5	0.63	-0.08	0.026				-15	0.50	-0.12	0.017	0.16	0.06	0.08
90	-0.01		0.006	0.05		0.04	5	0.30	-0.04	0.011	0.15	0.04	0.08	-10	0.45	-0.09	0.017	0.18	0.06	0.07
165	-0.06		0.004	0.06		0.04	15	0.08	-0.03	0.009	0.09	0.03	0.07	0	0.28	-0.05	0.015	0.17	0.04	0.08
185	-0.03		0.009	0.07		0.04	35	0.04	-0.03	0.004	0.08	0.03	0.07	10	0.10	-0.04	0.012	0.09	0.03	0.06
							65	0.01	-0.04	0.004	0.06	0.04	0.05	25	0.04	-0.04	0.004	0.08	0.04	0.07
							105	-0.03	-0.05	-0.002	0.07	0.04	0.05	55	0.02	-0.04	0.002	0.08	0.04	0.07
							135	-0.06	-0.04	0.002	0.06	0.04	0.05	95	-0.04	-0.04	-0.004	0.08	0.04	0.07
							155	-0.07		0.004	0.06		0.05	135	-0.08	-0.02	-0.003	0.08	0.04	0.08
							175	-0.09		0.000	0.07		0.05	155	-0.09		0.004	0.07		0.06
							185	-0.08		0.004	0.07		0.05	175	-0.13		0.005	0.06		0.05
														185	-0.15		0.005	0.06		0.05

Expt. 4F5.3Y200 - Cont'd

At x = 200 mm							At x = 250 mm							At x = 300 mm						
y (mm)	u (m/s)	v (m/s)	w (m/s)	$\sqrt{\overline{u'^2}}$ (m/s)	$\sqrt{\overline{v'^2}}$ (m/s)	$\sqrt{\overline{w'^2}}$ (m/s)	y (mm)	u (m/s)	v (m/s)	w (m/s)	$\sqrt{\overline{u'^2}}$ (m/s)	$\sqrt{\overline{v'^2}}$ (m/s)	$\sqrt{\overline{w'^2}}$ (m/s)	y (mm)	u (m/s)	v (m/s)	w (m/s)	$\sqrt{\overline{u'^2}}$ (m/s)	$\sqrt{\overline{v'^2}}$ (m/s)	$\sqrt{\overline{w'^2}}$ (m/s)
-70	-0.02	0.00	0.000				-70	0.14	0.00	0.012				-50	-0.02	0.03	0.002			
-55	0.13	-0.03	0.010				-60	0.23	-0.01	0.007				-30	0.31	0.09	0.009			
-45	0.29	-0.09	0.008	0.22	0.11	0.11	-50	0.32	-0.01	0.010				-5	0.28	0.12	0.007	0.11	0.08	0.08
-35	0.41	-0.11	0.012	0.18	0.09	0.10	-40	0.36	-0.01	0.010	0.16	0.08	0.09	10	0.19	0.08	-0.002	0.12	0.08	0.08
-30	0.41	-0.10	0.011	0.17	0.08	0.10	-30	0.35	0.00	0.008	0.15	0.07	0.09	25	0.12	0.04	-0.001	0.10	0.07	0.07
-20	0.34	-0.07	0.011	0.18	0.06	0.09	-20	0.29	0.00	0.013	0.15	0.07	0.08	45	0.06	0.00	-0.001	0.07	0.06	0.07
-10	0.28	-0.05	0.009	0.20	0.05	0.09	-10	0.22	0.00	0.005	0.16	0.06	0.08	75	-0.01	-0.04	0.007	0.07	0.06	0.07
0	0.17	-0.05	0.007	0.16	0.05	0.07	5	0.12	-0.02	-0.001	0.13	0.05	0.07	105	-0.05	-0.03	0.005	0.08	0.06	0.08
15	0.07	-0.05	-0.002	0.08	0.04	0.06	25	0.05	-0.04	-0.001	0.09	0.05	0.07	135	-0.11	-0.01	-0.005	0.08	0.06	0.07
35	0.02	-0.05	0.000	0.06	0.04	0.06	55	0.00	-0.05	-0.004	0.08	0.05	0.07	155	-0.14		0.002	0.08		0.07
65	-0.01	-0.06	0.004	0.07	0.05	0.06	95	-0.06	-0.05	0.004	0.08	0.05	0.08	175	-0.21		-0.005	0.08		0.07
95	-0.04	-0.05	0.002	0.07	0.05	0.06	135	-0.10	-0.02	-0.002	0.08	0.05	0.09	185	-0.25		-0.009	0.07		0.08
135	-0.09	-0.02	-0.005	0.07	0.05	0.07	155	-0.13		-0.003	0.07		0.07							
155	-0.12		0.000	0.07		0.06	175	-0.18		0.000	0.07		0.07							
175	-0.16		-0.003	0.07		0.06	185	-0.22		0.001	0.07		0.07							
185	-0.19		0.002	0.06		0.06														

Expt. 4F5.3Y200 - Cont'd

At x = 350 mm							At x = 400 mm							At x = 450 mm						
y (mm)	u (m/s)	v (m/s)	w (m/s)	$\sqrt{\overline{u'^2}}$ (m/s)	$\sqrt{\overline{v'^2}}$ (m/s)	$\sqrt{\overline{w'^2}}$ (m/s)	y (mm)	u (m/s)	v (m/s)	w (m/s)	$\sqrt{\overline{u'^2}}$ (m/s)	$\sqrt{\overline{v'^2}}$ (m/s)	$\sqrt{\overline{w'^2}}$ (m/s)	y (mm)	u (m/s)	v (m/s)	w (m/s)	$\sqrt{\overline{u'^2}}$ (m/s)	$\sqrt{\overline{v'^2}}$ (m/s)	$\sqrt{\overline{w'^2}}$ (m/s)
-10	0.14	0.19	0.008				20	0.04	0.07	0.003				40	0.03	0.02	-0.006	0.11	0.05	0.08
0	-0.04	-0.02	0.007				30	-0.15	0.00	0.008				50	0.11	0.06	-0.006	0.14	0.07	0.08
35	0.23	0.18	0.003	0.09	0.09	0.08	40	-0.31	0.12	0.007				60	0.13	0.08	-0.004	0.15	0.07	0.08
55	0.15	0.12	0.003	0.08	0.10	0.08	50	-0.25	0.04	0.006				75	0.18	0.15	0.000	0.14	0.08	0.09
75	0.07	0.06	-0.002	0.08	0.09	0.08	65	0.23	0.21	0.009	0.08	0.09	0.08	95	0.19	0.18	0.002	0.10	0.08	0.08
105	-0.01	0.02	-0.004	0.08	0.08	0.08	85	0.16	0.18	0.002	0.09	0.11	0.08	115	0.15	0.18	0.002	0.10	0.09	0.07
135	-0.09	0.01	-0.005	0.08	0.07	0.08	110	0.07	0.14	-0.002	0.09	0.10	0.08	140	0.08	0.14	-0.001	0.09	0.10	0.08
155	-0.13		-0.003	0.08		0.08	140	-0.04	0.08	-0.007	0.08	0.10	0.08	160	0.06		0.000	0.09		0.07
175	-0.20		-0.008	0.07		0.08	160	-0.07		-0.002	0.08		0.08	180	0.00		-0.003	0.08		0.08
185	-0.23		-0.010	0.07		0.09	180	-0.14		-0.009	0.07		0.08	190	-0.02		-0.009	0.08		0.10
							190	-0.17		-0.001	0.07		0.11							
At x = 500 mm							At x = 550 mm							At x = 600 mm						
55	0.01	0.00	0.004	0.06	0.03	0.07	75	0.04	0.00	0.001	0.07	0.04	0.07	85	0.05	0.00	-0.003	0.06	0.03	0.06
65	0.06	0.02	0.002	0.12	0.06	0.08	85	0.08	0.01	0.002	0.09	0.05	0.08	95	0.09	0.00	0.005	0.08	0.04	0.07
80	0.09	0.04	0.005	0.12	0.07	0.08	95	0.11	0.02	0.010	0.09	0.06	0.07	105	0.12	0.00	0.010	0.07	0.05	0.07
100	0.14	0.08	-0.001	0.12	0.07	0.08	105	0.13	0.02	0.006	0.11	0.06	0.09	130	0.17	0.01	0.010	0.08	0.06	0.07
120	0.15	0.09	0.006	0.10	0.07	0.08	120	0.16	0.03	0.004	0.09	0.06	0.07	140	0.19	0.01	0.011	0.07	0.06	0.07
140	0.15	0.09	0.001	0.09	0.08	0.07	140	0.18	0.03	0.007	0.08	0.07	0.07	160	0.21		0.005	0.07		0.06
160	0.17		-0.004	0.08		0.07	160	0.21		0.007	0.07		0.06	180	0.23		0.012	0.07		0.06
180	0.13		0.003	0.09		0.07	180	0.20		0.006	0.08		0.07	190	0.26		0.017	0.07		0.07
190	0.11		-0.005	0.08		0.09	190	0.21		0.020	0.08		0.08							

Expt. No.: = 4F5.3Y160 **U_0 = 0.79 m/s** **F_0 = 5.3** **y_t/b_0 = 10.0**

At x = 50 mm							At x = 100 mm							At x = 150 mm						
y (mm)	u (m/s)	v (m/s)	w (m/s)	$\sqrt{\overline{u'^2}}$ (m/s)	$\sqrt{\overline{v'^2}}$ (m/s)	$\sqrt{\overline{w'^2}}$ (m/s)	y (mm)	u (m/s)	v (m/s)	w (m/s)	$\sqrt{\overline{u'^2}}$ (m/s)	$\sqrt{\overline{v'^2}}$ (m/s)	$\sqrt{\overline{w'^2}}$ (m/s)	y (mm)	u (m/s)	v (m/s)	w (m/s)	$\sqrt{\overline{u'^2}}$ (m/s)	$\sqrt{\overline{v'^2}}$ (m/s)	$\sqrt{\overline{w'^2}}$ (m/s)
5	0.89		-0.009	0.02		0.02	-30	-0.05	0.04	0.003	0.11	0.06	0.08	-55	-0.06	0.03	0.001	0.09	0.05	0.08
10	0.81		-0.017	0.06		0.03	-20	0.21	-0.03	0.014				-45	0.00	0.01	0.007	0.15	0.09	0.10
15	0.45		-0.009	0.11		0.06	-15	0.54	-0.10	0.036				-35	0.15	-0.03	0.008			
25	0.05		0.007	0.05		0.05	-10	0.71	-0.12	0.039				-20	0.48	-0.13	0.024	0.18	0.09	0.10
40	0.03		0.009	0.05		0.04	-5	0.68	-0.09	0.039				-15	0.50	-0.12	0.024	0.16	0.07	0.09
60	0.02		0.009	0.05		0.04	0	0.52	-0.06	0.025	0.16	0.05	0.08	-5	0.40	-0.07	0.023	0.20	0.05	0.09
90	-0.01		0.003	0.06		0.05	10	0.19	-0.03	0.004	0.13	0.04	0.08	10	0.16	-0.04	0.013	0.14	0.04	0.08
120	-0.05		0.002	0.07		0.05	20	0.05	-0.03	0.005	0.08	0.03	0.07	30	0.05	-0.04	0.009	0.09	0.04	0.07
150	-0.06		0.001	0.08		0.05	40	0.02	-0.03	0.005	0.08	0.04	0.07	50	0.02	-0.04	0.011	0.07	0.04	0.06
							70	0.00	-0.04	0.004	0.06	0.04	0.05	70	0.00	-0.04	0.011	0.07	0.05	0.06
							100	-0.05	-0.04	0.003	0.07	0.04	0.06	100	-0.05	-0.03	-0.006	0.08	0.05	0.06
							120	-0.06		0.000	0.06		0.05	120	-0.08		0.000	0.08		0.06
							140	-0.09		0.003	0.08		0.05	140	-0.13		-0.001	0.08		0.06
							150	-0.08		0.004	0.08		0.05	150	-0.16		-0.002	0.08		0.06

Expt. 4F5.3Y160 - Cont'd

At x = 200 mm							At x = 250 mm							At x = 300 mm						
y (mm)	u (m/s)	v (m/s)	w (m/s)	$\sqrt{\overline{u'^2}}$ (m/s)	$\sqrt{\overline{v'^2}}$ (m/s)	$\sqrt{\overline{w'^2}}$ (m/s)	y (mm)	u (m/s)	v (m/s)	w (m/s)	$\sqrt{\overline{u'^2}}$ (m/s)	$\sqrt{\overline{v'^2}}$ (m/s)	$\sqrt{\overline{w'^2}}$ (m/s)	y (mm)	u (m/s)	v (m/s)	w (m/s)	$\sqrt{\overline{u'^2}}$ (m/s)	$\sqrt{\overline{v'^2}}$ (m/s)	$\sqrt{\overline{w'^2}}$ (m/s)
-65	0.00	-0.01	0.006	0.13	0.07	0.11	-60	0.15	0.01	0.014				-40	-0.06	0.05	0.013			
-55	0.12	-0.03	0.014	0.19	0.10	0.10	-40	0.33	0.02	0.019				-35	-0.07	0.05	0.007			
-45	0.26	-0.08	0.018	0.22	0.10	0.10	-30	0.35	0.02	0.016	0.15	0.08	0.10	-5	0.32	0.16	0.013	0.12	0.08	0.09
-35	0.36	-0.09	0.018	0.19	0.09	0.10	-20	0.33	0.02	0.018	0.15	0.07	0.09	5	0.27	0.15	0.013	0.11	0.08	0.08
-25	0.39	-0.08	0.026	0.16	0.07	0.09	-10	0.28	0.02	0.023	0.15	0.07	0.07	20	0.21	0.10	0.015	0.10	0.08	0.08
-15	0.35	-0.06	0.021	0.18	0.06	0.08	0	0.20	0.01	0.021	0.15	0.06	0.07	40	0.11	0.04	0.013	0.09	0.07	0.07
-5	0.24	-0.04	0.024	0.19	0.05	0.08	10	0.12	-0.01	0.019	0.11	0.05	0.07	70	0.02	0.00	0.001	0.08	0.07	0.08
5	0.15	-0.04	0.019	0.15	0.05	0.08	30	0.07	-0.02	0.019	0.09	0.06	0.07	100	-0.08	-0.01	-0.010	0.09	0.07	0.08
20	0.06	-0.04	0.009	0.10	0.05	0.08	60	0.01	-0.04	0.006	0.08	0.06	0.07	120	-0.13		-0.011	0.09		0.07
40	0.03	-0.05	0.010	0.07	0.05	0.06	100	-0.08	-0.03	-0.015	0.09	0.06	0.07	140	-0.21		-0.014	0.08		0.08
70	-0.02	-0.05	0.003	0.08	0.05	0.06	120	-0.12		-0.011	0.09		0.07	150	-0.26		-0.015	0.07		0.09
100	-0.07	-0.03	-0.009	0.08	0.05	0.07	140	-0.20		-0.011	0.08		0.07							
120	-0.10		-0.005	0.09		0.07	150	-0.24		-0.016	0.07		0.08							
140	-0.16		-0.011	0.08		0.07														
150	-0.20		-0.006	0.07		0.07														

Expt. 4F5.3Y160 - Cont'd

At x = 350 mm							At x = 400 mm							At x = 450 mm						
y (mm)	u (m/s)	v (m/s)	w (m/s)	$\sqrt{\overline{u'^2}}$ (m/s)	$\sqrt{\overline{v'^2}}$ (m/s)	$\sqrt{\overline{w'^2}}$ (m/s)	y (mm)	u (m/s)	v (m/s)	w (m/s)	$\sqrt{\overline{u'^2}}$ (m/s)	$\sqrt{\overline{v'^2}}$ (m/s)	$\sqrt{\overline{w'^2}}$ (m/s)	y (mm)	u (m/s)	v (m/s)	w (m/s)	$\sqrt{\overline{u'^2}}$ (m/s)	$\sqrt{\overline{v'^2}}$ (m/s)	$\sqrt{\overline{w'^2}}$ (m/s)
5	0.22	0.20	0.023	0.15	0.07	0.09	25	0.04	0.02	-0.003	0.12	0.06	0.08	45	0.01	0.00	-0.007	0.07	0.03	0.07
10	0.27	0.20	0.025				35	0.20	0.13	0.010	0.15	0.08	0.08	55	0.08	0.03	-0.003	0.13	0.06	0.07
15	0.27	0.21	0.020				45	0.19	0.15	0.005	0.15	0.08	0.08	65	0.12	0.06	-0.002	0.13	0.07	0.07
35	0.27	0.23	0.011	0.11	0.08	0.10	55	0.22	0.19	0.008	0.14	0.08	0.10	75	0.15	0.08	0.000	0.14	0.08	0.09
50	0.22	0.21	0.006	0.10	0.09	0.09	70	0.21	0.22	0.008	0.11	0.08	0.09	90	0.17	0.11	0.004	0.11	0.07	0.08
70	0.14	0.16	0.007	0.10	0.09	0.09	85	0.17	0.20	0.006	0.09	0.09	0.08	105	0.17	0.10	-0.001	0.10	0.08	0.08
100	0.00	0.08	-0.008	0.10	0.09	0.09	105	0.09	0.15	-0.004	0.10	0.10	0.08	125	0.19		-0.008	0.09		0.07
120	-0.06		-0.006	0.09		0.08	125	0.07		-0.005	0.09		0.07	145	0.13		-0.008	0.09		0.07
140	-0.16		-0.002	0.08		0.08	145	-0.03		-0.009	0.08		0.08	155	0.11		0.000	0.09		0.09
150	-0.21		-0.011	0.07		0.09	155	-0.05		-0.002	0.08		0.10							
At x = 500 mm							At x = 550 mm							At x = 600 mm						
65	0.08	0.01	-0.005	0.10	0.05	0.07	75	0.09	0.00	0.000	0.06	0.03	0.06	80	0.12	0.00	-0.004	0.06	0.03	0.06
75	0.11	0.01	0.001	0.10	0.06	0.07	85	0.15	0.00	-0.002	0.08	0.05	0.07	85	0.14	-0.01	-0.001	0.06	0.04	0.06
85	0.14	0.02	0.001	0.10	0.06	0.07	95	0.18	0.00	0.004	0.08	0.05	0.07	95	0.17	-0.01	0.001	0.06	0.04	0.06
95	0.17	0.03	0.002	0.10	0.07	0.08	105	0.19	0.00	0.004	0.09	0.05	0.08	105	0.19	-0.01	0.005	0.07	0.05	0.06
105	0.19	0.03	0.004	0.10	0.06	0.08	125	0.23		-0.006	0.07		0.06	125	0.22		-0.006	0.06		0.06
125	0.23		-0.012	0.08		0.07	145	0.26		0.001	0.07		0.05	145	0.25		-0.002	0.06		0.05
145	0.24		-0.002	0.08		0.06	155	0.28		0.005	0.07		0.07	155	0.27		0.003	0.06		0.06
155	0.23		0.010	0.08		0.08														